Saarland University
Faculty of Natural Science and Technology I
Department of Computer Science
Master's Program in Visual Computing

Master's Thesis

Hamilton-Jacobi Equations for Computer Vision: Application in Shape from Shading

Yong Chul Ju

May 17, 2010

Supervisor Prof. Dr. Joachim Weickert
Advisor PD Dr. Michael Breuß
Reviewers Prof. Dr. Joachim Weickert
PD Dr. Michael Breuß

Affidavit

I hereby declare that this master's thesis has been written only by undersigned and without any assistance from third parties. Furthermore, I confirm that no sources have been used in the preparation of this thesis other than those indicated in the thesis itself.

Saarbrücken, 17-05-2010

Declaration of Consent

Herewith I agree with that this thesis will be made available through the library of the Computer Science Department. This consent explicitly includes both the printed, as well as the electronic form attached to the last page of this thesis. I confirm that the electronic and the printed version are of identical content.

Saarbrücken, 17-05-2010

Acknowledgements

The presented work could never have been accomplished without contributions of many people.

First of all, I owe my gratitude to Prof. Dr. Joachim Weickert for giving me a chance to work under his supervision.

Then, I should thank my advisor PD Dr. Michael Breuß for giving me an interesting and challenging topic, fruitful discussion on various mathematical issues and spending much of his time on proofreading many draft versions.

I also wish to express my appreciation to Oliver Vogel for giving me a good advice on the topic and all the nice people in Mathematical Image Analysis group for providing me with a nice working atmosphere and being kind and helpful all the time.

Last but not least, I would like to express my sincere gratitude to my mother for her unlimited support and patience during my work and my father who is still alive in my heart.

Abstract

Hamilton-Jacobi equations arise in many areas of science such as classical mechanics or geometric optics. After Berthold K. P. Horn formulated the Shape from Shading problem using a Hamilton-Jacobi equation in 1970, they have also been playing an important role on computer vision.

This thesis deals with Hamilton-Jacobi equations in theoretical and numerical point of view especially focusing on the application in Shape from Shading.

The first part covers the solution theory under the notion of continuous viscosity solutions proposed by Crandall and Lions. The advantage of this approach is mainly twofold. One is the well-posedness properties we can obtain in this framework which cannot be achieved with the classical method. The other is that it provides a framework in which we can derive a simple explicit scheme to approximate solutions and prove the convergence of the scheme.

The second part concentrates on the model extension accomplished by the change of surface reflectance from Lambertian to non-Lambertian in the modelling process which causes non-convexities in the Hamiltonian. By employing critical points analysis for the Hamiltonian we investigate one of the simplest non-convex models by the Vogel-Breuß-Weickert model, and we provide conditions to circumvent the non-convex properties theoretically. This gives us a deeper insight into the model.

The last part concerns numerical aspects for solving Hamilton-Jacobi equations in the viscosity framework. Due to our special interest in the non-convex Hamiltonian one of the main difficulties in numerical analysis lies in assuring the convergence of a scheme. In this work, we have shown the convergence of an explicit scheme for the Vogel-Breuß-Weickert model in one-dimensional case and present the experimental results.

Contents

Chapter 1

Introduction

Hamilton-Jacobi equations are the mathematical language for describing natural phenomena and thereby arise naturally in numerous subfields of science such as classical mechanics or geometric optics in physics.

Since it was shown by Berthold K. P. Horn that the Shape from Shading problem can be formulated by these equations, this thesis put emphasis upon both theoretical and numerical perspectives for this nonlinear first-order partial differential equation especially focusing on the application in the Shape from Shading.

In the present chapter, we first give an overview of Shape from Shading problems and modelling issues on which we focus for this work. The detailed mathematical exposition for Hamilton-Jacobi equations is postponed until Chapter 2 and thereafter.

After we set goals for this thesis, short summaries of each chapter and the outline are provided at the end.

Main references for this chapter are papers on Shape from Shading such as [14, 27, 84, 85, 96].

1.1 Shape from Shading

As one might guess from the name, the task of *Shape from Shading (SfS)* is to compute a three-dimensional depth information of the object (*Shape*) from a given single grey value image (*Shading*), see Figure 1.1.

This classical inverse problem is one of the research topics in computer vision and has several practical applications. As an example, in astronomy this technique is used to reconstruct the terrain on a planet from a photograph acquired by a spacecraft. Another example can be found in endoscopy, where this method is helpful for recovering the surface of human internal organs for various medical reasons [9, 20, 40, 105, 108].

This problem was first formulated by Berthold K. P. Horn as finding solutions of nonlinear first-order partial differential equation called the *brightness equation* under certain

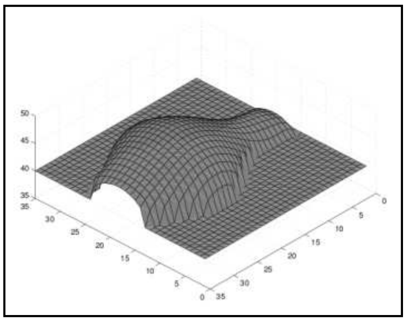

Input image $\xrightarrow{\text{SfS}}$ Recover the 3-D surface of the object

Figure 1.1: Illustration of the Shape from Shading (SfS) problem. The goal of this problem is to obtain the same image as the input one (left) when we take a picture of the recovered scene (right) that we have computed. Adapted from [3].

assumptions on the scenes [14, 45]. It was also he who coined the term "Shape from Shading". After he described the problem in 1970, a lot of efforts were made to solve this problem based on his work.

Roughly speaking, this brightness equation describes the relationship between image intensities and the variation of these intensities according to the slope of unknown surface, so that the shape can be reconstructed from the shading. Nevertheless, in order to solve this problem correctly it is also important for us to know exactly how the image is acquired from the scene. Then, we can make reasonable assumptions based on the image acquisition process. When the assumptions could not reflect physical phenomena correctly, the proposed model made by unrealistic assumptions would not work, which could yield unreasonable or poor results.

In the matter of SfS problem, it mainly involves three modelling issues of the scene: surface, illumination and camera setup. The details in need will be discussed in Section 5.1. In this thesis, we are primarily interested in surface and camera model.

Before we turn our attention to these modelling issues, we briefly see how progress has been made in this area.

1.1.1 Brief History and Related Works

According to [84], in the first stage (1980s) the efforts were made by only trying to compute numerical solutions directly without considering the existence and uniqueness of solutions except the work of Bruss and Brooks [16, 17], which showed important aspects in mathematics.

In the last decades, these questions were the central topics of the problem due to the poor quality of the results despite the huge amount of papers. For this reason, it drew the attention of mathematicians, and it turned out that the problem itself is in general ill-posed[1]. For example, in [79] the so-called "convex-concave ambiguities" show these difficulties which we shall discuss in Section 4.4.

As a result, tremendous attempts were made to alleviate these problems both in solution theory[2] of partial differential equations and in the modelling process. Among them *viscosity solutions*[3] and perspective camera model attract our interest, since we are allowed to obtain desired results within these frameworks [27, 29, 84]. Hence, we utilise these methods in this thesis.

1.1.2 Modelling Issues

As noted before, there are mainly three modelling components involved in Shape from Shading problem and we briefly discuss here each one. The mathematical details about this process is presented in Section 5.1.

Camera Model

The camera model is about how to map the surface point to the image plane.

As can be observed in Figure 1.2a, in an orthographic camera model the surface point is directly projected onto the retinal plane. In contrast to this, in a perspective one the surface point is mapped to the point on the retinal plane along the line starting from the optical centre, see Figure 1.2b.

According to [10, 27, 84], a perspective projection model enables us to step forward in dealing with ill-posedness with the help of viscosity framework, which is why we are specially interested in.

Illumination

The illumination model explains how the light intensities on the surface are stored on the image plane which is described by a brightness equation. Simply speaking, SfS problem is equivalent to solve this brightness equation. It has the form

$$I\left(x_1, x_2\right) = R\left(\mathbf{n}\left(x_1, x_2\right)\right), \tag{1.1}$$

where I denotes the image intensities at the point $\left(x_1, x_2\right)$ and R is the reflectance map depending on the surface normal vector $\mathbf{n}$ at the position $\left(x_1, x_2\right)$ and can be computed by $R = \cos\left(\mathbf{L}, \mathbf{n}\right) = \frac{\mathbf{L}}{|\mathbf{L}|} \cdot \frac{\mathbf{n}}{|\mathbf{n}|}$, see Figure 1.2.

[1]The meaning here is that solutions of the problem do not exist or the retrieved solution is not unique. This is the opposite concept of well-posedness which will be explained in more detail in Section 2.2

[2]Actually, this theory was not developed solely for SfS problem but for other model problems, e.g. in physics. SfS has benefited from its fruit.

[3]This theory was mainly developed to provide the well-posedness on the problem.

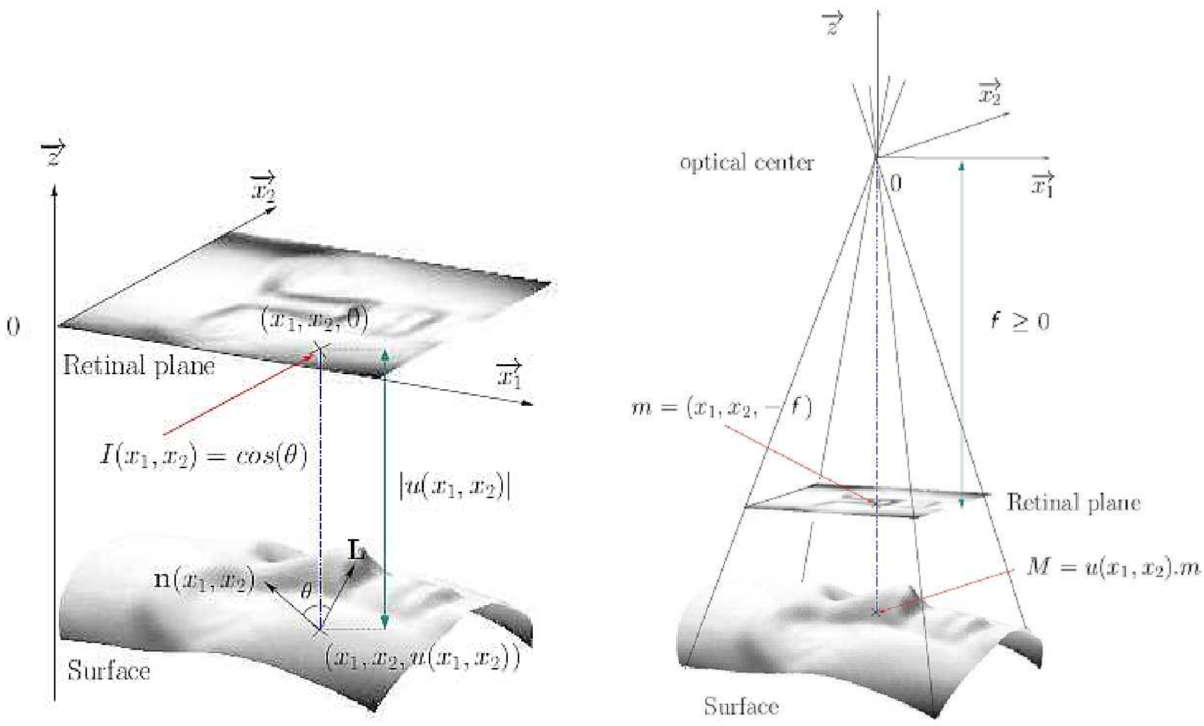

(a) Orthographic camera model

(b) Perspective camera model

Figure 1.2: Orthographic and perspective camera models. In 1.2a, $I(x_1, x_2)$ denotes image intensities at the point (x_1, x_2), $\mathbf{n}$ represents a normal vector of the surface at the point (x_1, x_2), $\mathbf{L}$ is the normalised light direction, θ is the angle between $\mathbf{n}$ and $\mathbf{L}$, and $u(x_1, x_2)$ is the unknown surface depth. In 1.2b, $\mathtt{f}$ denotes a focal length of a camera. Adapted from [85].

A usual assumption on the scene is that the light intensity on the surface point is directly saved on the image plane without any loss and the surface is Lambertian[4].

Surface

In the matter of surface, most SfS models incorporate Lambertian surfaces for both an orthographic setting and a perspective one. Comparing to huge amount of work for Lambertian surfaces, non-Lambertian ones constitute only a small portion. Although some attempts were already made for orthographic projections [56, 97], these models suffer from ill-posedness as we mentioned earlier.

Despite the fact that non-Lambertian reflectance is more realistic than Lambertian one, counting both non-Lambertian surfaces and a perspective camera model makes a brightness equation more complicated and difficult to deal with, since we have to cope with

[4] Basic properties of Lambertian surface will be explained in Section 5.1

non-convex problems in general [5, 75]. The comparison between models is presented in Table 6.1 and we shall account for these topics in Chapter 6.

So far, we have seen a brief overview of a SfS problem and its modelling issues. This may be the moment that we set goals for this thesis.

1.2 Goals of the Thesis

1.2.1 Motivation

First, we have flooded with theoretical results specially of viscosity solutions which are quite effective for SfS problems. Nonetheless, they are scattered all over the literature.

Second, theoretical works are sometimes considerably difficult to access.

Third, non-convex SfS models are up to now not analysed.

1.2.2 Goals

In this thesis, we aim at reaching following goals:

First, we try to collect all necessary theoretical ingredients from literature and give them structure in a reasonable way.

Second, we perform a first investigation of simplest non-convex model.

Third, we evaluate a non-convex model with respect to numerical algorithms.

1.3 Organisation and Chapter Summary

This thesis is composed of nine chapters and the outline is given in Figure 1.3. For the purpose of an overview, we summarise each chapter shortly.

In **chapter 2**, we give basic mathematical backgrounds on Hamilton-Jacobi equations including partial differential equations, well-posedness, notion of continuous viscosity solutions and Legendre transform.

In **chapter 3**, we consider a compatibility condition on the boundary data which is required to the existence of viscosity solutions.

In **chapter 4**, we investigate the uniqueness of the solution which can be explained by comparison theorem.

In **chapter 5**, mathematical modelling process of perspective SfS and the details of Prados and Faugeras model are studied including convexity and well-posedness.

In **chapter 6**, non-convex Vogel-Breuß-Weickert model is presented and analysed. The properties of a Hamiltonian and critical points are provided.

In **chapter 7**, basics knowledge of numerical analysis is given including consistency, stability and monotonicity. Afterwards, we examine the notion on the convergence of a numerical scheme and see how it works in the viscosity framework. In addition, we proved the convergence of one-dimensional explicit scheme for the VBW model.

In **chapter 8**, numerical experiments are performed in one- and two-dimension and results are presented.

In **chapter 9**, we conclude this work by giving a summary and discussing possible outlooks.

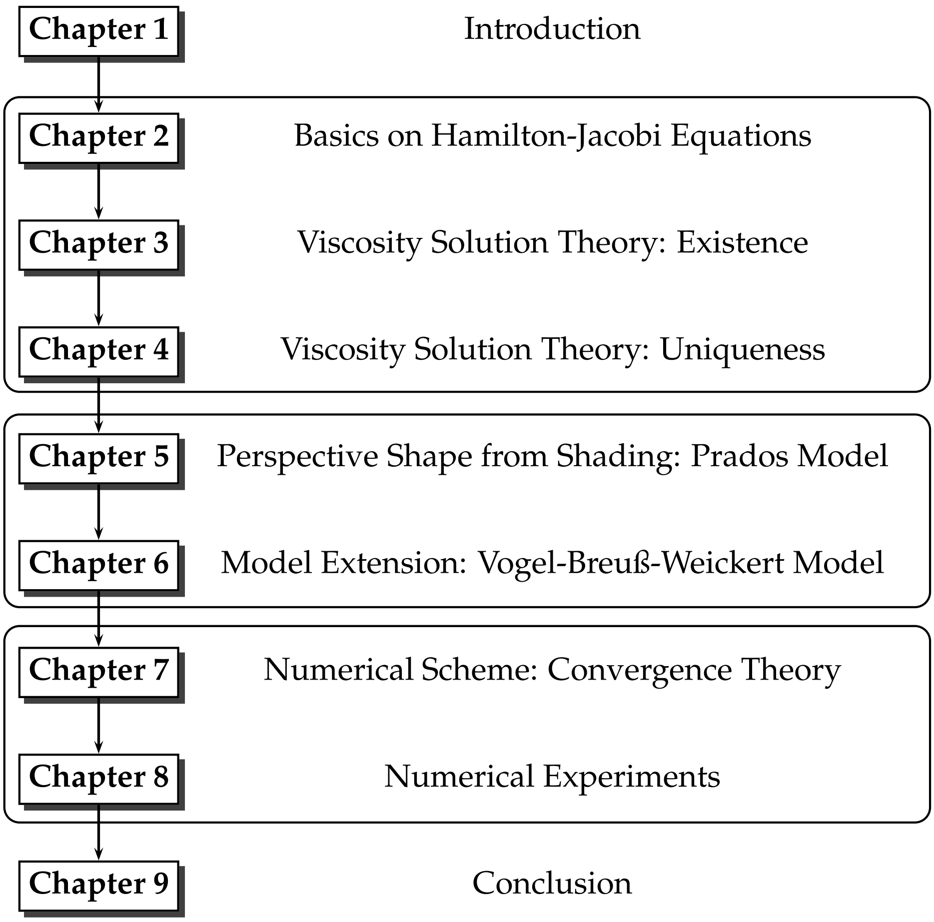

Figure 1.3: Structure of the present thesis.

Chapter 2

Mathematical Background on Hamilton-Jacobi Equations

In this chapter, we shall survey the important mathematical tools which will appear in this thesis. Our major concern is to solve the Shape from Shading problems which are described by partial differential equations. Among all different types of partial differential equations what we are specially interested in is a Hamilton-Jacobi equation. This introduces a new concept of solutions for the Shape from Shading problems.

The chapter is organised as follows.

In the first section we begin with a question "What is a Hamilton-Jacobi equation?", then think about "What is the reasonable meaning of solving this problem?", in other words "In what sense are we seeking for a solution?".

Afterwards, it can be realised that we encounter some problems when we approach with a classical method to solve a one-dimensional eikonal[1] equation, which brings us naturally a new notion of a solution.

Then, we investigate a new concept of a solution. Our contribution here is to present a detailed analytical exposition of a viscosity solution concept by making use of a one-dimensional eikonal equation.

Finally, we shall have a look at the Legendre transform which plays a significant role in the solution theory of a Hamilton-Jacobi equation.

To this end, we have used a certain range of the references depending on the topics. The main references for the general theory of partial differential equations are [32, 83] and for the well-posedness [11, 53] are used. In addition, we mainly follow [12, 67] for the viscosity solution theory and [7, 42–44, 46, 71, 91] for Legendre transform theory, respectively.

[1] $\varepsilon\iota\kappa\acute{\omega}\nu$ (or $\varepsilon\iota\kappa o\nu$) means "an image" in Greek

2.1 What is a Hamilton-Jacobi Equation?

In order to answer this question, we should first clarify what a partial differential equation is.

A *partial differential equation (PDE)* is an equation which describes the relationship between an unknown function u of two or more variables and its partial derivatives. In general, for a fixed integer $k \geq 1$ it has the form:

Definition 2.1.1 (Partial Differential Equation).

$$F\left(\mathbf{x}, u(\mathbf{x}), Du(\mathbf{x}), \ldots, D^{k-1}u(\mathbf{x}), D^k u(\mathbf{x})\right) = 0, \tag{2.1}$$

where $u : \Omega \to \mathbb{R}$ and Ω is any open subset in $\mathbb{R}^n$. We often take $\Omega = \mathbb{R}^n$. Here the notation $D^k u(\mathbf{x})$ denotes the vector containing all kth order partial derivatives. For example,

$$Du(\mathbf{x}) = \left(\frac{\partial u}{\partial x_1}, \ldots, \frac{\partial u}{\partial x_n}\right)^{\mathrm{T}} \tag{2.2}$$

and

$$D^2 u(\mathbf{x}) = \left(\frac{\partial^2 u}{\partial x_i \partial x_j}\right)^{\mathrm{T}}_{1 \leq i,j \leq n} \tag{2.3}$$

and so on. Sometimes we write $\frac{\partial u}{\partial x_i}$ as u_{x_i}.

As an example, when we consider the spatially two-dimensional case, which means $\mathbf{x} = (x_1, x_2)^T \in \mathbb{R}^2$, a general expression of a PDE has the following form:

$$F(x_1, x_2, u, u_{x_1}, u_{x_2}, u_{x_1 x_2}, u_{x_2 x_1}, u_{x_1 x_1}, u_{x_2 x_2}) = 0, \tag{2.4}$$

where x_1 and x_2 are independent variables in $\mathbb{R}$, $u(x_1, x_2) : \mathbb{R} \times \mathbb{R} \to \mathbb{R}$ is the unknown function, and u_{x_i} with $i \in \{1,2\}$ denotes the partial derivative $\frac{\partial u}{\partial x_i}$ with $i \in \{1,2\}$. As we can see in (2.4), the functional F "defines" the equation by involving u and its partial derivatives.

In general, a solution technique of a PDE heavily depends on its type, therefore we are in need of classifying this PDE into different types. To this end, we pay attention to the *order* and the *linearity* of a PDE [32, 83].

The Order of a PDE

The first classification is according to the *order* of the PDE.

Definition 2.1.2 (Order of a PDE). The *order* of a PDE is defined to be the order of the highest derivative present in the given PDE.

When the highest derivative is of order k, then the order of a PDE is said to be of order k. Let us have a look at some examples. A PDE $u_{x_1x_1} + u_{x_2x_2} = 0$ is called a second order PDE, since its highest derivative order is two. While the PDE $u_{x_1}^2 + u_{x_2}^2 = 1$ is said to be a first order, since this PDE involves only first derivatives.

Linear PDE

Another important classification criterion of a PDE is about *linear* versus *nonlinear*. A PDE is called *linear* when a functional F in (2.4) behaves linearly with respect to the unknown function u and its derivatives. Otherwise, it is called *nonlinear*. As an example, a PDE $x^2 u_{x_1} + e^{x_1 x_2} u_{x_2} + \sin(x_1^2 + x_2^2) u = x^3$ is a linear one but with *variable coefficients*, because we can rewrite this PDE as $\alpha_1 u_{x_1} + \alpha_2 u_{x_2} + \alpha_3 u + \alpha_4 = 0$, where $\alpha_1 = x^2$, $\alpha_2 = e^{x_1 x_2}$, $\alpha_3 = \sin(x_1^2 + x_2^2)$, and $\alpha_4 = -x^3$, which means that the coefficient functions do not depend on the unknown function u and its derivatives. However, in contrast to the previous example a PDE $u_{x_1}^2 + u_{x_2}^2 = 1$ is a nonlinear one, since the functional F in (2.4) does not behave linearly with respect to the derivatives of unknown function u in this case.

Going back to the question "What is the Hamilton-Jacobi equation?" gives the answer that a Hamilton-Jacobi equation (HJE) is a first order, nonlinear PDE. For the HJE, attention will be focused on the following two classes of problems. One is

Definition 2.1.3 (Dirichlet Problem for Hamilton-Jacobi Equation).

$$\begin{cases} H(\mathbf{x}, u(\mathbf{x}), Du(\mathbf{x})) & = & 0 & \text{in} & \Omega \\ u(\mathbf{x}) & = & \varphi(\mathbf{x}) & \text{on} & \partial\Omega, \end{cases} \tag{2.5}$$

where $H(\mathbf{x}, u(\mathbf{x}), Du(\mathbf{x})) : \Omega \times \mathbb{R} \times \mathbb{R}^n \to \mathbb{R}$ is a given function called *Hamiltonian*, $u(x) : \Omega \to \mathbb{R}$ with $\mathbf{x} \in \Omega = \mathbb{R}^n$ is the unknown function that we want to seek, and $\partial\Omega$ denotes the boundary of Ω.

The other is

Definition 2.1.4 (Cauchy Problem for Hamilton-Jacobi Equation).

$$\begin{cases} \dfrac{\partial u}{\partial t} + H(\mathbf{x}, t, u(\mathbf{x}, t), Du(\mathbf{x}, t)) & = & 0 & \text{in} & \Omega \times]0, T] \\ u(\mathbf{x}, t) & = & \varphi(\mathbf{x}, t) & \text{on} & \partial\Omega \times]0, T] \\ u(\mathbf{x}, 0) & = & u_0(\mathbf{x}) & \text{in} & \Omega, \end{cases} \tag{2.6}$$

where $\mathbf{x} \in \Omega = \mathbb{R}^n$ usually denotes a space variable and $t \in]0, T]$ with $T \in \mathbb{R}$ is for time. The function $u(\mathbf{x}, t) : \mathbb{R}^n \times \ ]0, T] \to \mathbb{R}$ is the unknown and $u_0(\mathbf{x}) : \mathbb{R}^n \to \mathbb{R}$ is the *initial condition*.

As an example, in the spatially two-dimensional case with one time variable a Cauchy Problem HJE has the expression

$$\begin{cases} \frac{\partial u}{\partial t} + H(x_1, x_2, t, u, u_{x_1}, u_{x_2}) & = & 0 & \text{in} & \Omega \times]0, T] \\ u(x_1, x_2, t) & = & \varphi(x_1, x_2, t) & \text{on} & \partial\Omega \times]0, T] \\ u(x_1, x_2, 0) & = & u_0(x_1, x_2) & \text{in} & \Omega, \end{cases} \tag{2.7}$$

where $\Omega \subset \mathbb{R}^2$, $u_{x_i} = \frac{\partial u}{\partial x_i}$ with $i \in \{1, 2\}$, and $u = u(x_1, x_2, t)$ is the unknown function.

Remark 2.1.1. These types of PDEs were extensively invetigated by the Irish mathematician William Rowan Hamilton (1805-1865) who made important contributions to the problems in optics and classical mechanics [106, 107], extended by Carl Gustav Jacob Jacobi (1804-1851), and named after them in honour of their achievements.

2.2 Well-Posedness

Our attention is now turned into the question "What does it mean to solve a PDE?". In general, solving a PDE is not an easy task depending on the particular structures of the problem at hand. To deal with this problem, Jacques Salomon Hadamard (1865-1963) presented guidelines in [41]. Having thought of a boundary value problem (BVP) for a PDE, he claims that a mathematical model for a physical problem has to be *well-posed* in the sense that it has the following three properties:

Definition 2.2.1 (Well-Posedness).

1. [**Existence**] There exists a solution of the problem.
2. [**Uniqueness**] There is at most one solution of the problem.
3. [**Stability**] The solution depends continuously on the given data in the problem.

If one of these conditions is not satisfied, the problem is said to be *ill-posed*.

Let us discuss briefly why these criteria are useful for solving a PDE.

The existence of a solution directly involves a question what requirements we ask for the solution. For example, is it enough for a solution u to be just a continuous function? Or does it have to be infinitely many differentiable? Depending on these requirements, the answer will be changed. For this matter, we shall see an example that a one-dimensional eikonal equation equipped with boundary value has no solution in C^1, but it does have a solution which belongs to C^0 in Section 2.3. Therefore, mathematically speaking, the existence of a solution can be enforced by enlarging the solution space. The concept of *weak*, *generalised*, or *distributional solutions* is developed to cope with these circumstances.

In the matter of uniqueness, we can think of a two-dimensional eikonal equation $u_{x_1}^2 + u_{x_2}^2 = n^2$ which describes the property of a traversal path of a ray as formulated by Hamilton, which can be seen in Figure 2.1. When a ray hits a denser homogenous medium, it chooses its propogation path according to the Fermat's principle, which states that the ray of a light takes the path along which it can be traversed in the least amount of time [77]. This suggests that the solution must fulfil the extremum condition indicating that the solution is not a dashed curve path but actually a line path from A to B in Figure 2.1. So, if a problem has more than one solution, then this can be understood as missing information by the model which would enable us to single out the solution. In this case, additional information, such as boundary conditions or initial conditions can be added into the model to resolve this situation.

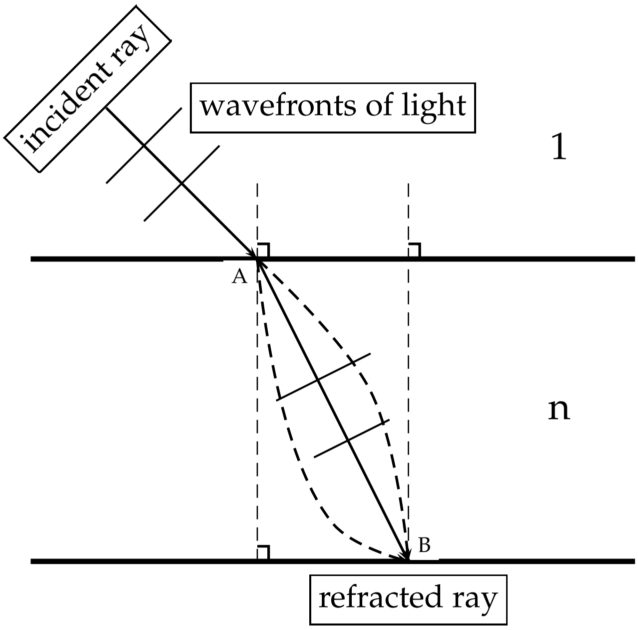

Figure 2.1: Refraction of a ray when the light transmitted into the denser medium ($n > 1$).

Regarding the stability, it implicates that the solution should change only a little bit when we change the problem a little. The requirement of this property is of great importance in practice. When we compute the solution of a problem using a numerical scheme, the convergence of the numerical scheme towards a true solution when the grid size vanishes is always an issue. According to [80] without the property of stability, the convergence of the scheme cannot be guaranteed. Therefore, if the solution does not depend continuously on the given data in the problem, then in general the computed solution is not related with the true solution.

Hence, it is a desirable strategy for us to seek for a solution to a given PDE which satisfies well-posedness properties in the sense of Hadamard.

2.3 Notion of a Solution

In this section, a simple example of a HJE is considered which makes trouble from the perspective of well-posedness when we approach with the classical methods. This discussion leads, afterwards, to a new concept of a solution called *viscosity solutions* in order to get around this problem.

2.3.1 Need for a New Concept of a Solution

Why do we need a new concept of a solution? At the first stage, let us try to solve with a classical method the following one-dimensional eikonal equation with Dirichlet boundary conditions (DBC) from geometric optics:

$$\begin{cases} |\nabla u(x)| &= 1, \quad x \in (0,1) \\ u(x) &= 0, \quad x \in \{0,1\}, \end{cases} \tag{2.8}$$

where $|\cdot|$ denotes the Euclidean norm.

Seeking the solution of the above problem (2.8) with the classical method, which means that we want to find a continuous and differentiable function u over the entire domain where x is defined, we encounter several questions concerned with the well-posedness.

The first question is about the existence of solutions. The PDE (2.8) has no solutions in C^1, which can be proved by contradiction. Suppose that there exist such solutions. In that case, we must be able to find a point $x_0 \in (0,1)$ which satisfies $u'(x_0) = 0$ by Rolle's theorem [8], which states that a differentiable and continuous function which attains equal values at end points of the interval must have a point x_0 between the interval $(0,1)$ where the slope of the tangent line at that point is zero which implies $u'(x_0) = 0$, see Figure 2.2. However, this contradicts the fact that for the every point $x_0 \in (0,1)$ the slope is already given by $|u'(x_0)| = 1$ in the problem (2.8). Therefore, (2.8) cannot admit a solution in C^1.

The second question is about the uniqueness of the solution. Now, let us expand our solution space from C^1 to C^0, since we have failed in looking for a solution in C^1. But this leads to another problem. As an example, we can easily confirm that the function $u^+(x) = \frac{1}{2} - \left|\frac{1}{2} - x\right|$ is a solution of (2.8) for almost every $x \in (0,1)$ as follows.

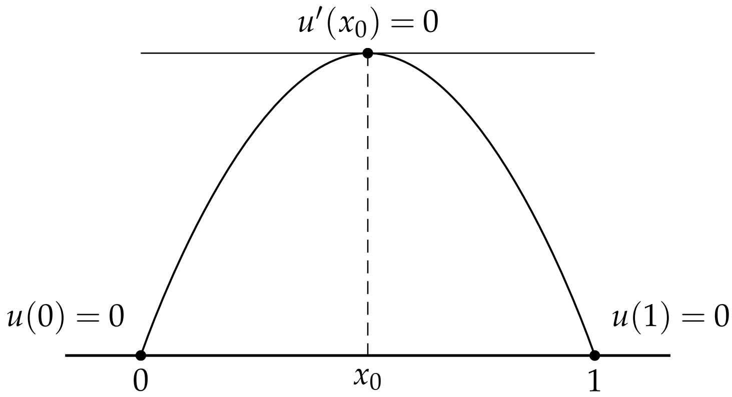

Figure 2.2: Rolle's theorem for PDE (2.8).

First, we check the boundary conditions:

$$\begin{aligned} u^+(0) &= \frac{1}{2} - \left|\frac{1}{2} - 0\right| \\ &= \frac{1}{2} - \frac{1}{2} \\ &= 0, \\ u^+(1) &= \frac{1}{2} - \left|\frac{1}{2} - 1\right| \\ &= \frac{1}{2} - \frac{1}{2} \\ &= 0. \end{aligned}$$

Second, we consider the case when $0 < x < \frac{1}{2}$. In this case, we receive $\left|\frac{1}{2} - x\right| = \left(\frac{1}{2} - x\right)$. Therefore, $u^+(x) = \frac{1}{2} - \left|\frac{1}{2} - x\right|$ becomes

$$\begin{aligned} u^+(x) &= \frac{1}{2} - \left|\frac{1}{2} - x\right| \\ &= \frac{1}{2} - \left(\frac{1}{2} - x\right) \\ &= x. \end{aligned}$$

Since $u^+(x) \to 0$ as $x \to 0$, we have $u^+(x) = x$ when $0 \le x < \frac{1}{2}$.

Next, we treat the case when $\frac{1}{2} \le x < 1$. In this case, we have $\left|\frac{1}{2} - x\right| = -\left(\frac{1}{2} - x\right)$. Thus,

$u^+(x) = \frac{1}{2} - \left|\frac{1}{2} - x\right|$ becomes

$$
\begin{aligned}
u^+(x) &= \frac{1}{2} - \left|\frac{1}{2} - x\right| \\
&= \frac{1}{2} + \left(\frac{1}{2} - x\right) \\
&= 1 - x.
\end{aligned}
$$

Extending the considered domain to $\frac{1}{2} \leq x \leq 1$, we also obtain $u^+(x) = 1 - x$, because $u^+(x) \to 0$ as $x \to 1$.

So, $u^+(x)$ has the form in the whole interval $[0, 1]$

$$
u^+(x) = \begin{cases} x & \text{if} \quad 0 \leq x < \dfrac{1}{2}, \\ 1 - x & \text{if} \quad \dfrac{1}{2} \leq x \leq 1, \end{cases} \tag{2.9}
$$

which can be seen in Figure 2.3. Now, we can clearly see that $u^+(x)$ has a slope 1 when $0 \leq x < \frac{1}{2}$ and slope -1 when $\frac{1}{2} < x \leq 1$, which indicates that $u^+(x)$ is a solution to the (2.8) except the point $x = \frac{1}{2}$. The point to be stressed out here is that the situation is delicate when $x = \frac{1}{2}$, since at this point $u^+(x)$ is not differentiable. That's why $u^+(x)$ is referred to as the solution which holds *almost everywhere* (a.e.), which implies in this case excluding the point where the function is not differentiable. The treatment of this problem will be more carefully handled in Section 2.3.2.

In the same way as we treated $u^+(x)$ above, we can also verify that $u^-(x) = -u^+(x)$ is a solution to (2.8) at the same time. In fact, for the equation (2.8) there are an infinite number of solutions of the form [11]:

$$
\begin{cases}
u_n(0) & = 0, \\
u_n(1) & = 0, \\
u_n'(x) & = 1 \quad \text{if} \quad x \in \left]\dfrac{2k}{2^n}, \dfrac{2k+1}{2^n}\right[, \qquad k = 0, \ldots, 2^n - 1, \\
u_n'(x) & = -1 \quad \text{if} \quad x \in \left]\dfrac{2k+1}{2^n}, \dfrac{2k+2}{2^n}\right[, \qquad k = 0, \ldots, 2^n - 1,
\end{cases} \tag{2.10}
$$

where $n \in \mathbb{N}$, which we can see in the Figure 2.3. Notice that $u^+(x)$ is the largest solution of (2.8) in a pointwise sense and $u^-(x)$ is the smallest one.

Another problem that we can notice is that 0 is not a solution of 2.8, although $u_n(x) \to 0$ uniformly when $n \to +\infty$.

Considering the given circumstances, we need clearly another strategy to deal with these difficulties.

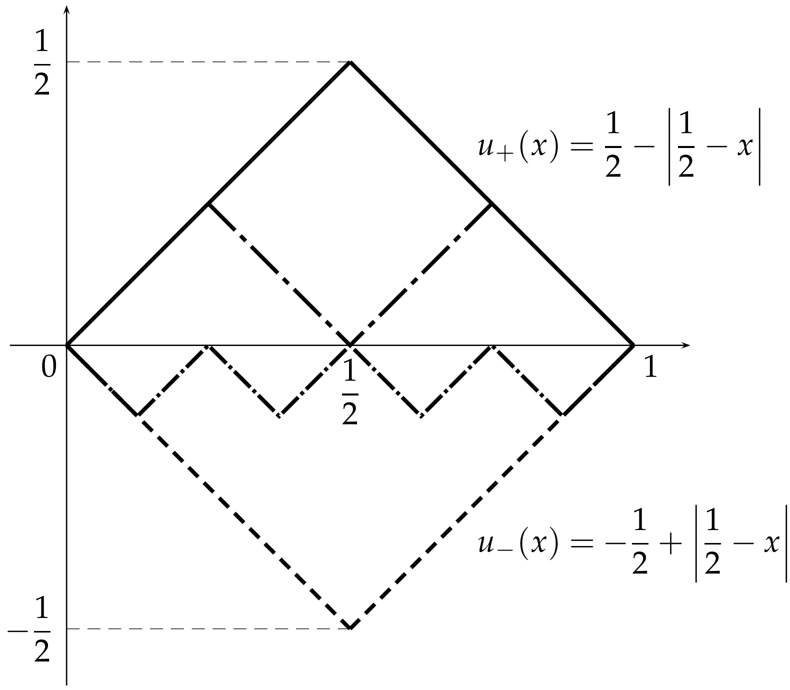

Figure 2.3: Examples of admissible solutions of a one-dimensional eikonal equation. Adapted from [11].

2.3.2 Viscosity Solutions

For the matter of viscosity solutions, we start with giving a brief history about solving a HJE in the sense of well-posedness. Then, we investigate the definitions of viscosity solutions in detail. This shows us how they are applied and helpful in the one-dimensional eikonal equation with which we have already encountered problems with the classical method.

Brief History

As we have already seen in the one-dimenstional eikonal equation problem, it is well known that a HJE is in general ill-posed. In early 1980s, the theory of viscosity solutions was introduced by Michael G. Crandall and Pierre-Louis Lions in [22, 23] for giving us useful mathematical tools to overcome the previously mentioned inherent ill-posed properties of the given HJE. However, before that another effort was already made and the way was paved by the Russian mathematician S. N. Kružkov. In 1975, he proposed a concept of generalised solutions of eikonal-type HJEs[2] in [99]. In the work [100] it was shown that he also put a further, physically meaningful constraint to receive existence

[2]eikonal-type HJE means that the hamiltonian $H(x, u, \nabla u)$ is independent of u and only depends on ∇u.

and uniqueness property of solutions. Although the mathematical details between viscosity solutions by Michael G. Crandall and Pierre-Louis Lions and generalised solutions by S. N. Kružkov are different, the basic idea of both theories is the same in the sense that they all want to turn an ill-posed HJE into a well-posed one by imposing some constraints on the problems.

As we have encountered several problems with the one-dimensional eikonal equation in the previous section, we pay more our attention to the eikonal-type HJE with the help of the viscosity theory rather than the general one. For more details and mathematical rigourousness about generalised theory, we refer to [22, 23, 34, 60, 66, 67, 69] and the references therein.

We present here two definitions of viscosity solutions which can be found in [12, 67]. One is defined making use of a test function $\varphi \in C^1$, and the other one uses super- and subdifferential. As the super- and subdifferential characterise the nondifferentiable local maxima and minima, both definitions are equivalent, which is proved in [12].

The point to be stressed for the viscosity solutions is that the solution u need not be everywhere differentiable. It may happen that the derivative Du does not exist, as e.g. in the case of $|x|$. Even if the derivative Du does not exist at some point, the super- and subdifferential are defined at that point and take the place of the derivative, which makes u only belong to C^0. Notice that, specially the notion of the subdifferential is also extensively investigated in the convex analysis literature such as [42–44, 94].

For the given Hamilton-Jacobi equation with DBC:

$$\begin{cases} H(x, \nabla u(x)) = 0 & \text{in } \Omega \\ u(x) = \varphi(x) & \text{on } \partial\Omega, \end{cases} \tag{2.11}$$

a continuous viscosity solution $u \in C^0$ of an equation (2.11) is defined as follows.

Definition 2.3.1 (Continuous Viscosity Solution I). A continuous function $u \in C^0$ is a viscosity solution of the equation (2.11) if the following conditions are satisfied:

(i) **(Viscosity subsolution)** For any test function $\varphi \in C^1(\Omega)$, if $x_0 \in \Omega$ is a local maximum point for $(u - \varphi)$, then

$$H(x_0, \nabla\varphi(x_0)) \leq 0 \tag{2.12}$$

(ii) **(Viscosity supersolution)** For any test function $\varphi \in C^1(\Omega)$, if $x_1 \in \Omega$ is a local minimum point for $(u - \varphi)$, then

$$H(x_1, \nabla\varphi(x_1)) \geq 0. \tag{2.13}$$

This is equivalent to:

Definition 2.3.2 (Continuous Viscosity Solution II). A continuous function $u \in C^0$ is a *viscosity solution* of the equation (2.11) if the following conditions are satisfied:

(i) **(Viscosity subsolution)** $H(x,p) \leq 0 \quad \forall\, x \in \mathbb{R}^n, \quad \forall p \in D^+u,$

(ii) **(Viscosity supersolution)** $H(x,q) \geq 0 \quad \forall\, x \in \mathbb{R}^n, \quad \forall q \in D^-u,$

where

$$D^+u(x) = \left\{ p \in \mathbb{R}^n : \limsup_{y \to x} \frac{u(y) - u(x) - p \cdot (y-x)}{|y-x|} \leq 0 \right\} \tag{2.14}$$

and

$$D^-u(x) = \left\{ q \in \mathbb{R}^n : \liminf_{y \to x} \frac{u(y) - u(x) - q \cdot (y-x)}{|y-x|} \geq 0 \right\}. \tag{2.15}$$

The sets $D^+u(x)$ and $D^-u(x)$ are called the *super-* and the *subdifferential* of u at x, respectively. In [12], the properties of these sets are collected in the following:

Lemma 2.3.1.

(i) $D^+u(x)$ and $D^-u(x)$ are closed convex (possibly empty) subsets of $\mathbb{R}^n$.

(ii) If u is differentiable at x, then

$$\{Du(x)\} = D^+u(x) = D^-u(x)\,. \tag{2.16}$$

(iii) If for some x both $D^+u(x)$ and $D^-u(x)$ are nonempty, then

$$\{Du(x)\} = D^+u(x) = D^-u(x)\,. \tag{2.17}$$

Remark 2.3.1. To understand the situation when u is nondifferentiable at x, propositional logic would be helpful. With the contraposition of the second property in Lemma 2.3.1 we are able to obtain

$$\begin{aligned} & (u \text{ is differentiable at } x) \Rightarrow \left(D^+u(x) = \{Du(x)\}\right) \wedge \left(D^-u(x) = \{Du(x)\}\right) \\ \Leftrightarrow\quad & \left(D^+u(x) \neq \{Du(x)\}\right) \vee \left(D^-u(x) \neq \{Du(x)\}\right) \Rightarrow \neg(u \text{ is differentiable at } x) \\ \Leftrightarrow\quad & \left(D^+u(x) \neq \{Du(x)\}\right) \vee \left(D^-u(x) \neq \{Du(x)\}\right) \Rightarrow (u \text{ is not differentiable at } x) \end{aligned}$$

This says that u is nondifferentiable at x if one of the super- or subdifferential of u is different from the derivative.

The last property of Lemma 2.3.1 basically tells us that the nondifferentiable points belong to only one set, i.e. they are either super- or subdifferentials, since the third statement in Lemma 2.3.1 can be formulated as follows:

$$\begin{aligned} & \left(D^+u(x) \neq \emptyset\right) \wedge \left(D^-u(x) \neq \emptyset\right) \Rightarrow \left(D^+u(x) = \{Du(x)\}\right) \wedge \left(D^-u(x) = \{Du(x)\}\right) \\ & \text{considering the contraposition of the above} \\ \Leftrightarrow\quad & \left(D^+u(x) \neq \{Du(x)\}\right) \vee \left(D^-u(x) \neq \{Du(x)\}\right) \Rightarrow \left(D^+u(x) = \emptyset\right) \vee \left(D^-u(x) = \emptyset\right). \end{aligned}$$

As mentioned above, one of super- or subdifferential of u at x is empty set if one of them are different from the derivative.

Therefore, with the second property of Lemma 2.17 nondifferentiable points cannot have the nonempty super- and subdifferential at the same time.

In [12] some algebraic properties on the super- and subdifferentials are given as follows.

Lemma 2.3.2.

(i) $D^{+}(\alpha u)(x) = \alpha D^{+}u(x)$ *if* $\alpha > 0$,

(ii) $D^{+}(\alpha u)(x) = \alpha D^{-}u(x)$ *if* $\alpha < 0$,

(iii) $D^{+}(u+\varphi)(x) = D^{+}u(x) + D\varphi(x)$ *if* $\varphi \in C^{1}(\Omega)$,

(iv) $D^{+}u_{\alpha}(x) = \alpha D^{+}u(x) + (1-\alpha) D\varphi(x)$ *if* $\varphi \in C^{1}(\Omega)$,

where $u_{\alpha}(x) := \alpha u(x) + (1-\alpha)\varphi(x)$ *with* $\alpha \in [0,1]$.

Now, we are in the position to realise that super- and subdifferential are the same as the classical derivative when the function is differentiable at a certain point. The only difference is made when the function is not differentiable. Whenever super- and subdifferential are not empty, according to the Definition 2.3.2, u is a *viscosity solution* of a HJE (2.11) if it is simultaneouly a viscosity sub- and supersolution. However, if we think of this situation by virtue of Lemma 2.3.1 and its remark, it occurs only when the points are differentiable. Otherwise, they have only one nonempty set from super- and subdifferential and the other set is empty, which implies that there exists only viscosity super- or subsolution.

After we have a look how the sub- and superdifferential are determined for the non-differentiable points of the function $|x|$, we shall apply Definition 2.3.2 to the one-dimensional eikonal equation, so that we can make this concept more clear.

In order to understand the Definition 2.3.2, let us first review the notions of subdifferential for the one-dimensional function $u(x) = |x|$ that we have already seen in convex analysis [42–44, 94].

Example 2.3.1 (Subdifferential of $|x|$)**.**

Since $u(x) = |x| = \begin{cases} x & \text{if } x \geq 0, \\ -x & \text{if } x < 0, \end{cases}$ we investigate this case by case as follows. We begin the case distinction with $x = 0$.

I. $x = 0$

(i) $y \geq 0$

$$\begin{aligned} & \liminf_{y \to x} \frac{u(y) - u(x) - q\,(y - x)}{|y - x|} \geq 0 \\ \Leftrightarrow \quad & \liminf_{y \to x} \frac{y - qy}{y} \geq 0 \\ \Leftrightarrow \quad & \liminf_{y \to x} \frac{(1 - q)\,y}{y} \geq 0 \\ \Leftrightarrow \quad & 1 - q \geq 0 \\ \Leftrightarrow \quad & q \leq 1 \end{aligned}$$

(ii) $y < 0$

$$\begin{aligned} & \liminf_{y \to x} \frac{u(y) - u(x) - q\,(y - x)}{|y - x|} \geq 0 \\ \Leftrightarrow \quad & \liminf_{y \to x} \frac{-y - qy}{-y} \geq 0 \\ \Leftrightarrow \quad & \liminf_{y \to x} \frac{-\,(1 + q)\,y}{-y} \geq 0 \\ \Leftrightarrow \quad & 1 + q \geq 0 \\ \Leftrightarrow \quad & q \geq -1 \end{aligned}$$

Hence, we receive the subdifferential $q \in [-1,1]$ when $x = 0$.

II. $x > 0$

(i) $x > 0, y > 0$

(a) $y > x > 0 \quad \Leftrightarrow \quad y - x > 0$

$$\begin{aligned} & \liminf_{y \to x} \frac{u(y) - u(x) - q\,(y - x)}{|y - x|} \geq 0 \\ \Leftrightarrow \quad & \liminf_{y \to x} \frac{(y - x) - q\,(y - x)}{(y - x)} \geq 0 \\ \Leftrightarrow \quad & \liminf_{y \to x} \frac{(1 - q)\,(y - x)}{(y - x)} \geq 0 \\ \Leftrightarrow \quad & 1 - q \geq 0 \\ \Leftrightarrow \quad & q \leq 1 \end{aligned}$$

(b) $x > y > 0 \quad \Leftrightarrow \quad y - x < 0 \quad \Leftrightarrow \quad -(y-x) > 0$

$$\begin{aligned}
&\liminf_{y \to x} \frac{u(y) - u(x) - q\,(y-x)}{|y-x|} \geq 0 \\
\Leftrightarrow\quad &\liminf_{y \to x} \frac{(y-x) - q\,(y-x)}{-(y-x)} \geq 0 \\
\Leftrightarrow\quad &\liminf_{y \to x} \frac{(1-q)\,(y-x)}{-(y-x)} \geq 0 \\
\Leftrightarrow\quad &-(1-q) \geq 0 \\
\Leftrightarrow\quad &1 - q \leq 0 \\
\Leftrightarrow\quad &q \geq 1
\end{aligned}$$

(ii) $x > 0, y < 0$

$$\begin{aligned}
&\liminf_{y \to x} \frac{u(y) - u(x) - q\,(y-x)}{|y-x|} \geq 0 \\
\Leftrightarrow\quad &\liminf_{y \to x} \frac{(-y-x) - q\,(y-x)}{-(y-x)} \geq 0 \\
\Leftrightarrow\quad &\liminf_{y \to x} \frac{-(1+q)\,y + (q-1)\,x}{-(y-x)} \geq 0 \\
\Leftrightarrow\quad &(q-1)\underbrace{x}_{>0} \geq (1+q)\underbrace{y}_{<0} \\
\Leftrightarrow\quad &(q - 1 \geq 0) \ \wedge \ (1 + q \geq 0) \\
\Leftrightarrow\quad &(q \geq 1) \ \wedge \ (q \geq -1) \\
\Leftrightarrow\quad &q \geq 1
\end{aligned}$$

Therefore, considering all the cases when $x > 0$, we receive the subdifferential $q = \{1\}$ for $u(x) = |x|$. Next, let us move on to the next case when $x < 0$.

III. $x < 0$

(i) $x < 0, y < 0$

(a) $y < x < 0 \quad \Leftrightarrow \quad y - x < 0 \quad \Leftrightarrow \quad -(y-x) > 0$

$$\begin{aligned}
& \liminf_{y\to x} \frac{u(y) - u(x) - q\,(y-x)}{|y-x|} \geq 0 \\
\Leftrightarrow \quad & \liminf_{y\to x} \frac{(-y+x) - q\,(y-x)}{-\,(y-x)} \geq 0 \\
\Leftrightarrow \quad & \liminf_{y\to x} \frac{-\,(1+q)\,(y-x)}{-\,(y-x)} \geq 0 \\
\Leftrightarrow \quad & 1 + q \geq 0 \\
\Leftrightarrow \quad & q \geq -1
\end{aligned}$$

(b) $x < y < 0 \quad \Leftrightarrow \quad y - x > 0$

$$\begin{aligned}
& \liminf_{y\to x} \frac{u(y) - u(x) - q\,(y-x)}{|y-x|} \geq 0 \\
\Leftrightarrow \quad & \liminf_{y\to x} \frac{(-y+x) - q\,(y-x)}{(y-x)} \geq 0 \\
\Leftrightarrow \quad & \liminf_{y\to x} \frac{-\,(1+q)\,(y-x)}{(y-x)} \geq 0 \\
\Leftrightarrow \quad & -\,(1+q) \geq 0 \\
\Leftrightarrow \quad & (1+q) \leq 0 \\
\Leftrightarrow \quad & q \leq -1
\end{aligned}$$

(ii) $x < 0, y > 0$

$$\begin{aligned}
& \liminf_{y\to x} \frac{u(y) - u(x) - q\,(y-x)}{|y-x|} \geq 0 \\
\Leftrightarrow \quad & \liminf_{y\to x} \frac{(y+x) - q\,(y-x)}{(y-x)} \geq 0 \\
\Leftrightarrow \quad & \liminf_{y\to x} \frac{(1-q)\,y + (1+q)\,x}{(y-x)} \geq 0 \\
\Leftrightarrow \quad & (1-q)\,\underbrace{y}_{>0} \geq (1+q)\,\underbrace{(-x)}_{>0} \\
\Leftrightarrow \quad & (1 - q \geq 0) \ \wedge \ (1 + q \leq 0) \\
\Leftrightarrow \quad & (1 \geq q) \ \wedge \ (q \leq -1) \\
\Leftrightarrow \quad & q \leq -1
\end{aligned}$$

Thus, taking all the cases above into account when $x < 0$, we receive subdifferential $q = \{-1\}$ for $u(x) = |x|$.

So, the result of Example 2.3.1 enables us to formulate the subdifferential of the function $u(x) = |x|$ depending on x as follows, see Figure 2.4.

$$D^{-}u(x) = \begin{cases} -1 & \text{if } x < 0, \\ [-1, 1] & \text{if } x = 0, \\ 1 & \text{if } x > 0. \end{cases} \tag{2.18}$$

As we did for the subdifferential, this time we proceed to the superdifferential of $|x|$. First we take care of the case when $x = 0$.

Example 2.3.2 (Superdifferential of $|x|$)**.**

I. $x = 0$

(i) $y \geq 0$

$$\begin{aligned} & \limsup_{y \to x} \frac{u(y) - u(x) - p(y - x)}{|y - x|} \leq 0 \\ \Leftrightarrow \quad & \limsup_{y \to x} \frac{y - py}{y} \leq 0 \\ \Leftrightarrow \quad & \limsup_{y \to x} \frac{(1 - p)y}{y} \leq 0 \\ \Leftrightarrow \quad & 1 - p \leq 0 \\ \Leftrightarrow \quad & p \geq 1 \end{aligned}$$

(ii) $y < 0$

$$\begin{aligned} & \limsup_{y \to x} \frac{u(y) - u(x) - p(y - x)}{|y - x|} \leq 0 \\ \Leftrightarrow \quad & \limsup_{y \to x} \frac{-y - py}{-y} \leq 0 \\ \Leftrightarrow \quad & \limsup_{y \to x} \frac{-(1 + p)y}{-y} \leq 0 \\ \Leftrightarrow \quad & 1 + p \leq 0 \\ \Leftrightarrow \quad & p \leq -1 \end{aligned}$$

Hence, we receive the superdifferential $p = \emptyset$ when $x = 0$.

II. $x > 0$

(i) $x > 0, y > 0$

(a) $y > x > 0 \quad \Leftrightarrow \quad y - x > 0$

$$\begin{aligned} & \limsup_{y \to x} \frac{u(y) - u(x) - p\,(y - x)}{|y - x|} \leq 0 \\ \Leftrightarrow \quad & \limsup_{y \to x} \frac{(y - x) - p\,(y - x)}{(y - x)} \leq 0 \\ \Leftrightarrow \quad & \limsup_{y \to x} \frac{(1 - p)\,(y - x)}{(y - x)} \leq 0 \\ \Leftrightarrow \quad & 1 - p \leq 0 \\ \Leftrightarrow \quad & p \geq 1 \end{aligned}$$

(b) $x > y > 0 \quad \Leftrightarrow \quad y - x < 0 \quad \Leftrightarrow \quad -(y - x) > 0$

$$\begin{aligned} & \limsup_{y \to x} \frac{u(y) - u(x) - p\,(y - x)}{|y - x|} \leq 0 \\ \Leftrightarrow \quad & \limsup_{y \to x} \frac{(y - x) - p\,(y - x)}{-(y - x)} \leq 0 \\ \Leftrightarrow \quad & \limsup_{y \to x} \frac{(1 - p)\,(y - x)}{-(y - x)} \leq 0 \\ \Leftrightarrow \quad & -(1 - p) \leq 0 \\ \Leftrightarrow \quad & 1 - p \geq 0 \\ \Leftrightarrow \quad & p \leq 1 \end{aligned}$$

Therefore, considering all the cases when $x > 0$, $y > 0$ we receive the superdifferential $p = \{1\}$ for $u(x) = |x|$. Next, let us move on to the case when $x > 0, y < 0$.

(c) $x > 0, y < 0$

$$\begin{aligned}
& \limsup_{y \to x} \frac{u(y) - u(x) - p\,(y - x)}{|y - x|} \leq 0 \\
\Leftrightarrow \quad & \limsup_{y \to x} \frac{(-y - x) - p\,(y - x)}{-\,(y - x)} \leq 0 \\
\Leftrightarrow \quad & \limsup_{y \to x} \frac{-\,(1 + p)\,y + (p - 1)\,x}{-\,(y - x)} \leq 0 \\
\Leftrightarrow \quad & (1 + p)\,\underbrace{(-y)}_{>0} \leq (1 - p)\,\underbrace{x}_{>0} \\
\Leftrightarrow \quad & (1 + p \leq 0) \ \wedge \ (1 - p \geq 0) \\
\Leftrightarrow \quad & p \leq -1
\end{aligned}$$

This case describes the situation when $y < 0$ crosses over the point 0 and approaches $x > 0$. However, there is no solution set which satisfies this condition since $\{p\,|(p \geq 1) \cap (p \leq 1) \cap (p \leq -1)\} = \emptyset$. The reason is that there is no superdifferential at $x = 0$.

Therefore, considering all the cases when $x > 0$, we receive the superdifferential $p = \{1\}$ for $u(x) = |x|$ only when $y > 0$. Next, let us move on to the case when $x < 0$.

III. $x < 0$

(i) $x < 0, y < 0$

(a) $y < x < 0 \quad \Leftrightarrow \quad y - x < 0 \quad \Leftrightarrow \quad -\,(y - x) > 0$

$$\begin{aligned}
& \limsup_{y \to x} \frac{u(y) - u(x) - p\,(y - x)}{|y - x|} \leq 0 \\
\Leftrightarrow \quad & \limsup_{y \to x} \frac{(-y + x) - p\,(y - x)}{-\,(y - x)} \leq 0 \\
\Leftrightarrow \quad & \limsup_{y \to x} \frac{-\,(1 + p)\,(y - x)}{-\,(y - x)} \leq 0 \\
\Leftrightarrow \quad & 1 + p \leq 0 \\
\Leftrightarrow \quad & p \leq -1
\end{aligned}$$

(b) $x < y < 0 \quad \Leftrightarrow \quad y - x > 0$

$$\begin{aligned}
&\limsup_{y\to x} \frac{u(y)-u(x)-p\,(y-x)}{|y-x|} \leq 0 \\
\Leftrightarrow\quad &\limsup_{y\to x} \frac{(-y+x)-p\,(y-x)}{(y-x)} \leq 0 \\
\Leftrightarrow\quad &\limsup_{y\to x} \frac{-\,(1+p)\,(y-x)}{(y-x)} \leq 0 \\
\Leftrightarrow\quad &-\,(1+p) \leq 0 \\
\Leftrightarrow\quad &(1+p) \geq 0 \\
\Leftrightarrow\quad &p \geq -1
\end{aligned}$$

Thus, taking all the cases above into account when $x < 0, y < 0$ we receive the superdifferential $p = \{-1\}$ for $u(x) = |x|$.

(ii) $x < 0, y > 0$

$$\begin{aligned}
&\limsup_{y\to x} \frac{u(y)-u(x)-p\,(y-x)}{|y-x|} \leq 0 \\
\Leftrightarrow\quad &\limsup_{y\to x} \frac{(y+x)-p\,(y-x)}{(y-x)} \leq 0 \\
\Leftrightarrow\quad &\limsup_{y\to x} \frac{(1-p)\,y+(p+1)\,x}{(y-x)} \leq 0 \\
\Leftrightarrow\quad &(p+1)\underbrace{x}_{<0} \leq (p-1)\underbrace{y}_{>0} \\
\Leftrightarrow\quad &(p+1 \geq 0)\ \wedge\ (p-1 \geq 0) \\
\Leftrightarrow\quad &p \geq 1
\end{aligned}$$

This case is similar as that of $x > 0$, $y < 0$. So, there is no solution set which satisfies this condition since $\{p\,|\,(p \geq -1) \cap (p \leq -1) \cap (p \geq 1)\} = \emptyset$.

Therefore, considering all the cases when $x < 0$, we receive the superdifferential $p = \{-1\}$ for $u(x) = |x|$ only when $y < 0$.

Based on the result of Example 2.3.2, we can write the superdifferential of the function $u(x) = |x|$ depending on x as follows.

$$D^+u(x) = \begin{cases} -1 & \text{if } x < 0, \\ \emptyset & \text{if } x = 0, \\ 1 & \text{if } x > 0. \end{cases} \tag{2.19}$$

As we can see in Figure 2.4, the subdifferential of a convex function $|x|$ is actually not different from the slope of function $|x|$, when the function is differentiable. The only difference is made when the function is not differentiable.

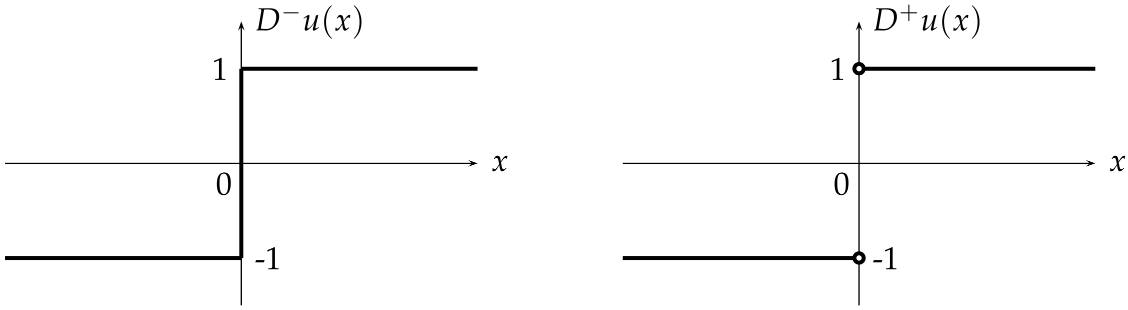

(a) Subdifferential $D^{-}u(x)$ of $u(x) = |x|$.

(b) Superdifferential $D^{+}u(x)$ of $u(x) = |x|$.

Figure 2.4: Sub- and superdifferential of a convex function $u(x) = |x|$.

Analogously, the super- and subdifferential of concave function $u(x) = -|x|$ can be obtained as follow. For the superdifferential of $-|x|$, we have

$$D^{+}u(x) = \begin{cases} 1 & \text{if } x < 0, \\ [-1,1] & \text{if } x = 0, \\ -1 & \text{if } x > 0. \end{cases} \tag{2.20}$$

As a subdifferential of $-|x|$, we receive

$$D^{-}u(x) = \begin{cases} 1 & \text{if } x < 0, \\ \emptyset & \text{if } x = 0, \\ -1 & \text{if } x > 0. \end{cases} \tag{2.21}$$

It turns out that the super- and subdifferential of concave function $-|x|$ just exchange the roles of sub- and superdifferential of the convex function $|x|$ as can be seen in Figure 2.5.

Using these results, let us find the solution $u \in C^0$ of the following one-dimensional eikonal-type HJE equipped with DBC in the viscosity sense:

$$\begin{cases} |\nabla u(x)| & = & 1, & x \in (-1,1), \\ u(x) & = & 0, & x \in \{-1,1\}. \end{cases} \tag{2.22}$$

We begin with the convex Hamiltonian $H(x,p) = |p| - 1$ for this problem, where p denotes $\nabla u(x)$. As we have already seen in the problem (2.8), we have an existence result

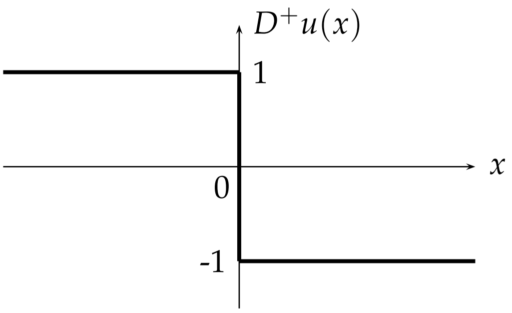

(a) Superdifferential $D^+u(x)$ of $u(x) = -|x|$.

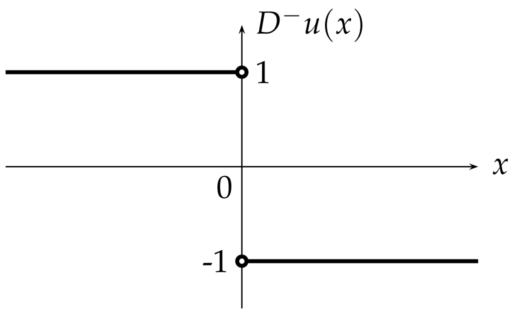

(b) Subdifferential $D^-u(x)$ of $u(x) = -|x|$.

Figure 2.5: Super- and subdifferential of a concave function $u(x) = -|x|$.

by expanding our solution space from C^1 to C^0, and there are infinitely many possible solutions belonging to C^0 for this problem. The solution candidates can be seen in Figure 2.6b. However, the only "viscosity solution" for this problem with the Hamiltonian $H(x,p) = |p| - 1$ turns out to be $u_{c_+}(x) = 1 - |x|$ and we verify that in the following. To this end, we pay special attention to the treatment for nondifferentiable points using sub- and superdifferential, which enables us to single out a solution.

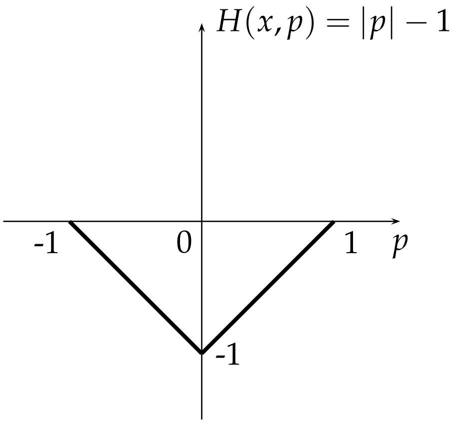

(a) Convex Hamiltonian $H(x,p) = |p| - 1$.

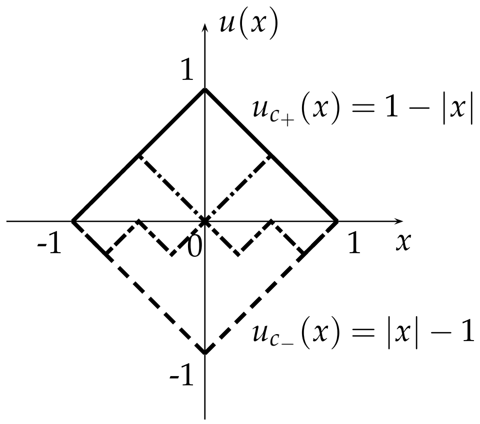

(b) Solution candidates for $H(x,p) = |p| - 1$.

Figure 2.6: One-dimensional convex Hamiltonian $H(x,p) = |p| - 1$ and solution candidates, where p denotes $\nabla u(x)$.

Since the super- and subdifferential of the function $u_{c+} = 1 - |x|$ is the same as those of

$-|x|$, we have the superdifferential $D^+u_{c_+}(x)$ of $u_{c+} = 1 - |x|$

$$D^+u_{c_+}(x) = \begin{cases} 1 & \text{if } x < 0, \\ \{p : |p| \leq 1\} & \text{if } x = 0, \\ -1 & \text{if } x > 0, \end{cases} \tag{2.23}$$

and as a subdifferential $D^-u_{c_+}(x)$ of $u_{c+} = 1 - |x|$, we receive

$$D^-u_{c_+}(x) = \begin{cases} 1 & \text{if } x < 0, \\ \emptyset & \text{if } x = 0, \\ -1 & \text{if } x > 0. \end{cases} \tag{2.24}$$

Now, we check whether $u_{c+} = 1 - |x|$ fulfils both viscosity sub- and supersolution conditions in Definition 2.3.2.

Since $u_{c+} = 1 - |x|$ satisfies $H(x, D^+u_{c_+}(x)) = |p| - 1 \leq 0$ by (2.23), so that $u_{c+} = 1 - |x|$ is a viscosity subsolution. Since the subdifferential $D^-u_{c_+}(x)$ is the empty set, we need not to take care of this case. Therefore, $u_{c+} = 1 - |x|$ is a viscosity solution for the HJE (2.22) with the Hamiltonian $H(x, p) = |p| - 1$.

How about the other solution candidates in Figure 2.6b? Let us try with $u_{c_-}(x) = |x| - 1$. Since sub- and superdifferential of $u_{c_-}(x) = |x| - 1$ are the same as those of $|x|$, we have the superdifferential $D^+u_{c_-}(x)$ of $u_{c-} = |x| - 1$

$$D^+u_{c_-}(x) = \begin{cases} -1 & \text{if } x < 0, \\ \emptyset & \text{if } x = 0, \\ 1 & \text{if } x > 0, \end{cases} \tag{2.25}$$

and as a subdifferential $D^-u_{c_-}(x)$ of $u_{c_-}(x) = |x| - 1$, we receive

$$D^-u_{c_-}(x) = \begin{cases} -1 & \text{if } x < 0, \\ \{p : |p| \leq 1\} & \text{if } x = 0, \\ 1 & \text{if } x > 0. \end{cases} \tag{2.26}$$

In a similar way, this time we test whether $u_{c_-}(x) = |x| - 1$ fulfils both the viscosity super- and subsolution requirements.

Since the superdifferential is the empty set, we don't need to treat this case. Plugging the subdifferential $D^-u_{c_-}(x)$ into the Hamiltonian $H(x, p) = |p| - 1$ yields $H(x, D^-u_{c_-}(x)) = |p| - 1 \leq 0$ by (2.26), which does not satisfy the viscosity supersolution condition. Thus, $u_{c-} = |x| - 1$ is not accepted as a viscosity solution for the HJE (2.22) with the Hamiltonian $H(x, p) = |p| - 1$. This can be interpreted as follows.

The one-dimensional convex Hamiltonian $H(x,p) = |p| - 1$ of HJE (2.22) does not admit the solution which has local minima at the nondifferentiable points by the viscosity supersolution criterion, which suggests that every other solution candidate (dashed lines in Figure 2.6b) except $u_{c_+}(x) = 1 - |x|$ can be filtered out by the viscosity supersolution criteria. Hence, this process makes $u_{c_+}(x) = 1 - |x|$ the unique viscosity solution for the given HJE (2.22), which can be seen in Figure 2.7b.

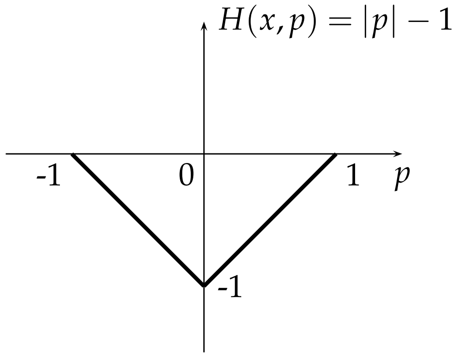

(a) Convex Hamiltonian $H(x,p) = |p| - 1$.

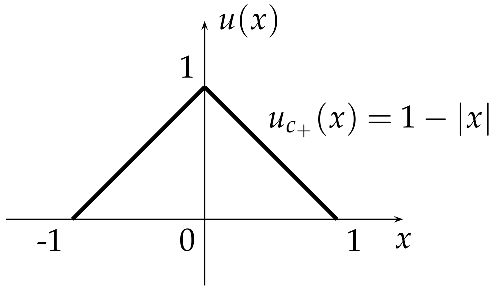

(b) Viscosity solution of $H(x,p) = |p| - 1$.

Figure 2.7: One-dimensional convex Hamiltonian $H(x,p) = |p| - 1$ and a viscosity solution, where p denotes $\nabla u(x)$.

What happens if we use non-convex Hamiltonian $H(x,p) = 1 - |p|$ for the same HJE (2.22)? Following the same procedure as in the convex Hamiltonian case, we obtain a different viscosity solution $u_{c_-}(x) = |x| - 1$ which is convex, see Figure 2.8b. This is not a surprising fact comparing to the convex Hamiltonian case that we have already seen in Figure 2.7.

Therefore, a striking difference between a viscosity solution and a classical one to be pointed out here is that viscosity solutions are not preserved by changing of the sign in the equation, which can be seen by comparing the Figure 2.7 with the Figure 2.8. In other words, a viscosity solution for the given problem does not depend on the given HJE itself but on the type of Hamiltonian that we choose for the given problem.

2.4 Legendre Transform

We begin with a question where the Legendre transform comes from by considering a differentiable function, being in addition an invertible mapping. Afterwards, we shall see how it is extended when the function has nondifferentiable points and the mapping is not unique. Then, the coercivity of a function will be discussed as well.

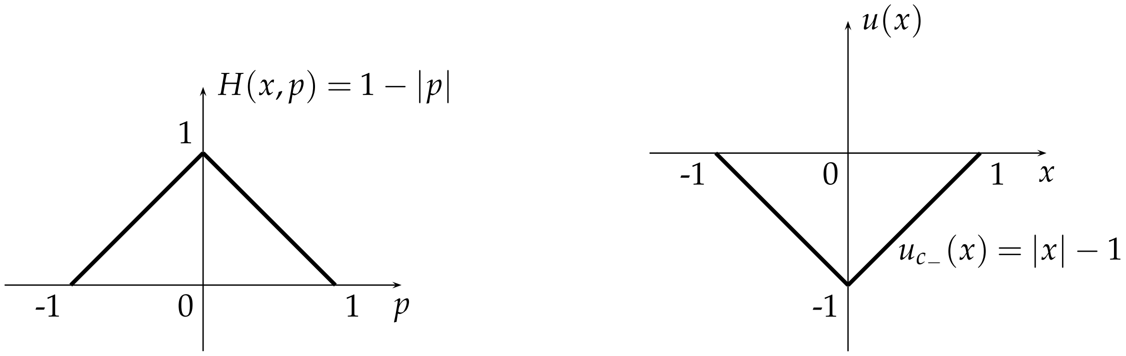

(a) Non-Convex Hamiltonian $H(x,p) = 1 - |p|$. (b) Viscosity solution of $H(x,p) = 1 - |p|$.

Figure 2.8: One-dimensional non-convex Hamiltonian $H(x,p) = 1 - |p|$ and a viscosity solution, where p denotes $\nabla u(x)$.

2.4.1 Classical Definition

In classical real analysis, the gradient of a differentiable function $f : \mathbb{R}^n \to \mathbb{R}$ plays a key role as a first optimality condition in order to find extrema. Let us consider this gradient as a mapping. Since

$$f : \mathbb{R}^n \to \mathbb{R}, \tag{2.27}$$

and a gradient ∇ has influence on f, a gradient mapping can be understood as

$$\nabla f : \mathbb{R}^n \xrightarrow{f} \mathbb{R} \xrightarrow{\nabla} \mathbb{R}^n. \tag{2.28}$$

At this point, what we are really interested in its inverse mapping $(\nabla f)^{-1}$. Namely, our concern is to find x satisfying the condition $s = \nabla f(x)$ when $s \in S$ is given. By virtue of (2.28) this can be described as

$$\left\{ \begin{array}{lccccc} \nabla f(x) : & x \in \mathbb{R}^n & \xrightarrow{f} & f(x) \in \mathbb{R} & \xrightarrow{\nabla} & \nabla f(x) \in \mathbb{R}^n \\ (\nabla f)^{-1}(s) : & f^{-1}\nabla^{-1}(s) \in \mathbb{R}^n & \xleftarrow[f^{-1}]{} & \nabla^{-1}(s) \in \mathbb{R} & \xleftarrow[\nabla^{-1}]{} & s \in \mathbb{R}^n. \end{array} \right. \tag{2.29}$$

Since it turns out that the inverse mapping $x(s) = (\nabla f)^{-1}(s)$ itself is also a gradient mapping, by renaming ∇^{-1} and f^{-1} as h and ∇ respectively, we can reformulate (2.29) as follows

$$\begin{array}{rlccccc} & (\nabla f)^{-1}(s) : & s \in \mathbb{R}^n & \xrightarrow{\nabla^{-1}} & \nabla^{-1}(s) \in \mathbb{R} & \xrightarrow{f^{-1}} & f^{-1}\nabla^{-1}(s) \in \mathbb{R}^n \\ \Leftrightarrow & \nabla h(s) : & s \in \mathbb{R}^n & \xrightarrow{h} & h(s) \in \mathbb{R} & \xrightarrow{\nabla} & \nabla h(s) \in \mathbb{R}^n. \end{array} \tag{2.30}$$

Sometimes the above inverse process does not make sense, because not every mapping is invertible. Therefore, we make this problem meaningful by assuming that such x exists and is unique. The natural choice for this setup is to pick up a smooth and strictly convex function. Since ∇f and ∇h are inverse to each other by the construction in (2.29) and (2.30), this makes the following reciprocal correspondence valid

$$\begin{aligned} & s && = && \nabla f(x) \\ \Leftrightarrow\quad & (\nabla f)^{-1}(s) && = && (\nabla f)^{-1}(\nabla f)(x) \\ \Leftrightarrow\quad & (\nabla f)^{-1}(s) && = && x \\ \overset{(2.30)}{\Leftrightarrow}\quad & \nabla h(s) && = && x\,. \end{aligned} \tag{2.31}$$

Now, let us think about this situation in a one-dimensional case.

For a given function $f = f(x)$ with the differential

$$\frac{df}{dx} = s\,, \tag{2.32}$$

our task is to find a function $h = h(s)$ satisfying (2.30), which means

$$\frac{dh}{ds} = x\,. \tag{2.33}$$

This can be done as follows.

From (2.32) we can deduce

$$\begin{aligned} & \frac{df}{dx} && = && s \\ \Leftrightarrow\quad & df && = && s\,dx \\ & && && \text{by product rule: } d(sx) = s\,dx + x\,ds \\ & && = && d(sx) - x\,ds \\ \Leftrightarrow\quad & d(f - sx) && = && -x\,ds \\ \Leftrightarrow\quad & d(sx - f) && = && x\,ds \\ \Leftrightarrow\quad & \frac{d}{ds}\underbrace{(sx - f)}_{\overset{(2.33)}{=} h} && = && x\,. \end{aligned} \tag{2.34}$$

Therefore, when the function f is differentiable and every mapping in (2.29) is invertible, the *classical Legendre transform* is naturally defined by

Definition 2.4.1 (Classical Legendre Transform).

$$S \ni s \mapsto h(s) = \langle s, x(s) \rangle - f(x(s)), \tag{2.35}$$

where $h : S \subset \mathbb{R}^n \rightarrow \mathbb{R}$ and $\langle \cdot, \cdot \rangle$ denotes the scalar product. This definition also makes the following statement vaild

$$f(x) + h(s) = \langle s, x \rangle. \tag{2.36}$$

At this point, one may raise a question, why man does not define a Legendre transform simply by exchanging the roles between x and s as we have seen in (2.31), because what we are looking for is just inverse. However, this approach makes trouble in backtransform. Let us make this clear with following example.

Assume that the transform were defined as

$$\begin{array}{rcl} \dfrac{df}{dx} & = & s\,(x) \text{ : compute } s \text{ for a given } f \\ \Rightarrow \quad x & = & x\,(s) \text{ : compute the representaion of } x \text{ from above expression} \\ \Rightarrow \quad h\,(s) & = & f\,[x\,(s)] \text{ : plug this } x \text{ into the original function } f. \end{array} \tag{2.37}$$

Now, we transform two functions $f_1(x) = x^2$ and $f_2(x) = (x+c)^2$ with $c \neq 0$ according to (2.37). This yields

$$\begin{array}{l} \left\{ \begin{array}{lllll} s & = & \dfrac{df_1}{dx} & = & 2x \\ s & = & \dfrac{df_2}{dx} & = & 2\,(x+c) \end{array} \right. \\ \Rightarrow \left\{ \begin{array}{lll} x & = & \dfrac{s}{2} \\ x & = & \dfrac{s}{2} - c \end{array} \right. \\ \Rightarrow \left\{ \begin{array}{lllllll} h_1\,(s) & = & f_1\left(\dfrac{s}{2}\right) & = & \left(\dfrac{s}{2}\right)^2 & = & \dfrac{s^2}{4} \\ h_2\,(s) & = & f_2\left(\dfrac{s}{2} - c\right) & = & \left(\dfrac{s}{2} - c + c\right)^2 & = & \dfrac{s^2}{4}. \end{array} \right. \end{array} \tag{2.38}$$

As we can see in (2.38), we have same transform result for the two different functions, which makes problem in the backtransform.

In contrast to the above example, when we abide by the Definition 2.4.1 for the same functions f_1 and f_2, the Legendre transform of each function is unique, since

$$\left\{ \begin{array}{lllll} s & = & \dfrac{df_1}{dx} & = & 2x \\ s & = & \dfrac{df_2}{dx} & = & 2\,(x+c) \end{array} \right. \tag{2.39}$$

$$\Rightarrow \left\{ \begin{array}{lll} x & = & \dfrac{s}{2} \\ x & = & \dfrac{s}{2} - c \end{array} \right. \tag{2.40}$$

$$\Rightarrow \begin{cases} h_1(s) &= sx(s) - f_1(x(s)) \\ &= s\left(\frac{s}{2}\right) - f_1\left(\frac{s}{2}\right) \\ &= \left(\frac{s^2}{2}\right) - \left(\frac{s}{2}\right)^2 \\ &= \frac{s^2}{4} \\ h_2(s) &= sx(s) - f_2(x(s)) \\ &= s\left(\frac{s}{2} - c\right) - f_2\left(\frac{s}{2} - c\right) \\ &= s\left(\frac{s}{2} - c\right) - \left(\frac{s}{2} - c + c\right)^2 \\ &= \frac{s^2}{4} - sc\,. \end{cases} \tag{2.41}$$

Furthermore, we can also confirm that the backtransform is unique, since

$$\begin{cases} h_1(s) &= \frac{s^2}{4} \\ h_2(s) &= \frac{s^2}{4} - sc \end{cases} \tag{2.42}$$

$$\Rightarrow \begin{cases} x = \frac{dh_1}{ds} = \frac{s}{2} & \Leftrightarrow \quad s = 2x \\ x = \frac{dh_2}{ds} = \frac{s}{2} - c & \Leftrightarrow \quad s = 2(x+c) \end{cases} \tag{2.43}$$

$$\Rightarrow \begin{cases} f_1(x) &= x\,s(x) - h_1(s(x)) \\ &= x\,(2x) - h_1\,(2x) \\ &= 2x^2 - \frac{(2x)^2}{4} \\ &= x^2 \\ f_2(x) &= x\,s(x) - h_2(s(x)) \\ &= x \cdot 2(x+c) - \left(\frac{2^2(x+c)^2}{4} - 2(x+c)c\right) \\ &= x \cdot 2(x+c) - (x+c)^2 + 2(x+c)c \\ &= 2(x+c)(x+c) - (x+c)^2 \\ &= 2(x+c)^2 - (x+c)^2 \\ &= (x+c)^2\,. \end{cases} \tag{2.44}$$

This process is described in Figure 2.9.

$$
\begin{tikzcd}
& f(x) \arrow[d] & = & x\,s(x) - h\,(s\,(x)) & \\
x = x(s) \arrow[dr] & s = \dfrac{df}{dx} \arrow[l] \arrow[d] & & x = \dfrac{dh}{ds} \arrow[u] \arrow[r] & s = s(x) \arrow[ul] \\
& s\,x\,(s) - f\,(x\,(s)) & = & h(s) \arrow[u] &
\end{tikzcd}
$$

Figure 2.9: Schema of a Legendre transform in one-dimension. Adapted from [71].

In particular, classical Legendre transform distinguishes itself in that it is its own inverse. This property is sometimes called *involutive*. This can be verified as follows. Applying the classical Legendre transform to h, we can go back to the f, since

$$
\begin{aligned}
\mathcal{L}(\mathcal{L}(f)) &= \langle s, x\rangle - \mathcal{L}(f) \\
&= \langle s, x\rangle - (\langle s, x\rangle - f) \\
&= f,
\end{aligned}
$$

where $h = \mathcal{L}(f) = \langle s, x\rangle - f$ denotes the classical Legendre transform. This is one of the important properties of the Legendre transform.

Geometrical Interpretation

In one-dimensional case, the Legendre transform $f^*(s)$ computes geometrically a negative y-interception of the tangential line of f with the slope s, which we shall substantiate in the next paragraph. This problem involves finding an inverse mapping in (2.29) and (2.30) and it turns out that this is equivalent to find x_0 such that the hyperplane $H(s)$ which passes through $(x_0, f(x_0))$ is tangent to gr f at x_0, see Figure 2.10. Such x_0 exists and is unique, since we have chosen a smooth and strictly convex function.

First, for a function $f : D \to \mathbb{R}$ the *graph* of f is defined by

Definition 2.4.2 (Graph of f).

$$
\operatorname{gr} f := \{(x, r) : x \in D \quad \text{and} \quad r = f(x)\}\,. \tag{2.45}
$$

In Figure 2.10, for a given point $(x_0, f(x_0))$ we draw a tangential line $H(s)$. Let the slope of this tangential line at this point be s, which can be formulated as

$$
s = \frac{d}{dx} f(x)\bigg|_{x=x_0}\,. \tag{2.46}
$$

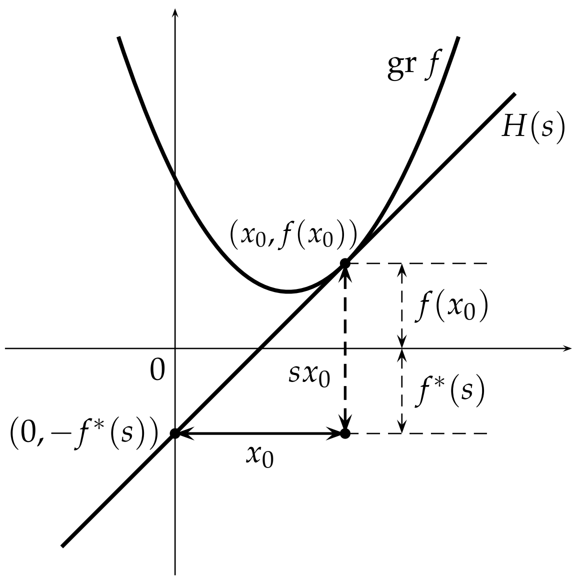

Figure 2.10: Illustration of a Legendre transform in one-dimension.

Then, we have the tangential line equation

$$\begin{aligned} y &= s(x - x_0) + f(x_0) \\ &= sx - sx_0 + f(x_0) \\ &= sx - (sx_0 - f(x_0)) \\ &\overset{(2.35)}{=} sx - f^*(s) \,, \end{aligned} \tag{2.47}$$

which explains the geometrical interpretation of Legendre transform. The last equality can be also explained as follows. When we consider the length of horizontal arrowed line labeled by x_0, its corresponding function value is the vertical dashed line denoted by $f(x_0)$. Since we assumed that the slope of the tangential line at this point is s, the length of the thick arrowed vertical line corresponds to sx_0. Here, the difference value $f^*(s) = sx_0 - f(x_0)$ in this case is encoded as a function of slope s, which coincides with the Definition 2.4.1. The Figure 2.10 also confirms the symmetric relationship (2.36) as well.

Remark 2.4.1. As we have seen so far, the Legendre transform generates a new function which contains the same information as the old, but is of a different independent variable. Mathematically, the Legendre transform is a symmetric equation whose structure can be clarified both algebraically and geometrically. This technique is useful for formulating model problems in the branch of physics, e.g. Hamilton-Lagrange mechanics or thermodynamics. From the viewpoint of physics, the Legendre transform can be interpreted as an issue of choosing independent variables that can be more easily controlled.

As an example in thermodynamics, it is impossible to have the entropy of the system at constant volume as the controllable variable in practical application, and it is much easier and intuitive to measure and control the temperature. More details about this theory, we refer to [91].

2.4.2 Generalised Legendre Transform

What we have discussed so far is about the case when the mapping $(\nabla f)^{-1}$ is well-defined. Let us turn our attention into the case when the mapping is not uniquely determined and a function has nondifferentiable points, e.g. $|x|$. Convex analysis, however, provides a nice framework to get around this situation. Let us see how the classical Legendre tansform is generalised.

First, the mapping $x \mapsto \nabla f(x)$ is replaced by a *set-valued* mapping $x \mapsto \partial f(x)$, where $\partial f(x)$ denotes the subdifferential which we have already seen in the Definition 2.3.2. To invert this mapping means that we want to find x such that $\partial f(x)$ contains a given s and we allow a nonunique such x. Therefore, a set-valued inverse mapping $(\partial f)^{-1}$ will be obtained.

Second, the $x(s)$ is constructed in such a way that the relationship $0 \in \partial f(x) - \{s\}$ holds. Thanks to the convexity of f this relationship means that x minimises $f - \langle s, \cdot \rangle$ over $\mathbb{R}^n$. In other words, to find $x(s)$, we have to solve

$$\inf\{f(x) - \langle s, x \rangle : x \in \mathbb{R}^n\}. \tag{2.48}$$

This is the possible way to define the Legendre transform unambiguously. In the classical Legendre transform, this problem is well-definded so that it has a unique solution. Therefore, we have the following more general definition of Legendre transform using (2.48)

Definition 2.4.3 (Generalised Legendre Transform).

$$\mathbb{R}^n \ni s \mapsto f^*(s) := \sup_x \{\langle s, x \rangle - f(x) : x \in \operatorname{dom} f\}, \tag{2.49}$$

where dom f denotes the set $\{x : f(x) < +\infty\} \neq \emptyset$. The mapping $f \mapsto f^*$ is also called the *conjugacy* operation or the *Legendre-Fenchel* transform. In order to avoid any confusedness with a classical definition, from now on "Legendre transform" is assumed to be referred as this generalised definition.

Remark 2.4.2. As in [46], a Legendre transform can also be defined using an infimum rather than a supremum:

$$g^*(k) = \inf_x \{\langle k, x \rangle - g(x)\}. \tag{2.50}$$

Transforming one version of the Legendre transform into the other is just a matter of introducing a minus sign at the right place. Indeed, with the relationship between supremum and infimum

$$\inf(A) = -\sup(-A), \tag{2.51}$$

where $-A = \{-a | a \in A\}$, we obtain

$$\begin{aligned}
& f^*(k) &=& \sup_x \{\langle k,x\rangle - f(x)\} \\
\Leftrightarrow\quad & -f^*(k) &=& -\sup_x \{\langle k,x\rangle - f(x)\} \\
\overset{(2.51)}{\Leftrightarrow}\quad & -f^*(k) &=& \inf_x \{-\langle k,x\rangle + f(x)\} \\
\Leftrightarrow\quad & -f^*(k) &=& \inf_x \{\langle -k,x\rangle - (-f(x))\}\,.
\end{aligned} \tag{2.52}$$

Thus,

$$g^*(q) = \inf_x \{\langle q, x\rangle - g(x)\}, \tag{2.53}$$

makes the transformations $g(x) = -f(x)$ and $g^*(q = -k) = -f^*(k = -q)$.

Let us make this clear by having a look at an example how a Legendre transform works for a nondifferentiable function $|x|$.

Example 2.4.1 (Legendre transform of $|x|$). Since

$$|x| = \begin{cases} x & \text{if} \quad x > 0 \\ -x & \text{if} \quad x \le 0 \end{cases}, \tag{2.54}$$

by the Definition 2.4.3 a Legendre transform of $|x|$ gives

$$\begin{aligned}
f^*(s) &= \sup \{sx - |x|\} \\
&= \sup \begin{cases} sx - x & \text{if} \quad x > 0 \\ sx + x & \text{if} \quad x \le 0 \end{cases} \\
&= \sup \begin{cases} (s-1)\,x & \text{if} \quad x > 0 \\ (s+1)\,x & \text{if} \quad x \le 0 \end{cases}.
\end{aligned} \tag{2.55}$$

As a Legendre transform is involved with a supremum, we have to think about the upper bound of (2.55). In order to achieve $f^*(s) < +\infty$, we need the following conditions

$$\begin{cases} s+1 \le 0 & \text{if} \quad x > 0 \\ s-1 \ge 0 & \text{if} \quad x \le 0, \end{cases} \tag{2.56}$$

which means $|s| \le 1$, see Figure 2.11a. Otherwise there does not exist a upper bound of $f^*(s)$, see Figure 2.11b. Therefore, we have the following result

$$f^*(s) = \begin{cases} 1 & \text{if} \quad |s| \le 1 \\ +\infty & \text{if} \quad |s| > 1, \end{cases} \tag{2.57}$$

which can be explained by Figure 2.4a.

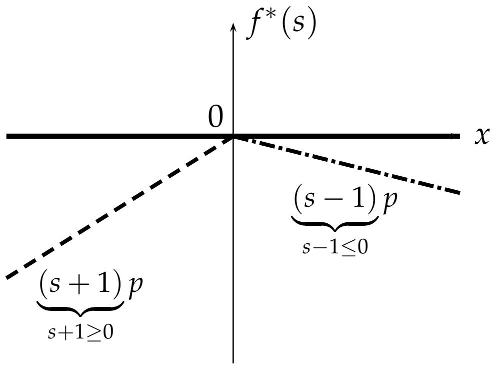

(a) When there is a upper bound for a Legendre transform of $|x|$.

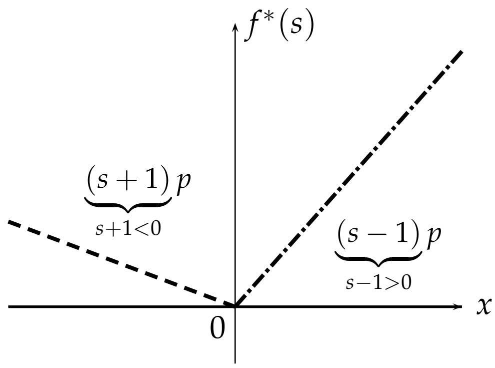

(b) When there is no upper bound for a Legendre transform of $|x|$.

Figure 2.11: Legendre transform of $|x|$.

2.4.3 Legendre Transform and Coercivity

A major concern in (2.53) is whether an infimum exists or not and this depends on the behaviour of g at infinity, which is why we are in need of the concept of coercivity. One important property of a coercive function is that a continuous function $g(x)$ defined on all $\mathbb{R}^n$ has at least one global minimum if $g(x)$ is coercive, which is proved in [7].

Considering (2.53), we can recognise that a function $g(x)$ should be greater than the linear function $\langle q, x\rangle$ for the existence of an infimum. The coercivity characterises this behaviour of g at infinity. After appreciatiating the definitions and some properties of coercivities, we shall see an example about this matter.

According to [42, 43], a convex function f which has an unambiguous Legendre transform satisfies the following properties

(i) differentiability (almost everywhere) - so that there is something to invert,

(ii) strict convexity - to have uniqueness in (2.48),

(iii) $\nabla f(\mathbb{R}^n) = \mathbb{R}^n$ - so that (2.48) does have a solution for all $s \in \mathbb{R}^n$.

The last property essentially means that, when $\|x\| \to \infty$, $f(x)$ increases faster than any other linear funcion. This function f is said to be *1-coercive*.

For the coercivities of the functions, the following definitions are given.

Definition 2.4.4 (0-Coercive Function). A continuous function $f : \mathbb{R}^n \to \mathbb{R} \cup \{+\infty\}$ which satisfies that $f \not\equiv +\infty$ and there is an affine function minorising f on $\mathbb{R}^n$ is said to be 0-coercive when

$$\lim_{\|x\| \to +\infty} f(x) = +\infty. \tag{2.58}$$

0-coercive is sometimes called *uniform coercive* as well.

Left us take a look at some examples.

Example 2.4.2 (Examples of Uniform Coercive Functions).

(a) Let $f(\mathbf{x}) = f(x_1, x_2) = x_1^2 + x_2^2 = |\mathbf{x}|^2$.

Then, we have

$$\lim_{|\mathbf{x}| \to \infty} f(\mathbf{x}) = \lim_{|\mathbf{x}| \to \infty} |\mathbf{x}|^2 \to \infty. \tag{2.59}$$

Thus, $f(x_1, x_2) = |\mathbf{x}|^2$ is uniform coercive by Definition 2.4.4.

(b) Let $f(\mathbf{x}) = f(x_1, x_2) = x_1^4 + x_2^4 - 3x_1x_2$.

Since $f(\mathbf{x})$ is dominated by higher order terms as $|\mathbf{x}| \to \infty$, we receive

$$\begin{aligned} f(x_1, x_2) &= \left(x_1^4 + x_2^4\right) - 3x_1x_2 \\ &= \left(x_1^4 + x_2^4\right)\left(1 - \frac{3x_1x_2}{x_1^4 + x_2^4}\right). \end{aligned} \tag{2.60}$$

Then, we deduce

$$\lim_{|(x_1,x_2)| \to \infty} f(x_1, x_2) = \lim_{|(x_1,x_2)| \to \infty} \left(x_1^4 + x_2^4\right)\left(1 - \underbrace{\frac{3x_1x_2}{x_1^4 + x_2^4}}_{\to 0}\right) \to \infty. \tag{2.61}$$

Therefore, by Definition 2.4.4 $f(x_1, x_2) = x_1^4 + x_2^4 - 3x_1x_2$ is uniform coercive as well.

Remark 2.4.3. It is insufficient to conclude $f(\mathbf{x})$ is uniform coercive, if we only know that $f(\mathbf{x}) \to \infty$ along each coordinate axis. A uniform coercive function must increase without a limit on any path that tends to infinity. Thus, if we can show that on a certain path in $\mathbb{R}^n$, $f(\mathbf{x})$ is bounded from above as $|\mathbf{x}| \to \infty$, then $f(\mathbf{x})$ must not be coercive. The following example explains this point.

Example 2.4.3 (Examples of Non-uniform Coercive Functions).

(a) Let $f(x_1, x_2) = x_1^2 - 2x_1x_2 + x_2^2$.

Then, we have:

(i) for each fixed $x_2 = y_2$, we receive

$$\lim_{|x_1| \to \infty} f(x_1, y_2) = \lim_{|x_1| \to \infty} x_1^2 - 2x_1y_2 + y_2^2 \to \infty. \tag{2.62}$$

(ii) for each fixed $x_1 = y_1$, we receive

$$\lim_{|x_2|\to\infty} f(y_1,x_2) = \lim_{|x_2|\to\infty} y_1^2 - 2y_1x_2 + x_2^2 \to \infty. \tag{2.63}$$

(iii) However, $f(x_1,x_2) = x_1^2 - 2x_1x_2 + x_2^2$ is not uniform coercive. This can be verified as follows.
Since $f(x_1,x_2) = x_1^2 - 2x_1x_2 + x_2^2$ can be reformulated as

$$f(x_1,x_2) = x_1^2 - 2x_1x_2 + x_2^2 = (x_1 - x_2)^2, \tag{2.64}$$

$f(x_1,x_2) = (x_1 - x_2)^2 \to 0$ even if $|(x_1,x_2)|$ goes to infinity along the line $x_2 = x_1$.
Hence,

$$\lim_{|(x_1,x_2)|\to\infty} f(x_1,x_2) \nrightarrow \infty, \tag{2.65}$$

which means that $f(x_1,x_2)$ not uniform coercive by Definition 2.4.4.

(b) Linear functions on $\mathbb{R}^2$ cannot be uniform coercive.

Such functions can be expressed as

$$f(x_1,x_2) = ax_1 + bx_2 + c, \tag{2.66}$$

where either $a \neq 0$ or $b \neq 0$. To see that $f(x_1,x_2) = ax_1 + bx_2 + c$ is not uniform coercive, we can observe that in a simple case. Along the line

$$ax_1 + bx_2 = 0, \tag{2.67}$$

$f(x_1,x_2)$ is equal to c. Although the line $ax_1 + bx_2 = 0$ is unbounded, the function $f(x_1,x_2) = ax_1 + bx_2 + c$ is constant, which confirms the assertion.

Definition 2.4.5 (1-Coercive Function). A continuous function $f : \mathbb{R}^n \to \mathbb{R} \cup \{+\infty\}$ which satisfies that $f \not\equiv +\infty$ and there is an affine function minorising f on $\mathbb{R}^n$ is said to be 1-coercive when

$$\lim_{\|x\|\to+\infty} \frac{f(x)}{\|x\|} = +\infty. \tag{2.68}$$

Notice that for the 1-coercivity, it is not sufficient to conclude that function has 1-coercive property if we only know that $f(x) \to +\infty$. For example, a function $f(x) = |x|$ is 0-coercive but not 1-coercive. Since it satisfies 0-coercive condition

$$\lim_{|x|\to+\infty} f(x) = \lim_{|x|\to+\infty} |x| \to +\infty, \tag{2.69}$$

but does not fulfil the 1-coercive requirement

$$\lim_{|x|\to+\infty} \frac{f(x)}{|x|} = \lim_{|x|\to+\infty} \frac{|x|}{|x|} = 1 \nrightarrow +\infty. \tag{2.70}$$

Concerning the coercivities, the following proposition will be used for the analysis of the properties of Hamiltonians. The proof can be found in [43].

Proposition 2.4.1. *If a continuous function $f : \mathbb{R}^n \to \mathbb{R} \cup \{+\infty\}$ which satisfies that $f \not\equiv +\infty$ and there is an affine function minorising f on $\mathbb{R}^n$ is 1-coercive, then $f^* < +\infty$ for all $s \in \mathbb{R}^n$.*

Remark 2.4.4. This proposition basically states that a function must satisfy the convexity and 1-coercive condition in order that the Legendre transform of f exists for all $s \in \mathbb{R}^n$, which is useful when we analyse the properties of a Hamiltonian.

Let us take a look at an example for this matter.

Example 2.4.4. Consider the following three one-dimensional functions $f_1(x) = c$ with $c \in \mathbb{R}$, $f_2(x) = |x|$, and $f_3(x) = x^2$.

First, we check the coercivities of functions. As we already know the result for f_2 and f_3, here we only test for f_1. It turns out that f_1 is neither 0-coercive nor 1-coercive, since

$$\lim_{|x|\to+\infty} f_3(x) = c \nrightarrow +\infty \tag{2.71}$$

and

$$\lim_{|x|\to+\infty} \frac{f_1(x)}{|x|} = \lim_{|x|\to+\infty} \frac{c}{|x|} = 0 \nrightarrow +\infty. \tag{2.72}$$

Next, we compute the Legendre transform of functions. The result of f_2 and f_3 is known in (2.57) and (2.41). In order to find the Legendre transform of f_1, by following the Definition 2.4.3 we have to find

$$\sup\{sx - f_1(x)\} = \sup\{sx - c\}. \tag{2.73}$$

Therefore, we have

$$f_1^*(s) = \begin{cases} -c, & s = 0 \\ +\infty, & s \neq 0. \end{cases} \tag{2.74}$$

As can be seen in (2.74), the Legendre transform of f_1 only exists when $s = 0$, since f_1 is neither 0-coercive nor 1-coercive in view of Proposition 2.4.1. In an analogous way, the case of f_2 can be explained as well. f_2 is convex and 0-coercive but not 1-coercive. Hence, its Legendre transform only exists when $|s| \leq 1$, see (2.57). In the case of f_3, it is convex and 1-coercive, so the Legendre transform of f_3 exists for all $s \in \mathbb{R}$, see (2.41).

2.5 Summary

In this chapter, we have explorered the important mathematical concepts which will be used in this thesis.

First, we have started with the topic of a Hamilton-Jacobi equation and thought about why we need the viscosity solution concept based on the well-posedness perspective by considering a one-dimensional eikonal equation with the classical methods.

Afterwards, we have investigated the notions of viscosity solutions and how we can obtain the viscosity solution for the one-dimensional eikonal equation.

Finally, the Legendre transform has been studied by classifying the cases when a considered function is differentiable and nondifferentiable.

In the next chapter, we shall have a look at the conditions for the existence of continuous viscosity solutions.

Chapter 3

Compatibility Condition on the Boundary Data

In the preceding chapter, we have gone through the viscosity solution concept with the example of the one-dimensional eikonal equation equipped with Dirichlet boundary conditions. In this chapter, we shall study a compatibility condition which is the systematic way to check the existence of the solutions for the Hamilton-Jacobi equations with Dirichlet boundary conditions.

This chapter proceeds as follows.

We commence giving the starting point for a compatibility condition by recalling the properties of the viscosity solutions in the previous chapter.

Then, our attention will be focused on how we can characterise and formulate such condition when a solution exists, which implies “necessary” requirements for the existence of the solution.

Afterwards, some examples will be provided, so that we can see how these conditions are applied for the Dirichlet boundary value problems.

Our contribution here is the analysis and elaboration on the exposition of Lion’s work [60] in an accessible way with an example of a one-dimensional eikonal equation.

For this chapter, we mainly follow the result of [13, 60, 93].

3.1 Introduction

Investigating the existence of viscosity solutions raises naturally the following questions. Is there any formal and systematic way to check whether there exist solutions for the given HJE with DBC in the viscosity framework? Or is there any proper conditions for the existence of the viscosity solutions? The compatibility condition concerning the Dirichlet boundary problems is studied to answer these questions, so that we can at least recognise that under certain conditions there do not exist such solutions.

To this end, we consider the following eikonal-type HJE with DBC

$$\begin{cases} |Du(x)| & = f(x) \quad \text{in} \quad \Omega \\ u(x) & = \varphi(x) \quad \text{on} \quad \partial\Omega, \end{cases} \tag{3.1}$$

where φ is given on $\partial\Omega$.

In the whole chapter, we assumed that Ω is a bounded, smooth and connected domain in $\mathbb{R}^n$ and we will use the following convex Hamiltonian

$$H(x,p) = |p| - f(x), \tag{3.2}$$

where p denotes Du and $f \in C(\overline{\Omega})$ and $f \geq 0$ in $\overline{\Omega}$ to be assumed. In addition, H is also assumed to satisfy the uniform coercivity condition, which means $H(x,p) \to +\infty$ uniformly for $x \in \overline{\Omega}$, as $|p| \to +\infty$. Notice that H is 0-coercive but not 1-coercive as we have already seen in (2.69) and (2.70).

Remark 3.1.1. As can be seen in the Subsection 2.3.2, making use of a convex Hamiltonian 3.2 implies that a viscosity subsolution plays a significant role.

Then, how can we characterise a condition if a continuous viscosity solution exists? If such solution exists, by the Definition 2.3.2 we should necessarily have the viscosity subsolution relationship on $\partial\Omega$ as follows

$$H(x,\partial\varphi) = |\partial\varphi| - f(x) \leq 0, \tag{3.3}$$

where $\partial\varphi$ denotes the tangential gradient of φ on $\partial\Omega$.

This is basically the starting point of formulating the compatibility condition on the boundary data.

Since we are looking for a continuous viscosity solution for the given boundary condition, existence of a solution suggests that there is a continuous path from one boundary point to the other. As an example, let us revisit the one-dimensional eikonal equation

$$\begin{cases} |\nabla u| - 1 & = & 0 \quad x \in (-1,1) \\ \varphi(x) & = & 0 \quad x \in \{\pm 1\}. \end{cases} \tag{3.4}$$

As we have already seen in Figure 2.7b, the continuous viscosity solution of (3.4) is $1 - |x|$ with $x \in [-1,1]$. Apparently, we are able to find a continuous path $1 - |x|$ between boundary points $x \in [-1,1]$ along which we can integrate. Hence, a necessary condition for the existence of continuous viscosity solutions can be formulated via an integration with the help of a viscosity subsolution criterion (3.3). Let us see how it is formulated in the sequel.

3.2 Formulation of a Compatibility Condition

In this section, we shall see how a compatibility condition on the boundary data is formulated.

First, we construct a path formulation between boundary points of a solution using integration. Then, we take care of the viscosity subsolution criterion, which leads to a compatibility condition. Finally, the Legendre transfomation version will be derived.

3.2.1 Integration Path between Boundary Data

Let $x, y \in \overline{\Omega}$, and $\xi(t) : [0,T] \rightarrow (\xi_1, \xi_2, \ldots, \xi_n)^T \in \mathbb{R}^n$ be a Lipschitz-continuous path function such that $\xi(0) = x$, $\xi(T) = y$, and $|\xi'(t)| \leq 1$ a.e. $\forall\, t \in [0,T]$ and u is parameterised by $\xi(s)$, which means $u\left(\xi\left(s\right)\right)$.

Now, we formulate the integration path between boundary points making use of "fundamental theorem of line integral" [8, 54, 102]

$$\int_0^T \nabla u\left(\xi\left(s\right)\right) \left|\xi'\left(s\right)\right| ds = \int_{\xi(0)}^{\xi(T)} \nabla u\left(\tau\right) d\tau\,. \tag{3.5}$$

With the above assumptions this leads to

$$\begin{aligned} \int_{\xi(0)}^{\xi(T)} \nabla u\left(\tau\right) d\tau &= \int_{\xi(0)=x}^{\xi(T)=y} \nabla u\left(\tau\right) d\tau \\ &= \left[u\left(\tau\right)\right]_x^y \\ &= u\left(y\right) - u\left(x\right)\,. \end{aligned} \tag{3.6}$$

Therefore, we formally establish

$$u(y) - u(x) = \int_0^T \nabla u\left(\xi(s)\right) \left|\xi'(s)\right| ds\,. \tag{3.7}$$

3.2.2 Viscosity Subsolution Criterion

As noted before, what we are interested in is the viscosity subsolution criterion, since we deal with the convex Hamiltonian. It turns out that the basic idea of compatibility condition stems from the viscosity subsolution criterion.

From (3.3) with the properties of estimation of integraion and the assumption $f \geq 0$ and

$|\xi'| \leq 1$ we deduce

$$
\begin{array}{cccccc}
(3.3) & |Du(\xi(s))| & \leq & f(\xi(s)) & & \\
\Leftrightarrow & |Du(\xi(s))|\,|\xi'(s)| & \leq & f(\xi(s))\,|\xi'(s)| & \leq & f(\xi(s)) \\
\Leftrightarrow & \left|\int_0^T Du(\xi(s))\,|\xi'(s)|\,ds\right| & \leq & \int_0^T f(\xi(s))\,|\xi'(s)|\,ds & \leq & \int_0^T f(\xi(s))\,ds \\
\overset{(3.5)}{\Leftrightarrow} & \left|\int_x^y Du(\tau)\,d\tau\right| & \leq & \int_x^y f(\tau)\,d\tau & \leq & \int_0^T f(\xi(s))\,ds \\
\Leftrightarrow & |u(y)-u(x)| & \leq & \int_x^y f(\tau)\,d\tau & \leq & \int_0^T f(\xi(s))\,ds.
\end{array}
\tag{3.8}
$$

Hence, we have the relationship

$$|u(y)-u(x)| \leq \int_0^T f(\xi(s))ds \tag{3.9}$$

from which we can receive

$$|u(y)-u(x)| \leq L(x,y), \tag{3.10}$$

where

$$
\begin{aligned}
L(x,y) = \inf_{\xi,T}\Bigg\{ \int_0^T f(\xi(s))ds;\ \xi(0)=x,\ \xi(T)=y,& \\
|\xi'(t) \leq 1| \text{ a.e. in } [0,T],\ \xi(t) \in \overline{\Omega}\ \ \forall\, t \in [0,T] \Bigg\}&.
\end{aligned}
\tag{3.11}
$$

In particular, writing this "necessary" condition (3.10) for the boundary data, we deduce

$$|\varphi(y)-\varphi(x)| \leq L(x,y) \quad \forall\,(x,y) \in \partial\Omega \times \partial\Omega, \tag{3.12}$$

which is called a *compatibility condition* on the boundary data.

Remark 3.2.1. In fact, it turns out that (3.12) is also a "sufficient" existence condition, which is shown in [60]. Furthermore, according to [60] when a compatibility condition on the boundary data (3.12) holds, a viscosity solution of (3.1) is given by

$$u(x) = \inf_{y\in\partial\Omega}\left[\varphi(y)+L(x,y)\right]. \tag{3.13}$$

This is based on the fact that a path integral from y to x is the same as that from x to y, which suggests $L(x,y) = L(y,x)$. Hence, we have

$$
\begin{array}{ccl}
& \varphi(x)-\varphi(y) & \leq L(x,y) \quad \forall x,y \in \partial\Omega \\
\Leftrightarrow & \varphi(x) & \leq \varphi(y)+L(x,y) \\
\Leftrightarrow & \varphi(x) & = \inf_{y\in\partial\Omega}\{\varphi(y)+L(x,y)\} \\
\Leftrightarrow & u(x) & = \inf_{y\in\partial\Omega}\{\varphi(y)+L(x,y)\}.
\end{array}
\tag{3.14}
$$

3.2.3 Compatibility Condition with a Legendre Transform

Since we have used a convex Hamiltonian, the $L(x,y)$ in (3.11) and (3.14) can be defined as a Lagrangian function with the Legendre transform as well. Now we are in need of a infimum version of Legendre tranform for $L(x,y)$, by the Remark 2.4.2 we receive

$$\begin{aligned}
& H^*(x,q) = \sup_{p\in\mathbb{R}^n} \{\langle p,q\rangle - H(x,p)\} \\
\Leftrightarrow & - H^*(x,q) = - \sup_{p\in\mathbb{R}^n} \{\langle p,q\rangle - H(x,p)\} \\
\overset{(2.51)}{\Leftrightarrow} & - H^*(x,q) = \inf_{p\in\mathbb{R}^n} \{-\langle p,q\rangle + H(x,p)\} \\
\Leftrightarrow & - H^*(x,q) = \inf_{p\in\mathbb{R}^n} \{\langle p,-q\rangle - (-H(x,p))\} \\
& \text{by the Remark 2.4.2} \\
\Leftrightarrow & H^*(x,-q) = \inf_{p\in\mathbb{R}^n} \{\langle p,-q\rangle - (-H(x,p))\}.
\end{aligned} \tag{3.15}$$

This leads to

$$\begin{aligned}
L(x,y) = \inf_{\xi,T} \Bigg\{ \int_0^T H^*\left(\xi(s), -\frac{d\xi}{ds}\right) ds;\ \xi(0) = x,\ \xi(T) = y, \\
\xi(t) \in \overline{\Omega}\ \ \forall\, t \in [0,T], \frac{d\xi}{dt} \in L^\infty(0,T) \Bigg\},
\end{aligned} \tag{3.16}$$

where $L^\infty(0,T)$ denotes the set of bounded measurable functions defined on the interval $(0,T)$ and takes the value in $\mathbb{R}^n$. With the result of (3.16), (3.13) can be formulated as

$$u(x) = \inf_{\xi} \left\{ \int_0^T H^*\left(\xi(s), -\xi'(s)\right) + \varphi(\xi(T)) \right\}, \tag{3.17}$$

which is actually explained in terms of Theorem 5.3 in [60]. This result is used for the Prados model in the next chapter.

Coercivity of a Hamiltonian. One more point to be discussed here is the condition $|\xi'(t) \le 1|$ in (3.11), which can be explained by the 0-coercivity of a convex Hamiltonian $H(p) = |p| - 1$.

According to Definition 2.4.4 and Definition 2.4.5, $H(p) = |p| - 1$ is 0-coercive but not 1-coercive, since

$$\lim_{|p|\to+\infty} H(p) = \lim_{|p|\to+\infty} |p| - 1 \to +\infty \tag{3.18}$$

and

$$\lim_{|p|\to+\infty} \frac{H(p)}{|p|} = \lim_{|p|\to+\infty} \frac{|p|-1}{|p|} \to 1 \neq +\infty. \tag{3.19}$$

By virtue of Proposition 2.4.1, we need a constraint to receive a finite $H^*(s)$. Here, we proceed as we did in Example 2.4.1.

Since

$$|p| = \begin{cases} p & \text{if} \quad p > 0 \\ -p & \text{if} \quad p \leq 0 \end{cases}, \tag{3.20}$$

by the Definition 2.4.3 a Legendre transform of $H(p) = |p| - 1$ yields

$$\begin{aligned} H^*(s) &= \sup_p \{sp - (|p| - 1)\} \\ &= \sup_p \begin{cases} sp - p + 1 & \text{if} \quad p > 0 \\ sp + p + 1 & \text{if} \quad p \leq 0 \end{cases} \\ &= \sup_p \begin{cases} (s-1)p + 1 & \text{if} \quad p > 0 \\ (s+1)p + 1 & \text{if} \quad p \leq 0 \end{cases}. \end{aligned} \tag{3.21}$$

As a Legendre transform is involved with a supremum, we have to think about the upper bound of (3.21). In order to achieve $H^*(s) < +\infty$, we need the following conditions

$$\begin{cases} s + 1 \leq 0 & \text{if} \quad p > 0 \\ s - 1 \geq 0 & \text{if} \quad p \leq 0, \end{cases} \tag{3.22}$$

which means $|s| \leq 1 \; \forall p$, see Figure 3.1a. Otherwise there does not exist a upper bound of $H^*(s)$, see Figure 3.1b. Therefore, we have the following result

$$H^*(s) = \begin{cases} 1 & \text{if} \quad |s| \leq 1 \\ +\infty & \text{if} \quad |s| > 1, \end{cases} \tag{3.23}$$

which explains the constraint $\left|\frac{d\xi}{ds}\right| \leq 1$ a.e. in (3.11).

3.3 Application of a Compatibility Condition

In this section, we shall see some examples how a compatibility condition is applied for the boundary value problems.

To this end, let us reconsider the following one-dimensional eikonal equation that we have seen in Section 2.3.

Example 3.3.1 (Compatibility Condition for 1-D Eikonal Equation 1).

$$\begin{cases} |\nabla u(x)| - 1 = 0, & x \in (0,1) \\ \varphi(x) = 0, & x \in \{0,1\}. \end{cases} \tag{3.24}$$

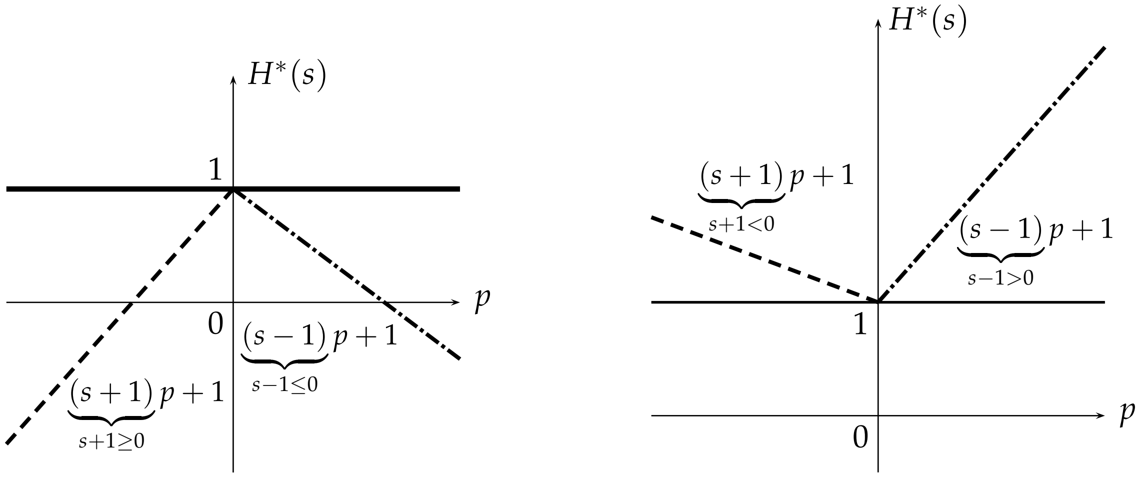

(a) When there is a upper bound for a Legendre transform of $H(p) = |p| - 1$.

(b) When there is no upper bound for a Legendre transform of $H(p) = |p| - 1$.

Figure 3.1: Legendre transform of a convex Hamiltonian $H(p) = |p| - 1$.

In order to have a compatibility condition for this problem, we first estimate $L(x,y)$ in (3.11). So, from (3.11) we have

$$\begin{aligned} L(x,y) &= \inf \int_0^T f(\xi(s))\, ds \\ &\overset{(3.8)}{=} \int_x^y f(\tau)\, d\tau \\ &= \int_x^y 1\, d\tau \\ &= y - x. \end{aligned} \tag{3.25}$$

Thus, by (3.12) we have the compatibility condition

$$|\varphi(y) - \varphi(x)| \leq |y - x|, \tag{3.26}$$

where $|\cdot|$ reflects that path integral is nonnegative. This states that the positive difference between boundary function values must be less than that of boundary points for the requirement of the existence of a solution. This fact can be validated as follows.

Computing the compatibility condition on the boundary data for this problem is therefore given by

$$\begin{aligned}
& |\varphi(0)-\varphi(1)| && \leq L(0,1) = 1-0 = 1 \\
\Leftrightarrow \quad & |0-0| && \leq L(0,1) = 1 \\
\Leftrightarrow \quad & 0 && \leq L(0,1) = 1, \\
\text{or} \quad & && \\
& |\varphi(1)-\varphi(0)| && \leq L(1,0) = |0-1| = 1 \\
\Leftrightarrow \quad & |0-0| && \leq L(1,0) = 1 \\
\Leftrightarrow \quad & 0 && \leq L(1,0) = 1.
\end{aligned} \tag{3.27}$$

From the Section 2.3 we already know that this problem has a viscosity solution $u(x) = \frac{1}{2} - \left|\frac{1}{2} - x\right|$. This can be explained by the result of (3.27), see Figure 3.2a.

Now, let us have a look at the next example.

Example 3.3.2 (Compatibility Condition for 1-D Eikonal Equation 2).

$$\begin{cases} |\nabla u| - 1 & = 0 \quad \text{if} \quad x \in (0,1) \\ \varphi(0) & = 1 \\ \varphi(1) & = 0 \end{cases} \tag{3.28}$$

Analogously, the compatibility condition for this problem can be formulated as

$$\begin{aligned}
& |\varphi(0)-\varphi(1)| && \leq L(0,1) = 1-0 = 1 \\
\Leftrightarrow \quad & |1-0| && \leq L(0,1) = 1 \\
\Leftrightarrow \quad & 1 && \leq L(0,1) = 1, \\
\text{or} \quad & && \\
& |\varphi(1)-\varphi(0)| && \leq L(1,0) = |0-1| = 1 \\
\Leftrightarrow \quad & |0-1| && \leq L(1,0) = 1 \\
\Leftrightarrow \quad & 1 && \leq L(1,0) = 1.
\end{aligned} \tag{3.29}$$

Based on this result, we conclude that there exists a solution and actually it does, see Figure 3.2b.

The last example shows us when the compatibility condition is useful.

Example 3.3.3 (Compatibility Condition for 1-D Eikonal Equation 3).

$$\begin{cases} |\nabla u| - 1 & = \quad 0 \quad \text{if} \quad x \in (0,1) \\ \varphi(0) & = \quad 0 \\ \varphi(1) & = \quad 1.5 \end{cases} \tag{3.30}$$

This problem does not satisfy the compatibility condition on the boundary data, which can be seen as follows

$$\begin{aligned} & |\varphi(0)-\varphi(1)| && \overset{?}{\leq} L(0,1) = 1-0 = 1 \\ \Leftrightarrow \quad & |0-1.5| && \nleq L(0,1) = 1 \\ \Leftrightarrow \quad & 1.5 && \nleq L(0,1) = 1\,, \\ \text{or} & && \\ & |\varphi(1)-\varphi(0)| && \overset{?}{\leq} L(1,0) = |0-1| = 1 \\ \Leftrightarrow \quad & |1.5-0| && \nleq L(1,0) = 1 \\ \Leftrightarrow \quad & 1.5 && \nleq L(1,0) = 1\,. \end{aligned} \tag{3.31}$$

As we can see in the Figure 3.2c, it is clear that we need a function whose slope is $\frac{3}{2}$ so as to fulfil the boundary condition in (3.30). However, the absolute value of the slope of our unknown function is already given 1. This means that there is no way to satisfy this requirement, which is confirmed in (3.31). As a consequence, we conclude that this problem has no solution by the compatibility condition on the boundary data.

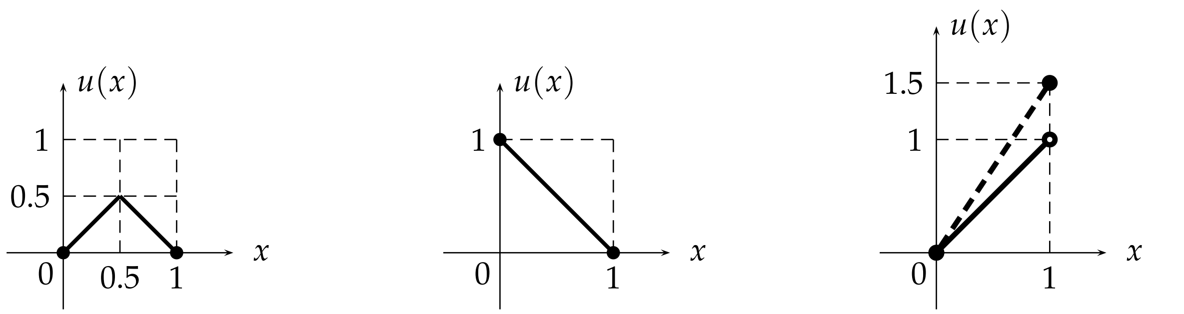

(a) Compatibility condition for (3.24).

(b) Compatibility condition for (3.28).

(c) Compatibility condition for (3.30).

Figure 3.2: Compatibility conditions on the boundary data.

3.4 Summary

In this chapter, we have investigated the compatibility condition on the boundary data. This condition serves as necessary and sufficient condition for the existence of solutions and enables us to recognise when the boundary points are not compatible with the problem.

First, we have started with formulating the integration path between bounday points by considering the necessary condition for the existence of solutions.

Then, having considered the viscosity subsolution criterion gives us the compatibility condition formulation.

Afterwards, we have thought about how this compatibility condition is formulated by Legendre transform as well.

Finally, some examples are provided how this condition is applied for the one-dimensional eikonal equation.

In the next chapter, we shall study the uniqueness of a solution which is also an essential part of the solution theory.

Chapter 4

Uniqueness of a Solution

In the previous chapter, the compatibility condition on the boundary data was discussed for the existence of solutions. In this chapter, we shall study the uniqueness of solutions, which is another major issue in the viscosity solution theory.

This chapter is planned as follows.

First, we begin with a classical comparison theorem as an introduction from which we can grasp the basic idea for the purpose.

Then, we investigate the comparison theorem in the viscosity framework. The key idea of an argumentation on this matter relies on [12].

Finally, the convex and concave ambiguity of Shape from Shading problems in the perspective of well-posedness will be discussed.

For this purpose, we mainly follow the result of [12, 47, 67, 69] for the comparison theorem and [26] for Shape from Shading modelling and the analysis of convex and concave ambiguity, respectively.

4.1 Introduction

The uniqueness result of a viscosity solution is, actually, a direct consequence based on the comparison theorem which can be found in [23, 60]. The uniqueness theory of a generalised HJE with the Dirichlet boundary problem, i.e.

$$\begin{cases} H(x, u(x), Du(x)) = 0 & \text{in} \quad \Omega \\ u(x) = \varphi(x) & \text{on} \quad \partial\Omega \end{cases} \tag{4.1}$$

is already well developed since the notion of viscosity solutions has been introduced.

However, it is not a simple task to apply directly the above mentioned uniqueness theory in [23] into the eikonal-type Hamiltonian, since it is independent of u, e.g. in the case of $H(x, p) = |p| - n(x)$. As a consequence, in [47] Ishii presented and proved the comparision theorem specially for this eikonal-type Hamiltonian.

Although in [47] a different technique was used for the proof in the viscosity framework comparing to the work in [23, 60, 99], the original setting was based on [99]. In this case, the convexity of H with respect to p plays an essential role.

The comparison theorem for uniqueness theory has several versions depending on the types of Hamilton-Jacobi equations that can be found in [12, 60]. Here, we make use of the version for the eikonal-type Hamiltonian in [12, 47].

4.2 Classical Comparison Theorem

To begin with, we think about the basic idea of comparison theorem in the classical sense and see how this is useful for the uniqueness of the solution.

As an introduction, let us consider the following problem.

Suppose that u_1, $u_2 \in C^0\left(\overline{\Omega}\right) \cap C^1\left(\Omega\right)$ satisfy the inequalities

$$\begin{cases} u_1(x) + H(x, Du_1(x)) & \leq 0 \\ u_2(x) + H(x, Du_2(x)) & \geq 0 \end{cases} \tag{4.2}$$

for $x \in \Omega$ and

$$u_1 \leq u_2 \quad \text{on} \quad \partial\Omega. \tag{4.3}$$

Assume also that Ω is bounded and let x_0 be a maximum point for $u_1 - u_2$ on $\overline{\Omega}$. When $x_0 \in \Omega$ is the case, by the first optimality condition we can receive

$$Du_1(x_0) = Du_2(x_0). \tag{4.4}$$

Let us think of (4.2) as

$$u_1(x) + H(x, Du_1(x)) \leq 0 \tag{4.5}$$

$$-u_2(x) - H(x, Du_2(x)) \leq 0. \tag{4.6}$$

Then, adding (4.6) to (4.5) using (4.4) yields

$$u_1(x) - u_2(x) \overset{(*)}{\leq} u_1(x_0) - u_2(x_0) \leq 0 \quad \forall x \in \overline{\Omega}, \tag{4.7}$$

where $(*)$ is valid because x_0 is assumed to be a maximum point of $u_1 - u_2$.

If $x_0 \in \partial\Omega$, then by (4.3) we have the same result as (4.7)

$$u_1(x) - u_2(x) \leq u_1(x_0) - u_2(x_0) \leq 0 \quad \forall x \in \overline{\Omega}. \tag{4.8}$$

As a consequence, we are able to obtain

$$u_1 \leq u_2 \quad \forall x \in \overline{\Omega}. \tag{4.9}$$

Changing the roles of u_1 and u_2 enables us to have the uniqueness of the classical solution of the Dirichlet problem

$$\begin{cases} u(x) + H(x, Du(x)) & = & 0 & \text{in} & \Omega \\ u(x) & = & \varphi(x) & \text{on} & \partial\Omega, \end{cases} \tag{4.10}$$

since as we have in (4.9)

$$\begin{cases} u_1 \leq u_2 & \forall x \in \overline{\Omega} \\ u_1 \geq u_2 & \forall x \in \overline{\Omega} \end{cases} \quad \Rightarrow \quad u_1 = u_2 \quad \forall x \in \overline{\Omega}. \tag{4.11}$$

The preceding technique does not work if u_1, u_2 satisfying (4.2) are the viscosity solutions, because in that case Du_i, $i \in \{1,2\}$ may not exist at x_0. However, the viscosity solution framework is strong enough to allow us to extend the previous result to the continuous viscosity solutions of HJE for the various Hamiltonian.

4.3 Comparison Theorem

In this section, we shall look into the details of comparison theorem so that how this really works in the viscosity framework.

Considering the eikonal-type Hamiltonian, we discuss specially the following problem

$$H(x, Du(x)) = 0, \quad x \in \Omega. \tag{4.12}$$

First, we give the definition of *modulus* for the hypotheses on which the comparison theorem rely on [47].

Definition 4.3.1 (Modulus). A function $m : [0, +\infty[\to [0, +\infty[$ is called *modulus* if it is continuous and nondecreasing and satisfies $m(0) = 0$.

In addition, the following hypotheses on H will be used.

(H1) There is a modulus m such that

$$|H(x,p) - H(y,p)| \leq m(|x-y|(1+|p|))$$

for $x, y \in \Omega$ and $p \in \mathbb{R}^n$.

(H2) The function $p \to H(x,p)$ is convex on $\mathbb{R}^n$ for each $x \in \Omega$.

Now, we give a comparison theorem.

Theorem 4.3.1 (Comparison Theorem). *Let Ω be a bounded open subset of $\mathbb{R}^n$. Assume that (H1) and (H2) hold. Let $\underline{u}, \overline{u} \in C^0(\overline{\Omega})$ be, respectively, viscosity sub- and supersolution of (4.12) with*

$$\underline{u} \leq \overline{u} \quad \textit{on} \quad \partial\Omega. \tag{4.13}$$

Assume also that

(H3) there is a function $\varphi \in C^1(\Omega) \cap C^0(\overline{\Omega})$ *such that* $\varphi \leq \underline{u}$ *in* $\overline{\Omega}$ *and*

$$\sup_{x \in \omega} H(x, D\varphi(x)) < 0, \qquad \forall \omega \subset\subset \Omega.$$

Then $\underline{u} \leq \overline{u}$ *in* Ω.

Here, we elaborate on the proof which is given in [12] based on [47], thereby clarifying the steps therein.

Proof. The proof of this theorem proceeds in three steps and method of "proof by contradiction" will be used, see Figure 4.1 for the outline of the proof. First, we set up an auxiliary function u_α satisfying (H3), which suggests that $\varphi \leq u_\alpha \leq \underline{u}$ in $\overline{\Omega}$. Then, using the convexity assumption of (H2) we derive a relationship. Finally, we show that this relationship implies $u_\alpha \leq \overline{u}$ in Ω by contradition. This leads to the conclusion $(u_\alpha \to \underline{u}) \leq \overline{u}$ as $\alpha \to 1$.

Step 1. This step is a preparation stage by building up a function u_α which can approach to $\underline{u}$ for the later use. We shall see how it behaves.

For $\alpha \in (0,1)$ we define a function u_α as

$$u_\alpha = \alpha\, \underline{u}(x) + (1-\alpha)\, \varphi(x), \quad x \in \overline{\Omega}. \tag{4.14}$$

As $\underline{u} \in C^0(\overline{\Omega})$ and by (H3) $\varphi \in C^1(\Omega) \cap C^0(\overline{\Omega})$, it is clear that

$$u_\alpha = \alpha \underline{u} + (1-\alpha)\, \varphi \in C^0(\overline{\Omega}). \tag{4.15}$$

Using $\varphi \leq \underline{u}$ in $\overline{\Omega}$ of (H3) we receive

$$\begin{array}{ccccc} & \varphi & \leq & \underline{u} & \\ \Leftrightarrow & \alpha\varphi & \leq & \alpha\underline{u} & \alpha \in (0,1) \\ \Leftrightarrow & \varphi + \alpha\varphi & \leq & \varphi + \alpha\underline{u} & \alpha \in (0,1) \\ \Leftrightarrow & \varphi & \leq & \underbrace{\alpha\underline{u} + (1-\alpha)\,\varphi}_{=\,u_\alpha} & \alpha \in (0,1) \\ \Leftrightarrow & \varphi & \leq & u_\alpha & \alpha \in (0,1) \end{array} \tag{4.16}$$

and

$$\begin{array}{ccccc} & \varphi & \leq & \underline{u} & \\ \Leftrightarrow & (1-\alpha)\,\varphi & \leq & (1-\alpha)\,\underline{u} & \alpha \in (0,1) \\ \Leftrightarrow & \underbrace{\alpha\underline{u} + (1-\alpha)\,\varphi}_{=\,u_\alpha} & \leq & \underline{u} & \alpha \in (0,1) \\ \Leftrightarrow & u_\alpha & \leq & \underline{u} & \alpha \in (0,1)\,. \end{array} \tag{4.17}$$

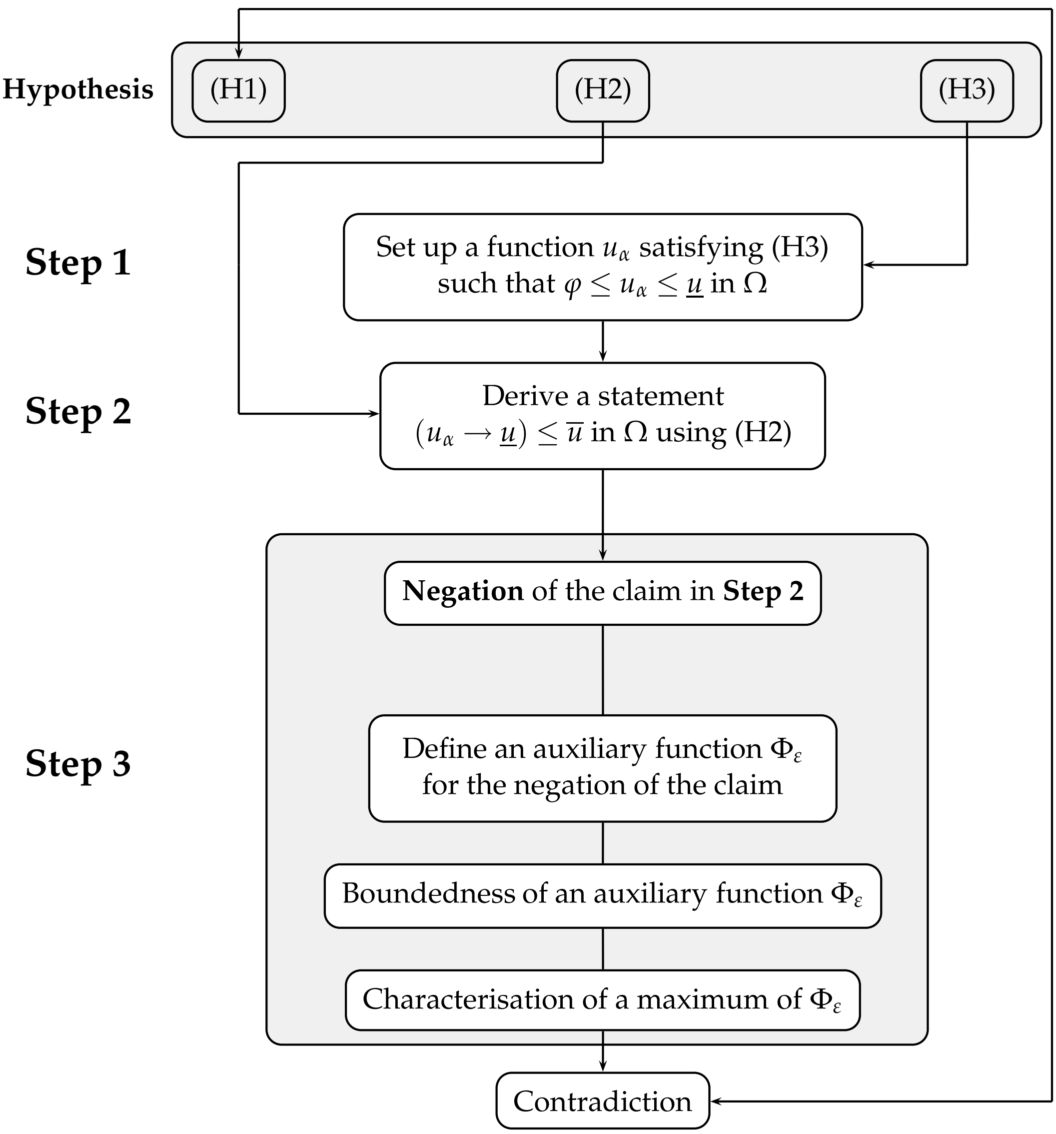

Figure 4.1: Outline of the proof for the comparison theorem.

Therefore, by virtue of (4.16) and (4.17) it follows

$$\varphi \leq u_\alpha \leq \underline{u} \quad \text{in} \quad \overline{\Omega}. \tag{4.18}$$

Following the Lemma 2.3.2 we obtain following property of u_α

$$D^+ u_\alpha(x) = \{q \in \mathbb{R}^n \mid q = \alpha p + (1-\alpha) D\varphi(x),\ p \in D^+ \underline{u}(x),\ \forall \alpha \in (0,1)\}\,. \tag{4.19}$$

In addition, from (4.14) we also have

$$u_\alpha \longrightarrow \underline{u} \quad \text{as} \quad \alpha \longrightarrow 1. \tag{4.20}$$

At this stage with (4.18) and (4.20) we have the relationship

$$\begin{cases} \varphi \le u_\alpha \le \underline{u} \le \overline{u} & \text{on} \quad \partial\Omega \\ \varphi \le u_\alpha \le \underline{u} & \text{in} \quad \Omega. \end{cases} \tag{4.21}$$

Step 2. Based on the former step, here we derive a statement that will be proved in the next step using the method by contradiction.
By (H2) for any $q \in D^+ u_\alpha(x)$ in (4.19) we receive

$$H(x,q) \overset{(4.19)}{=} H(x, \alpha p + (1-\alpha) D\varphi(x)) \overset{(H2)}{\le} \alpha H(x,p) + (1-\alpha) H(x, D\varphi(x)), \tag{4.22}$$

for some $p \in D^+\underline{u}(x)$ and $\forall \alpha \in (0,1)$.
From (4.22) for $p \in D^+\underline{u}(x)$ and $\forall \alpha \in (0,1)$ we deduce the following

$$\begin{array}{lrcl} (4.22) & H(x,q) & \le & \alpha H(x,p) + (1-\alpha) H(x, D\varphi(x)) \\ \Leftrightarrow & H(x,q) - (1-\alpha) H(x, D\varphi(x)) & \le & \alpha H(x,p) \\ & \text{since } \underline{u} \text{ is a subsolution of (4.12):} & & H(x,p) \le 0 \Leftrightarrow \alpha H(x,p) \le 0 \\ \Leftrightarrow & H(x,q) - (1-\alpha) H(x, D\varphi(x)) & \le & \alpha H(x,p) \le 0 \\ \Leftrightarrow & H(x,q) - (1-\alpha) H(x, D\varphi(x)) & \le & 0. \end{array} \tag{4.23}$$

This means that for any $\alpha \in [0,1]$ u_α is a viscosity subsolution of

$$H(x, Du_\alpha(x)) - (1-\alpha) H(x, D\varphi(x)) = 0 \quad x \in \Omega, \tag{4.24}$$

where $H(x, D\varphi(x)) \in C^0(\Omega)$.
The claim here is that this implies

$$u_\alpha \le \overline{u} \quad \text{in} \quad \Omega, \quad \forall \alpha \in (0,1). \tag{4.25}$$

As $\alpha \longrightarrow 1$ u_α converges to $\underline{u}$ in (4.25) based on the (4.20). This comes to the conclusion $\underline{u} \le \overline{u}$ in Ω. The proof of (4.25) proceeds in the next step.

Step 3. Our goal is to show $\underline{u} \le \overline{u}$ in Ω. As pointed out in the last part of the previous step, this corresponds to show (4.25). In this step, we first set up an auxiliary function by negating the statement in the previous step. Then, the properties of this auxiliary function will be discussed. These are about the boundedness and the properties of maximum points of this function. Having a look at the behaviour of these points tells us the status of interior of the domain. Afterwards, proceeding within this negated setup comes to the contradiction, which confirms the original assertion.

Negation of the claim. In order to prove (4.25), as mentioned before let us suppose by contradiction that for some $\beta \in (0,1)$

$$\sup_{x\in\Omega} \left(u_\beta - \overline{u}\right)(x) = \delta > 0. \tag{4.26}$$

Define an auxiliary function. Consider now for $\varepsilon > 0$ the auxiliary function

$$\Phi_\varepsilon(x,y) = u_\beta(x) - \overline{u}(y) - \frac{|x-y|^2}{2\varepsilon} \tag{4.27}$$

and assume that there exists a maximum of (4.27) at $(x_\varepsilon, y_\varepsilon) \in \overline{\omega} \times \overline{\omega}$. Then, using (4.27) we obtain

$$\sup_{x\in\overline{\omega}} \left(u_\beta - \overline{u}\right)(x) = \sup_{x\in\overline{\omega}} \Phi_\varepsilon(x,x) \leq \sup_{(x,y)\in\overline{\omega}\times\overline{\omega}} \Phi_\varepsilon(x,y) = \Phi_\varepsilon(x_\varepsilon, y_\varepsilon). \tag{4.28}$$

Here, the open set ω can be set as

$$\omega = \left\{ x \in \Omega \middle| \left(u_\beta - \overline{u}\right)(x) > \frac{\delta}{2} \right\}. \tag{4.29}$$

This leads to

$$\overline{\omega} = \left\{ x \in \Omega \middle| \left(u_\beta - \overline{u}\right)(x) \geq \frac{\delta}{2} \right\}, \tag{4.30}$$

which satisfies (4.26) and so does the condition $\omega \subset\subset \Omega \Leftrightarrow \overline{\omega} \subset \Omega$ in (H3).

Boundedness of an auxiliary function. First, we investigate the boundedness property of this auxiliary function by looking into (4.37). Otherwise there does not exist a maximum and the exposition in (4.37) does not make sense.

Recalling in the Definition 2.3.2 that a viscosity supersolution $\overline{u}$ has lower semicontinuous property gives us the fact that there is a lower bound for $\overline{u}$. In other words, $-\overline{u}$ is bounded above. Analogously, a viscosity subsolution $\underline{u}$ is upper semicontinuios, so it has an upper bound. Therefore, choosing a suitable test function φ allows u_β to have an upper bound as well. Now, we are about to take a look at the properties of $\frac{|x-y|^2}{2\varepsilon}$ in (4.27).

From (4.37) we have

$$\begin{aligned}
& \Phi_\varepsilon(x_\varepsilon, x_\varepsilon) && \leq && \Phi_\varepsilon(x_\varepsilon, y_\varepsilon) \\
\overset{(4.27)}{\Leftrightarrow} \quad & u_\beta(x_\varepsilon) - \overline{u}(x_\varepsilon) - \frac{|x_\varepsilon - x_\varepsilon|^2}{2\varepsilon} && \leq && u_\beta(x_\varepsilon) - \overline{u}(y_\varepsilon) - \frac{|x_\varepsilon - y_\varepsilon|^2}{2\varepsilon} \\
\Leftrightarrow \quad & u_\beta(x_\varepsilon) - \overline{u}(x_\varepsilon) - 0 && \leq && u_\beta(x_\varepsilon) - \overline{u}(y_\varepsilon) - \frac{|x_\varepsilon - y_\varepsilon|^2}{2\varepsilon} \\
\Leftrightarrow \quad & -\overline{u}(x_\varepsilon) && \leq && -\overline{u}(y_\varepsilon) - \frac{|x_\varepsilon - y_\varepsilon|^2}{2\varepsilon} \\
\Leftrightarrow \quad & \frac{|x_\varepsilon - y_\varepsilon|^2}{2\varepsilon} && \leq && \overline{u}(x_\varepsilon) - \overline{u}(y_\varepsilon)\,.
\end{aligned} \tag{4.31}$$

This formulation can be further expanded as

$$\begin{aligned}
\text{from (4.31)} \quad \frac{|x_\varepsilon - y_\varepsilon|^2}{2\varepsilon} &\leq \overline{u}(x_\varepsilon) - \overline{u}(y_\varepsilon) \\
\Leftrightarrow \quad |x_\varepsilon - y_\varepsilon|^2 &\leq 2\varepsilon\left(\overline{u}(x_\varepsilon) - \overline{u}(y_\varepsilon)\right) \\
\Rightarrow \quad |x_\varepsilon - y_\varepsilon| &\leq \sqrt{2\varepsilon\left|\overline{u}(x_\varepsilon) - \overline{u}(y_\varepsilon)\right|} \\
\Leftrightarrow \quad |x_\varepsilon - y_\varepsilon| &\leq (C\varepsilon)^{\frac{1}{2}}\,,
\end{aligned} \tag{4.32}$$

where $C = 2\left|\overline{u}(x_\varepsilon) - \overline{u}(y_\varepsilon)\right|$ depends only on the maximum of $|\overline{u}|$ in $\overline{\omega}$. Therefore, in (4.32) we obtain

$$|x_\varepsilon - y_\varepsilon| \to 0 \quad \text{as} \quad \varepsilon \to 0. \tag{4.33}$$

In addition, due to $\overline{u}(x_\varepsilon) - \overline{u}(y_\varepsilon) \leq \left|\overline{u}(x_\varepsilon) - \overline{u}(y_\varepsilon)\right|$ from (4.32) we have

$$\frac{|x_\varepsilon - y_\varepsilon|^2}{2\varepsilon} \leq \overline{u}(x_\varepsilon) - \overline{u}(y_\varepsilon) \leq \left|\overline{u}(x_\varepsilon) - \overline{u}(y_\varepsilon)\right|. \tag{4.34}$$

By the continuity of $\overline{u}$ (4.34) leads to

$$\frac{|x_\varepsilon - y_\varepsilon|^2}{2\varepsilon} \leq \overline{u}(x_\varepsilon) - \overline{u}(y_\varepsilon) \leq \left|\overline{u}(x_\varepsilon) - \overline{u}(y_\varepsilon)\right| \leq m_1\,|x_\varepsilon - y_\varepsilon|\,, \tag{4.35}$$

where m_1 is a modulus of a continuity for $\overline{u}$. Then, together with (4.33) we receive

$$\frac{|x_\varepsilon - y_\varepsilon|^2}{2\varepsilon} \to 0 \quad \text{as} \quad \varepsilon \to 0. \tag{4.36}$$

Hence, with the property of (4.36) Φ_ε is bounded above for each $\varepsilon > 0$ as well.

Characterisation of a maximum of Φ_ε. Let us now characterise the maximum of Φ_ε at the point $(x_\varepsilon, y_\varepsilon)$. Since $\omega \subset\subset \Omega$ from (4.37) we can derive

$$\delta \overset{(4.26)}{=} \sup_{x\in\omega} \left(u_\beta - \overline{u}\right)(x) = \sup_{x\in\omega} \Phi_\varepsilon(x,x) \leq \sup_{(x,y)\in\omega\times\omega} \Phi_\varepsilon(x,y) = \Phi_\varepsilon(x_\varepsilon, y_\varepsilon)\,. \tag{4.37}$$

This implies that $(x_\varepsilon, y_\varepsilon) \in \omega \times \omega$ for sufficiently small ε. If this were not the case, then either x_ε or y_ε would belong to $\partial\omega$. This statement makes trouble. We can confirm that as follows. Assuming $x_\varepsilon \in \partial\omega$ we have

$$\begin{array}{rrcl} \text{from (4.37)} & \left(u_\beta - \overline{u}\right)(x_\varepsilon) = \delta & \leq & \Phi_\varepsilon(x_\varepsilon, y_\varepsilon) \\ \overset{(4.35)}{\Leftrightarrow} & \delta - m_2\left|x_\varepsilon - y_\varepsilon\right| & \leq & \Phi_\varepsilon(x_\varepsilon, y_\varepsilon) - \left(\overline{u}(x_\varepsilon) - \overline{u}(y_\varepsilon)\right), \end{array} \tag{4.38}$$

where m_2 is a modulus of continuity for $\overline{u}$. Since we have assumed the maximum is attatined on $\partial\omega$ $(*)$, by (4.30) we obtain

$$\delta - m_2\left|x_\varepsilon - y_\varepsilon\right| \leq \Phi_\varepsilon(x_\varepsilon, y_\varepsilon) - \left(\overline{u}(x_\varepsilon) - \overline{u}(y_\varepsilon)\right) \overset{(*)}{\leq} u_\beta(x_\varepsilon) - \overline{u}(x_\varepsilon) \overset{(4.30)}{=} \frac{\delta}{2}. \tag{4.39}$$

Taking (4.33) into account yields $\delta \leq \dfrac{\delta}{2}$ for $\delta > 0$, which makes no sense. As a result, a maximum of (4.27) can be attained only at the interior of the domain ω.

Contradiction. Now, we are about to set up the statement (4.24). In order to exploit the Definition 2.3.1, we interpret the maximum of Φ_ε at $(x_\varepsilon, y_\varepsilon)$ in a different way. In view of (4.27), a maximum of Φ_ε can be attained when we subtract a local minimum of $\overline{u}$ at y_ε from a local maximum of u_β at x_ε. This can be viewed as follows:
x_ε is a local maximum for

$$x \mapsto u_\beta(x) - \left(\overline{u}(y_\varepsilon) + \frac{\left|x - y_\varepsilon\right|^2}{2\varepsilon}\right) \tag{4.40}$$

and y_ε is a local minimum for

$$y \mapsto \overline{u}(y) - \left(u_\beta(x_\varepsilon) - \frac{\left|x_\varepsilon - y\right|^2}{2\varepsilon}\right). \tag{4.41}$$

Since a maximum of (4.40) is attained at x_ε, computing a superdifferential of (4.40) gives

$$\begin{aligned}
& D^+\left(u_\beta(x)-\left(\overline{u}(y_\varepsilon)+\frac{|x-y_\varepsilon|^2}{2\varepsilon}\right)\right)\ni 0\\
\Leftrightarrow\quad & D^+u_\beta(x)-\underbrace{D^+\overline{u}(y_\varepsilon)}_{=0}-D^+\left(\frac{|x-y_\varepsilon|^2}{2\varepsilon}\right)\ni 0\\
\Leftrightarrow\quad & D^+u_\beta(x)-\frac{2(x-y_\varepsilon)}{2\varepsilon}\ni 0\\
& \text{a maximum is attatined at } x_\varepsilon\\
\Leftrightarrow\quad & D^+u_\beta(x_\varepsilon)-\frac{(x_\varepsilon-y_\varepsilon)}{\varepsilon}=0\\
\Leftrightarrow\quad & D^+u_\beta(x_\varepsilon)=\frac{(x_\varepsilon-y_\varepsilon)}{\varepsilon}.
\end{aligned}\tag{4.42}$$

Using the fact that u_β is a viscosity subsolution of (4.24), we plug the result of (4.42) into (4.24). This process yields

$$H\left(x_\varepsilon,\frac{x_\varepsilon-y_\varepsilon}{\varepsilon}\right)-(1-\beta)H(x_\varepsilon,D\varphi(x_\varepsilon))\leq 0.\tag{4.43}$$

In a similar way, calculating a subdifferential of (4.41) gives

$$\begin{aligned}
& D^-\left(\overline{u}(y)-\left(u_\beta(x_\varepsilon)-\frac{|x_\varepsilon-y|^2}{2\varepsilon}\right)\right)\ni 0\\
\Leftrightarrow\quad & D^-\overline{u}(y)-\underbrace{D^-u_\beta(x_\varepsilon)}_{=0}+D^-\left(\frac{|x_\varepsilon-y|^2}{2\varepsilon}\right)\ni 0\\
\Leftrightarrow\quad & D^-\overline{u}(y)-\frac{2(x_\varepsilon-y)}{2\varepsilon}\ni 0\\
& \text{a minimum is attatined at } x_\varepsilon\\
\Leftrightarrow\quad & D^-u_\beta(x_\varepsilon)-\frac{(x_\varepsilon-y_\varepsilon)}{\varepsilon}=0\\
\Leftrightarrow\quad & D^-u_\beta(x_\varepsilon)=\frac{(x_\varepsilon-y_\varepsilon)}{\varepsilon}.
\end{aligned}\tag{4.44}$$

As $\overline{u}$ is a viscosity supersolution of (4.12), by plugging (4.44) into (4.12) we obatin

$$H\left(y_\varepsilon,\frac{x_\varepsilon-y_\varepsilon}{\varepsilon}\right)\geq 0.\tag{4.45}$$

The claim here is that (4.43) and (4.45) disobeys (H1) in view of (4.33) and (4.36).

By virtue of (H3), for all small ε there exists $\rho > 0$ such that

$$(1-\beta) H(x_\varepsilon, D\varphi(x_\varepsilon)) \leq -\rho < 0. \tag{4.46}$$

Then, from (4.43) we deduce

$$\begin{aligned}
& H\left(x_\varepsilon, \frac{x_\varepsilon - y_\varepsilon}{\varepsilon}\right) - (1-\beta) H(x_\varepsilon, D\varphi(x_\varepsilon)) \leq 0 \\
\Leftrightarrow \quad & -(1-\beta) H(x_\varepsilon, D\varphi(x_\varepsilon)) \leq -H\left(x_\varepsilon, \frac{x_\varepsilon - y_\varepsilon}{\varepsilon}\right) \\
\Leftrightarrow \quad & 0 < \rho \overset{(4.46)}{\leq} -(1-\beta) H(x_\varepsilon, D\varphi(x_\varepsilon)) \leq -H\left(x_\varepsilon, \frac{x_\varepsilon - y_\varepsilon}{\varepsilon}\right) \\
\overset{(4.45)}{\Leftrightarrow} \quad & 0 < \rho \leq H\left(y_\varepsilon, \frac{x_\varepsilon - y_\varepsilon}{\varepsilon}\right) - H\left(x_\varepsilon, \frac{x_\varepsilon - y_\varepsilon}{\varepsilon}\right) \\
\Leftrightarrow \quad & 0 < \rho \leq H\left(y_\varepsilon, \frac{x_\varepsilon - y_\varepsilon}{\varepsilon}\right) - H\left(x_\varepsilon, \frac{x_\varepsilon - y_\varepsilon}{\varepsilon}\right) \overset{(H1)}{\leq} m_2\left(|x_\varepsilon - y_\varepsilon|\left(1 + \frac{|x_\varepsilon - y_\varepsilon|}{\varepsilon}\right)\right).
\end{aligned} \tag{4.47}$$

Following (4.43) and (4.45) allows the right hand side of (4.47) to approach 0. Then, (4.47) leads to

$$0 < \rho \leq H\left(y_\varepsilon, \frac{x_\varepsilon - y_\varepsilon}{\varepsilon}\right) - H\left(x_\varepsilon, \frac{x_\varepsilon - y_\varepsilon}{\varepsilon}\right) \leq 0, \tag{4.48}$$

which is a contradiction. This completes the proof. □

As a direct consequence of this comparison theorem, we obtain the following uniqueness result.

Corollary 4.3.2. *Let u, v the two viscosity solutions of (4.10) such that $u = v$ on $\partial\Omega$. Then $u = v$. Therefore, the Dirichlet problem*

$$\begin{cases} H(x, Du(x)) = 0 & \text{in } \Omega \\ u(x) = \varphi(x) & \text{on } \partial\Omega, \end{cases} \tag{4.49}$$

has at most one continuous viscosity solution.

Proof. Since for all x on $\partial\Omega$ $u = v$ and u, v are both viscosity sub- and supersolution, the comparison principle implies that $u \leq v$ and $v \leq u$ on $\overline{\Omega}$. Thus, the conclusion follows. □

Remark 4.3.1. Theorem 4.3.1 can be applied to the eikonal equation $|D(x)| = f(x)$ if f is uniformly continuous in Ω and strictly positive. As an example, let us recall the one-dimenstional eikonal equation

$$\begin{cases} |u'(x)| = 1 & x \in (-1, 1) \\ u(x) = 0 & x = \{\pm 1\}. \end{cases} \tag{4.50}$$

Using a convex Hamiltonian $H(x,p) = |p| - 1$, we can find a φ which satisfies (H3) by taking $\varphi = 0$. This case is clear, since $H(x,0) = 0 - 1 = -1 < 0$. This can be interpreted as follows. In fact, we take φ such that

$$\varphi(x) \equiv \min_{\overline{\Omega}} \underline{u}, \tag{4.51}$$

where $\underline{u}$ denotes the viscosity subsolution of a convex Hamiltonian $H(x,p) = |p| - 1$. As we have seen in the Figure 2.7, $\underline{u} = 1 - |x|$ has a minimum value 0 at the boundary of the domain. Hence, (4.50) has a unique continuous viscosity solution by Theorem 4.3.1. However, the difficulty of this approach lies in the fact that it is, in general, not trivial to find φ satisfying (H3).

With the help of this theorem, one can also verify that under suitable assumptions Shape from Shading models proposed by Prados and Faugeras in [31, 85, 88] have a unique continuous viscosity solution.

4.4 Convex-Concave Ambiguity

Shape from Shading is well-known to be an ill-posed problem, so there are several articles in which specially the nonuniqueness property of the solution called "convex-concave ambiguity" was investigated [16, 25, 26, 30, 31, 72, 79].

Other than convex/concave ambiguity there are other points to make Shape from Shading problems ill-posed. According to [81] one of the reasons for that is so-called "bas-relief ambiguity" which basically says that this type of ambiguity is caused by the fact that the mathematical model does not reflect the physical phenomenon exactly or some information is missing in the modelling process, e.g. the surface reflectance map at some point is not defined or the focal length of a camera is unknown and so forth. Therefore, this makes also the problem ill-posed. However, assuming all these informations are at hand, this is still not good enough to resolve all the situations completely [25, 26, 28, 31, 72, 82]. This suggests that we still suffer from the convex/concave ambiguity.

In this section, the convex/concave ambiguity of the Shape from Shading problem will be briefly discussed in the viscosity framework. It turns out that the problem of a convex/concave ambiguity stems from the existence of singular points [1] [26]. So, convex/concave ambiguity can be characterised by the singular points. For this purpose, we shall use the following eikonal-type Hamiltonian which is designed for the orthographic Shape from Shading model by Rouy and Tourin [26]

$$H^{\text{orth}}_{\text{Eikonal}}(\mathbf{x},\mathbf{p}) = |\mathbf{p}| - \sqrt{\frac{1}{I(\mathbf{x})^2} - 1}, \tag{4.52}$$

[1] The points where the normalised image intensity is one are called "singular points" or sometimes "critical points." This phenomenon occurs when the surface normal coincides with the light direction [29].

where $\mathbf{x} = (x_1,\ x_2)^{\mathrm{T}} \in \mathbb{R}^2$, $\mathbf{p} = \nabla u(\mathbf{x})$ and $I(\mathbf{x}) > 0$ denotes the normalised image intensity.

Now, let us consider the uniqueness property of (4.52) by focusing on the requirement (H3) for the Theorem 4.3.1. Then, with the help of Remark 4.3.1 this problem turns out to be a question how the term $\sqrt{\frac{1}{I(\mathbf{x})^2} - 1}$ in (4.52) behaves. Since $I(\mathbf{x}) > 0$ is normalised image intensity, we have

$$\begin{aligned}
& \sqrt{\frac{1}{I(\mathbf{x})^2} - 1} && > 0 \\
\Leftrightarrow \quad & \sqrt{\frac{1 - I(\mathbf{x})^2}{I(\mathbf{x})^2}} && > 0 \\
\overset{I(\mathbf{x})>0}{\Leftrightarrow} \quad & \underbrace{\frac{1}{I(\mathbf{x})}}_{>0} \sqrt{1 - I(\mathbf{x})^2} && > 0 \\
\Leftrightarrow \quad & 1 - I(\mathbf{x})^2 && > 0 \\
\Leftrightarrow \quad & I(\mathbf{x})^2 && < 1 \\
\Leftrightarrow \quad & |I(\mathbf{x})| && < 1.
\end{aligned} \tag{4.53}$$

Therefore, it can be realised that we have a uniqueness result by the Theorem 4.3.1 as long as the normalised image intensity holds $0 < I(\mathbf{x}) < 1$.

This naturally raises a question "What if the normalised image intensity is one?" When the singular points occur, we lose the uniqueness property immediately, since it is impossible for us to find $\varphi(x)$ at those points satisfying (H3) for the Theorem 4.3.1. This can be understood as follows. At the singular points the Hamiltonian 4.52 is turned into

$$H^{\text{orth}}_{\text{Eikonal}}(\mathbf{x}, \nabla u(\mathbf{x})) = |\nabla u(\mathbf{x})| \,. \tag{4.54}$$

When we think of (4.54) as

$$H^{\text{orth}}_{\text{Eikonal}}(\mathbf{x}, \nabla u(\mathbf{x})) = |\nabla u(\mathbf{x})| = 0\,, \tag{4.55}$$

it is obvious that every constant vector $u(\mathbf{x}) = (c_1, c_2)^{\mathrm{T}} \in \mathbb{R}^2$ is a viscosity solution of (4.55). Therefore, the uniqueness does not hold.

This can be verified by the Theorem 4.3.1 as well. In (H3) finding $\varphi(x)$ means that

$$H^{\text{orth}}_{\text{Eikonal}}(\mathbf{x}, \nabla \varphi(\mathbf{x})) = |\nabla \varphi(\mathbf{x})| < 0. \tag{4.56}$$

It is clear that this is an impossible task, since $|\nabla \varphi(\mathbf{x})| \geq 0$.

Remark 4.4.1. As can be seen in the above, it can be noticed that for the eikonal-type Hamiltonian

$$H(x, Du(x)) = 0 \tag{4.57}$$

a nonuniqueness phenomenon may appear even in the viscosity framework.

Remark 4.4.2. Strong efforts were already made to make Shape from Shading problem well-posed, e.g. [16, 55, 73] using eikonal-type Hamiltonian. However, as can be noticed previously, an eikonal-type Hamiltonian is not good enough to reconstruct the surface completely when the singular points occur. Furthermore, since a gradient itself is invariant under shifting, it is not a good idea when we only try to extract the information of the gradient. Hence, it would be better if we had the information of the surface itself. This means that we have to change our Hamiltonian from the eikonal-type to the general one. In the viscosity frame work, this is done by Prados and Faugeras [29, 87].

4.5 Summary

In this chapter, we have looked into the details of a comparison theorem in the viscosity framework which plays a significant role in the uniqueness theory.

First, we have seen the classical comparison theorem in order to have basic idea.

Then, a comparison theorem for the eikonal-type Hamilton-Jecobi equation has been investigated throughly in the viscosity framework. The convexity of a Hamiltonian has been the essential part in this theorem.

Finally, convex-concave ambiguities of Shape from Shading problems are discussed in the context of well-posedness as well.

In the next chapter, we shall see how the mathematical tools that we went through in this chapter will be applied for the Shape from Shading problems based on the model which is proposed by Prados and Faugeras.

Chapter 5

The Prados Model for Shape from Shading

So far, we have reviewed the theoretical background for Shape from Shading problems, one of whose main part is the concept of viscosity solution and its existence and uniqueness property in the solution theory.

In this chapter, we shall see how this theory is applied in the perpective Shape from Shading models.

The outline of this chapter is as follows.

We begin with how the Shape from Shading problem is modelled mathematically and investigate two different cases of using the perspective projections. The first one is when a point light source lies at infinity and the other is when a point light source is located at the optical centre, respectively.

Afterwards, we pay special attention to the properties of the "generic" Hamiltonians proposed by Prados and Faugeras [84, 85, 88]. This setup gives us an efficient framework in which the proposed model can be handled effectively. Our contribution here is to provide every step that Prados and Faugeras have taken for granted.

Then, we shall see how we can receive the well-posedness properties for the Shape from Shading problem in the viscosity sense. This requires our knowledge of the viscosity theory that we have gone through in the previous chapters.

Our references for this chapter are mainly the papers by Prados and Faugeras [31, 84, 85, 88], which deal with the topic of perspective Shape from Shading models.

5.1 Mathematical Modelling

In this section, we first have a look how a surface and an illumination model is formulated mathematically and then how they are connected to the perspective projection camera setup. Here, we mainly follow the concept from [29, 84, 85, 88].

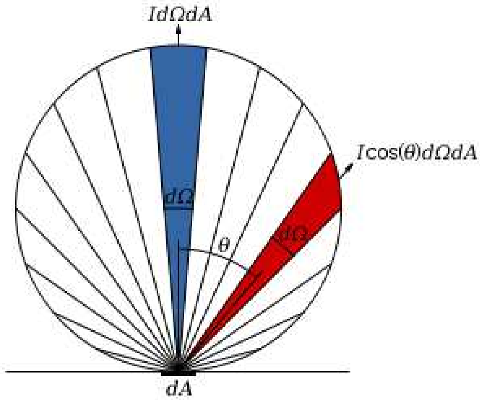

Figure 5.1: Lambert's cosine law. Each piece has same solid angle $d\Omega$. dA denotes area. Adapted from [2].

5.1.1 Lambertian Surfaces and Surface Parametrisation

Before we formulate the surface, we suppose the surface is Lambertian, which means that the surface has perfectly matte properties which adheres to Lambert's cosine law. The Lambert's cosine law in [57] states that the reflected radiant intensity in any direction of Lambertian surface depends only on the cosine of the angle θ between the surface normal and the light direction. As a direct consequence of Lambert's cosine law, the radiance[1] of that surface is the same regardless of the viewing angle, which can be formulated as

$$R(x_1, x_2, x_3) = \sigma \frac{\mathbf{n}}{|\mathbf{n}|} \cdot \mathbf{L}, \tag{5.1}$$

where $R(x_1, x_2, x_3)$ denotes reflected light intensity, $\mathbf{n}$ is for surface normal, σ is proportion factor and $|\cdot|$ Euclidean norm, see Figure 5.1.
Since the reconstructed scene in the Shape from Shading problem is represented by the surface $\mathcal{S}$, we assume that $\mathcal{S}$ can be parametrised by a function

$$S(x_1, x_2) : \overline{\Omega} \in \mathbb{R}^2 \mapsto \mathbb{R}^3, \tag{5.2}$$

where $\Omega \in \mathbb{R}^2$ is the rectangular image domain $]0, X[\times]0, Y[$. Therefore, the surface $\mathcal{S}$ can be formulated as following:

$$\mathcal{S} = \left\{ S(x_1, x_2) \in \mathbb{R}^3 | \, (x_1, x_2) \in \overline{\Omega} \right\}. \tag{5.3}$$

[1]Radiance is radiometric measurement which describes the amount of light that passes through or is emitted from a particular area, and falls within a given solid angle in a specific direction [76, 77]. The radiance is usually denoted as L and the SI unit of radiance is watt per steradian per square meter $\left[\mathbf{W} \cdot \mathbf{sr}^{-1} \cdot \mathbf{m}^{-2}\right]$. The corresponding photometric term is *luminance*.

5.1.2 Illumination Model and Brightness Equation

For the illumination model, we assume a single point light source and the light position is always known in order to avoid bas-relief ambiguity. This enables us to have the information about the unit light vector $\mathbf{L}$ pointing to the light source. The image intensity is modelled as a function $I(x_1, x_2)$ by

$$I(x_1, x_2) : \overline{\Omega} \mapsto [0, 1]\,. \tag{5.4}$$

In addition, the light intensity at each point on the surface $\mathcal{S}$ is assumed to be the same as the given image intensity $I(x_1, x_2)$. Therefore, for all $\mathbf{x} = (x_1, x_2) \in \overline{\Omega}$ the normalised image intensity $I(\mathbf{x})$ is the light intensity at the point $S(\mathbf{x})$ on the surface $\mathcal{S}$. With this assumption and (5.1) we have following *image irradiance*[2] *equation* (or sometimes called *brightness equation*)

$$I(\mathbf{x}) = \frac{\mathbf{n}}{|\mathbf{n}|} \cdot \mathbf{L}(S(\mathbf{x}))\,. \tag{5.5}$$

The next point we think about is the perspective projection camera setup. Comparing to the orthographic framework, a typical pinhole camera model is assumed here which is represented by its optical and its retinal plane. It is characterised by its focal length, see Figure 1.2b.

Light Source at Infinity

First, we assume that the light source is at the infinity. In this case, the scene is assumed to be parameterised by a surface $\mathcal{S}$ defined by

$$\mathcal{S} = \left\{ u(x_1, x_2) \begin{bmatrix} x_1 \\ x_2 \\ -\mathtt{f} \end{bmatrix} \middle| (x_1, x_2) \in \overline{\Omega} \right\}, \tag{5.6}$$

where $u(x_1, x_2)$ is the depth map that we are looking for and $\mathtt{f}$ is a focal length. Taking partial derivative of $\mathcal{S}$ with respect to x_1 gives

$$\mathcal{S}_{x_1} = \begin{bmatrix} u + x_1\, u_{x_1} \\ x_2\, u_{x_1} \\ -\mathtt{f}\, u_{x_1} \end{bmatrix}. \tag{5.7}$$

Analogously, we obtain the partial derivative of $\mathcal{S}$ with respect to x_2 as following

$$\mathcal{S}_{x_2} = \begin{bmatrix} x_1\, u_{x_2} \\ u + x_2\, u_{x_2} \\ -\mathtt{f}\, u_{x_2} \end{bmatrix}. \tag{5.8}$$

[2] Irradiance is radiometry terms which describes total amount of radiative flux incident upon a point on a surface from all directions above the surface ("hemisphere"). This can be calculated as an integration of radiance along the solid angle. It is usually denoted as E and its SI unit is watts per square meter $[\mathbf{W}/\mathbf{m}^2]$ [76, 77]. The corresponding phtometric terms is *illuminance.*

By taking the cross product between $\mathcal{S}_{x_1}$ and $\mathcal{S}_{x_2}$

$$\mathbf{n}(\mathbf{x}) = \mathcal{S}_{x_1} \times \mathcal{S}_{x_2} = \begin{bmatrix} \mathtt{f}\, u_{x1} \\ \mathtt{f}\, u_{x2} \\ u + (x_1 u_{x_1} + x_2 u_{x_2}) \end{bmatrix} \tag{5.9}$$

yields the surface normal vector $\mathbf{n}(\mathbf{x})$. The light can be represented by a constant unit vector $\mathbf{L} = (\alpha, \beta, \gamma)$, with $\gamma > 0$. By plugging (5.9) and light vector $\mathbf{L}$ into equation (5.5) we receive the following brightness equation

$$I(\mathbf{x}) = \frac{\mathtt{f}\,\mathbf{l} \cdot \nabla u(\mathbf{x}) + \gamma\,(\mathbf{x} \cdot \nabla u(\mathbf{x}) + u(\mathbf{x}))}{\sqrt{\mathtt{f}^2\,|\nabla u(\mathbf{x})|^2 + (\mathbf{x} \cdot \nabla u(\mathbf{x}) + u(\mathbf{x}))^2}}, \tag{5.10}$$

where $\mathbf{l} = (\alpha, \beta)$.

By changing the variable $v(\mathbf{x}) = \ln u(\mathbf{x})$, we obtain $\nabla v(\mathbf{x}) = \dfrac{\nabla u(\mathbf{x})}{u(\mathbf{x})}$. This can be confirmed as follows. Since $v(\mathbf{x}) = \ln u(\mathbf{x}) \;\Leftrightarrow\; v(x_1, x_2) = \ln u(x_1, x_2)$, we receive

$$\begin{aligned} v_{x_1} &= \frac{\partial v(x_1,x_2)}{\partial x_1} = \frac{\partial \ln u(x_1,x_2)}{\partial x_1} = \frac{1}{u}\frac{\partial u}{\partial x_1} = \frac{1}{u} u_{x_1}\,, \\ v_{x_2} &= \frac{\partial v(x_1,x_2)}{\partial x_2} = \frac{\partial \ln u(x_1,x_2)}{\partial x_2} = \frac{1}{u}\frac{\partial u}{\partial x_2} = \frac{1}{u} u_{x_2}\,. \end{aligned} \tag{5.11}$$

Plugging $\nabla u = u \nabla v$ into equation (5.10) gives

$$\begin{aligned} I(\mathbf{x}) &= \frac{\mathtt{f}\;\mathbf{l} \cdot u(\mathbf{x}) \nabla v(\mathbf{x}) + \gamma\,(\mathbf{x} \cdot u(\mathbf{x}) \nabla v(\mathbf{x}) + u(\mathbf{x}))}{\sqrt{\mathtt{f}^2\,|u(\mathbf{x}) \nabla v(\mathbf{x})|^2 + (\mathbf{x} \cdot u(\mathbf{x}) \nabla v(\mathbf{x})) + u(\mathbf{x}))^2}} \\ &= \frac{u(\mathbf{x})\,[\mathtt{f}\,\mathbf{l} \cdot \nabla v(\mathbf{x}) + \gamma\,(\mathbf{x} \cdot \nabla v(\mathbf{x}) + 1)]}{u(\mathbf{x}) \left[\sqrt{\mathtt{f}^2\,|\nabla v(\mathbf{x})|^2 + (\mathbf{x} \cdot \nabla v(\mathbf{x})) + 1)^2}\right]} \\ &= \frac{\mathtt{f}\,\mathbf{l} \cdot \nabla v(\mathbf{x}) + \gamma\,(\mathbf{x} \cdot \nabla v(\mathbf{x}) + 1)}{\sqrt{\mathtt{f}^2\,|\nabla v(\mathbf{x})|^2 + (\mathbf{x} \cdot \nabla v(\mathbf{x})) + 1)^2}}\,. \end{aligned} \tag{5.12}$$

Therefore, perspective Shape from Shading problem when the light source is at infinity corresponds to solve the following PDE

$$I(\mathbf{x}) \sqrt{\mathtt{f}^2\,|\nabla v(\mathbf{x})|^2 + (\mathbf{x} \cdot \nabla v(\mathbf{x}) + 1)^2} - (\mathtt{f}\;\mathbf{l} + \gamma\,\mathbf{x}) \cdot \nabla v(\mathbf{x}) - \gamma = 0\,. \tag{5.13}$$

Light Source at Optical Centre

Now, we consider the case when the light is at optical centre. For this case, as we can see in Figure 5.2, the surface $\mathcal{S}$ is parameterised by

$$\mathcal{S} = \left\{ \frac{\mathtt{f}}{\sqrt{|\mathbf{x}|^2 + \mathtt{f}^2}} u(x_1, x_2) \begin{bmatrix} x_1 \\ x_2 \\ -\mathtt{f} \end{bmatrix} \middle| (x_1, x_2) \in \overline{\Omega} \right\}. \tag{5.14}$$

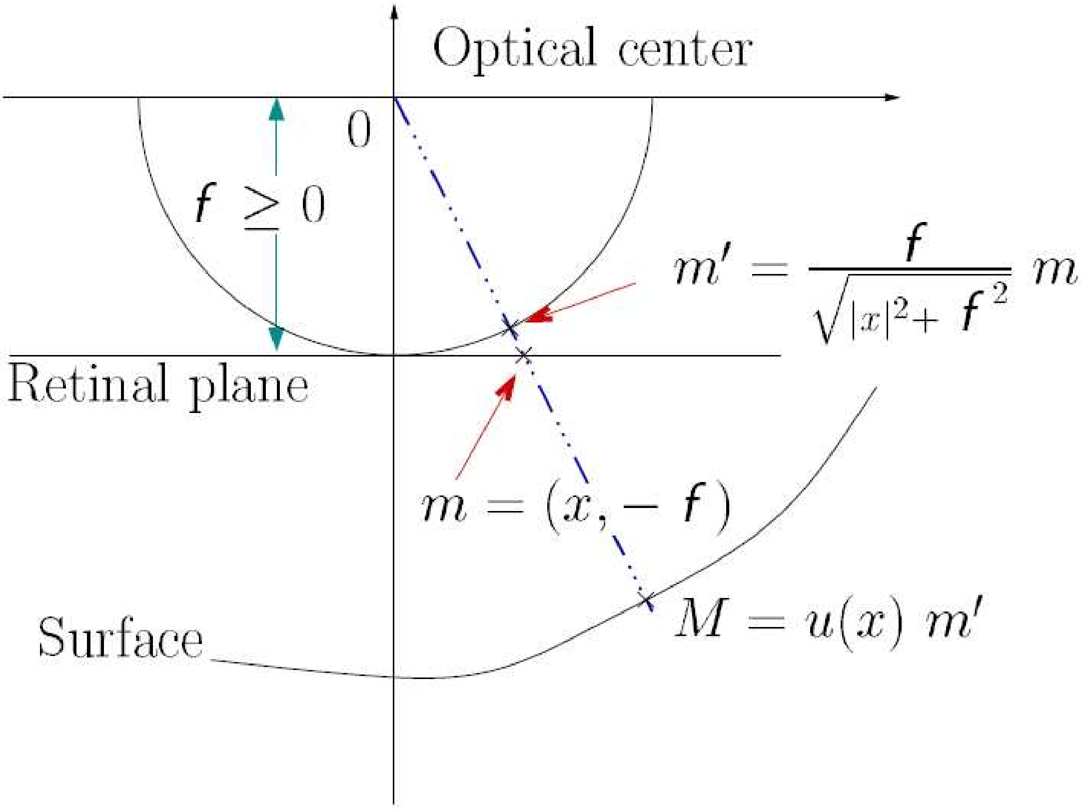

Figure 5.2: Perspective projection with a point light source located at the optical center. Adapted from [85].

The Figure 5.2 shows that the image intensity at the pixel $(\mathbf{x}, -f)$ is the intensity of the point on the surface $\mathcal{S}$. This framework is specially useful when a flash of a camera pops up in the night, or for endoscopy modelling.

Similar to the previous model, in order to find a surface normal vector we first take the partial derivative of $\mathcal{S}$ with respect to x_1

$$\mathcal{S}_{x_1} = \frac{\mathtt{f}}{\sqrt{|\mathbf{x}|^2 + \mathtt{f}^2}} \begin{bmatrix} (u + x_1 u_{x_1}) - \dfrac{x_1^2 u}{|\mathbf{x}|^2 + \mathtt{f}^2} \\ x_2 u_{x_1} - \dfrac{u x_2 x_1}{|\mathbf{x}|^2 + \mathtt{f}^2} \\ -\mathtt{f}\, u_{x_1} + \dfrac{\mathtt{f}\, u x_1}{|\mathbf{x}|^2 + \mathtt{f}^2} \end{bmatrix}. \tag{5.15}$$

Then, we compute the partial derivative of $\mathcal{S}$ with respect to x_2

$$\mathcal{S}_{x_2} = \frac{\mathtt{f}}{\sqrt{|\mathbf{x}|^2 + \mathtt{f}^2}} \begin{bmatrix} u_{x_2} x_1 - \dfrac{u x_2 x_1}{|\mathbf{x}|^2 + \mathtt{f}^2} \\ (u_{x_2} x_2 + u) - \dfrac{x_2^2 u}{|\mathbf{x}|^2 + \mathtt{f}^2} \\ -\mathtt{f} u_{x_2} + \dfrac{\mathtt{f}\, u x_2}{|\mathbf{x}|^2 + \mathtt{f}^2} \end{bmatrix}. \tag{5.16}$$

Thus, by taking cross product between $\mathcal{S}_{x_1}$ and $\mathcal{S}_{x_2}$ yields the surface normal vector

$$\mathbf{n}(\mathbf{x}) = \mathcal{S}_{x_1} \times \mathcal{S}_{x_2} = \begin{bmatrix} \mathtt{f} u_{x_1} \\ \mathtt{f} u_{x_2} \\ x_1 u_{x_1} + x_2 u_{x_2} \end{bmatrix} - \frac{\mathtt{f}}{|\mathbf{x}|^2 + \mathtt{f}^2} \begin{bmatrix} x_1 u \\ x_2 u \\ -\mathtt{f}\, u \end{bmatrix}. \tag{5.17}$$

In addition, as we can see in Figure 5.2 the single light source is located at the optical centre, the unit light vector $\mathbf{L}$ at point $S(\mathbf{x})$ is given by the vector

$$\mathbf{L}(S(\mathbf{x})) = \frac{1}{\sqrt{|\mathbf{x}|^2 + \mathtt{f}^2}} \begin{bmatrix} -x_1 \\ -x_2 \\ \mathtt{f} \end{bmatrix}. \tag{5.18}$$

Plugging (5.17) and (5.18) into the brightness equation (5.5) gives the PDE

$$I(\mathbf{x}) \sqrt{\left(\frac{|\mathbf{x}|^2 + \mathtt{f}^2}{\mathtt{f}^2}\right) \left[\mathtt{f}^2 |\nabla u(\mathbf{x})|^2 + (\nabla u(\mathbf{x}) \cdot \mathbf{x})^2\right] + u(\mathbf{x})^2} - u(\mathbf{x}) = 0. \tag{5.19}$$

As we did in the previous case, we plug the result $\nabla v(\mathbf{x}) = \dfrac{\nabla u(\mathbf{x})}{u(\mathbf{x})}$ of changing the variable $v(\mathbf{x}) = \ln u(\mathbf{x})$ into the PDE (5.19), we obtain the following brightness equation

$$\begin{aligned}
& I(\mathbf{x})\sqrt{\left(\frac{|\mathbf{x}|^2+\mathtt{f}^2}{\mathtt{f}^2}\right)\left[\mathtt{f}^2|\nabla u(\mathbf{x})|^2+(\nabla u(\mathbf{x})\cdot\mathbf{x})^2\right]+u(\mathbf{x})^2}-u(\mathbf{x}) &=& 0\\
\Leftrightarrow\ & I(\mathbf{x})\sqrt{\left(\frac{|\mathbf{x}|^2+\mathtt{f}^2}{\mathtt{f}^2}\right)\left[\mathtt{f}^2|u(\mathbf{x})\nabla v(\mathbf{x})|^2+(u(\mathbf{x})\nabla v(\mathbf{x})\cdot\mathbf{x})^2\right]+u(\mathbf{x})^2}-u(\mathbf{x}) &=& 0\\
\Leftrightarrow\ & I(\mathbf{x})\sqrt{\left(\frac{|\mathbf{x}|^2+\mathtt{f}^2}{\mathtt{f}^2}\right)u(\mathbf{x})^2\left[\mathtt{f}^2|\nabla v(\mathbf{x})|^2+(\nabla v(\mathbf{x})\cdot\mathbf{x})^2\right]+u(\mathbf{x})^2}-u(\mathbf{x}) &=& 0
\end{aligned}$$

assuming the Surface $\mathcal{S}$ is visible and $u(\mathbf{x}) \geq \dfrac{\sqrt{|\mathbf{x}|^2+\mathtt{f}^2}}{\mathtt{f}} \geq 1$ gives

$$\Leftrightarrow\ I(\mathbf{x})\sqrt{\left(\frac{|\mathbf{x}|^2+\mathtt{f}^2}{\mathtt{f}^2}\right)\left[\mathtt{f}^2|\nabla v(\mathbf{x})|^2+(\nabla v(\mathbf{x})\cdot\mathbf{x})^2\right]+1}-1 = 0. \tag{5.20}$$

This is equivalent to deal with the following PDE

$$I(\mathbf{x})\sqrt{\left[\mathtt{f}^2|\nabla v(\mathbf{x})|^2+(\nabla v(\mathbf{x})\cdot\mathbf{x})^2\right]+\frac{\mathtt{f}^2}{|\mathbf{x}|^2+\mathtt{f}^2}}-\frac{\mathtt{f}}{\sqrt{|\mathbf{x}|^2+\mathtt{f}^2}}=0. \tag{5.21}$$

Hence, as we can see in equation (5.13) and equation (5.21), Hamilton-Jacobi equations arise for the perspective Shape from Shading problems.

5.2 The Prados and Faugeras Model

In this section, we shall see how the perspective Shape from Shading model can be formulated under the framework called "generic" Hamiltonian which was proposed by Prados and Faugeras in [84, 85, 88]. Afterwards, we investigate the properties of Hamiltonian, which includes the convexity of the model.

5.2.1 Generic Hamiltonian

Motivation

In [84, 85, 88] Prados and Faugeras proposed a "generic" Hamiltonian which can unify both orthographic[3] and perspective Shape from Shading models. This generic Hamiltonian simplifies the formulation of the problem and, in particular, all theorems about

[3]Here, the orthographic Shape from Shading model means the one proposed by Rouy and Tourin in [26].

the characterisation and the approximation of the solution can be applied within this setup. Therefore, from a practical point of view, a unique code can be used to numerically solve these two problems. Another useful point is that it can give us the possibility of efficiency when we analyse the properites of Hamiltonian, e.g. convexity. However, one of the drawbacks of this framework is that it is not always possible to formulate the Shape from Shading problem with this method specially when we want to deal with a more complicated model.

Now, we are about to see how the generic Hamiltonian is organised.

As we already have seen in (5.21), when the light source is at optical centre, the Hamiltonian of the perspective projection model by Prados and Faugeras can be read as:

$$H_{\text{Foc}}^{\text{pers}}(\mathbf{x}, \nabla v) = I(\mathbf{x})\sqrt{\mathtt{f}^2|\nabla v|^2 + (\nabla v \cdot \mathbf{x})^2 + Q(\mathbf{x})^2} - Q(\mathbf{x}), \tag{5.22}$$

where $Q(\mathbf{x}) = \sqrt{\dfrac{\mathtt{f}^2}{|\mathbf{x}|^2 + \mathtt{f}^2}}$, $|\mathbf{x}| = \sqrt{x_1^2 + x_2^2}$ for $\mathbf{x} = (x_1, x_2)^{\mathrm{T}} \in \mathbb{R}^2$ denotes a Euclidean norm and $\mathtt{f}$ indicates the focal length of a camera.

Similarly, when the light source is at infinity, by (5.13) the Hamiltonian of the perspective projection model by Prados and Faugeras can be read as:

$$H_{\text{Inf}}^{\text{pers}}(\mathbf{x}, \nabla v) = I(\mathbf{x})\sqrt{\mathtt{f}^2|\nabla \mathbf{v}|^2 + (\mathbf{x} \cdot \nabla v + 1)^2} - (\mathtt{f}\,\mathbf{l} + \gamma\mathbf{x}) \cdot \nabla v - \gamma. \tag{5.23}$$

The proposition made by Prados and Faugeras in [84, 85, 88] was that both Hamiltonians, (5.22) and (5.23), are the special cases of the following "generic" Hamiltonian:

$$H_{\mathrm{g}}(\mathbf{x}, \mathbf{p}) = \widetilde{H}(\mathbf{x}, \mathbf{A}_{\mathbf{x}}\mathbf{p} + \mathbf{v}_{\mathbf{x}}) + \mathbf{w}_{\mathbf{x}} \cdot \mathbf{p} + c_{\mathbf{x}} \tag{5.24}$$

with $\widetilde{H}(\mathbf{x}, \mathbf{q}) = \kappa_{\mathbf{x}}\sqrt{|\mathbf{q}|^2 + K_{\mathbf{x}}^2}$,

- $\kappa_{\mathbf{x}} > 0$ and $K_{\mathbf{x}} \geq 0$,
- $\mathbf{A}_{\mathbf{x}} = \mathbf{D}_{\mathbf{x}}\mathbf{R}_{\mathbf{x}}$, where
  - $\mathbf{D}_{\mathbf{x}} = \begin{bmatrix} \mu_{\mathbf{x}} & 0 \\ 0 & \nu_{\mathbf{x}} \end{bmatrix}$, $\mu_{\mathbf{x}}, \nu_{\mathbf{x}} \neq 0$,
  - if $\mathbf{x} \neq \mathbf{0}$, $\mathbf{R}_{\mathbf{x}}$ is the rotation matrix: $\mathbf{R}_{\mathbf{x}} = \begin{bmatrix} \cos\theta & \sin\theta \\ -\sin\theta & \cos\theta \end{bmatrix}$, where $\cos\theta = \dfrac{x_2}{|\mathbf{x}|}$ and $\sin\theta = -\dfrac{x_1}{|\mathbf{x}|}$,
  - if $\mathbf{x} = \mathbf{0}$, $\mathbf{R}_{\mathbf{x}} = \begin{bmatrix} 1 & 0 \\ 0 & 1 \end{bmatrix}$;
- $\mathbf{v}_{\mathbf{x}}, \mathbf{w}_{\mathbf{x}} \in \mathbb{R}^2$

- $c_\mathbf{x} \in \mathbb{R}$.

The main point to validate this idea is to reformulate both (5.22) and (5.23) in terms of generic Hamiltonian notations. In other words, our major concern is to figure out how the expressions in $H_{\text{Inf}}^{\text{pers}}$[4] and $H_{\text{Foc}}^{\text{pers}}$[5] appear in the generic Hamiltonian $H_g(x,p)$. For this purpose, we use the following lemma from [84, 85]. In particular, this lemma is useful to find corresponding terms of (5.22) and (5.23) to $\mathbf{v_x}$ in (5.24). We describe here how it is achieved.

Lemma 5.2.1. *By*

$$\left| \begin{bmatrix} \mathtt{f}_1 & 0 \\ 0 & \sqrt{\mathtt{f}_1^2 + \mathtt{f}_2^2 |\mathbf{x}|^2} \end{bmatrix} \mathbf{R_x p} \right|^2 = \mathtt{f}_1^2 |\mathbf{p}|^2 + \mathtt{f}_2^2 (\mathbf{x}\cdot\mathbf{p})^2, \tag{5.25}$$

we have $\mathtt{f}^2 |\mathbf{p}|^2 + (\mathbf{x}\cdot\mathbf{p})^2 = |\mathbf{D_x R_x p}|^2$ *with* $\mu_\mathbf{x} = \mathtt{f}$ *and* $\nu_\mathbf{x} = \sqrt{\mathtt{f}^2 + |\mathbf{x}|^2}$.

We elaborate here on the proof given in [84, 85], clarifying thereby the steps within.

Proof. This lemma says that we can reformulate the expression $\mathtt{f}_1^2 |\mathbf{p}|^2 + \mathtt{f}_2^2 (\mathbf{x}\cdot\mathbf{p})^2$ as the Euclidean square norm of the matrix vector product $\mathbf{D_x R_x p}$. The proof proceeds in three steps. First, we begin with rewriting the matrix vector product $\mathbf{R_x p}$ with $\mathbf{x}$, $\mathbf{x}^\perp$ and $|\mathbf{x}|$. Then, we reformulate $\mathbf{D_x R_x p}$ using the previous result. Finally, computing the Euclidean norm square of $\mathbf{D_x R_x p}$ leads to the conclusion.

Let us denote $\mathbf{x}^\perp := \begin{bmatrix} x_2 \\ -x_1 \end{bmatrix}$ and $\mathbf{p} := \begin{bmatrix} p_1 \\ p_2 \end{bmatrix}$. Therefore, we have

$$\begin{aligned} \mathbf{R_x p} &= \frac{1}{|\mathbf{x}|} \begin{bmatrix} x_2 & -x_1 \\ x_1 & x_2 \end{bmatrix} \begin{bmatrix} p_1 \\ p_2 \end{bmatrix} \\ &= \frac{1}{|\mathbf{x}|} \begin{bmatrix} x_2 p_1 - x_2 p_2 \\ x_1 p_1 + x_2 p_2 \end{bmatrix} \\ &= \frac{1}{|\mathbf{x}|} \begin{bmatrix} \mathbf{x}^\perp \cdot \mathbf{p} \\ \mathbf{x}\cdot\mathbf{p} \end{bmatrix}. \end{aligned} \tag{5.26}$$

This leads to

$$\begin{aligned} \begin{bmatrix} \mathtt{f}_1 & 0 \\ 0 & \sqrt{\mathtt{f}_1^2 + \mathtt{f}_2^2 |\mathbf{x}|^2} \end{bmatrix} \mathbf{R_x p} &\overset{(5.26)}{=} \frac{1}{|\mathbf{x}|} \begin{bmatrix} \mathtt{f}_1 & 0 \\ 0 & \sqrt{\mathtt{f}_1^2 + \mathtt{f}_2^2 |\mathbf{x}|^2} \end{bmatrix} \begin{bmatrix} \mathbf{x}^\perp \cdot \mathbf{p} \\ \mathbf{x}\cdot\mathbf{p} \end{bmatrix} \\ &= \frac{1}{|\mathbf{x}|} \begin{bmatrix} \mathtt{f}_1 \left(\mathbf{x}^\perp \cdot \mathbf{p}\right) \\ \sqrt{\mathtt{f}_1^2 + \mathtt{f}_2^2 |\mathbf{x}|^2} \left(\mathbf{x}\cdot\mathbf{p}\right) \end{bmatrix}. \end{aligned} \tag{5.27}$$

[4] This Hamiltonian has been established by Prados and Faugeras in [31].
[5] This Hamiltonian has been introduced by Prados and Faugeras in [85, 88].

Computing the square norm of (5.27) yields:

$$
\begin{aligned}
& \left| \frac{1}{|\mathbf{x}|} \left[\frac{\mathtt{f}_1 \left(\mathbf{x}^\perp \cdot \mathbf{p} \right)}{\sqrt{\mathtt{f}_1^2 + \mathtt{f}_2^2 |\mathbf{x}|^2} (\mathbf{x} \cdot \mathbf{p})} \right] \right|^2 \\
= & \ \frac{1}{|\mathbf{x}|^2} \left[\mathtt{f}_1^2 \left(\mathbf{x}^\perp \cdot \mathbf{p} \right)^2 + \left(\mathtt{f}_1^2 + \mathtt{f}_2^2 |\mathbf{x}|^2 \right) (\mathbf{x} \cdot \mathbf{p})^2 \right] \\
= & \ \frac{1}{|\mathbf{x}|^2} \left[\mathtt{f}_1^2 \left(\mathbf{x}^\perp \cdot \mathbf{p} \right)^2 + \mathtt{f}_1^2 (\mathbf{x} \cdot \mathbf{p})^2 + \mathtt{f}_2^2 |\mathbf{x}|^2 (\mathbf{x} \cdot \mathbf{p})^2 \right] \\
= & \ \frac{1}{|\mathbf{x}|^2} \left[\mathtt{f}_1^2 \left(\left(\mathbf{x}^\perp \cdot \mathbf{p} \right)^2 + (\mathbf{x} \cdot \mathbf{p})^2 \right) + \mathtt{f}_2^2 |\mathbf{x}|^2 (\mathbf{x} \cdot \mathbf{p})^2 \right] \\
= & \ \frac{1}{|\mathbf{x}|^2} \left[\mathtt{f}_1^2 \left((x_2 p_1 - x_1 p_2)^2 + (x_1 p_1 + x_2 p_2)^2 \right) + \mathtt{f}_2^2 |\mathbf{x}|^2 (\mathbf{x} \cdot \mathbf{p})^2 \right] \\
= & \ \frac{1}{|\mathbf{x}|^2} \left[\mathtt{f}_1^2 \left[\left(x_2^2 p_1^2 - 2 x_1 x_2 p_1 p_2 + x_1^2 p_2^2 \right) + \left(x_1^2 p_1^2 + 2 x_1 x_2 p_1 p_2 + x_2^2 p_2^2 \right) \right] \right] \\
& \quad + \frac{1}{|\mathbf{x}|^2} \left[\mathtt{f}_2^2 |\mathbf{x}|^2 (\mathbf{x} \cdot \mathbf{p})^2 \right] \\
= & \ \frac{1}{|\mathbf{x}|^2} \left[\mathtt{f}_1^2 \left(x_2^2 p_1^2 + x_1^2 p_1^2 + x_1^2 p_2^2 + x_2^2 p_2^2 \right) + \mathtt{f}_2^2 |\mathbf{x}|^2 (\mathbf{x} \cdot \mathbf{p})^2 \right] \\
= & \ \frac{1}{|\mathbf{x}|^2} \left[\mathtt{f}_1^2 \left(p_1^2 \left(x_1^2 + x_2^2 \right) + p_2^2 \left(x_1^2 + x_2^2 \right) \right) + \mathtt{f}_2^2 |\mathbf{x}|^2 (\mathbf{x} \cdot \mathbf{p})^2 \right] \\
= & \ \frac{1}{|\mathbf{x}|^2} \left[\mathtt{f}_1^2 \underbrace{\left(p_1^2 + p_2^2 \right)}_{=|\mathbf{p}|^2} \underbrace{\left(x_1^2 + x_2^2 \right)}_{=|\mathbf{x}|^2} + \mathtt{f}_2^2 |\mathbf{x}|^2 (\mathbf{x} \cdot \mathbf{p})^2 \right] \\
= & \ \frac{1}{|\mathbf{x}|^2} \left[\mathtt{f}_1^2 |\mathbf{p}|^2 |\mathbf{x}|^2 + \mathtt{f}_2^2 |\mathbf{x}|^2 (\mathbf{x} \cdot \mathbf{p})^2 \right] \\
= & \ \frac{1}{|\mathbf{x}|^2} |\mathbf{x}|^2 \left[\mathtt{f}_1^2 |\mathbf{p}|^2 + \mathtt{f}_2^2 (\mathbf{x} \cdot \mathbf{p})^2 \right] \\
= & \ \mathtt{f}_1^2 |\mathbf{p}|^2 + \mathtt{f}_2^2 (\mathbf{x} \cdot \mathbf{p})^2 .
\end{aligned}
$$

□

By comparing $H_g(\mathbf{x}, \mathbf{p})$ from (5.24)

$$
H_g(\mathbf{x}, \mathbf{p}) = \kappa_{\mathbf{x}} \sqrt{|\mathbf{A}_{\mathbf{x}} \mathbf{p} + \mathbf{v}_{\mathbf{x}}|^2 + K_{\mathbf{x}}^2} + \mathbf{w}_{\mathbf{x}} \cdot \mathbf{p} + c_{\mathbf{x}},
$$

with H_{Foc}^{pers} from (5.22)

$$H_{Foc}^{pers}(\mathbf{x},\mathbf{p}) = I(\mathbf{x}) \sqrt{\underbrace{\mathtt{f}^2|\mathbf{p}|^2 + (\mathbf{p}\cdot\mathbf{x})^2}_{=|\mathbf{D_x R_x p}|^2} + \frac{\mathtt{f}^2}{\mathtt{f}^2+|\mathbf{x}|^2}} - \sqrt{\frac{\mathtt{f}^2}{\mathtt{f}^2+|\mathbf{x}|^2}},$$

and using Lemma 5.2.1, we obtain

$$\begin{aligned} \mu_\mathbf{x} &= \mathtt{f}, & \nu_\mathbf{x} &= \sqrt{\mathtt{f}^2+|\mathbf{x}|^2}, \\ \kappa_\mathbf{x} &= I(\mathbf{x}), & K_\mathbf{x} &= \sqrt{\frac{\mathtt{f}^2}{\mathtt{f}^2+|\mathbf{x}|^2}}, \\ \mathbf{w_x} &= \mathbf{0}, & \mathbf{v_x} &= \mathbf{0}, \\ c_\mathbf{x} &= -K_\mathbf{x}. \end{aligned} \tag{5.28}$$

Plugging this into the generic Hamiltonian (5.24) for the $H_{\text{Foc}}^{\text{pers}}$ model yields the expression

$$H_{\text{Foc}_\text{g}}^{\text{pers}}(\mathbf{x},\mathbf{p}) = I(\mathbf{x})\sqrt{|\mathbf{D_x R_x p}|^2 + K_\mathbf{x}^2} - K_\mathbf{x}, \tag{5.29}$$

where $\mathbf{D_x} = \begin{bmatrix} \mathtt{f} & 0 \\ 0 & \sqrt{\mathtt{f}^2+|\mathbf{x}|^2} \end{bmatrix}$, $\mathbf{R_x} = \frac{1}{|\mathbf{x}|}\begin{bmatrix} x_2 & -x_1 \\ x_1 & x_2 \end{bmatrix}$ and $K_\mathbf{x} = \sqrt{\frac{\mathtt{f}^2}{\mathtt{f}^2+|\mathbf{x}|^2}}$.

In an analogous way, we can also find the corresponding terms of $H_\text{g}(\mathbf{x},\mathbf{p})$ from (5.24) for $H_{\text{Inf}}^{\text{pers}}$ from (5.23):

$$\begin{aligned} \mu_\mathbf{x} &= \mathtt{f}, & \nu_\mathbf{x} &= \sqrt{\mathtt{f}^2+|\mathbf{x}|^2}, \\ \kappa_\mathbf{x} &= I(\mathbf{x}), & K_\mathbf{x} &= \sqrt{\frac{\mathtt{f}^2}{\mathtt{f}^2+|\mathbf{x}|^2}}, \\ \mathbf{w_x} &= -(\mathtt{f}\,\mathbf{1} + \gamma\mathbf{x}), & \mathbf{v_x} &= \mathbf{D_x}^{-1}\mathbf{R_x x} = \begin{bmatrix} 0 \\ \frac{|\mathbf{x}|}{\sqrt{\mathtt{f}^2+|\mathbf{x}|^2}} \end{bmatrix}, \\ c_\mathbf{x} &= -\gamma. \end{aligned} \tag{5.30}$$

Now, we are about to see how this is achieved.

As can be seen in the following, the main idea of doing this is to exploit the properties of diagonal and rotational matrix with the help of Lemma 5.2.1:

$$\begin{aligned}
\mathtt{f}^2 |\mathbf{p}|^2 + (\mathbf{x}\cdot\mathbf{p}+1)^2 &= \mathtt{f}^2 |\mathbf{p}|^2 + (\mathbf{x}\cdot\mathbf{p})^2 + 2(\mathbf{x}\cdot\mathbf{p}) + 1 \\
&\overset{\text{Lemma 5.2.1}}{=} |\mathbf{D_x R_x p}|^2 + 2(\mathbf{x}\cdot\mathbf{p}) + 1 \\
&= |\mathbf{D_x R_x p}|^2 + 2\mathbf{x}\cdot\left(\underbrace{\mathbf{R_x}^{-1}\mathbf{D_x}^{-1}\mathbf{D_x R_x}}_{=I}\mathbf{p}\right) + 1 \\
&\overset{(a)}{=} |\mathbf{D_x R_x p}|^2 + 2\left[\left(\mathbf{R_x}^{-1}\mathbf{D_x}^{-1}\right)^{\mathsf{T}}\mathbf{x}\right]\cdot(\mathbf{D_x R_x p}) + 1 \qquad (5.31) \\
&\overset{(b)}{=} |\mathbf{D_x R_x p}|^2 + 2\left[\mathbf{D_x}^{-1}\mathbf{R_x x}\right]\cdot(\mathbf{D_x R_x p}) + 1 \\
&\overset{(c)}{=} \left|\mathbf{D_x R_x p} + \left[\mathbf{D_x}^{-1}\mathbf{R_x x}\right]\right|^2 - \left|\mathbf{D_x}^{-1}\mathbf{R_x x}\right|^2 + 1 \\
&\overset{(d)}{=} \left|\mathbf{D_x R_x p} + \left[\mathbf{D_x}^{-1}\mathbf{R_x}\right]\right|^2 + K_{\mathbf{x}}^2 .
\end{aligned}$$

Here, we validate the steps indicated by (a) to (d) in the above computation. The (a) holds since

$$\begin{aligned}
\mathbf{x}\cdot\left(\mathbf{R_x}^{-1}\mathbf{D_x}^{-1}\mathbf{D_x R_x p}\right) &= \mathbf{x}^{\mathsf{T}}\left(\mathbf{R_x}^{-1}\mathbf{D_x}^{-1}\mathbf{D_x R_x p}\right) \\
&= \left(\mathbf{x}^{\mathsf{T}}\mathbf{R_x}^{-1}\mathbf{D_x}^{-1}\right)(\mathbf{D_x R_x}) \\
&= \left[\left(\mathbf{D_x}^{-1}\right)^{\mathsf{T}}\left(\mathbf{R_x}^{-1}\right)^{\mathsf{T}}\mathbf{x}\right]^{\mathsf{T}}(\mathbf{D_x R_x p}) \qquad (5.32) \\
&= \left[\left(\mathbf{D_x}^{-1}\right)^{\mathsf{T}}\left(\mathbf{R_x}^{-1}\right)^{\mathsf{T}}\mathbf{x}\right]\cdot(\mathbf{D_x R_x p}) \\
&= \left[\left(\mathbf{R_x}^{-1}\mathbf{D_x}^{-1}\right)^{\mathsf{T}}\mathbf{x}\right]\cdot(\mathbf{D_x R_x p}),
\end{aligned}$$

and (b) holds by the properties of orthogonal and diagonal matrix, i.e.:

$$\left(\mathbf{R_x}^{-1}\mathbf{D_x}^{-1}\right)^{\mathsf{T}} = \left(\mathbf{D_x}^{-1}\right)^{\mathsf{T}}\left(\mathbf{R_x}^{-1}\right)^{\mathsf{T}}$$

here, rotation matrix, $\mathbf{R_x}$, is an orthogonal matrix: $\mathbf{R_x}^{-1} = \mathbf{R_x}^{\mathsf{T}}$

$$= \left(\mathbf{D_x}^{-1}\right)^{\mathsf{T}}(\mathbf{R_x}^{\mathsf{T}})^{\mathsf{T}}$$

$\mathbf{D_x}$ is a diagonal matrix: $\left(\mathbf{D_x}^{-1}\right)^{\mathsf{T}} = \mathbf{D_x}^{-1}$

$$= \mathbf{D_x}^{-1}\mathbf{R_x}.$$

The transition to (c) is valid by the following fact:

$$|\mathbf{q}|^2 + 2\mathbf{v}\cdot\mathbf{q} = |\mathbf{q}+\mathbf{v}|^2 - |\mathbf{v}|^2 . \qquad (5.33)$$

When we plug $\mathbf{q} =: \mathbf{D_x R_x p}$ and $\mathbf{v} =: \mathbf{D_x}^{-1}\mathbf{R_x x}$ into equation (5.33), the assertion follows. Furthermore, we can also confirm that

$$
\begin{aligned}
\mathbf{D_x}^{-1}\mathbf{R_x x} &= \frac{1}{|\mathbf{x}|}\begin{bmatrix} \mathtt{f} & 0 \\ 0 & \sqrt{\mathtt{f}^2+|\mathbf{x}|^2} \end{bmatrix}^{-1}\begin{bmatrix} x_2 & -x_1 \\ x_1 & x_2 \end{bmatrix}\begin{bmatrix} x_1 \\ x_2 \end{bmatrix} \\
&= \frac{1}{|\mathbf{x}|}\begin{bmatrix} \frac{1}{\mathtt{f}} & 0 \\ 0 & \frac{1}{\sqrt{\mathtt{f}^2+|\mathbf{x}|^2}} \end{bmatrix}\begin{bmatrix} \underbrace{x_2x_1 - x_1x_2}_{=0} \\ \underbrace{x_1^2 + x_2^2}_{=|\mathbf{x}|^2} \end{bmatrix} \\
&= \begin{bmatrix} 0 \\ \frac{|\mathbf{x}|}{\sqrt{\mathtt{f}^2+|\mathbf{x}|^2}} \end{bmatrix}.
\end{aligned}
$$

The last step, (d), can be verified as

$$
\begin{aligned}
1 - \left|\mathbf{D_x}^{-1}\mathbf{R_x x}\right|^2 &= 1 - \left(\frac{|\mathbf{x}|}{\sqrt{\mathtt{f}^2+|\mathbf{x}|^2}}\right)^2 \\
&= \frac{\left(\mathtt{f}^2+|\mathbf{x}|^2\right) - |\mathbf{x}|^2}{\mathtt{f}^2+|\mathbf{x}|^2} \\
&= K_{\mathbf{x}}^2.
\end{aligned}
$$

Hence, another expression of generic Hamiltonian from (5.24) for $H_{\text{Inf}}^{\text{pers}}$ can be read as

$$
H_{\text{Inf}_g}^{\text{pers}}(\mathbf{x},\mathbf{p}) = I(\mathbf{x})\sqrt{\left|\mathbf{D_x R_x p} + \left[\mathbf{D_x}^{-1}\mathbf{R_x x}\right]\right|^2 + K_{\mathbf{x}}^2} + \mathbf{w_x}\cdot\mathbf{x} + c_{\mathbf{x}}\,, \tag{5.34}
$$

where $\mathbf{w_x} = -(\mathtt{f}\,\mathbf{1} + \gamma\,\mathbf{x})$ and $c_{\mathbf{x}} = -\gamma$.

5.2.2 Properties of the Hamiltonian

As we have seen in the preceding chapter, the convexity of a Hamiltonian plays a significant role on the solution theory. Therefore, it is worthwhile for us here to investigate the convexity of Prados and Faugeras model. With the help of generic Hamiltonian, we can treat convexity of the Hamiltonian efficiently, e.g. compare $H_{\text{Foc}}^{\text{pers}}$ with (5.22). In what follows, we substantiate the convexity of both Hamiltonians $H_{\text{Foc}}^{\text{pers}}$ and $H_{\text{Inf}}^{\text{pers}}$.

Positive Definite Matrices and Sylvester's Criterion

Before we go into the analysis of the convexity of the Hamiltonian, we should first decide which tool we are going to use to confirm the convexity. Since we are interested in the second derivative test to analyse Hessian matrix properties of the Hamiltonian, the Sylvester's criterion which can be found, for example, in [39, 52, 63, 64, 104] draws our attention. Thus, we look into this criterion.

Sylvester's criterion enables us to characterise the positive definite matrices without computing eingenvalues directly and can be explained by linear algebra knowledge. We begin here by giving a well-known definition of a positive definite matrix from which this criterion can be derived. To this end, we mainly follow the arguments in [19, 64, 98, 104]. Another approach and other properties of positive definite matrices can be found, e.g. in [38, 50, 62, 63, 104]. The definitions of principal submatrices and principal minors are borrowed from [39].

Having mentioned the background we need, we proceed to the definition of positive definite matrices.

Definition 5.2.1 (Positive Definite). A real and symmetric matrix $\mathbf{A} \in \mathbb{R}^{n\times n}$ is called *positive definite* if for every nonzero vector $\mathbf{x} \in \mathbb{R}^n$, $\mathbf{x}^{\mathrm{T}}\mathbf{A}\mathbf{x} > 0$.

This involves the following eingenvalue chracterisation of positive definite matrices as well.

Theorem 5.2.1. *A real and symmetric matrix $\mathbf{A} \in \mathbb{R}^{n\times n}$ is positive definite if and only if all its eigenvalues are positive.*

Proof. The sufficiency can be deduced from the definition of eigenvalues. The necessity is a direct consequence of the spectral theorem, e.g. which can be found in [52, 63, 104].

"⇒". We use the definition of eigenvalues for this direction.

Suppose that λ_i is eigenvalue of $\mathbf{A}$ and $\mathbf{x}_i$ is the corresponding unit eigenvector. Then, we can obtain the following

$$
\begin{array}{rrcl}
 & \mathbf{A}\mathbf{x}_i & = & \lambda_i \mathbf{x}_i \\
\Leftrightarrow & \mathbf{x}_i^T \mathbf{A}\mathbf{x}_i & = & \mathbf{x}_i^T \lambda_i \mathbf{x}_i \\
 & & & \lambda_i \text{ is scalar} \\
\Leftrightarrow & \mathbf{x}_i^T \mathbf{A}\mathbf{x}_i & = & \lambda_i \mathbf{x}_i^T \mathbf{x}_i \\
 & & & \mathbf{x}_i \text{ is a unit eigenvector so } \mathbf{x}_i^T\mathbf{x}_i = 1 \\
\Leftrightarrow & \mathbf{x}_i^T \mathbf{A}\mathbf{x}_i & = & \lambda_i \\
 & & & \text{since } \forall i \ \mathbf{x}_i^T \mathbf{A}\mathbf{x}_i > 0 \\
\Leftrightarrow & \mathbf{x}_i^T \mathbf{A}\mathbf{x}_i & = & \lambda_i > 0\,.
\end{array}
\tag{5.35}
$$

"⇐". For this direction we use the spectral theorem (also known as principal axis theorem), which states that a real symmetric matrix $\mathbf{A}$ can be factored into $\mathbf{P}^T\mathbf{A}\mathbf{P} = \mathbf{D}$, where a diagonal matrix $\mathbf{D} = \operatorname{diag}(\lambda_1, \lambda_2, \dots, \lambda_n)$ is real and $\mathbf{P}$ denotes an orthogonal matrix.

Let

$$\mathbf{y} = \mathbf{P}^T \mathbf{x}. \tag{5.36}$$

Since an orthogonal matrix $\mathbf{P}$ has the property of $\mathbf{P}^{-1} = \mathbf{P}^T$ we can derive

$$\mathbf{x} = \mathbf{P}\mathbf{y}. \tag{5.37}$$

Now, considering the quadratic form $\mathbf{x}^T\mathbf{A}\mathbf{x}$ with (5.37) gives

$$\begin{aligned}
\mathbf{x}^T\mathbf{A}\mathbf{x} &= (\mathbf{P}\mathbf{y})^T \mathbf{A} (\mathbf{P}\mathbf{y}) \\
&= \mathbf{y}^T\mathbf{P}^T\mathbf{A}\mathbf{P}\mathbf{y} \\
&\quad \text{by spectral theorem } \mathbf{P}^T\mathbf{A}\mathbf{P} = \mathbf{D} \\
&= \mathbf{y}^T\mathbf{D}\mathbf{y} \\
&= \sum_{i=1}^{n} \lambda_i y_i^2 \\
&\quad \text{since } \forall i\, \lambda_i > 0 \\
&= \sum_{i=1}^{n} \lambda_i y_i^2 > 0.
\end{aligned} \tag{5.38}$$

This holds for all $\mathbf{x} \neq \mathbf{0}$. □

Another definition that we need is about principal submatrices and principal minors.

Definition 5.2.2 (Principal Submatrix and Principal Minor). Let $\mathbf{A} \in \mathbb{R}^{n\times n}$ be a matrix. For $1 \leq k \leq n$, the *k-th principal submatrix of* $\mathbf{A}$ is the $k \times k$ submatrix formed from the first k rows and first k columns of $\mathbf{A}$. Hence, there are n principal submatrices for $\mathbf{A} \in \mathbb{R}^{n\times n}$.

$$\mathbf{A}_1 = [\mathbf{a}_{11}], \quad \mathbf{A}_2 = \begin{bmatrix} \mathbf{a}_{11} & \mathbf{a}_{12} \\ \mathbf{a}_{21} & \mathbf{a}_{22} \end{bmatrix}, \quad \mathbf{A}_3 = \begin{bmatrix} \mathbf{a}_{11} & \mathbf{a}_{12} & \mathbf{a}_{13} \\ \mathbf{a}_{21} & \mathbf{a}_{22} & \mathbf{a}_{23} \\ \mathbf{a}_{31} & \mathbf{a}_{32} & \mathbf{a}_{33} \end{bmatrix},$$
$$\mathbf{A}_4 = \begin{bmatrix} \mathbf{a}_{11} & \mathbf{a}_{12} & \mathbf{a}_{13} & \mathbf{a}_{14} \\ \mathbf{a}_{21} & \mathbf{a}_{22} & \mathbf{a}_{23} & \mathbf{a}_{24} \\ \mathbf{a}_{31} & \mathbf{a}_{32} & \mathbf{a}_{33} & \mathbf{a}_{34} \\ \mathbf{a}_{41} & \mathbf{a}_{42} & \mathbf{a}_{34} & \mathbf{a}_{44} \end{bmatrix}, \quad \ldots, \quad \mathbf{A}_n = \begin{bmatrix} \mathbf{a}_{11} & \mathbf{a}_{12} & \cdots & \mathbf{a}_{1n} \\ \mathbf{a}_{21} & \mathbf{a}_{22} & \cdots & \mathbf{a}_{2n} \\ \vdots & \vdots & \ddots & \vdots \\ \mathbf{a}_{n1} & \mathbf{a}_{n2} & \cdots & \mathbf{a}_{nn} \end{bmatrix}. \tag{5.39}$$

Its determinant is the k-th *principal minor*

$$\mathbf{a}_{11}, \quad \begin{vmatrix} \mathbf{a}_{11} & \mathbf{a}_{12} \\ \mathbf{a}_{21} & \mathbf{a}_{22} \end{vmatrix}, \quad \begin{vmatrix} \mathbf{a}_{11} & \mathbf{a}_{12} & \mathbf{a}_{13} \\ \mathbf{a}_{21} & \mathbf{a}_{22} & \mathbf{a}_{23} \\ \mathbf{a}_{31} & \mathbf{a}_{32} & \mathbf{a}_{33} \end{vmatrix},$$
$$\begin{vmatrix} \mathbf{a}_{11} & \mathbf{a}_{12} & \mathbf{a}_{13} & \mathbf{a}_{14} \\ \mathbf{a}_{21} & \mathbf{a}_{22} & \mathbf{a}_{23} & \mathbf{a}_{24} \\ \mathbf{a}_{31} & \mathbf{a}_{32} & \mathbf{a}_{33} & \mathbf{a}_{34} \\ \mathbf{a}_{41} & \mathbf{a}_{42} & \mathbf{a}_{43} & \mathbf{a}_{44} \end{vmatrix}, \quad \ldots, \quad \begin{vmatrix} \mathbf{a}_{11} & \mathbf{a}_{12} & \cdots & \mathbf{a}_{1n} \\ \mathbf{a}_{21} & \mathbf{a}_{22} & \cdots & \mathbf{a}_{2n} \\ \vdots & \vdots & \ddots & \vdots \\ \mathbf{a}_{n1} & \mathbf{a}_{n2} & \cdots & \mathbf{a}_{nn} \end{vmatrix}. \tag{5.40}$$

As we have seen the principal minors above, let us think about the following lemma. This lemma is useful for the proof of sufficiency in Sylvester's criterion.

Lemma 5.2.2. *Let*

$$\mathbf{A} = \begin{bmatrix} \mathbf{A}_{n-1} & \mathbf{a}_n \\ \mathbf{a}_n^T & a_{nn} \end{bmatrix} \tag{5.41}$$

be an n-th order symmetric real matrix, where $\mathbf{A}_{n-1} \in \mathbb{R}^{(n-1)\times(n-1)}$ *the symmetric submatrix consisting of first* $n-1$ *rows and columns of* $\mathbf{A}$*. In addition,* $\mathbf{a}_n \in \mathbb{R}^{(n-1)\times 1}$ *and* $\mathbf{a}_n^T \in \mathbb{R}^{1\times(n-1)}$ *are vectors consisting of last column and last row of* $\mathbf{A}$ *without* $a_{nn} \in \mathbb{R}$*. Then, if* $\mathbf{A}_{n-1}$ *is nonsingular, there is a nonsingular matrix* $\mathbf{P}$ *such that*

$$\mathbf{P}^T\mathbf{A}\mathbf{P} = \begin{bmatrix} \mathbf{A}_{n-1} & \mathbf{0} \\ \mathbf{0}^\mathbf{T} & b_{nn} \end{bmatrix}. \tag{5.42}$$

If, in addition, $\det \mathbf{A}_{n-1}$ *and* $\det \mathbf{A}$ *are positive, then* a_{nn} *is positive.*

Here, we elaborate on the proof given in [98], thereby clarify the steps therein.

Proof. The main point of this proof is to construct the matrix $\mathbf{P}$ using some linear algebra knowledge. Then, we can come to the conclusion by the assupmtion without any pain.

Since $\mathbf{A}_{n-1}$ is nonsingular, there is a unique nontrivial solution of

$$\mathbf{A}_{n-1}\mathbf{p} = \mathbf{a}_n\,. \tag{5.43}$$

This indicates that $\mathbf{a}_n$ can be uniquely represented as a linear combination of column vectors of $\mathbf{A}$. When we think of (5.41) as

$$\mathbf{A} = \left[\begin{array}{c|c} \begin{bmatrix} \\ \mathbf{a}_1 \\ \\ \end{bmatrix} \cdots \begin{bmatrix} \\ \mathbf{a}_{n-1} \\ \\ \end{bmatrix} & \mathbf{a}_n \\ \hline \mathbf{a}^T & a_{nn} \end{array}\right], \tag{5.44}$$

we receive

$$\mathbf{a}_n \;=\; \alpha_1 \begin{bmatrix} \\ \mathbf{a}_1 \\ \\ \end{bmatrix} + \cdots + \alpha_{n-1} \begin{bmatrix} \\ \mathbf{a}_{n-1} \\ \\ \end{bmatrix} \tag{5.45}$$

and

$$\mathbf{a}_n^T \;=\; \alpha_1\mathbf{a}_1^T + \cdots + \alpha_{n-1}\mathbf{a}_{n-1}^T, \tag{5.46}$$

where $\alpha_1, \ldots, \alpha_{n-1}$ are the corresponding coefficients for the solution of (5.43).

Constructing the matrix $\mathbf{P}^T$ by replacing the last rows of the identity matrix with

$$\left[\underbrace{-\alpha_1, \ldots, -\alpha_{n-1}, 1}_{:=\mathbf{q}_{n-1}^T} \right], \tag{5.47}$$

gives

$$\begin{aligned}
\mathbf{P}^T\mathbf{A}\mathbf{P} &= \left[\begin{array}{ccc|c} 1 & & & \\ & \ddots & & \mathbf{0} \\ & & 1 & \\ \hline -\alpha_1 & \cdots & -\alpha_{n-1} & 1 \end{array}\right] \left[\begin{array}{ccc|c} \begin{bmatrix} \mathbf{a}_1 \end{bmatrix} & \cdots & \begin{bmatrix} \mathbf{a}_{n-1} \end{bmatrix} & \mathbf{a}_n \\ \hline & \mathbf{a}^T & & a_{nn} \end{array}\right] \left[\begin{array}{ccc|c} 1 & & & -\alpha_1 \\ & \ddots & & \vdots \\ & & 1 & -\alpha_{n-1} \\ \hline & \mathbf{0^T} & & 1 \end{array}\right] \\
&= \left[\begin{array}{c|c} \begin{bmatrix} \mathbf{a}_1 \end{bmatrix} \cdots \begin{bmatrix} \mathbf{a}_{n-1} \end{bmatrix} & \mathbf{a}_n \\ \hline \underbrace{\underbrace{-\alpha_1\mathbf{a}_1^T - \cdots - \alpha_{n-1}\mathbf{a}_{n-1}^T}_{\overset{(5.46)}{=} -\mathbf{a}^T} + \mathbf{a}^T}_{=\mathbf{0}^T} & \underbrace{\mathbf{q}_{n-1}^T\mathbf{a}_n}_{\text{by (5.47)}} + a_{nn} \end{array}\right] \left[\begin{array}{ccc|c} 1 & & & -\alpha_1 \\ & \ddots & & \vdots \\ & & 1 & -\alpha_{n-1} \\ \hline & \mathbf{0^T} & & 1 \end{array}\right] \\
&= \left[\begin{array}{c|c} \begin{bmatrix} \mathbf{a}_1 \end{bmatrix} \cdots \begin{bmatrix} \mathbf{a}_{n-1} \end{bmatrix} & \underbrace{\underbrace{-\alpha_1\mathbf{a}_1 \cdots - \alpha_{n-1}\mathbf{a}_{n-1}}_{\overset{(5.45)}{=} -\mathbf{a}_n} + \mathbf{a}_n}_{=\mathbf{0}} \\ \hline \mathbf{0}^T & \mathbf{q}_{n-1}^T\mathbf{a}_n + a_{nn} \end{array}\right] \\
&= \begin{bmatrix} \mathbf{A}_{n-1} & \mathbf{0} \\ \mathbf{0^T} & b_{nn} \end{bmatrix}.
\end{aligned} \tag{5.48}$$

Since $\mathbf{P}$ is nonsingular, by means of the properties of determinants we can derive

$$\begin{aligned} \det \mathbf{P}^T\mathbf{A}\mathbf{P} &= \det\mathbf{P}^T \det\mathbf{A} \det\mathbf{P} \\ & \quad \text{since } \det\mathbf{P}^T = \det\mathbf{P} \\ &= (\det\mathbf{P})^2 \underbrace{\det\mathbf{A}}_{>0} \\ &= b_{nn} \underbrace{\det\mathbf{A}_{n-1}}_{>0}. \end{aligned} \tag{5.49}$$

Considering the assumptions $\det\mathbf{A}_n > 0$ and $\det\mathbf{A}_{n-1} > 0$ in (5.49), b_{nn} must be positive. Thus, the assertion follows. □

As we have all the background that we need, we now present the Sylvester's criterion.

Theorem 5.2.2 (Sylvester's Criterion). *A real and symmetric matrix $\mathbf{A} \in \mathbb{R}^{n\times n}$ is positive definite if and only if all its principal minors are positive.*

The proof given here is the detailed version whose exposition is based on [24, 98, 104].

Proof. For the necessity case, we can directly derive from the Definition 5.2.1 with the Theorem 5.2.1 and the sufficiency can be shown by mathematical induction with the Lemma 5.2.2.

"⇒". The idea of this direction is to consider vectors $\mathbf{x}_k$ whose first k elements are nonzero and whose last $n-k$ elements are all zero $\mathbf{x} = \left[\begin{array}{c|c} \underbrace{\mathbf{x}_k^T}_{\in\mathbb{R}^{1\times k}} & \underbrace{\mathbf{0}^T}_{\in\mathbb{R}^{1\times(n-k)}} \end{array}\right]^T$. This vector allows us to extract the k-th principal submatrices of $\mathbf{A}$ and we can directly see the result. So, the corresponding quadratic form is

$$
\begin{aligned}
\mathbf{x}^T\mathbf{A}\mathbf{x} &= \underbrace{\left[\begin{array}{c|c} \underbrace{\mathbf{x}_k^T}_{\in\mathbb{R}^{1\times k}} & \underbrace{\mathbf{0}^T}_{\in\mathbb{R}^{1\times(n-k)}} \end{array}\right]}_{\in\mathbb{R}^{1\times n}} \underbrace{\left[\begin{array}{c|c} \underbrace{\mathbf{A}_k}_{\in\mathbb{R}^{k\times k}} & \underbrace{\mathbf{B}}_{\in\mathbb{R}^{k\times(n-k)}} \\ \hline \underbrace{\mathbf{B}^T}_{\in\mathbb{R}^{(n-k)\times k}} & \underbrace{\mathbf{C}}_{\in\mathbb{R}^{(n-k)\times(n-k)}} \end{array}\right]}_{\in\mathbb{R}^{n\times n}} \underbrace{\left[\begin{array}{c} \underbrace{\mathbf{x}_k}_{\in\mathbb{R}^{k\times 1}} \\ \hline \underbrace{\mathbf{0}}_{\in\mathbb{R}^{(n-k)\times 1}} \end{array}\right]}_{\in\mathbb{R}^{n\times 1}} \\
&= \underbrace{\left[\begin{array}{c|c} \underbrace{\mathbf{x}_k^T\mathbf{A}_k}_{\in\mathbb{R}^{1\times k}} + \underbrace{\mathbf{0}^T\mathbf{B}^T}_{\in\mathbb{R}^{1\times k}} & \underbrace{\mathbf{x}_k^T\mathbf{B}}_{\in\mathbb{R}^{1\times(n-k)}} + \underbrace{\mathbf{0}^T\mathbf{C}}_{\in\mathbb{R}^{1\times(n-k)}} \end{array}\right]}_{\in\mathbb{R}^{1\times n}} \underbrace{\left[\begin{array}{c} \underbrace{\mathbf{x}_k}_{\in\mathbb{R}^{k\times 1}} \\ \hline \underbrace{\mathbf{0}}_{\in\mathbb{R}^{(n-k)\times 1}} \end{array}\right]}_{\in\mathbb{R}^{n\times 1}} \\
&= \underbrace{\left[\begin{array}{c|c} \underbrace{\mathbf{x}_k^T\mathbf{A}_k}_{\in\mathbb{R}^{1\times k}} & \underbrace{\mathbf{x}_k^T\mathbf{B}}_{\in\mathbb{R}^{1\times(n-k)}} \end{array}\right]}_{\in\mathbb{R}^{1\times n}} \underbrace{\left[\begin{array}{c} \underbrace{\mathbf{x}_k}_{\in\mathbb{R}^{k\times 1}} \\ \hline \underbrace{\mathbf{0}}_{\in\mathbb{R}^{(n-k)\times 1}} \end{array}\right]}_{\in\mathbb{R}^{n\times 1}} \\
&= \mathbf{x}_k^T\mathbf{A}_k\mathbf{x}_k\,.
\end{aligned} \tag{5.50}
$$

Since the original quadratic form $\mathbf{x}^T\mathbf{A}\mathbf{x}$ is assumed to be positive definite, so does that of principal submatrices $\mathbf{x}_k^T\mathbf{A}_k\mathbf{x}_k$ by (5.50). As k can be varied from 1 to n, this includes $\mathbf{A}$ itself. This implies that all eigenvalues of principal submatrices of $\mathbf{A}$ are positive by the Theorem 5.2.1. Therefore, from the fact that a determinant of a matrix is multiplication of all its eigenvalues, all determinants of principal submatrices are positive.

"$\Leftarrow$". As mentioned above, we make use of a mathematical induction.

For the base case when $n = 1$, it is clear that the statement holds, as there is only one element in the matrix and the element itself is a determinant of a matrix.

For the induction hypothesis, let us suppose that the it is true when $n-1$ and let $\mathbf{A}$ be an n-th order symmetric matrix with positive leading principal minors.

Now comes to the inductive step. By the induction hypothesis $\mathbf{A}$ fulfils the conditions of the Lemma 5.2.2. Therefore, positive definiteness of $\mathbf{x}^T \mathbf{A}\mathbf{x}$ is equivalent to that of

$$\begin{aligned}
\mathbf{x}^T \mathbf{P}^T \mathbf{A}\mathbf{P}\mathbf{x} &\overset{(5.42)}{=} \mathbf{x}^T \begin{bmatrix} \mathbf{A}_{n-1} & \mathbf{0} \\ \mathbf{0}^{\mathbf{T}} & b_{nn} \end{bmatrix} \mathbf{x} \\
&= \left[\underbrace{\mathbf{x}_{n-1}^T}_{\in\mathbb{R}^{1\times(n-1)}} \middle| \underbrace{x_n}_{\in\mathbb{R}} \right] \left[\begin{array}{c|c} \underbrace{\mathbf{A}_{n-1}}_{\in\mathbb{R}^{(n-1)\times(n-1)}} & \underbrace{\mathbf{0}}_{\in\mathbb{R}^{(n-1)\times 1}} \\ \hline \underbrace{\mathbf{0}^{\mathbf{T}}}_{\in\mathbb{R}^{1\times(n-1)}} & \underbrace{b_{nn}}_{\in\mathbb{R}} \end{array} \right] \left[\begin{array}{c} \underbrace{\mathbf{x}_{n-1}}_{\in\mathbb{R}^{(n-1)\times 1}} \\ \hline \underbrace{x_n}_{\in\mathbb{R}} \end{array} \right] \\
&= \left[\underbrace{\mathbf{x}_{n-1}^T \mathbf{A}_{n-1}}_{\in\mathbb{R}^{1\times(n-1)}} \middle| \underbrace{x_n b_{nn}}_{\in\mathbb{R}} \right] \left[\begin{array}{c} \underbrace{\mathbf{x}_{n-1}}_{\in\mathbb{R}^{(n-1)\times 1}} \\ \hline \underbrace{x_n}_{\in\mathbb{R}} \end{array} \right] \\
&= \mathbf{x}_{n-1}^T \mathbf{A}_{n-1} \mathbf{x}_{n-1} + x_n^2 b_{nn}\,,
\end{aligned} \tag{5.51}$$

where $\mathbf{x}_{n-1}$ denotes the first $n-1$ elements in $\mathbf{x}_n$.

Following the induction hypothesis the first term of (5.51) is positive definite, since every principal minor of $\mathbf{A}$ is also the principal minor of $\mathbf{A}_{n-1}$. In addition, the second term is also positive by the Lemma 5.2.2. □

Convexity of $H_{\mathrm{Foc}}^{\mathrm{pers}}$

In order to verify the convexity of H with respect to p, we deal with the properties of the generic Hamiltonian. For this, we use the formulations of H in the generic terms, c.f. (5.28) and (5.29).

Since rotation matrix, $\mathbf{R}_\mathbf{x}$, is a unitary matrix, we can rewrite and expand (5.29) as following:

$$\begin{aligned}
H_{\mathrm{Foc_g}}^{\mathrm{pers}}(\mathbf{x},\mathbf{p}) &= I(\mathbf{x})\sqrt{|\mathbf{D_x R_x p}|^2 + K_\mathbf{x}^2} - K_\mathbf{x} \\
&= I(\mathbf{x})\sqrt{|\mathbf{D_x p}|^2 + K_\mathbf{x}^2} - K_\mathbf{x} \\
&= I(\mathbf{x})\sqrt{\left| \begin{bmatrix} \mathtt{f} & 0 \\ 0 & \sqrt{\mathtt{f}^2 + |\mathbf{x}|^2} \end{bmatrix} \begin{bmatrix} p_1 \\ p_2 \end{bmatrix} \right|^2 + K_\mathbf{x}^2} - K_\mathbf{x} \\
&= I(\mathbf{x})\sqrt{\left| \begin{bmatrix} \mathtt{f} p_1 \\ \sqrt{\mathtt{f}^2 + |\mathbf{x}|^2} p_2 \end{bmatrix} \right|^2 + K_\mathbf{x}^2} - K_\mathbf{x} \\
&= I(\mathbf{x})\sqrt{\mathtt{f}^2 p_1^2 + (\mathtt{f}^2 + |\mathbf{x}|^2)\, p_2^2 + K_\mathbf{x}^2} - K_\mathbf{x}\,,
\end{aligned} \tag{5.52}$$

where $K_\mathbf{x} = \sqrt{\dfrac{\mathtt{f}^2}{\mathtt{f}^2 + |\mathbf{x}|^2}}$.

Now, we are checking the properties of Hessian matrix of

$$h(p_1, p_2) =: I(\mathbf{x})\sqrt{\mathtt{f}^2 p_1^2 + (\mathtt{f}^2 + |\mathbf{x}|^2)\, p_2^2 + K_{\mathbf{x}}^2} - K_{\mathbf{x}} \tag{5.53}$$

First, taking partial derivatives of $h(p_1, p_2)$ with respect to each variable p_1 and p_2 leads to

$$h_{p_1} = I(\mathbf{x})\frac{\mathtt{f}^2 p_1}{\sqrt{\mathtt{f}^2 p_1^2 + (\mathtt{f}^2 + |\mathbf{x}|^2)\, p_2^2 + K_{\mathbf{x}}^2}}, \tag{5.54}$$

$$h_{p_2} = I(\mathbf{x})\frac{\left(\mathtt{f}^2 + |\mathbf{x}|^2\right) p_2}{\sqrt{\mathtt{f}^2 p_1^2 + (\mathtt{f}^2 + |\mathbf{x}|^2)\, p_2^2 + K_{\mathbf{x}}^2}}. \tag{5.55}$$

Computing the second partial derivatives yields:

$$Hess(h) = \begin{bmatrix} h_{p_1 p_1} & h_{p_1 p_2} \\ h_{p_2 p_1} & h_{p_2 p_2} \end{bmatrix}, \tag{5.56}$$

where

$$\begin{aligned} h_{p_1 p_1} &= I(\mathbf{x})\frac{\mathtt{f}^2\sqrt{\mathtt{f}^2 p_1^2 + (\mathtt{f}^2 + |\mathbf{x}|^2)\, p_2^2 + K_{\mathbf{x}}^2} - \dfrac{\mathtt{f}^4 p_1^2}{\sqrt{\mathtt{f}^2 p_1^2 + (\mathtt{f}^2 + |\mathbf{x}|^2)\, p_2^2 + K_{\mathbf{x}}^2}}}{\left(\sqrt{\mathtt{f}^2 p_1^2 + (\mathtt{f}^2 + |\mathbf{x}|^2)\, p_2^2 + K_{\mathbf{x}}^2}\right)^2} \\ &= I(\mathbf{x})\frac{\mathtt{f}^2\left(\mathtt{f}^2 p_1^2 + \left(\mathtt{f}^2 + |\mathbf{x}|^2\right) p_2^2 + K_{\mathbf{x}}^2\right) - \mathtt{f}^4 p_1^2}{\left(\sqrt{\mathtt{f}^2 p_1^2 + (\mathtt{f}^2 + |\mathbf{x}|^2)\, p_2^2 + K_{\mathbf{x}}^2}\right)^3} \\ &= I(\mathbf{x})\frac{\mathtt{f}^2\left(\left(\mathtt{f}^2 + |\mathbf{x}|^2\right) p_2^2 + K_{\mathbf{x}}^2\right)}{\left(\sqrt{\mathtt{f}^2 p_1^2 + (\mathtt{f}^2 + |\mathbf{x}|^2)\, p_2^2 + K_{\mathbf{x}}^2}\right)^3} > 0, \end{aligned} \tag{5.57}$$

$$
\begin{aligned}
h_{p_2p_2} &= I(\mathbf{x})\frac{\left(\mathtt{f}^2+|\mathbf{x}|^2\right)\sqrt{\mathtt{f}^2p_1^2+\left(\mathtt{f}^2+|\mathbf{x}|^2\right)p_2^2+K_{\mathbf{x}}^2}}{\left(\sqrt{\mathtt{f}^2p_1^2+\left(\mathtt{f}^2+|\mathbf{x}|^2\right)p_2^2+K_{\mathbf{x}}^2}\right)^2} \\
&\quad - I(\mathbf{x})\frac{\left(\mathtt{f}^2+|\mathbf{x}|^2\right)p_2\dfrac{\left(\mathtt{f}^2+|\mathbf{x}|^2\right)p_2}{\sqrt{\mathtt{f}^2p_1^2+\left(\mathtt{f}^2+|\mathbf{x}|^2\right)p_2^2+K_{\mathbf{x}}^2}}}{\left(\sqrt{\mathtt{f}^2p_1^2+\left(\mathtt{f}^2+|\mathbf{x}|^2\right)p_2^2+K_{\mathbf{x}}^2}\right)^2} \qquad (5.58)\\
&= I(\mathbf{x})\frac{\left(\mathtt{f}^2+|\mathbf{x}|^2\right)\left(\mathtt{f}^2p_1^2+\left(\mathtt{f}^2+|\mathbf{x}|^2\right)p_2^2+K_{\mathbf{x}}^2\right)-\left(\mathtt{f}^2+|\mathbf{x}|^2\right)^2p_2^2}{\left(\sqrt{\mathtt{f}^2p_1^2+\left(\mathtt{f}^2+|\mathbf{x}|^2\right)p_2^2+K_{\mathbf{x}}^2}\right)^3} \\
&= I(\mathbf{x})\frac{\left(\mathtt{f}^2+|\mathbf{x}|^2\right)\left(\mathtt{f}^2p_1^2+K_{\mathbf{x}}^2\right)}{\left(\sqrt{\mathtt{f}^2p_1^2+\left(\mathtt{f}^2+|\mathbf{x}|^2\right)p_2^2+K_{\mathbf{x}}^2}\right)^3} > 0,
\end{aligned}
$$

and

$$
\begin{aligned}
h_{p_1p_2} &= I(\mathbf{x})\frac{0-\mathtt{f}^2p_1\dfrac{\left(\mathtt{f}^2+|\mathbf{x}|^2\right)p_2}{\sqrt{\mathtt{f}^2p_1^2+\left(\mathtt{f}^2+|\mathbf{x}|^2\right)p_2^2+K_{\mathbf{x}}^2}}}{\left(\sqrt{\mathtt{f}^2p_1^2+\left(\mathtt{f}^2+|\mathbf{x}|^2\right)p_2^2+K_{\mathbf{x}}^2}\right)^2} \qquad (5.59)\\
&= -I(\mathbf{x})\frac{\mathtt{f}^2\left(\mathtt{f}^2+|\mathbf{x}|^2\right)p_1p_2}{\left(\sqrt{\mathtt{f}^2p_1^2+\left(\mathtt{f}^2+|\mathbf{x}|^2\right)p_2^2+K_{\mathbf{x}}^2}\right)^3},
\end{aligned}
$$

$$
\begin{aligned}
h_{p_2p_1} &= I(\mathbf{x})\frac{0-\left(\mathtt{f}^2+|\mathbf{x}|^2\right)p_2\dfrac{\mathtt{f}^2p_1}{\sqrt{\mathtt{f}^2p_1^2+\left(\mathtt{f}^2+|\mathbf{x}|^2\right)p_2^2+K_{\mathbf{x}}^2}}}{\left(\sqrt{\mathtt{f}^2p_1^2+\left(\mathtt{f}^2+|\mathbf{x}|^2\right)p_2^2+K_{\mathbf{x}}^2}\right)^2} \qquad (5.60)\\
&= -I(\mathbf{x})\frac{\mathtt{f}^2\left(\mathtt{f}^2+|\mathbf{x}|^2\right)p_1p_2}{\left(\sqrt{\mathtt{f}^2p_1^2+\left(\mathtt{f}^2+|\mathbf{x}|^2\right)p_2^2+K_{\mathbf{x}}^2}\right)^3}.
\end{aligned}
$$

This confirms $h_{p_1p_2} = h_{p_2p_1}$.

Assuming image intensity $I(x)$ and focal length $\mathtt{f}$ are not zero gives $h_{p_1p_1} > 0$ and $h_{p_2p_2} >$

0. In addition, computing the determinant of $Hess(h)$ gives

$$
\begin{aligned}
&|Hess(h)| \\
&= I(\mathbf{x})^2 \frac{\mathtt{f}^2\left(\left(\mathtt{f}^2+|\mathbf{x}|^2\right)p_2^2+K_{\mathbf{x}}^2\right)\left(\mathtt{f}^2+|\mathbf{x}|^2\right)\left(\mathtt{f}^2p_1^2+K_{\mathbf{x}}^2\right)}{\left(\sqrt{\mathtt{f}^2p_1^2+\left(\mathtt{f}^2+|\mathbf{x}|^2\right)p_2^2+K_{\mathbf{x}}^2}\right)^6} \\
&\quad - I(\mathbf{x})^2 \frac{\left[\mathtt{f}^2\left(\mathtt{f}^2+|\mathbf{x}|^2\right)p_1p_2\right]^2}{\left(\sqrt{\mathtt{f}^2p_1^2+\left(\mathtt{f}^2+|\mathbf{x}|^2\right)p_2^2+K_{\mathbf{x}}^2}\right)^6} \\
&= I(\mathbf{x})^2 \frac{\mathtt{f}^2\left(\left(\mathtt{f}^2+|\mathbf{x}|^2\right)p_2^2+K_{\mathbf{x}}^2\right)\left(\mathtt{f}^2+|\mathbf{x}|^2\right)\left(\mathtt{f}^2p_1^2+K_{\mathbf{x}}^2\right)}{\left(\sqrt{\mathtt{f}^2p_1^2+\left(\mathtt{f}^2+|\mathbf{x}|^2\right)p_2^2+K_{\mathbf{x}}^2}\right)^6} \\
&\quad - I(\mathbf{x})^2 \frac{\mathtt{f}^4\left(\mathtt{f}^2+|\mathbf{x}|^2\right)^2p_1^2p_2^2}{\left(\sqrt{\mathtt{f}^2p_1^2+\left(\mathtt{f}^2+|\mathbf{x}|^2\right)p_2^2+K_{\mathbf{x}}^2}\right)^6} \\
&= I(\mathbf{x})^2\mathtt{f}^2\underbrace{\left(\mathtt{f}^2+|\mathbf{x}|^2\right)}_{=:A>0} \frac{\left(\underbrace{\left(\mathtt{f}^2+|\mathbf{x}|^2\right)}_{=:A>0}p_2^2+K_{\mathbf{x}}^2\right)\left(\mathtt{f}^2p_1^2+K_{\mathbf{x}}^2\right)}{\left(\sqrt{\mathtt{f}^2p_1^2+\left(\mathtt{f}^2+|\mathbf{x}|^2\right)p_2^2+K_{\mathbf{x}}^2}\right)^6} \\
&\quad - I(\mathbf{x})^2\mathtt{f}^2\underbrace{\left(\mathtt{f}^2+|\mathbf{x}|^2\right)}_{=:A>0} \frac{\mathtt{f}^2\overbrace{\left(\mathtt{f}^2+|\mathbf{x}|^2\right)}^{=:A>0}p_1^2p_2^2}{\left(\sqrt{\mathtt{f}^2p_1^2+\left(\mathtt{f}^2+|\mathbf{x}|^2\right)p_2^2+K_{\mathbf{x}}^2}\right)^6} \\
&= I(\mathbf{x})^2\mathtt{f}^2A \frac{\left(Ap_2^2+K_{\mathbf{x}}^2\right)\left(\mathtt{f}^2p_1^2+K_{\mathbf{x}}^2\right)-\mathtt{f}^2Ap_1^2p_2^2}{\left(\sqrt{\mathtt{f}^2p_1^2+\left(\mathtt{f}^2+|\mathbf{x}|^2\right)p_2^2+K_{\mathbf{x}}^2}\right)^6} \\
&= I(\mathbf{x})^2\mathtt{f}^2A \frac{A\mathtt{f}^2p_1^2p_2^2+AK_{\mathbf{x}}^2p_2^2+\mathtt{f}^2p_1^2K_{\mathbf{x}}^2+K_{\mathbf{x}}^4-\mathtt{f}^2Ap_1^2p_2^2}{\left(\sqrt{\mathtt{f}^2p_1^2+\left(\mathtt{f}^2+|\mathbf{x}|^2\right)p_2^2+K_{\mathbf{x}}^2}\right)^6} \\
&= I(\mathbf{x})^2\mathtt{f}^2A \frac{AK_{\mathbf{x}}^2p_2^2+\mathtt{f}^2p_1^2K_{\mathbf{x}}^2+K_{\mathbf{x}}^4}{\left(\sqrt{\mathtt{f}^2p_1^2+\left(\mathtt{f}^2+|\mathbf{x}|^2\right)p_2^2+K_{\mathbf{x}}^2}\right)^6} > 0.
\end{aligned}
\tag{5.61}
$$

As we can see in (5.57) and (5.61), $h_{p_1p_1}$ and determinant of Hessian matrix of are both positive, so the convexity of h holds by the Theorem 5.2.1.

Convexity of $H_{\text{Inf}}^{\text{pers}}$

For the case of $H_{\text{Inf}}^{\text{pers}}$, see (5.23) and (5.34), we can also reformulate the Hamiltonian using the generic formulation as in the previous case:

$$
\begin{aligned}
&H_{\text{Inf}_g}^{\text{pers}}(\mathbf{x},\mathbf{p}) \\
&= I(\mathbf{x})\sqrt{\left|\mathbf{D_x R_x p} + \left[\mathbf{D_x}^{-1}\mathbf{R_x x}\right]\right|^2 + K_{\mathbf{x}}^2} + \mathbf{w_x}\cdot\mathbf{p} + c_{\mathbf{x}} \\
&= I(\mathbf{x})\sqrt{\left|\mathbf{D_x p} + \left[\mathbf{D_x}^{-1}\mathbf{x}\right]\right|^2 + K_{\mathbf{x}}^2} + \mathbf{w_x}\cdot\mathbf{p} + c_{\mathbf{x}} \\
&= I(\mathbf{x})\sqrt{\left|\begin{bmatrix} \mathtt{f} & 0 \\ 0 & \sqrt{\mathtt{f}^2+|\mathbf{x}|^2}\end{bmatrix}\begin{bmatrix} p_1 \\ p_2\end{bmatrix} + \begin{bmatrix} \frac{1}{\mathtt{f}} & 0 \\ 0 & \frac{1}{\sqrt{\mathtt{f}^2+|\mathbf{x}|^2}}\end{bmatrix}\begin{bmatrix} x_1 \\ x_2\end{bmatrix}\right|^2 + K_{\mathbf{x}}^2} + \mathbf{w_x}\cdot\mathbf{p} + c_{\mathbf{x}} \\
&= I(\mathbf{x})\sqrt{\left|\begin{bmatrix} f p_1 \\ \sqrt{\mathtt{f}^2+|\mathbf{x}|^2}p_2\end{bmatrix} + \begin{bmatrix} \frac{1}{\mathtt{f}}x_1 \\ \frac{1}{\sqrt{\mathtt{f}^2+|\mathbf{x}|^2}}x_2\end{bmatrix}\right|^2 + K_{\mathbf{x}}^2} + \mathbf{w_x}\cdot\mathbf{p} + c_{\mathbf{x}} \\
&= I(\mathbf{x})\sqrt{\left|\begin{bmatrix} \mathtt{f} p_1 + \frac{1}{\mathtt{f}}x_1 \\ \sqrt{f^2+|\mathbf{x}|^2}p_2 + \frac{1}{\sqrt{\mathtt{f}^2+|\mathbf{x}|^2}}x_2\end{bmatrix}\right|^2 + K_{\mathbf{x}}^2} + \mathbf{w_x}\cdot\mathbf{p} + c_{\mathbf{x}} \\
&= I(\mathbf{x})\sqrt{\left(\mathtt{f} p_1 + \underbrace{\frac{1}{\mathtt{f}}x_1}_{=:\,\alpha}\right)^2 + \left(\sqrt{\mathtt{f}^2+|\mathbf{x}|^2}p_2 + \underbrace{\frac{1}{\sqrt{\mathtt{f}^2+|\mathbf{x}|^2}}x_2}_{=:\,\beta}\right)^2 + K_{\mathbf{x}}^2} + \mathbf{w_x}\cdot\mathbf{p} + c_{\mathbf{x}},
\end{aligned}
\tag{5.62}
$$

where $K_{\mathbf{x}} = \sqrt{\frac{\mathtt{f}^2}{\mathtt{f}^2+|\mathbf{x}|^2}}$, $\mathbf{w_x} = -(\mathtt{f}\,\mathbf{1} + \gamma\,\mathbf{x})$, and $c_{\mathbf{x}} = -\gamma$.

Therefore, we only need to analyse the properties of Hessian matrix of

$$
d(p_1,p_2) =: \sqrt{(\mathtt{f}p_1+\alpha)^2 + \left(\sqrt{\mathtt{f}^2+|\mathbf{x}|^2}p_2+\beta\right)^2 + K_{\mathbf{x}}^2}, \tag{5.63}
$$

because $(\mathbf{w_x}\cdot\mathbf{p} + c_{\mathbf{x}})$ does not give a contribution to the second derivatives with respect to $\mathbf{p}$.

Taking partial derivatives of $d(p_1,p_2)$ with respect to each variable p_1 and p_2 leads to

$$d_{p_1} = \frac{(\mathtt{f}p_1+\alpha)\,\mathtt{f}}{\sqrt{(\mathtt{f}p_1+\alpha)^2+\left(\sqrt{\mathtt{f}^2+|\mathbf{x}|^2}p_2+\beta\right)^2+K_{\mathbf{x}}^2}} \tag{5.64}$$

and

$$d_{p_2} = \frac{\left(\sqrt{\mathtt{f}^2+|\mathbf{x}|^2}p_2+\beta\right)\sqrt{\mathtt{f}^2+|\mathbf{x}|^2}}{\sqrt{(\mathtt{f}p_1+\alpha)^2+\left(\sqrt{\mathtt{f}^2+|\mathbf{x}|^2}p_2+\beta\right)^2+K_{\mathbf{x}}^2}}. \tag{5.65}$$

With taking second derivatives of d, we can compute the Hessian matrix of d as following

$$Hess(d) = \begin{bmatrix} d_{p_1p_1} & d_{p_1p_2} \\ d_{p_2p_1} & d_{p_2p_2} \end{bmatrix}, \tag{5.66}$$

where

$$\begin{aligned} d_{p_1p_1} &= \frac{\mathtt{f}^2\sqrt{(\mathtt{f}p_1+\alpha)^2+\left(\sqrt{\mathtt{f}^2+|\mathbf{x}|^2}p_2+\beta\right)^2+K_{\mathbf{x}}^2}}{\left(\sqrt{(\mathtt{f}p_1+\alpha)^2+\left(\sqrt{\mathtt{f}^2+|\mathbf{x}|^2}p_2+\beta\right)^2+K_{\mathbf{x}}^2}\right)^2} \\ &\quad - \frac{(\mathtt{f}p_1+\alpha)\,\mathtt{f}\dfrac{(\mathtt{f}p_1+\alpha)\,\mathtt{f}}{\sqrt{(\mathtt{f}p_1+\alpha)^2+\left(\sqrt{\mathtt{f}^2+|\mathbf{x}|^2}p_2+\beta\right)^2+K_{\mathbf{x}}^2}}}{\left(\sqrt{(\mathtt{f}p_1+\alpha)^2+\left(\sqrt{\mathtt{f}^2+|\mathbf{x}|^2}p_2+\beta\right)^2+K_{\mathbf{x}}^2}\right)^2} \\ &= \frac{\mathtt{f}^2\left[(\mathtt{f}p_1+\alpha)^2+\left(\sqrt{\mathtt{f}^2+|\mathbf{x}|^2}p_2+\beta\right)^2+K_{\mathbf{x}}^2\right]-(\mathtt{f}p_1+\alpha)^2\mathtt{f}^2}{\left(\sqrt{(\mathtt{f}p_1+\alpha)^2+\left(\sqrt{\mathtt{f}^2+|\mathbf{x}|^2}p_2+\beta\right)^2+K_{\mathbf{x}}^2}\right)^3} \\ &= \frac{\mathtt{f}^2\left[\left(\sqrt{\mathtt{f}^2+|\mathbf{x}|^2}p_2+\beta\right)^2+K_{\mathbf{x}}^2\right]}{\left(\sqrt{(\mathtt{f}p_1+\alpha)^2+\left(\sqrt{\mathtt{f}^2+|\mathbf{x}|^2}p_2+\beta\right)^2+K_{\mathbf{x}}^2}\right)^3} > 0, \end{aligned} \tag{5.67}$$

$$\begin{aligned}
d_{p_2p_2} &= \frac{\left(\mathtt{f}^2+|\mathbf{x}|^2\right)\left[(\mathtt{f}p_1+\alpha)^2+\left(\sqrt{\mathtt{f}^2+|\mathbf{x}|^2}p_2+\beta\right)^2+K_{\mathbf{x}}^2\right]}{\left(\sqrt{(\mathtt{f}p_1+\alpha)^2+\left(\sqrt{\mathtt{f}^2+|\mathbf{x}|^2}p_2+\beta\right)^2+K_{\mathbf{x}}^2}\right)^3} \\
&\quad -\frac{\left(\sqrt{\mathtt{f}^2+|\mathbf{x}|^2}p_2+\beta\right)^2\left(\mathtt{f}^2+|\mathbf{x}|^2\right)}{\left(\sqrt{(\mathtt{f}p_1+\alpha)^2+\left(\sqrt{\mathtt{f}^2+|\mathbf{x}|^2}p_2+\beta\right)^2+K_{\mathbf{x}}^2}\right)^3} \\
&= \frac{\left(\mathtt{f}^2+|\mathbf{x}|^2\right)\left[(\mathtt{f}p_1+\alpha)^2+K_{\mathbf{x}}^2\right]}{\left(\sqrt{(\mathtt{f}p_1+\alpha)^2+\left(\sqrt{\mathtt{f}^2+|\mathbf{x}|^2}p_2+\beta\right)^2+K_{\mathbf{x}}^2}\right)^3},
\end{aligned} \tag{5.68}$$

and

$$\begin{aligned}
h_{p_1p_2} &= \frac{0-(\mathtt{f}p_1+\alpha)\,\mathtt{f}\dfrac{\left(\sqrt{\mathtt{f}^2+|\mathbf{x}|^2}p_2+\beta\right)\sqrt{\mathtt{f}^2+|\mathbf{x}|^2}}{\sqrt{(\mathtt{f}p_1+\alpha)^2+\left(\sqrt{\mathtt{f}^2+|\mathbf{x}|^2}p_2+\beta\right)^2+K_{\mathbf{x}}^2}}}{\left(\sqrt{(\mathtt{f}p_1+\alpha)^2+\left(\sqrt{\mathtt{f}^2+|\mathbf{x}|^2}p_2+\beta\right)^2+K_{\mathbf{x}}^2}\right)^2} \\
&= -\frac{(\mathtt{f}p_1+\alpha)\,\mathtt{f}\left(\sqrt{\mathtt{f}^2+|\mathbf{x}|^2}p_2+\beta\right)\sqrt{\mathtt{f}^2+|\mathbf{x}|^2}}{\left(\sqrt{(\mathtt{f}p_1+\alpha)^2+\left(\sqrt{\mathtt{f}^2+|\mathbf{x}|^2}p_2+\beta\right)^2+K_{\mathbf{x}}^2}\right)^3},
\end{aligned} \tag{5.69}$$

$$\begin{aligned}
h_{p_2p_1} &= \frac{0-\left(\sqrt{\mathtt{f}^2+|\mathbf{x}|^2}p_2+\beta\right)\sqrt{\mathtt{f}^2+|\mathbf{x}|^2}\dfrac{(\mathtt{f}p_1+\alpha)\,\mathtt{f}}{\sqrt{(\mathtt{f}p_1+\alpha)^2+\left(\sqrt{\mathtt{f}^2+|\mathbf{x}|^2}p_2+\beta\right)^2+K_{\mathbf{x}}^2}}}{\left(\sqrt{(\mathtt{f}p_1+\alpha)^2+\left(\sqrt{\mathtt{f}^2+|\mathbf{x}|^2}p_2+\beta\right)^2+K_{\mathbf{x}}^2}\right)^2} \\
&= -\frac{\left(\sqrt{\mathtt{f}^2+|\mathbf{x}|^2}p_2+\beta\right)\sqrt{\mathtt{f}^2+|\mathbf{x}|^2}\,(\mathtt{f}p_1+\alpha)\,\mathtt{f}}{\left(\sqrt{(\mathtt{f}p_1+\alpha)^2+\left(\sqrt{\mathtt{f}^2+|\mathbf{x}|^2}p_2+\beta\right)^2+K_{\mathbf{x}}^2}\right)^3}.
\end{aligned} \tag{5.70}$$

This verifies $d_{p_1p_2} = d_{p_2p_1}$.

Hence, the determinant of Hessian matrix is given by

$$
\begin{aligned}
&|Hess(d)| \\
&= \frac{\mathtt{f}^2 \left[\left(\sqrt{\mathtt{f}^2 + |\mathbf{x}|^2} p_2 + \beta \right)^2 + K_{\mathbf{x}}^2 \right] \left(\mathtt{f}^2 + |\mathbf{x}|^2 \right) \left[\left(\mathtt{f} p_1 + \alpha \right)^2 + K_{\mathbf{x}}^2 \right]}{\left(\sqrt{\left(\mathtt{f} p_1 + \alpha \right)^2 + \left(\sqrt{\mathtt{f}^2 + |\mathbf{x}|^2} p_2 + \beta \right)^2 + K_{\mathbf{x}}^2} \right)^6} \\
&\quad - \frac{\left(\mathtt{f} p_1 + \alpha \right)^2 \mathtt{f}^2 \left(\sqrt{\mathtt{f}^2 + |\mathbf{x}|^2} p_2 + \beta \right)^2 \left(\mathtt{f}^2 + |\mathbf{x}|^2 \right)}{\left(\sqrt{\left(\mathtt{f} p_1 + \alpha \right)^2 + \left(\sqrt{\mathtt{f}^2 + |\mathbf{x}|^2} p_2 + \beta \right)^2 + K_{\mathbf{x}}^2} \right)^6} \\
&= \mathtt{f}^2 \left(\mathtt{f}^2 + |\mathbf{x}|^2 \right) \frac{\left[\underbrace{\left(\sqrt{\mathtt{f}^2 + |\mathbf{x}|^2} p_2 + \beta \right)^2}_{=:A>0} + K_{\mathbf{x}}^2 \right] \left[\underbrace{\left(\mathtt{f} p_1 + \alpha \right)^2}_{=:B>0} + K_{\mathbf{x}}^2 \right]}{\left(\sqrt{\left(\mathtt{f} p_1 + \alpha \right)^2 + \left(\sqrt{\mathtt{f}^2 + |\mathbf{x}|^2} p_2 + \beta \right)^2 + K_{\mathbf{x}}^2} \right)^6} \\
&\quad - \mathtt{f}^2 \left(\mathtt{f}^2 + |\mathbf{x}|^2 \right) \frac{\underbrace{\left(\mathtt{f} p_1 + \alpha \right)^2}_{=:B>0} \underbrace{\left(\sqrt{\mathtt{f}^2 + |\mathbf{x}|^2} p_2 + \beta \right)^2}_{=:A>0}}{\left(\sqrt{\left(\mathtt{f} p_1 + \alpha \right)^2 + \left(\sqrt{\mathtt{f}^2 + |\mathbf{x}|^2} p_2 + \beta \right)^2 + K_{\mathbf{x}}^2} \right)^6} \\
&= \frac{\mathtt{f}^2 \left(\mathtt{f}^2 + |\mathbf{x}|^2 \right) \left[\left(B + K_{\mathbf{x}}^2 \right) \left(A + K_{\mathbf{x}}^2 \right) - BA \right]}{\left(\sqrt{\left(\mathtt{f} p_1 + \alpha \right)^2 + \left(\sqrt{\mathtt{f}^2 + |\mathbf{x}|^2} p_2 + \beta \right)^2 + K_{\mathbf{x}}^2} \right)^6} \\
&= \frac{\mathtt{f}^2 \left(\mathtt{f}^2 + |\mathbf{x}|^2 \right) \left[K_{\mathbf{x}}^4 + (A + B) K_{\mathbf{x}}^2 + AB - AB \right]}{\left(\sqrt{\left(\mathtt{f} p_1 + \alpha \right)^2 + \left(\sqrt{\mathtt{f}^2 + |\mathbf{x}|^2} p_2 + \beta \right)^2 + K_{\mathbf{x}}^2} \right)^6} \\
&= \frac{\mathtt{f}^2 \left(\mathtt{f}^2 + |\mathbf{x}|^2 \right) \left[K_{\mathbf{x}}^2 + (A + B) \right] K_{\mathbf{x}}^2}{\left(\sqrt{\left(\mathtt{f} p_1 + \alpha \right)^2 + \left(\sqrt{\mathtt{f}^2 + |\mathbf{x}|^2} p_2 + \beta \right)^2 + K_{\mathbf{x}}^2} \right)^6} > 0 .
\end{aligned}
\tag{5.71}
$$

This verifies the positive definiteness of $H_{\mathrm{Inf}}^{\mathrm{pers}}$ by the Theorem 5.2.2.

5.3 Well-posedness of Prados and Faugeras Model

So far, we have investigated the properties of Hamiltonian proposed by Prados and Faugeras. In this section, we shall think about the well-posedness of Prados and Faugeras model by taking the viscosity framework into account.

Shape from Shading has been a central problem in computer vision and also well known that this problem is ill-posed as we have discussed in Section 4.4. In the work of Prados and Faugeras [85, 88], they have tried to reformulate the problem using generic Hamiltonian in such a way that it can be interpreted as a well-posed problem in the viscosity sense. However, as we have seen in Remark 4.3.1, it has limitations owing to the properties of an eikonal-type Hamiltonian.

In this section, we investigate the requirements for the existence and uniqueness of the Prados and Faugeras model. To this end, we make use of the theorem adjusted to the Prados and Faugeras model which can be found in [84, 85, 88] based on the theory that we have studied in Chapter 3 and Chapter 4.

5.3.1 Existence of Continuous Viscosity Solutions

The following theorem summarises all the points that we need. After we discuss why we need these conditions, we shall check wheter the Prados and Faugeras models satisfy the requirements.

Theorem 5.3.1 (Existence of Continuous Viscosity Solutions for the Prados Model). *If*

(E1) [**Regularity**] $H \in C^0(\overline{\Omega} \times \mathbb{R}^2)$,

(E2) [**Convexity**] *H is convex with respect to $\mathbf{p}$ for all $\mathbf{x}$ in $\overline{\Omega}$,*

(E3) [**Subsolution**] $\inf_{\mathbf{p} \in \mathbb{R}^2} H(\mathbf{x}, \mathbf{p}) \leq 0$ *in* $\overline{\Omega}$,

(E4) [**Uniform Coercivity**] *$H(\mathbf{x}, \mathbf{p}) \to +\infty$ when $|\mathbf{p}| \to +\infty$ uniformly with respect to $\mathbf{x} \in \overline{\Omega}$,*

(E5) [**Compatibility**] *For all $\mathbf{x}, \mathbf{y} \in \partial\Omega$ if $\varphi(\mathbf{x}) - \varphi(\mathbf{y}) \leq L(\mathbf{x}, \mathbf{y})$ holds then the function u defined in $\overline{\Omega}$ by*

$$u(\mathbf{x}) = \inf_{\mathbf{y} \in \partial\Omega} \{\varphi(\mathbf{y}) + L(\mathbf{x}, \mathbf{y})\} \tag{5.72}$$

$$= \inf \left\{ \int_0^{T_0} H^*\left(\xi(s), -\xi'(s)\right) ds + \varphi(\xi(T_0)) \right\} \tag{5.73}$$

is a continuous viscosity solution of equation (in particular u verifies $u(\mathbf{x}) = \varphi(\mathbf{x})$ for all $\mathbf{x}$ in $\partial\Omega$), where $\mathbf{p}$ denotes ∇u.

Remark 5.3.1. (E1) [**Regularity**] Regarding regularity, the Hamiltonian must satisfy regularity, since we seek continuous soluions.

(E2) [**Convexity**] In order to apply the theory that we have investigated, the convexity of Hamiltonian is crucial.

(E3) [**Subsolution**] As we have seen in Section 2.3, a viscosity subsolution plays an essential role since we deal with a convex Hamiltonian.

(E4) [**Uniform Coercivity**] As discussed in 2.4.3 and 3.2.3, Hamiltonian should be at least uniform coercive when the Legendre transform of Hamiltonian is finite.

(E5) [**Compatibility**] Since the compatibility condition is necessary and sufficient condition for the existence of solutions by Remark 3.2.1, it must be fulfilled as well.

Thus, the model should be investigated whether all of these conditions are fulfilled. We examine one by one.

Before going into analysis, we first see the following lemma and proposition which will be used for the property of uniform coercivity for the Prados and Faugeras model.

Lemma 5.3.1. *Let Q be a function defined by*

$$\begin{array}{rccl} Q: & E\times\mathbb{R}^n & \rightarrow & \mathbb{R} \\ & (\mathbf{x},\mathbf{q}) & \mapsto & Q(\mathbf{x},\mathbf{q}) := |\mathbf{q}| + W(\mathbf{x})\cdot\mathbf{q} + C(\mathbf{x}), \end{array} \tag{5.74}$$

where E is any set, $C:\mathbf{x}\in E\mapsto C(\mathbf{x})\in\mathbb{R}$ is a function bounded below by $c\in\mathbb{R}$, and W is a function definded by $W:\mathbf{x}\in E\mapsto W(\mathbf{x})\in\mathbb{R}^n$.

If there exists $\varepsilon>0$ such that $\forall\mathbf{x}\in E$, $|W(\mathbf{x})|\leq 1-\varepsilon$ then $Q(\mathbf{x},\cdot):\mathbf{q}\mapsto Q(\mathbf{x},\mathbf{q})$ is coercive uniformly with respect to $\mathbf{x}$ in E.

Proof. The proof idea of this lemma is based on the Cauchy-Schwarz inequality. Estimating the components of (5.74) leads us to the conclusion.

By the the Cauchy-Schwarz inequality we have

$$\begin{array}{rrcl} & W(\mathbf{x})\cdot\mathbf{q} & \geq & -|W(\mathbf{x})|\,|\mathbf{q}| \\ \Leftrightarrow & |\mathbf{q}|+W(\mathbf{x})\cdot\mathbf{q} & \geq & |\mathbf{q}|-|W(\mathbf{x})|\,|\mathbf{q}| \\ \Leftrightarrow & |\mathbf{q}|+W(\mathbf{x})\cdot\mathbf{q} & \geq & |\mathbf{q}|\,(1-|W(\mathbf{x})|)\,. \end{array} \tag{5.75}$$

In addition, $|\mathbf{q}|\,(1-|W(\mathbf{x})|)$ in (5.75) can be estimated by

$$\begin{array}{rrcl} & |W(\mathbf{x})| & \leq & 1-\varepsilon \\ \Leftrightarrow & -|W(\mathbf{x})| & \geq & \varepsilon-1 \\ \Leftrightarrow & 1-|W(\mathbf{x})| & \geq & \varepsilon \\ \Leftrightarrow & |\mathbf{q}|\,(1-|W(\mathbf{x})|) & \geq & |\mathbf{q}|\,\varepsilon. \end{array} \tag{5.76}$$

Hence, from (5.75) and (5.76) we receive

$$\begin{array}{rrcrcl} & & & |\mathbf{q}| + W(\mathbf{x})\cdot\mathbf{q} & \geq & |\mathbf{q}|\varepsilon \\ \Leftrightarrow & & & |\mathbf{q}| + W(\mathbf{x})\cdot\mathbf{q} + c & \geq & |\mathbf{q}|\varepsilon + c \\ \Leftrightarrow & Q(\mathbf{x},\mathbf{q}) & \geq & |\mathbf{q}| + W(\mathbf{x})\cdot\mathbf{q} + c & \geq & |\mathbf{q}|\varepsilon + c \\ \Leftrightarrow & & & Q(\mathbf{x},\mathbf{q}) & \geq & |\mathbf{q}|\varepsilon + c\,. \end{array} \tag{5.77}$$

Since $Q(\mathbf{x},\mathbf{q})$ in (5.77) is bounded below but not above, the assertion follows. $\square$

Proposition 5.3.1. *Assume that $\kappa_{\mathbf{x}}, c_x, (\mathbf{R_x}^T\mathbf{A_x})^{-1}, \mathbf{w}_x, \mathbf{R_x}^T\mathbf{v}_x$ are continuous and bounded on the compact set $\overline{\Omega}$ in generic Hamiltonian H_g (5.24). If $\forall\mathbf{x}\in\overline{\Omega}$, $\left|\left(\mathbf{A_x}^{-1}\right)^T\mathbf{w}_x\right| < \kappa_{\mathbf{x}}$ then $H_g(\mathbf{x},\cdot)$ is coercive uniformly with respect to $\mathbf{x}$ in $\overline{\Omega}$.*

The proof given here is the elaborated version from [84, 85].

Proof. The main idea for the proof of this proposition relies on the Lemma 5.3.1. The proof proceeds in three steps.
First, we define an auxiliary Hamiltonian $\widehat{H}$ in such a way that the uniform coercivity of generic Hamiltonian H_g holds if we confirm the uniform coercivity of the auxiliary Hamiltonian $\widehat{H}$.
In the second step, we consider an adapted $Q(\mathbf{x},\mathbf{q})$ in Lemma 5.3.1 whose uniform coercivity still holds, so that we can make use of it for the proof of uniform coercivity of $\widehat{H}$.
As a third step, we show the uniform coercivity of $\widehat{H}$ using $Q(\mathbf{x},\mathbf{q})$ in the second step by reformulating the uniform coercivity, which leads to the conclusion.

Step 1. Let us define

$$\widehat{H}(\mathbf{x},\mathbf{p}) = \kappa_{\mathbf{x}}\,|\mathbf{A_x}\mathbf{p} + \mathbf{v_x}| + \mathbf{w_x}\cdot\mathbf{p} + c_{\mathbf{x}}\,. \tag{5.78}$$

Then, for $\mathbf{x}\in\overline{\Omega}$, $\forall\mathbf{p}\in\mathbb{R}^2$ we have

$$H_g(\mathbf{x},\mathbf{p}) \geq \widehat{H}(\mathbf{x},\mathbf{p})\,, \tag{5.79}$$

since by (5.24)

$$\begin{array}{rrcl} & \kappa_{\mathbf{x}}\sqrt{|\mathbf{A_x}\mathbf{p}+\mathbf{v_x}|^2 + K_{\mathbf{x}}^2} & \geq & \kappa_{\mathbf{x}}\,|\mathbf{A_x}\mathbf{p}+\mathbf{v_x}| \\ \Leftrightarrow & \kappa_{\mathbf{x}}\sqrt{|\mathbf{A_x}\mathbf{p}+\mathbf{v_x}|^2 + K_{\mathbf{x}}^2} + \mathbf{w_x}\cdot\mathbf{p} + c_{\mathbf{x}} & \geq & \kappa_{\mathbf{x}}\,|\mathbf{A_x}\mathbf{p}+\mathbf{v_x}| + \mathbf{w_x}\cdot\mathbf{p} + c_{\mathbf{x}}\,. \end{array} \tag{5.80}$$

Hence, if $\widehat{H}(\mathbf{x},\cdot):\mathbf{p}\mapsto\widehat{H}(\mathbf{x},\mathbf{p})$ is uniform coercive with repect to $\mathbf{x}$ then $H_g(\mathbf{x},\cdot)$ is uniform coercive with respect to $\mathbf{x}$ as well.

Step 2. Here, we consider

$$
\begin{aligned}
Q: \quad \overline{\Omega} \times \mathbb{R}^2 &\rightarrow \mathbb{R} \\
(\mathbf{x},\mathbf{q}) &\mapsto Q(\mathbf{x},\mathbf{q}) := |\mathbf{q}| + \underbrace{\frac{1}{\kappa_{\mathbf{x}}}\left[\left(\mathbf{A}_{\mathbf{x}}^{\mathbf{T}}\right)^{-1}\mathbf{w}_{\mathbf{x}}\right]}_{=:W(\mathbf{x})} \cdot \mathbf{q} + \underbrace{c_{\mathbf{x}} - \left[\left(\mathbf{A}_{\mathbf{x}}^{\mathbf{T}}\right)^{-1}\mathbf{w}_{\mathbf{x}}\right] \cdot \mathbf{v}_{\mathbf{x}}}_{=:C(\mathbf{x})} .
\end{aligned}
\tag{5.81}
$$

Since we have assumed that

(i) $c_{\mathbf{x}}$, $\mathbf{A}_{\mathbf{x}}^{-1}$, $\mathbf{w}_{\mathbf{x}}$, $\mathbf{v}_{\mathbf{x}}$ are bounded

and that

(ii) $\left|\left(\mathbf{A}_{\mathbf{x}}^{T}\right)^{-1}\mathbf{w}_{\mathbf{x}}\right| < \kappa_{\mathbf{x}}$,

by continuity there exists $\varepsilon > 0$ such that $\frac{1}{\kappa_{\mathbf{x}}}\left|\left(\mathbf{A}_{\mathbf{x}}^{T}\right)^{-1}\mathbf{w}_{\mathbf{x}}\right| \leq 1 - \varepsilon$ for all $\mathbf{x}$ in the compact set $\overline{\Omega}$. Therefore, by Lemma 5.3.1 $Q(\mathbf{x},\cdot)$ is uniform coercive with respect to $\mathbf{x}$ in $\overline{\Omega}$.

Step 3.

Reformulation of Coercivity. Here, we rewrite the uniform coercivity of $Q(\mathbf{x},\cdot)$ as follows: for all $a \in \mathbb{R}$ there exists $m \in \mathbb{R}$ such that $|\mathbf{q}| \geq m$ implies $Q(\mathbf{x},\mathbf{q}) \geq a$ for all $\mathbf{q} \in \mathbb{R}^2$ and $\mathbf{x} \in \overline{\Omega}$.

Now, let us fix a and m_1 such that the above implication is true with $m = m_1$. We consider $m_2 \in \mathbb{R}$ such that for all $\mathbf{x}$ in $\overline{\Omega}$

$$
m_2 \geq \frac{1}{\kappa_{\mathbf{x}}}\left|\mathbf{A}_{\mathbf{x}}^{-1}\right|\left(|m_1| + \kappa_{\mathbf{x}}|\mathbf{v}_{\mathbf{x}}|\right) . \tag{5.82}
$$

The first term in (5.82) is bounded, since $\kappa_{\mathbf{x}}^{-1}$ is bounded based on the fact that $\left|\mathbf{A}_{\mathbf{x}}^{-1}\mathbf{w}_{\mathbf{x}}\right| = \left|\left(\mathbf{A}_{\mathbf{x}}^{T}\right)^{-1}\mathbf{w}_{\mathbf{x}}\right| > 0$ and $\left|\mathbf{A}_{\mathbf{x}}^{-1}\mathbf{w}_{\mathbf{x}}\right| < \kappa_{\mathbf{x}}$ is continuous in the compact set $\overline{\Omega}$. In addition, we have assumed that $\mathbf{v}_{\mathbf{x}}$ and $\mathbf{A}_{\mathbf{x}}^{-1}$ are bounded, the second term $\left|\mathbf{A}_{\mathbf{x}}^{-1}\right||\mathbf{v}_{\mathbf{x}}|$ is bounded as well.

Uniform Coercivity of $\widehat{H}$. To show the uniform coercivity of $\widehat{H}$, we first see what $|\mathbf{p}| \geq m_2$ implies. This brings us to the position that we can use the uniform coercivity of $Q(\mathbf{x},\cdot)$ in step 2. Furthermore, it turns out that $\widehat{H}$ can be expressed by $Q(\mathbf{x},\cdot)$, which leads to the conclusion.

Implication of $|\mathbf{p}| \geq m_2$. By the triangle and Cauchy-Schwarz inequality, e.g. in [95], we can derive that $|\mathbf{p}| \geq m_2$ implies

$$
\begin{aligned}
& \kappa_{\mathbf{x}} |\mathbf{A}_{\mathbf{x}}\mathbf{p} + \mathbf{v}_{\mathbf{x}}| && \geq && \kappa_{\mathbf{x}} (|\mathbf{A}_{\mathbf{x}}\mathbf{p}| - |\mathbf{v}_{\mathbf{x}}|) \\
\Leftrightarrow \quad & \kappa_{\mathbf{x}} |\mathbf{A}_{\mathbf{x}}\mathbf{p} + \mathbf{v}_{\mathbf{x}}| && \geq && \kappa_{\mathbf{x}} (|\mathbf{A}_{\mathbf{x}}| \, |\mathbf{p}| - |\mathbf{v}_{\mathbf{x}}|) \\
\Leftrightarrow \quad & \kappa_{\mathbf{x}} |\mathbf{A}_{\mathbf{x}}\mathbf{p} + \mathbf{v}_{\mathbf{x}}| && \geq && \kappa_{\mathbf{x}} \left(\frac{1}{\left|{\mathbf{A}_{\mathbf{x}}}^{-1}\right|} |\mathbf{p}| - |\mathbf{v}_{\mathbf{x}}| \right) \\
\overset{|\mathbf{p}| \geq m_2}{\Leftrightarrow} \quad & \kappa_{\mathbf{x}} |\mathbf{A}_{\mathbf{x}}\mathbf{p} + \mathbf{v}_{\mathbf{x}}| && \geq && \kappa_{\mathbf{x}} \left(\frac{1}{\left|{\mathbf{A}_{\mathbf{x}}}^{-1}\right|} |m_2| - |\mathbf{v}_{\mathbf{x}}| \right) \\
\overset{(5.82)}{\Leftrightarrow} \quad & \kappa_{\mathbf{x}} |\mathbf{A}_{\mathbf{x}}\mathbf{p} + \mathbf{v}_{\mathbf{x}}| && \geq && \kappa_{\mathbf{x}} \left(\frac{1}{\left|{\mathbf{A}_{\mathbf{x}}}^{-1}\right|} \frac{1}{\kappa_{\mathbf{x}}} \left|\mathbf{A}_{\mathbf{x}}^{-1}\right| (|m_1| + \kappa_{\mathbf{x}} |\mathbf{v}_{\mathbf{x}}|) - |\mathbf{v}_{\mathbf{x}}| \right) \\
\Leftrightarrow \quad & \kappa_{\mathbf{x}} |\mathbf{A}_{\mathbf{x}}\mathbf{p} + \mathbf{v}_{\mathbf{x}}| && \geq && \kappa_{\mathbf{x}} \left(\frac{1}{\kappa_{\mathbf{x}}} (|m_1| + \kappa_{\mathbf{x}} |\mathbf{v}_{\mathbf{x}}|) - |\mathbf{v}_{\mathbf{x}}| \right) \\
\Leftrightarrow \quad & \kappa_{\mathbf{x}} |\mathbf{A}_{\mathbf{x}}\mathbf{p} + \mathbf{v}_{\mathbf{x}}| && \geq && |m_1| + \kappa_{\mathbf{x}} |\mathbf{v}_{\mathbf{x}}| - \kappa_{\mathbf{x}} |\mathbf{v}_{\mathbf{x}}| \\
\Leftrightarrow \quad & \kappa_{\mathbf{x}} |\mathbf{A}_{\mathbf{x}}\mathbf{p} + \mathbf{v}_{\mathbf{x}}| && \geq && m_1 \,.
\end{aligned}
\tag{5.83}
$$

Following the reformulation of the uniform coercivity using (5.83) and the result in step 2 leads us to:
for all $a \in \mathbb{R}$ there exists $m \in \mathbb{R}$ such that $|\mathbf{p}| \geq m_2$ implies $Q(\mathbf{x}, \kappa_{\mathbf{x}} (\mathbf{A}_{\mathbf{x}}\mathbf{p} + \mathbf{v}_{\mathbf{x}})) \geq a$ for all $\kappa_{\mathbf{x}} (\mathbf{A}_{\mathbf{x}}\mathbf{p} + \mathbf{v}_{\mathbf{x}}) \in \mathbb{R}^2$ and $\mathbf{x} \in \overline{\Omega}$.
Our rest job is to show that $\widehat{H}(\mathbf{x}, \mathbf{p})$ has same bound as that of $Q(\mathbf{x}, \kappa_{\mathbf{x}} (\mathbf{A}_{\mathbf{x}}\mathbf{p} + \mathbf{v}_{\mathbf{x}}))$.
Computing $Q(\mathbf{x}, \kappa_{\mathbf{x}} (\mathbf{A}_{\mathbf{x}}\mathbf{p} + \mathbf{v}_{\mathbf{x}}))$ in (5.81) gives

$$
\begin{aligned}
& Q(\mathbf{x}, \kappa_{\mathbf{x}} (\mathbf{A}_{\mathbf{x}}\mathbf{p} + \mathbf{v}_{\mathbf{x}})) \\
& = |\kappa_{\mathbf{x}} (\mathbf{A}_{\mathbf{x}}\mathbf{p} + \mathbf{v}_{\mathbf{x}})| + \frac{1}{\kappa_{\mathbf{x}}} \left[\left(\mathbf{A}_{\mathbf{x}}^{\mathbf{T}} \right)^{-1} \mathbf{w}_{\mathbf{x}} \right] \cdot \kappa_{\mathbf{x}} (\mathbf{A}_{\mathbf{x}}\mathbf{p} + \mathbf{v}_{\mathbf{x}}) + c_{\mathbf{x}} - \left[\left(\mathbf{A}_{\mathbf{x}}^{\mathbf{T}} \right)^{-1} \mathbf{w}_{\mathbf{x}} \right] \cdot \mathbf{v}_{\mathbf{x}} \\
& = \kappa_{\mathbf{x}} |(\mathbf{A}_{\mathbf{x}}\mathbf{p} + \mathbf{v}_{\mathbf{x}})| + \left[\left(\mathbf{A}_{\mathbf{x}}^{\mathbf{T}} \right)^{-1} \mathbf{w}_{\mathbf{x}} \right] \cdot (\mathbf{A}_{\mathbf{x}}\mathbf{p} + \mathbf{v}_{\mathbf{x}}) + c_{\mathbf{x}} - \left[\left(\mathbf{A}_{\mathbf{x}}^{\mathbf{T}} \right)^{-1} \mathbf{w}_{\mathbf{x}} \right] \cdot \mathbf{v}_{\mathbf{x}} \\
& = \kappa_{\mathbf{x}} |(\mathbf{A}_{\mathbf{x}}\mathbf{p} + \mathbf{v}_{\mathbf{x}})| + \left[\left(\mathbf{A}_{\mathbf{x}}^{\mathbf{T}} \right)^{-1} \mathbf{w}_{\mathbf{x}} \right] \cdot \mathbf{A}_{\mathbf{x}}\mathbf{p} + \left[\left(\mathbf{A}_{\mathbf{x}}^{\mathbf{T}} \right)^{-1} \mathbf{w}_{\mathbf{x}} \right] \mathbf{v}_{\mathbf{x}} + c_{\mathbf{x}} - \left[\left(\mathbf{A}_{\mathbf{x}}^{\mathbf{T}} \right)^{-1} \mathbf{w}_{\mathbf{x}} \right] \cdot \mathbf{v}_{\mathbf{x}} \\
& = \kappa_{\mathbf{x}} |(\mathbf{A}_{\mathbf{x}}\mathbf{p} + \mathbf{v}_{\mathbf{x}})| + \left[\left(\mathbf{A}_{\mathbf{x}}^{\mathbf{T}} \right)^{-1} \mathbf{w}_{\mathbf{x}} \right] \cdot \mathbf{A}_{\mathbf{x}}\mathbf{p} + c_{\mathbf{x}} \,.
\end{aligned}
\tag{5.84}
$$

The second term $\left[\left(\mathbf{A}_{\mathbf{x}}^{\mathbf{T}} \right)^{-1} \mathbf{w}_{\mathbf{x}} \right] \cdot \mathbf{A}_{\mathbf{x}}\mathbf{p}$ in (5.84) has the same bound as the second one $\mathbf{w}_{\mathbf{x}} \cdot \mathbf{p}$ in (5.78) by $\left| \left(\mathbf{A}^T \right)^{-1} \right| = |\mathbf{A}|^{-1}$ and Cauchy-Schwarz inequality. Therefore, $\widehat{H}(\mathbf{x}, \cdot)$

is uniform coercive with respect to $\mathbf{x}$ as well. As noted in step 1, this completes the proof. $\square$

In what follows, we check the first model $H_{\mathrm{Foc}}^{\mathrm{pers}}$.

(E1) [**Regularity**] Regarding the regularity, as soon as image intensity $I(\mathbf{x})$ is continuous, $H_{\mathrm{Foc}}^{\mathrm{pers}}$ is continuous in $\overline{\Omega} \times \mathbb{R}^2$.

(E2) [**Convexity**] Convexity of the model $H_{\mathrm{Foc}}^{\mathrm{pers}}$ is already verified in the previous section.

(E3) [**Uniform Coercivity**] For uniform coercivity we apply Proposition 5.3.1.

By (5.28) we plug corresponding terms into $\left|\left(\mathbf{A_x}^{-1}\right)^T \mathbf{w_x}\right| < \kappa_{\mathbf{x}}$. Since $\mathbf{w_x} = \mathbf{0}$ in this case, $\underbrace{\left|\left(\mathbf{A_x}^{-1}\right)^T \mathbf{w_x}\right|}_{=0} < \kappa_{\mathbf{x}}$ holds if $\kappa_{\mathbf{x}} = I(\mathbf{x}) > 0$. Therefore, as long as $I(\mathbf{x}) > 0$ $H_{\mathrm{Foc}}^{\mathrm{pers}}$ is uniform coercive.

(E4) [**Subsolution**] Considering the Definition 2.3.1 or Definition 2.3.2, we can confirm that all constant functions are strict viscosity subsolutions of the Hamiltonian $H_{\mathrm{Foc}}^{\mathrm{pers}}(\mathbf{x}, \mathbf{p})$. We validate the assertion as follows.

For all constant functions we have $\mathbf{p} = \begin{bmatrix} p_1 \\ p_2 \end{bmatrix} = \begin{bmatrix} 0 \\ 0 \end{bmatrix}$. Plugging $\mathbf{p} = \begin{bmatrix} 0 \\ 0 \end{bmatrix}$ into $H_{\mathrm{Foc}}^{\mathrm{pers}}(\mathbf{x}, \mathbf{p})$ gives

$$\begin{aligned} H(\mathbf{x}, \mathbf{0}) &= I(\mathbf{x}) Q(\mathbf{x}) - Q(\mathbf{x}) \\ &= (I(\mathbf{x}) - 1) Q(\mathbf{x}), \end{aligned} \tag{5.85}$$

where $Q(\mathbf{x}) = \sqrt{\dfrac{\mathfrak{f}^2}{\mathfrak{f}^2 + |\mathbf{x}|^2}}$.

As $Q(\mathbf{x}) > 0$, $H(\mathbf{x}, \mathbf{0}) < 0$ if $0 < I(\mathbf{x}) < 1$. Therefore, we have $H(\mathbf{x}, \mathbf{p}) \leq H(\mathbf{x}, \mathbf{0}) \leq 0$ as long as $0 < I(\mathbf{x}) < 1$, which verifies the statement.

(E5) [**Compatibility**]

$$\varphi(\mathbf{x}) - \varphi(\mathbf{y}) \leq L(\mathbf{x}, \mathbf{y}) = \inf_{\xi \in C_{\mathbf{x},\mathbf{y}}, T_0 > 0} \left\{ \int_0^{T_0} H^* \left(\xi(s), -\xi'(s)\right) ds \right\} \quad \forall \mathbf{x}, \mathbf{y} \in \partial\Omega$$

Hence, if the aforementioned regularity, convexity, existence of viscosity subsolution and uniform coercivity are fulfilled and furthermore if the compatibility condition is satisfied on $\partial\Omega$, which means the change of boundary values is less than the running cost, $H_{\mathrm{Foc}}^{\mathrm{pers}}$ has continuous viscosity solutions by Theorem 5.3.1.

In an analogous way, we examine the second model $H_{\mathrm{Inf}}^{\mathrm{pers}}$.

(E1) [**Regularity**] Regularity holds for $H^{\text{pers}}_{\text{Inf}}$ as well, as soon as image intensity $I(\mathbf{x})$ is continuous.

(E2) [**Convexity**] Convexity of the model $H^{\text{pers}}_{\text{Inf}}$ also holds, as we have seen in the previous section.

(E3) [**Uniform Coercivity**] In an analogous way in the case of $H^{\text{pers}}_{\text{Foc}}$, we can find the conditions for uniform coercivity for $H^{\text{pers}}_{\text{Inf}}$ using Proposition 5.3.1.

By (5.30), we have

$$\begin{aligned} \left|\left(\mathbf{A_x}^{-1}\right)^T \mathbf{w_x}\right|^2 &= \left|\left[\begin{array}{c} \dfrac{x_2\left(-\mathtt{f}\,\alpha-\gamma\,x_1\right)-x_1\left(-\mathtt{f}\,\beta-\gamma\,x_2\right)}{|\mathbf{x}|\,\mathtt{f}} \\ \dfrac{x_1\left(-\mathtt{f}\,\alpha-\gamma\,x_1\right)+x_2\left(-\mathtt{f}\,\beta-\gamma\,x_2\right)}{|\mathbf{x}|\sqrt{\mathtt{f}^2+|\mathbf{x}|^2}} \end{array}\right]\right|^2 \\ &= \left(\frac{x_2\left(-\mathtt{f}\,\alpha-\gamma\,x_1\right)-x_1\left(-\mathtt{f}\,\beta-\gamma\,x_2\right)}{|\mathbf{x}|\,\mathtt{f}}\right)^2 \\ &\quad+\left(\frac{x_1\left(-\mathtt{f}\,\alpha-\gamma\,x_1\right)+x_2\left(-\mathtt{f}\,\beta-\gamma\,x_2\right)}{|\mathbf{x}|\sqrt{\mathtt{f}^2+|\mathbf{x}|^2}}\right)^2, \end{aligned} \tag{5.86}$$

where $\mathbf{x}=(x_1,x_2)^{\mathrm{T}}\in\mathbb{R}^2$.

Since $\mathbf{L}=(\alpha,\beta,\gamma)$ is normalised light direction vector,

$$\alpha^2+\beta^2+\gamma^2=1 \tag{5.87}$$

holds. In addition, $\mathbf{l}$ denotes the vector $(\alpha,\beta)^{\mathrm{T}}\in\mathbb{R}^2$.

Now, plugging $\gamma=\sqrt{1-\alpha^2-\beta^2}$ from (5.87) into (5.86) and simplifying the terms gives rise to

$$\left|\left(\mathbf{A_x}^{-1}\right)^T \mathbf{w_x}\right|^2=\frac{1}{\mathtt{f}^2+|\mathbf{x}|^2}\left[\left|\gamma\,\mathbf{x}+\mathtt{f}\,\mathbf{l}\right|^2+\left(|\mathbf{x}|^2|\mathbf{l}|^2-(\mathbf{x}\cdot\mathbf{l})^2\right)\right]. \tag{5.88}$$

As a result, by Proposition 5.3.1 $H^{\text{pers}}_{\text{Inf}}$ is uniform coercive when

$$I\left(\mathbf{x}\right)^2>\frac{1}{\mathtt{f}^2+|\mathbf{x}|^2}\left[\left|\gamma\,\mathbf{x}+\mathtt{f}\,\mathbf{l}\right|^2+\left(|\mathbf{x}|^2|\mathbf{l}|^2-(\mathbf{x}\cdot\mathbf{l})^2\right)\right] \tag{5.89}$$

holds.

(E4) [**Subsolution**] Regarding the subsolution of $H^{\text{pers}}_{\text{Inf}}$, Prados and Faugeras provided the strict viscosity subsolution for $H^{\text{pers}}_{\text{Inf}}$ in [86], which is given by

$$\underline{u}(\mathbf{x})=-\ln\frac{\gamma}{\mathtt{f}}-\ln\left(\gamma\,\mathtt{f}-\mathbf{l}\cdot\mathbf{x}\right) \tag{5.90}$$

with the condition of $\gamma \mathtt{f} - \mathbf{l} \cdot \mathbf{x} > 0$, i.e. $\mathbf{L} \cdot (\mathbf{x}, -\mathtt{f}) < 0$, where $\mathbf{L} = (\alpha, \beta, \gamma)$ is the normalised light direction constant vector and $\mathbf{l}$ denotes (α, β). Assuming that the light source is above the surface makes $\gamma > 0$.

In what follows, we justify the strict viscosity subsolution of $H_{\text{Inf}}^{\text{pers}}$.

For the given subsolution (5.90), first we can find the gradient of subsolution (5.90)

$$\nabla \underline{u}(x) = \frac{\mathbf{l}}{\gamma \mathtt{f} - \mathbf{l} \cdot x}. \tag{5.91}$$

Plugging (5.91) into $H_{\text{Inf}}^{\text{pers}}$ yields

$$\begin{aligned}
&H(\mathbf{x}, \nabla \underline{u}(\mathbf{x})) \\
&= I(\mathbf{x}) \sqrt{\mathtt{f}^2 \left|\nabla \underline{u}\right|^2 + (\mathbf{x} \cdot \nabla \underline{u} + 1)^2} - (\mathtt{f}\,\mathbf{l} + \gamma \mathbf{x}) \cdot \nabla \underline{u} - \gamma \\
&= I(\mathbf{x}) \sqrt{\mathtt{f}^2 \left| \frac{\mathbf{l}}{\gamma \mathtt{f} - \mathbf{l} \cdot \mathbf{x}} \right|^2 + \left(\mathbf{x} \cdot \frac{\mathbf{l}}{\gamma \mathtt{f} - \mathbf{l} \cdot \mathbf{x}} + 1 \right)^2} - (\mathtt{f}\,\mathbf{l} + \gamma \mathbf{x}) \cdot \frac{\mathbf{l}}{\gamma \mathtt{f} - \mathbf{l} \cdot \mathbf{x}} - \gamma \\
&= I(\mathbf{x}) \sqrt{\frac{\mathtt{f}^2 |\mathbf{l}|^2}{(\gamma \mathtt{f} - \mathbf{l} \cdot \mathbf{x})^2} + \left(\frac{\mathbf{l} \cdot \mathbf{x} + \gamma \mathtt{f} - \mathbf{l} \cdot \mathbf{x}}{\gamma \mathtt{f} - \mathbf{l} \cdot \mathbf{x}} \right)^2} - \frac{(\mathtt{f}\,\mathbf{l} + \gamma \mathbf{x}) \cdot \mathbf{l}}{\gamma \mathtt{f} - \mathbf{l} \cdot \mathbf{x}} - \gamma \\
&= I(\mathbf{x}) \sqrt{\frac{f^2 \left(|\mathbf{l}|^2 + \gamma^2 \right)}{(\gamma \mathtt{f} - \mathbf{l} \cdot \mathbf{x})^2}} - \frac{\mathtt{f}\,|\mathbf{l}|^2 + \gamma (\mathbf{l} \cdot \mathbf{x})}{\gamma \mathtt{f} - \mathbf{l} \cdot \mathbf{x}} - \gamma \\
&\text{by the normalised light direction vector } |\mathbf{l}|^2 + \gamma^2 = \alpha^2 + \beta^2 + \gamma^2 = 1 \\
&= I(\mathbf{x}) \frac{\mathtt{f}}{\gamma \mathtt{f} - \mathbf{l} \cdot \mathbf{x}} - \frac{\mathtt{f}\,|\mathbf{l}|^2 + \gamma (\mathbf{l} \cdot \mathbf{x})}{\gamma \mathtt{f} - \mathbf{l} \cdot \mathbf{x}} - \frac{\gamma (\gamma \mathtt{f} - \mathbf{l} \cdot \mathbf{x})}{\gamma \mathtt{f} - \mathbf{l} \cdot \mathbf{x}} \\
&= I(\mathbf{x}) \frac{\mathtt{f}}{\gamma \mathtt{f} - \mathbf{l} \cdot \mathbf{x}} - \frac{\mathtt{f}\,|\mathbf{l}|^2 + \gamma (\mathbf{l} \cdot \mathbf{x}) + \gamma^2 \mathtt{f} - \gamma (\mathbf{l} \cdot \mathbf{x})}{\gamma \mathtt{f} - \mathbf{l} \cdot \mathbf{x}} \\
&= I(\mathbf{x}) \frac{\mathtt{f}}{\gamma \mathtt{f} - \mathbf{l} \cdot \mathbf{x}} - \frac{\mathtt{f} \left(|\mathbf{l}|^2 + \gamma^2 \right)}{\gamma \mathtt{f} - \mathbf{l} \cdot \mathbf{x}} \\
&\text{by the same reasoning of normalised light direction vector} \\
&= I(\mathbf{x}) \frac{\mathtt{f}}{\gamma \mathtt{f} - \mathbf{l} \cdot \mathbf{x}} - \frac{\mathtt{f}}{\gamma \mathtt{f} - \mathbf{l} \cdot \mathbf{x}} \\
&= \frac{\mathtt{f}}{\gamma \mathtt{f} - \mathbf{l} \cdot \mathbf{x}} (I(\mathbf{x}) - 1).
\end{aligned} \tag{5.92}$$

As we have already assumed $\gamma \mathtt{f} - \mathbf{l} \cdot \mathbf{x} > 0$, the only way to achieve strict subsolution of $H_{\text{Inf}}^{\text{pers}}$ is when $0 < I(\mathbf{x}) < 1$. Hence, under this condition $\underline{u}(\mathbf{x}) = -\ln \frac{\gamma}{\mathtt{f}} - \ln (\gamma \mathtt{f} - \mathbf{l} \cdot \mathbf{x})$ is the strict viscosity subsolution of $H_{\text{Inf}}^{\text{pers}}$.

(E5) [**Compatibility**] Compatibility conditions for $H_{\text{Inf}}^{\text{pers}}$ are expressed in the same way as in the case of $H_{\text{Foc}}^{\text{pers}}$.

Therefore, there exist continuous viscosity solutions for Prados and Faugeras model which are described as in (E5) under the adequate conditions (E1)-(E4).

5.3.2 Uniqueness of Viscosity Solution

For the uniqueness of the Prados model, we make use of Theorem 5.3.2 adjusted to the model which basically relies on the Theorem 4.3.1 discussed in Chapter 4. Although there are several common criterion between Theorem 5.3.1 and Theorem 5.3.2, the major difference is that uniqueness theorem requires the existence of the strict viscosity subsolution.

For the given eikonal-type HJE of the form

$$H\left(\mathbf{x},\nabla u\left(\mathbf{x}\right)\right)=0 \qquad \mathbf{x}\in\Omega, \tag{5.93}$$

if the image intensity I does not reach the maximal value 1, a uniqueness theorem can be formulated as follows.

Theorem 5.3.2 (Uniqueness of Continuous Viscosity Solutions for the Prados Model). *Let Ω be a bounded open subset of $\mathbb{R}^2$. If H satisfies*

(U1) [**Convexity**] *H is convex with respect to $\mathbf{p}$ for all $\mathbf{x}$ in Ω,*

(U2) [**Space variable regularity**] *There exists a nondecreasing function ω which goes to zero at zero, such that $\forall \mathbf{x},\mathbf{y}\in\Omega$, $\forall\mathbf{p}\in\mathbb{R}^2$, $\left|H\left(\mathbf{x},\mathbf{p}\right)-H\left(\mathbf{y},\mathbf{p}\right)\right|\leq\omega\left(\left|\mathbf{x}-\mathbf{y}\right|\left(1+\left|\mathbf{p}\right|\right)\right)$,*

(U3) [**Strict subsolution**] *There exists a strict viscosity subsoloution $\underline{u}\in C(\overline{\Omega})\cap C^1(\Omega)$ of (5.93), i.e. such that $H\left(\mathbf{x},\nabla\underline{u}\right)<0$ for all $\mathbf{x}$ in Ω,*

then there exists at most one continuous viscosity solution of (5.93) in $\overline{\Omega}$, such that

$$u(\mathbf{x})=\varphi(\mathbf{x}) \qquad \forall\mathbf{x}\in\partial\Omega. \tag{5.94}$$

In effect:

(U1) [**Convexity**] In Subsection 5.2.2, we have already seen that the convexity is true for both $H_{\text{Foc}}^{\text{pers}}$ and $H_{\text{Inf}}^{\text{pers}}$.

(U2) [**Space variable regularity**] This condition can be understood as $I\left(\mathbf{x}\right)$ is Lipschitz-continuous.

(U3) [**Strict subsolution**] The existence of the strict subsolution is basically one of the essential part in the comparison theorem for uniqueness theory. In the previous section, we have already confirmed that for both cases, $H_{\text{Foc}}^{\text{pers}}$ and $H_{\text{Inf}}^{\text{pers}}$, there exist subsolutions and they are actually strict subsolutions.

Therefore, as soon as the image intensity $I(\mathbf{x})$ is Lipschitz-continuous and verifies

$$0 < I(\mathbf{x}) < 1 \quad \forall \mathbf{x} \in \Omega, \tag{5.95}$$

Prados and Faugeras models have at most one continuous viscosity solution by Theorem 5.3.2.

Remark 5.3.2. However, there is a subtle issue to be discussed here. In practice, $I(\mathbf{x})$ can reach the value 1 in an arbitrary compact set in $\overline{\Omega}$, which insinuates that we lose the uniqueness properity by (U3) in Theorem 5.3.2. In order to remedy this situation, Prados and Faugeras extended the idea of Rouy and Tourin [26] to their perspective framework. In what follows, we shall see how this works.

Here denotes $\mathbf{S}$ the set of singular points (also called critical points)

$$\mathbf{S} = \{\mathbf{x} \in \Omega \mid I(\mathbf{x}) = 1\} \tag{5.96}$$

and assumes that $\mathbf{S}$ contains a finite number of singular points $\mathbf{S} = \{\mathbf{x}_1, \ldots, \mathbf{x}_n\}$, where the index n and real constants $c_i = u(\mathbf{x}_i) = \varphi(\mathbf{x}_i), (c_i)_{i,\ldots,n}$, are also assumed to be fixed. Then employing the DBC to the set $\partial\Omega \cup \mathbf{S}$ for the given Hamiltonian

$$\begin{cases} H(\mathbf{x}, \nabla u(\mathbf{x})) &= 0 & \text{in } \Omega \\ u(\mathbf{x}) &= \varphi(\mathbf{x}) & \text{on } \partial\Omega \end{cases} \tag{5.97}$$

yields

$$\begin{cases} H(\mathbf{x}, \nabla u(\mathbf{x})) &= 0 & \text{in } \Omega - \mathbf{S} \\ u(\mathbf{x}) &= \varphi(\mathbf{x}) & \text{on } \partial\Omega \cup \mathbf{S}, \end{cases} \tag{5.98}$$

which can be reformulated as

$$\begin{cases} H(\mathbf{x}, \nabla u(\mathbf{x})) &= 0 & \text{in } \Omega' \\ u(\mathbf{x}) &= \varphi(\mathbf{x}) & \text{on } \partial\Omega', \end{cases} \tag{5.99}$$

where $\Omega' = \Omega - \mathbf{S}$ and $\partial\Omega' = \partial\Omega \cup \mathbf{S}$.

Thanks to the refomulation (5.99), we can still have the existence and uniqueness property by applying the Theorem 5.3.1 and Theorem 5.3.2 into (5.99) if image intensity $I(\mathbf{x})$ is Lipschitz-continuous, since Ω' includes no singular points. In other words, although Hamiltonian (5.97) is ill-posed, we are still in the position to turn this problem into a well-posed one and obtain the continuous viscosity solutions which have mathematically nice properties by choosing arbitrarily the constants $c_i (= \varphi(\mathbf{x}_i))$ and solving (5.99).

One disadvantage to be pointed out about this framework is, namely, the assumptions. They assumed that all the informations about singular points and the values on the boundary are available, whereas in general the input data to a Shape from Shading problem consists only of an image, which leads to the restriction of this setup.

5.4 Summary

In this chapter, we have gone through the Shape from Shading model proposed by Prados and Faugeras based on the theory in preceding chapters.

First, we have seen how the perspective Shape from Shading problems are modelled mathematically.

Then, we have investigated the properties of generic Hamiltonian which has the capability of combining several Hamiltonians and the convexity of the Hamiltonians are examined as well.

Afterwards, the existence and uniqueness theories for the Prados and Faugeras model are looked into and verified for each case. For the uniqueness property, a caveat of the model is also mentioned.

In the next chapter, we shall discuss the model extension for the Shape from Shading problems.

Chapter 6

Discussion of Model Extensions

In the previous chapter, we have studied the Prados and Faugeras model extensively which involves perspective Shape from Shading problem. However, there is one important assumption that makes Prados and Faugeras model unrealistic, namely Lambertian surface. Therefore, we are also in need of the model which can describe non-Lambertian surfaces when we think of the application in real life situation.

In this chapter, we shall discuss the Vogel-Breuß-Weickert model which is more realistic than that of Prados and Faugeras. Nevertheless, dealing with non-Lambertian surfaces with the model by Vogel et al. gives rise to a non-convex general-type Hamiltonian which needs careful treatments.

This chapter is outlined as follows.

First, we shall look into how the new model is described and the brightness equation is formulated. This involves Phong reflection based perspective Shape from Shading model from [29, 87].

Then, we investigate the convexity of the model. It turns out that this type of Hamiltonian is in general not convex because of specular terms in the Phong model. Thus, we analyse the model when the non-convexities of the model occur and think about whether there is a way to get around these difficulties, so that we can have at least almost everywhere convexity properties.

Our contribution here is to provide the analysis of the critical points of the Hamiltonian and condition to circumvent the non-convex properties around the critical points.

The main reference for this chapter is the paper by the authors [75].

6.1 The Vogel-Breuß-Weickert Model

In this section, we shall see how the new model is described. To describe a model, we begin with the surface parametrisation for the perspective SfS that we have seen in Section 5.1.

6.1.1 Surface Parametrisation

By (5.14), we have surface parametrisation

$$\mathcal{S} = \left\{ \frac{\mathtt{f}}{\sqrt{|\mathbf{x}|^2 + \mathtt{f}^2}} u(x_1, x_2) \begin{bmatrix} x_1 \\ x_2 \\ -\mathtt{f} \end{bmatrix} \middle| (x_1, x_2) \in \overline{\Omega} \right\}, \tag{6.1}$$

where $u(x_1, x_2)$ denotes the unknown depth and $\mathcal{S} : \overline{\Omega} \to \mathbb{R}^3$ with $\Omega \subset \mathbb{R}^2$.

As we did in (5.15) and (5.16), taking partial derivative with respect to each variable and computing their cross product gives surface normal vector $\mathbf{n}(\mathbf{x})$ at $\mathcal{S}(\mathbf{x})$, which is the same result as in (5.17)

$$\mathbf{n}(\mathbf{x}) = \mathcal{S}_{x_1} \times \mathcal{S}_{x_2} = \begin{bmatrix} \mathtt{f} u_{x_1} \\ \mathtt{f} u_{x_2} \\ x_1 u_{x_1} + x_2 u_{x_2} \end{bmatrix} - \frac{\mathtt{f}}{|\mathbf{x}|^2 + \mathtt{f}^2} \begin{bmatrix} x_1 u \\ x_2 u \\ -\mathtt{f}\, u \end{bmatrix}. \tag{6.2}$$

Up till now, the process is identical to that of perspective SfS.

6.1.2 Brightness Equation for Phong-type Surfaces

As mentioned earlier, since the new model assumes Phong-type surfaces, the following image irradiance equation is introduced based on [18]

$$I(\mathbf{x}) = \underbrace{\kappa_a I_a}_{\text{ambient}} + \sum_{\text{light sources}} \frac{1}{r^2} \left(\underbrace{\kappa_d I_d \cos\phi}_{\text{diffuse}} + \underbrace{\kappa_s I_s (\cos\theta)^{\alpha}}_{\text{specular}} \right). \tag{6.3}$$

Remark 6.1.1. In (6.3) I_a, I_d, and I_s denote the image intensities of the ambient, diffuse, and specular components of the reflected light, respectively. Accordingly, k_a, k_d, and k_s represent the corresponding constants with $\kappa_a + \kappa_d + \kappa_s \leq 1$. In addition, the light attenuation factor $1/r^2$, where r is the distance between point light source and the surface, is incorporated relying on the inverse square law[1] in physics, see Figure 6.1.

In the diffuse term, ϕ is the angle between surface normal and light source direction, so the intensities of the diffuse light is proportional to $\cos\phi$. According to the Phong model, the diffuse term is not affected by the viewer direction.

In the specular term, θ is the angle between ideal mirror reflection of the incoming light and the viewer direction and α is a constant depending on the material of the surface. As α becomes larger, the model describes more mirror-like reflection. In contrast to the diffuse term, the specular term is largely influenced by the viewer direction, so the amount of specular light towards the viewer is proportional to $(\cos\theta)^{\alpha}$.

[1] In Figure 6.1 we assume that the total energy radiated from the light source **S** is distributed to spherical surface of radius r. Although the surface area with radius r is proportional to r^2, the total energy given off from the source remains the same. As a consequence, the absorbed energy per unit area is inversely proportional to square of the distance from the light source.

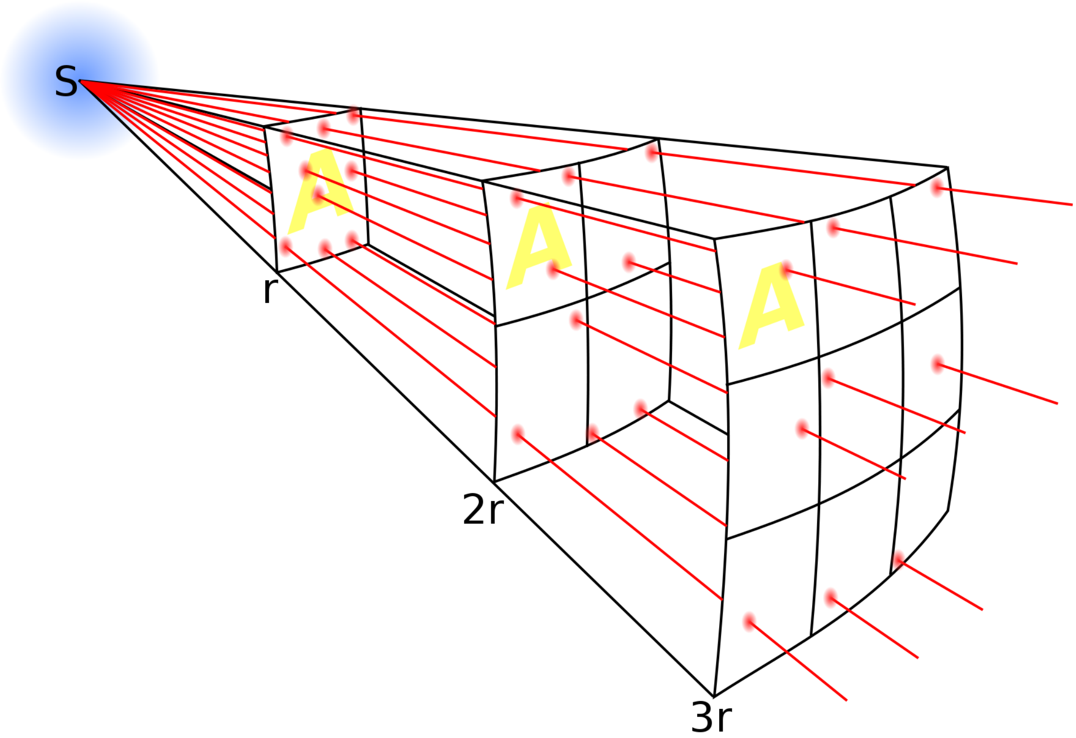

Figure 6.1: Visualisation of the inverse square law. **S** denotes the point light source, r represents the distance from **S**, and the red lines stand for the flux emanating from the source **S**. Adapted from [1].

Since this model is restricted to the case when a single light source is at the optical centre of the camera, (6.3) reduces to

$$I(\mathbf{x}) = \kappa_a I_a + \frac{1}{r^2}\left(\kappa_d I_d \cos\phi + \kappa_s I_s (\cos\theta)^{\alpha}\right) . \tag{6.4}$$

In addition, in this case viewer direction and light source direction are the same, see Figure 5.2, we can obtain

$$\theta = 2\phi , \tag{6.5}$$

which leads to

$$I(\mathbf{x}) = \kappa_a I_a + \frac{1}{r^2}\left(\kappa_d I_d \cos\phi + \kappa_s I_s (\cos 2\phi)^{\alpha}\right) . \tag{6.6}$$

Reformulating $cos\phi$ in (6.6) with scalar product between unit surface normal vector and normalised light direction vector yields

$$\cos\phi = \mathbf{N}\cdot\mathbf{L} , \tag{6.7}$$

where $\mathbf{N} = \frac{\mathbf{n}(\mathbf{x})}{|\mathbf{n}(\mathbf{x})|}$ and $\mathbf{L}$ is a normalised light direction vector. Additionally, employing trigonometric identities, e.g. in [70],

$$\cos 2\phi = 2(\cos\phi)^2 - 1 \tag{6.8}$$

with (6.7) makes (6.6) turn into

$$I(\mathbf{x}) = \kappa_a I_a + \frac{1}{r^2}\left(\kappa_d I_d (\mathbf{N}\cdot\mathbf{L}) + \kappa_s I_s \left(2(\mathbf{N}\cdot\mathbf{L})^2 - 1\right)^{\alpha}\right). \tag{6.9}$$

As the normalised light direction vector is already given in (5.17), the scalar product between surface normal vector and unit light direction vector gives

$$\begin{aligned}
&\mathbf{N}\cdot\mathbf{L}(S(\mathbf{x}))\\
&= \frac{\mathbf{n}(\mathbf{x})}{|\mathbf{n}(\mathbf{x})|}\cdot\left(\frac{1}{\sqrt{|\mathbf{x}|^2+\mathtt{f}^2}}\begin{bmatrix}-x_1\\-x_2\\\mathtt{f}\end{bmatrix}\right)\\
&\overset{(5.17)}{=} \frac{1}{|\mathbf{n}(\mathbf{x})|\sqrt{|\mathbf{x}|^2+\mathtt{f}^2}}\left(\begin{bmatrix}\mathtt{f}u_{x_1}\\\mathtt{f}u_{x_2}\\x_1u_{x_1}+x_2u_{x_2}\end{bmatrix} - \frac{\mathtt{f}}{|\mathbf{x}|^2+\mathtt{f}^2}\begin{bmatrix}x_1u\\x_2u\\-\mathtt{f}\,u\end{bmatrix}\right)\cdot\begin{bmatrix}-x_1\\-x_2\\\mathtt{f}\end{bmatrix}\\
&= \frac{1}{|\mathbf{n}(\mathbf{x})|\sqrt{|\mathbf{x}|^2+\mathtt{f}^2}}\left(-\mathtt{f}u_{x_1}x_1 + \frac{\mathtt{f}x_1^2u}{|\mathbf{x}|^2+\mathtt{f}^2} - \mathtt{f}u_{x_2}x_2 + \frac{\mathtt{f}x_2^2u}{|\mathbf{x}|^2+\mathtt{f}^2}\right)\\
&\quad + \frac{1}{|\mathbf{n}(\mathbf{x})|\sqrt{|\mathbf{x}|^2+\mathtt{f}^2}}\left(\mathtt{f}x_1u_{x_1} + \mathtt{f}x_2u_{x_2} + \frac{\mathtt{f}^3u}{|\mathbf{x}|^2+\mathtt{f}^2}\right)\\
&= \frac{1}{|\mathbf{n}(\mathbf{x})|\sqrt{|\mathbf{x}|^2+\mathtt{f}^2}}\frac{\mathtt{f}u}{|\mathbf{x}|^2+\mathtt{f}^2}\left(\underbrace{x_1^2+x_2^2}_{=|\mathbf{x}|^2}+\mathtt{f}^2\right)\\
&= \frac{\mathtt{f}u}{|\mathbf{n}(\mathbf{x})|\sqrt{|\mathbf{x}|^2+\mathtt{f}^2}}.
\end{aligned} \tag{6.10}$$

Making use of $r = \mathtt{f}u(\mathbf{x})$ for the light attenuation factor $1/r^2$ in (6.9) and plugging (6.10) into (6.9) yields

$$\begin{aligned}
&I(\mathbf{x})\\
&= \kappa_a I_a + \frac{1}{\mathtt{f}^2u(\mathbf{x})^2}\left(\kappa_d I_d\left(\frac{\mathtt{f}u(\mathbf{x})}{|\mathbf{n}(\mathbf{x})|\sqrt{|\mathbf{x}|^2+\mathtt{f}^2}}\right) + \kappa_s I_s\left(2\left(\frac{\mathtt{f}u(\mathbf{x})}{|\mathbf{n}(\mathbf{x})|\sqrt{|\mathbf{x}|^2+\mathtt{f}^2}}\right)^2 - 1\right)^{\alpha}\right)\\
&= \kappa_a I_a + \frac{1}{\mathtt{f}^2u(\mathbf{x})^2}\left(\kappa_d I_d\frac{u(\mathbf{x})Q(\mathbf{x})}{|\mathbf{n}(\mathbf{x})|} + \kappa_s I_s\left(2\left(\frac{u(\mathbf{x})Q(\mathbf{x})}{|\mathbf{n}(\mathbf{x})|}\right)^2 - 1\right)^{\alpha}\right),
\end{aligned} \tag{6.11}$$

where
$$|\mathbf{n}(\mathbf{x})| = \sqrt{\mathtt{f}^2 |\nabla u(\mathbf{x})|^2 + (\nabla u(\mathbf{x}) \cdot \mathbf{x})^2 + u(\mathbf{x})^2 Q(\mathbf{x})^2} \tag{6.12}$$
and $Q(\mathbf{x}) = \sqrt{\frac{\mathtt{f}^2}{|\mathbf{x}|^2 + \mathtt{f}^2}}$.

6.1.3 Hamiltonian of the Model

In order to exploit the change of the variables for the later use, we multiply $\frac{\mathtt{f}^2 |\mathbf{n}(\mathbf{x})|}{u(\mathbf{x})Q(\mathbf{x})}$ both sides of (6.11), which gives

$$(I(\mathbf{x}) - k_a I_a) \frac{\mathtt{f}^2 |\mathbf{n}(\mathbf{x})|}{Q(\mathbf{x})\, u(\mathbf{x})} - \frac{k_d I_d}{u(\mathbf{x})^2} - \frac{|\mathbf{n}(\mathbf{x})| k_s I_s}{u(\mathbf{x})^3 Q(\mathbf{x})} \left(\frac{2u(\mathbf{x})^2 Q(\mathbf{x})^2}{|n(\mathbf{x})|^2} - 1 \right)^{\alpha} = 0 . \tag{6.13}$$

Here, assuming that the surface $\mathcal{S}$ is always visible makes u strictly positive. Moreover, by applying the technique of change of variables $v(\mathbf{x}) = \ln u(\mathbf{x}) \Leftrightarrow \nabla u = u \nabla v$ to (6.12) we can obtain

$$\begin{aligned} |\mathbf{n}(\mathbf{x})| &= \sqrt{\mathtt{f}^2 |u(\mathbf{x}) \nabla v(\mathbf{x})|^2 + (u(\mathbf{x}) \nabla v(\mathbf{x}) \cdot \mathbf{x})^2 + u(\mathbf{x})^2 Q(\mathbf{x})^2} \\ \Leftrightarrow \quad \frac{|\mathbf{n}(\mathbf{x})|}{u(\mathbf{x})} &= \sqrt{\mathtt{f}^2 |\nabla v(\mathbf{x})|^2 + (\nabla v(\mathbf{x}) \cdot \mathbf{x})^2 + Q(\mathbf{x})^2} =: W(\mathbf{x}) . \end{aligned} \tag{6.14}$$

Since
$$\begin{aligned} v &= \ln u \\ \Leftrightarrow \quad e^{v} &= u \\ \Leftrightarrow \quad e^{-2v} &= u^{-2} , \end{aligned} \tag{6.15}$$

by plugging (6.15) into (6.13) and with the help of (6.14) HJE (6.13) can be reformulated as
$$(I(\mathbf{x}) - \kappa_a I_a) \frac{\mathtt{f}^2 W}{Q} - \kappa_d I_d e^{-2v} - \frac{W \kappa_s I_s}{Q} e^{-2v} \left(\frac{2Q^2}{W^2} - 1 \right)^{\alpha} = 0 , \tag{6.16}$$

which is also HJE and called "Phong SfS" problem.

Therefore, we obtain the Hamiltonian for the new model

$$H_{VBW} = (I(\mathbf{x}) - k_a I_a) \frac{\mathtt{f}^2}{Q(\mathbf{x})} \frac{|n(\mathbf{x})|}{u(\mathbf{x})} - \frac{k_d I_d}{u(\mathbf{x})^2} - \frac{|n(\mathbf{x})|}{u(\mathbf{x})} \frac{k_s I_s}{u(\mathbf{x})^2 Q(\mathbf{x})} \left(2Q(\mathbf{x})^2 \left(\frac{u(\mathbf{x})}{|n(\mathbf{x})|} \right)^2 - 1 \right)^{\alpha} \tag{6.17}$$

or

$$H_{VBW} = \underbrace{(I(\mathbf{x}) - k_a I_a) \frac{\mathtt{f}^2 W(\mathbf{x})}{Q(\mathbf{x})}}_{=:H_a} - \underbrace{k_d I_d e^{-2v(\mathbf{x})}}_{=:H_d} - \underbrace{e^{-2v(\mathbf{x})} \frac{k_s I_s W(\mathbf{x})}{Q(\mathbf{x})} \left(\frac{2Q(\mathbf{x})^2}{W(\mathbf{x})^2} - 1 \right)^{\alpha}}_{=:H_s} , \tag{6.18}$$

with $v = \ln u$.

Note that in the Phong model, the cosine in the specular term is usually replaced by zero if

$$\cos\theta = \frac{2Q(\mathbf{x})^2}{W(\mathbf{x})^2} - 1 < 0\,. \tag{6.19}$$

Remark 6.1.2. One important difference between the Hamiltonians of the model by Vogel et al. and those of the model by Prados and Faugeras that we have seen in Section 5.2 is the type of Hamiltonian. In fact, the latter is a eikonal type $H\left(\mathbf{x}, \nabla u\left(\mathbf{x}\right)\right)$ and the former is a general one $H\left(\mathbf{x}, u\left(\mathbf{x}\right), \nabla u\left(\mathbf{x}\right)\right)$.

As pointed out in [29, 87], the difference is made in the modelling process. In [84, 85, 88] Prados and Faugeras ignored the light attenuation factor $1/r^2$ influenced by inverse square law, which leads to the results. After that, they consider this effect and reformulated the brightness equation for the Lambertian surface in [29, 87], which we call here "Prados 04" in order to distinguish from the previous one. As one might expect, changing the image irradiance equation gives rise to a different type of Hamiltonian, which requires different solution theory than that of eikonal-type. We summarise this result in Table 6.1.

	Rouy & Tourin	**Prados**	**Prados 04**	**Vogel et al.**
Camera	Orthographic	Perspective	Perspective	Perspective
Surface	Lambertian	Lambertian	Lambertian	Non-Lambertian
Hamiltonian	Eikonal-type	Eikonal-type	General-type	General-type
Convexity	Convex	Convex	Convex	Non-convex

Table 6.1: Comparison between the Shape from Shading models.

The exposition of the problems can also be found in [29, 87] which basically relies on the generalised viscosity solution theory. More details about the solution theory for general-type Hamiltonians, we refer to [12, 23, 60, 67, 69] and the references therein.

6.2 Analysis of the Model

In this section, we investigate the convexity of the Hamiltonian of the model.

We begin with ambient H_a and diffuse terms H_d in (6.18). This leads to the fact that the convexity of the model is actually depends on the specular terms H_s.

Due to the complexities of the specular terms, here we only consider this problem in one-dimensional case, and yet the idea can be extended to the two-dimensional case.

6.2.1 Convexity of the Hamiltonian

Our task here is to check if H_{VBW} is convex with respect to ∇v.

Ambient and Diffuse Terms

As can be seen in (6.18), the diffuse term H_d has no influence on the convexity of H_{VBW}, so we turn our attention to H_a. Actually, H_a is convex, since the convexity of $W(\mathbf{x})$ is already verified in Section 5.2. Therefore, the convexity of the model boils down to check the property of the specular term H_s.

Now, we focus on the specular term H_s.

Convexity of the Functions

Before we test the convexity of H_s, we think about the properties of convex functions. In general, convex functions are not closed under minus operations, e.g. $x^4 - x^2$, despite the closedness under plus ones [103]. Therefore, H_s in (6.18) must be concave or "$-H_s$" must be convex so as to achieve the convexity of Hamiltonian H_{VBW}. We proceed with this kept in mind.

6.2.2 Analysis of H_s in One-Dimensional Case

We analyse H_s by characterising critical points whose behaviour can give us useful information about the Hamiltonian itself.

When we take H_s into account in one-dimension, it is equivalent to consider

$$h_s = \frac{W(x)}{Q(x)} \left(\frac{2Q(x)^2}{W(x)^2} - 1 \right)^{\alpha}, \tag{6.20}$$

where

$$W(x) = \sqrt{\mathtt{f}^2 p^2 + (px)^2 + Q(x)^2} \tag{6.21}$$

with $p = \nabla v$ and

$$Q(x) = \sqrt{\frac{\mathtt{f}^2}{x^2 + \mathtt{f}^2}}. \tag{6.22}$$

Since $\mathbf{x} \in \mathbb{R}^2$ is already known by pixel position of a given image, here we also assume x to be known.

Critical Points

In order to find critical points, we first differentiate (6.21) with respect to p for the later use

$$\begin{aligned} W_p &= \frac{\mathtt{f}^2 2p + 2px^2}{2\sqrt{\mathtt{f}^2 p^2 + p^2 x^2 + Q^2}} \\ &= \frac{2p\left(\mathtt{f}^2 + x^2\right)}{2\sqrt{\mathtt{f}^2 p^2 + p^2 x^2 + Q^2}} \\ &= \frac{p\left(\mathtt{f}^2 + x^2\right)}{W}. \end{aligned} \tag{6.23}$$

Now, by taking the first derivative of (6.20) with respect to p, we have

$$\begin{aligned} h_{s_p} &= \frac{1}{Q}\left[W_p\left(\frac{2Q^2}{W^2}-1\right)^{\alpha} + W\alpha\left(\frac{2Q^2}{W^2}-1\right)^{\alpha-1} 2Q^2\left(\frac{-2}{W^3}\frac{p\left(\mathtt{f}^2+p^2\right)}{W}\right)\right] \\ &\overset{(6.23)}{=} \frac{1}{Q}\left(\frac{2Q^2}{W^2}-1\right)^{\alpha-1}\left[\frac{p\left(\mathtt{f}^2+x^2\right)}{W}\left(\frac{2Q^2}{W^2}-1\right) - \frac{4\alpha Q^2 p\left(\mathtt{f}^2+p^2\right)}{W^3}\right] \\ &= \frac{1}{Q}\left(\frac{2Q^2}{W^2}-1\right)^{\alpha-1}\frac{p\left(\mathtt{f}^2+x^2\right)}{W}\left[\left(\frac{2Q^2}{W^2}-1\right) - \frac{4\alpha Q^2}{W^2}\right] \\ &= \frac{1}{Q}\left(\frac{2Q^2}{W^2}-1\right)^{\alpha-1}\frac{p\left(\mathtt{f}^2+x^2\right)}{W}\left[\frac{2Q^2\left(1-2\alpha\right)}{W^2}-1\right]. \end{aligned} \tag{6.24}$$

When we consider $h_{s_p} = 0$ under the assumption $Q \neq 0$, we have three possibilities:

$$\frac{2Q^2}{W^2} - 1 = 0, \tag{6.25}$$

$$p = 0, \tag{6.26}$$

or

$$\frac{2Q^2\left(1-2\alpha\right)}{W^2} - 1 = 0. \tag{6.27}$$

By virtue of specular exponent property in Phong reflectance model $\alpha \geq 2$, the left hand side of (6.27) becomes negative and cannot be zero. As a consequence, the task reduces to deal with (6.25) and (6.26).

Classification of Critical Points

In order to classify critical points, we compute the second derivative of h_s using product and chain rule. From (6.24) we can obtain

$$\begin{aligned} h_{s_{pp}} &= \frac{1}{Q}\left[\left(\frac{2Q^2}{W^2}-1\right)^{\alpha-1}\right]_p \frac{p\left(\mathtt{f}^2+x^2\right)}{W}\left[\frac{2Q^2\left(1-2\alpha\right)}{W^2}-1\right] \\ &\quad +\frac{1}{Q}\left(\frac{2Q^2}{W^2}-1\right)^{\alpha-1}\left[\frac{p\left(\mathtt{f}^2+x^2\right)}{W}\right]_p\left[\frac{2Q^2\left(1-2\alpha\right)}{W^2}-1\right] \\ &\quad +\frac{1}{Q}\left(\frac{2Q^2}{W^2}-1\right)^{\alpha-1}\frac{p\left(\mathtt{f}^2+x^2\right)}{W}\left[\frac{2Q^2\left(1-2\alpha\right)}{W^2}-1\right]_p . \end{aligned} \tag{6.28}$$

Now, we examine two cases (6.25) and (6.26), respectively.

Case: $\frac{2Q^2}{W^2}=1$. When we calculate this condition explicitly, we can obtain

$$\begin{aligned} & W^2 &=& \ 2Q^2 \\ \overset{(6.21)}{\Leftrightarrow} & \left(\mathtt{f}^2+x^2\right)p^2+Q^2 &=& \ 2Q^2 \\ \Leftrightarrow & p^2 &=& \ \frac{1}{\mathtt{f}^2+x^2}Q^2 \\ \overset{(6.22)}{\Leftrightarrow} & p &=& \ \pm\frac{\mathtt{f}}{\mathtt{f}^2+x^2} . \end{aligned} \tag{6.29}$$

In (6.28), we can easily see that $h_{s_{pp}}\Big|_{\frac{2Q^2}{W^2}=1}=0$.

Case: $p=0$. Evaluating (6.28) when $p=0$ gives

$$h_{s_{pp}}\Big|_{p=0}=\frac{\left(x^2+\mathtt{f}^2\right)^2}{\mathtt{f}^2}\left(1-4\alpha\right) . \tag{6.30}$$

Hence, h_s is concave as long as $\alpha>\frac{1}{4}$. Therefore, under this condition we can obtain convex property of h_s when $p=0$.

We sum up the investigation of sign changes around the critical points in Table 6.2, Table 6.3, and Table 6.4.

Remark 6.2.1. As can be seen in Table 6.3, we can recognise that convexity of the Hamiltonian H_{VBW} for the range of specular exponent $1\leq\alpha\leq 100$ still holds within the proximity of the critical point ($\frac{-0.05\mathtt{f}}{x^2+\mathtt{f}^2}\leq p\leq\frac{0.05\mathtt{f}}{x^2+\mathtt{f}^2}$) when $p=0$. From the theoretical point of view, we can also have similar effect when $x\gg\mathtt{f}$.

When $p=\pm\frac{\mathtt{f}}{x^2+\mathtt{f}^2}$, however, h_{s_p} vanishes, which makes $h_{s_{pp}}$ zero as well. Therefore, we can notice that around this point the Hamiltonian h_s is not strictly concave and thereby H_{VBW} loses strong convexity. As can be seen in Table 6.2 and Table 6.4, for the close

p	$p = \dfrac{-\mathtt{f}}{x^2+\mathtt{f}^2}$	$p = \dfrac{-0.95\mathtt{f}}{x^2+\mathtt{f}^2}$
h_{s_p}	0	$\begin{cases} + & \alpha > 0.0243 \\ - & \alpha < 0.0243 \end{cases}$
$h_{s_{pp}}$	0	$\begin{cases} + & \alpha > 1.0020 \\ - & 0.0007 < \alpha < 1.0020 \\ + & \alpha < 0.0007 \end{cases}$

Table 6.2: Investigation of sign changes of h_{s_p} and $h_{s_{pp}}$ around the critical point when $p = \frac{-\mathtt{f}}{x^2+\mathtt{f}^2}$.

p	$p = \dfrac{-0.05\mathtt{f}}{x^2+\mathtt{f}^2}$	$p = 0$	$p = \dfrac{0.05\mathtt{f}}{x^2+\mathtt{f}^2}$
h_{s_p}	$\begin{cases} + & \alpha > 0.2494 \\ - & \alpha < 0.2494 \end{cases}$	0	$\begin{cases} - & \alpha > 0.2494 \\ + & \alpha < 0.2494 \end{cases}$
$h_{s_{pp}}$	$\begin{cases} + & \alpha > 100.2525 \\ - & 0.2481 < \alpha < 100.2525 \\ + & \alpha < 0.2481 \end{cases}$	$\begin{cases} - & \alpha > \frac{1}{4} \\ + & \alpha < \frac{1}{4} \end{cases}$	$\begin{cases} + & \alpha > 100.2525 \\ - & 0.2481 < \alpha < 100.2525 \\ + & \alpha < 0.2481 \end{cases}$

Table 6.3: Investigation of sign changes of h_{s_p} and $h_{s_{pp}}$ around the critical point when $p = 0$.

point of $p = \pm\frac{\mathtt{f}}{x^2+\mathtt{f}^2}$ the valid α for the convexity of H_{VBW} is only when $\alpha = 1$, which is too small to be used in reality.

6.3 Summary

In this chapter, we have studied the Vogel-Breuß-Weickert model which involves non-Lambertian surfaces.

First, we have appreciated the new model. Compared to the Prados model in Chapter 5, it deals with Phong reflectance in consideration of light attenuation term. This change in model assumptions affects the type of Hamiltonian, which also has influence on the convexity.

Then, to understand the behaviour of Hamiltonian we have analysed the critical points

p	$p = \dfrac{0.95\mathtt{f}}{x^2+\mathtt{f}^2}$	$p = \dfrac{\mathtt{f}}{x^2+\mathtt{f}^2}$
h_{s_p}	$\begin{cases} - & \alpha > 0.0244 \\ + & \alpha < 0.0244 \end{cases}$	0
$h_{s_{pp}}$	$\begin{cases} + & \alpha > 1.0020 \\ - & 0.0007 < \alpha < 1.0020 \\ + & \alpha < 0.0007 \end{cases}$	0

Table 6.4: Investigation of sign changes of h_{s_p} and $h_{s_{pp}}$ around the critical point when $p = \frac{\mathtt{f}}{x^2+\mathtt{f}^2}$.

in one-dimensional case and have seen that under which circumstances the Hamiltonian can be convex.

In the next chapter, we shall discuss numerical schemes for solving Hamilton-Jacobi equations.

Chapter 7

Numerical Schemes

So far, we have investigated perspective Shape from Shading models describing Lambertian and non-Lambertian surfaces which actually deal with convex and non-convex Hamiltonians. However, besides theoretical point of view we are also in need of practical strategy in order to realise the model in real-life situations.

In this chapter, we shall study numerical methods to solve Hamilton-Jacobi equations in the viscosity framework. Since Hamilton-Jacobi equations belong to the class of nonlinear PDEs, there are more issues that we have to think about than those of linear ones. One important issue is about the criterion for the convergence of numerical schemes. Concerning the convergence matter, a scheme that approximates nonlinear PDEs to obtain viscosity solutions asks more requirements than those of Lax-Richtmyer equivalence theorem in the linear cases, which we shall discuss here.

The structure of this chapter is as follows.

We begin with the basic concepts that will be used for the analysis of numerical schemes in this chapter by examining upwind schemes approximating linear advection equation. This includes consistency, stability, monotonicity, and the fundamental theorem of numerical analysis.

After that we shall see how the convergence of numerical schemes works in the viscosity framework with these notions. This is actually the main point to prove the convergence of Rouy and Tourin scheme in [26]. To this end, we primarily follow the concepts and arguments from the work by Barles and Souganidis [37] and by Souganidis [101], both of which are based on the notion of weak limits.

Then, the attention will be paid to the scheme of Rouy and Tourin which is originally designed to obtain viscosity solutions of the eikonal-type Hamiltonian for the orthogonal Shape from Shading model.

Finally, we think of the Vogel-Breuß-Weickert model in a numerical point of view. Our contribution here is to provide the analysis of convergence for the explicit scheme in one-dimensional case.

To this end, we have used a certain range of literature depending on the topics. Main references for basic numerical concepts in this chapter are [6, 15, 33, 58, 59] and for the convergence theory in the viscosity framework [37, 101] are used. In addition, we mainly follow [26] for the scheme of Rouy and Tourin and [61, 74, 75] for numerical algorithms of Vogel-Breuß-Weickert model, respectively.

7.1 Basic Notions for Numerical Schemes

Since upwind-type schemes are used in the work by Rouy and Tourin [26] and Vogel et al. [75] in order to solve HJE numerically in the viscosity framework, here we briefly review the basics of these types of schemes.

7.1.1 Upwind Scheme

To illustrate the idea, first let us consider the following one-dimensional linear hyperbolic *advection equation*

$$u_t + a\,u_x = 0\,, \tag{7.1}$$

where $a \in \mathbb{R}$ with an initial condition

$$u\,(x,0) := u_0\,(x)\;. \tag{7.2}$$

The solution of (7.1) with (7.2) is known to be

$$u\,(x,t) := u_0\,(x - at) \tag{7.3}$$

for example in [51, 58, 59] and it is not difficult to show. Taking partial derivatives of (7.3) with respect to t and x yields

$$\begin{aligned}
\frac{\partial}{\partial t}u\,(x,t) &= \frac{\partial}{\partial t}u_0\,(x-at) \\
&\quad x - at =: x_0 \\
&= \frac{\partial}{\partial x_0}u_0\,(x_0)\,\frac{\partial x_0}{\partial t} \\
&\quad \text{since } \partial x_0 = \partial x \text{ and } \frac{\partial x_0}{\partial t} = -a \\
&= \frac{\partial}{\partial x}u_0\,(x-at)\,(-a)
\end{aligned} \tag{7.4}$$

and

$$\begin{aligned}
a\frac{\partial}{\partial x}u\,(x,t) &= a\frac{\partial}{\partial x}u_0\,(x-at) \\
&= a\frac{\partial}{\partial x}u_0\,(x-at)\;,
\end{aligned} \tag{7.5}$$

respectively. Plugging (7.4) and (7.5) into (7.1) gives

$$u_t + a\,u_x = \frac{\partial}{\partial x}u_0\,(x - at)\,(-a) + a\,\frac{\partial}{\partial x}u_0\,(x - at) = 0\,, \tag{7.6}$$

which verifies the assertion.

In one-dimensional case, the solution (7.3) basically states that the initial data u_0 propagates with the speed a in one direction, namely right if $a > 0$ or left if $a < 0$. This explains a spatially one-sided discretisation, see Figure 7.1.

Before we discretise spatial domain, temporal discretisation is taken into account first. For this purpose, we make use of explicit forward Euler method, which means

$$u_t \approx \frac{u_i^{n+1} - u_i^n}{\Delta t}\,. \tag{7.7}$$

Now, we consider the spatial discretisation. As mentioned earlier, the information is delivered from left to right when $a > 0$, so in this case the reasonable spatial approximation is

$$u_x \approx \frac{u_i^n - u_{i-1}^n}{\Delta x}\,. \tag{7.8}$$

In an analogous way, when $a < 0$ the information propagates from right to left, therefore we have the following spatial approximation

$$u_x \approx \frac{u_{i+1}^n - u_i^n}{\Delta x}\,. \tag{7.9}$$

Plugging (7.8) and (7.9) with (7.7) into (7.1) yields

$$\begin{aligned} \frac{u_i^{n+1} - u_i^n}{\Delta t} + a\,\frac{u_i^n - u_{i-1}^n}{\Delta x} &= 0 \qquad a > 0\,, \\ \frac{u_i^{n+1} - u_i^n}{\Delta t} + a\,\frac{u_{i+1}^n - u_i^n}{\Delta x} &= 0 \qquad a < 0\,, \end{aligned} \tag{7.10}$$

where

$$u_j^n = u\,(j\Delta x, n\Delta t) \qquad j \in \mathbb{Z}, n \in \mathbb{N}^+\,. \tag{7.11}$$

By sorting (7.10) out with respect to u_i^{n+1}, we can obtain the following upwind scheme:

$$u_i^{n+1} = u_i^n - a\,\frac{\Delta t}{\Delta x}\left(u_i^n - u_{i-1}^n\right) \qquad a > 0\,, \tag{7.12}$$

and

$$u_i^{n+1} = u_i^n - a\,\frac{\Delta t}{\Delta x}\left(u_{i+1}^n - u_i^n\right) \qquad a < 0\,. \tag{7.13}$$

Stencil diagrams for (7.12) and (7.13) are provided in Figure 7.1a and Figure 7.1b, respectively.

Remark 7.1.1. As can be noticed above, the basic idea of a upwind scheme boils down to determining propagation directions of information.

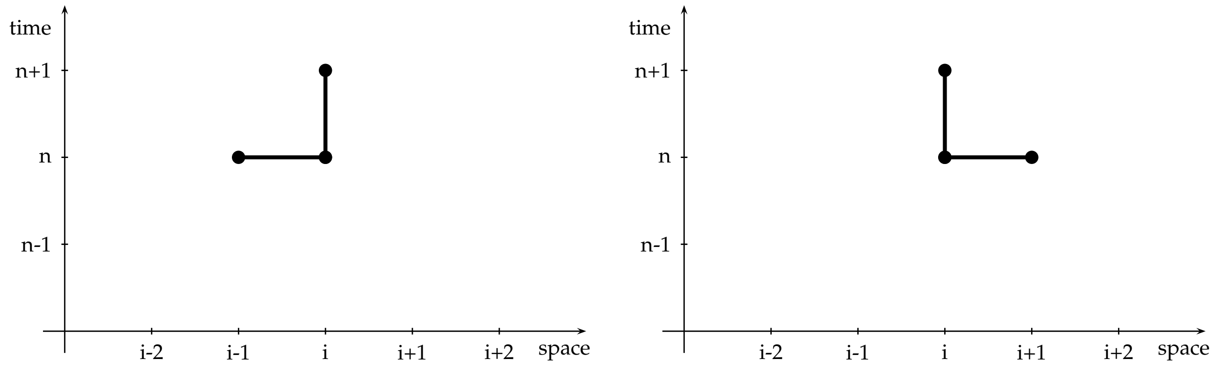

(a) Stencil diagram for the case of $a > 0$.

(b) Stencil diagram for the case of $a < 0$.

Figure 7.1: Stencil diagrams for upwind scheme in one-dimension.

7.1.2 Local Truncation Error and Consistency

In numerical analysis literature, e.g. in [58], *local truncation error* L is explained as a measure of how well the difference equation approximates the differential equation locally. It can be computed by replacing the approximate solution in the difference equation by the true solution. Let us have a look at the following example.

Here we think about the case of $a > 0$ in (7.12). Then, the local truncation error L can be understood as

$$\underbrace{u_t + a\,u_x}_{\text{original PDE}} = \underbrace{\frac{u_i^{n+1} - u_i^n}{\Delta t} + a\,\frac{u_i^n - u_{i-1}^n}{\Delta x}}_{\text{numerical scheme}} + \underbrace{L}_{\text{local truncation error}} . \tag{7.14}$$

In what follows, we shall see how local truncation error can be computed by making use of Taylor series expansion.

Under the smoothness assumption of u, by employing a notation

$$u\,(x,t) =: u := u\,(i\,\Delta x, n\,\Delta t) = u_i^n . \tag{7.15}$$

Taylor series expansions yield:

$$u_i^{n+1} = u + \Delta t\,u_t + \frac{\Delta^2}{2} u_{tt} + \frac{\Delta t^3}{6} + \mathcal{O}\left(\Delta t^4\right), \tag{7.16}$$

$$u_i^n = u\,, \tag{7.17}$$

and

$$u_{i-1}^n = u - \Delta x\,u_x + \frac{\Delta x^2}{2} u_{xx} - \frac{\Delta x^3}{6} u_{xxx} + \mathcal{O}\left(\Delta x^4\right). \tag{7.18}$$

Then, by (7.16), (7.17), and (7.18) the local truncation error L can be obtained by

$$\begin{aligned} L &= \frac{\left[u + \Delta t\, u_t + \frac{\Delta^2}{2} u_{tt} + \frac{\Delta t^3}{6} + \mathcal{O}\left(\Delta t^4\right)\right] - u}{\Delta t} \\ &\quad + \frac{a}{\Delta x}\left[u - \left[u - \Delta x\, u_x + \frac{\Delta x^2}{2} u_{xx} - \frac{\Delta x^3}{6} u_{xxx} + \mathcal{O}\left(\Delta x^4\right)\right]\right] \\ &= \underbrace{u_t + a\, u_x}_{\overset{(7.1)}{=} 0} + \frac{\Delta t}{2} u_{tt} + \frac{\Delta t^2}{6} u_{ttt} + \mathcal{O}\left(\Delta t^3\right) - \frac{a\,\Delta x}{2} u_{xx} + \frac{a\,\Delta x^2}{6} u_{xxx} + \mathcal{O}\left(\Delta x^3\right). \end{aligned} \tag{7.19}$$

Additionally, with

$$\lambda = \frac{\Delta t}{\Delta x} = \text{constant} \tag{7.20}$$

we are able to have the relationship

$$\mathcal{O}\left(\Delta t\right) = \mathcal{O}\left(\Delta x\right). \tag{7.21}$$

Hence, with the help of (7.21) and "big O" notation we can formulate the local truncation error L in (7.19) as

$$L = \mathcal{O}\left(\Delta x\right). \tag{7.22}$$

This defines the notion *consistency* of the numerical scheme, which means that local truncation error L goes to zero with the rate Δx as the mesh (or grid) size Δx vanishes. Thus, we can observe that upwind scheme (7.12) is consistent of first order in space and time with the PDE (7.1).

7.1.3 Necessary Notions for Convergence

The fundamental theorem of numerical analysis which will be the next topic is a primary building block for linear numerical methods. In order to appreciate this, some other notions are needed to be taken into account in addition to consistency and local truncation error.

In the theory of numerical analysis for PDEs, three notions are closely related, i.e. consistency, convergence, and stability. As we have studied the consistency just right before, let us start with the meaning of convergence and see how it is related to others. Besides that, monotonicity shall also be discussed as a nonlinear stability criterion.

Convergence

Convergence of a numerical scheme means that a solution of a difference equation obtained from a numerical scheme approximating an original PDE approaches a true solution of an original PDE with respect to a corresponding norm, as parameters in numerical methods, e.g. a mesh size Δx and a time step size Δt, vanish. Convergence of a scheme is the desired property of a numerical method, otherwise the result of a scheme is meaningless.

At this point, one may raise a question "Is consistency not good enough for the convergence of a scheme?" If not, why?

The answer to this question is "no" and the issue here is the total sum of accumulated truncation errors. The main reason for this problem lies in the approximation process of continuous problems in a discrete domain.

Since a truncation error occurs at each evaluation point of a numerical scheme as we go over all grid points within a discretisation domain, we definitely need an insurance policy which guarantees that these accumulated errors do not grow exponentially, which in mathematical terms is bounded above. If these computational errors are not bounded, they force us to solve different problems from the original ones, which makes the computed results of no use. *Stability* theory of numerical schemes is developed in order to take care of this phenomenon.

Stability

In [15], *stability* is described in three aspects, all of which are helpful to understand the convergence result in the next section. Here, we briefly appreciate them one by one.

First of all, stability means that solutions of a numerical approximation of a PDE mimics important structural properties of *analytic solutions* of an original PDE.

Among such properties, we can choose a maximum (or minimum) principle. So, if we have a maximum (or minimum) principle in analytic solutions, discrete solutions of a stable scheme must also obey a discrete maximum (or minimum) principle. This perspective leads to a notion of monotonicity of a scheme which will be discussed as a next topic.

Another perspective of stability is that it is relevant to give a bound on a numerical solution. This is reasonable in the sense that a bounded accumulated sum of errors lead to a bound on a numerical solution. Such a bound may depend on the norm in use. This aspect will be used for the convergence result in the next section.

As a result, in numerical analysis stability is an indispensable requirement to prove convergence of a scheme.

Remark 7.1.2. Notice that we only have discussed linear cases so far. Then, how about nonlinear ones? Not only for linear cases but also for nonlinear ones does a discrete maximum (or minimum) principle have a meaning as well, since it enables to avoid numerical oscillations which can be misinterpreted as noise.

In the sequel, we are about to see a property of *monotonicity* which can serve as a nonlinear stability criterion.

Monotonicity

Monotonicy implies that a discrete comparison principle holds for all time levels $n \in \mathbb{N}^+$. This suggests that for the given V^n and W^n with $V^n \geq W^n$ (pointwise) the inequality should not be changed as a time step n evolves. In other words, $V^{n+1} \geq W^{n+1}$ (pointwise) must also be valid at the next time level $n+1$ [58].

As a result, monotonicity mimics an *analytic comparison principle*: Given two initial conditions (or boundary conditions) $\Phi \geq \Psi$ (pointwise), then for the corresponding analytic solutions u_Φ and u_Ψ should hold $u_\Phi \geq u_\Psi$ (pointwise).

By monotonicity, a discrete maximum (or minimum) principle is immediately justified. This can be understood as follows. We may take sequences composed solely of the constants given by the maximum/minimum of some given sequences V^n. Applying a monotone scheme to V^n implies that this can never exceed the bounds.

Then, how can we verify monotonicity and why in that way?

According to [59], for a given explicit three points scheme by

$$u_i^{n+1} = \mathcal{G}\left(u_{i-1}^n, u_i^n, u_{i+1}^n\right), \tag{7.23}$$

to prove monotonicity we must show

$$(i)\ \frac{\partial \mathcal{G}}{\partial u_{i-1}^n} \geq 0, \quad (ii)\ \frac{\partial \mathcal{G}}{\partial u_i^n} \geq 0, \quad (iii)\ \frac{\partial \mathcal{G}}{\partial u_{i+1}^n} \geq 0. \tag{7.24}$$

This means that $\mathcal{G}$ should be a monotonically increasing function with respect to u_{i-1}^n, u_i^n, and u_{i+1}^n. To explain why this is the case, let us take the point of view that a set of data $V^n = \left\{\ldots, v_{i-1}^n, v_i^n, v_{i+1}^n, \ldots\right\}$ is given. The task is to validate a comparison principle as defined above. Thus, for comparison we take some data set W^n with $W^n \geq V^n$ in the pointwise sense.

Now, let $w_k^n = v_k^n$ for all indices k, except for $w_i^n > v_i^n$. What we expect when applying $\mathcal{G}$ in (7.23) for $\mathcal{G}$ monotone is $W^{n+1} \geq V^{n+1}$ in the pointwise sense.

First, we check the case of (i).

At point $i-1$, given $w_i^n > v_i^n$, it may in general only hold $w_{i-1}^{n+1} \geq v_{i-1}^{n+1}$. When we consider any positive perturbation δ of w_k^n

$$w_k^n = v_k^n + \delta, \tag{7.25}$$

this leads to

$$\begin{aligned}
& w_{i-1}^{n+1} \overset{(7.23)}{=} \mathcal{G}\left(w_{i-2}^n, w_{i-1}^n, w_i^n\right) \\
\Leftrightarrow\quad & w_{i-1}^{n+1} \overset{(7.25)}{=} \underbrace{\mathcal{G}\left(v_{i-2}^n, v_{i-1}^n, v_i^n + \delta\right) \overset{!}{\geq} \mathcal{G}\left(v_{i-2}^n, v_{i-1}^n, v_i^n\right)}_{(*)} \overset{(7.23)}{=} v_{i-1}^{n+1}.
\end{aligned} \tag{7.26}$$

The part $(*)$ which we really want in (7.26) can be expressed as

$$
\begin{aligned}
& \mathcal{G}\left(v_{i-2}^n, v_{i-1}^n, v_i^n+\delta\right)-\mathcal{G}\left(v_{i-2}^n, v_{i-1}^n, v_i^n\right) && \geq && 0 \quad \forall \delta>0 \\
\Leftrightarrow \quad & \frac{\mathcal{G}\left(v_{i-2}^n, v_{i-1}^n, v_i^n+\delta\right)-\mathcal{G}\left(v_{i-2}^n, v_{i-1}^n, v_i^n\right)}{\delta} && \geq && 0 \quad \forall \delta>0 .
\end{aligned} \tag{7.27}
$$

Taking $\delta \rightarrow 0$ gives the reason of the condition (iii) in (7.24) from (7.23).

In a similar way, by investigating the case at the point $i+1$ and i we can obtain the condition (i) and (ii) in (7.24) from (7.23), respectively.

Example 7.1.1 (Monotonocity of Upwind Scheme). Here we consider the condition for monotonicity of upwind scheme (7.12). When we rewrite (7.12) as

$$
\begin{aligned}
H\left(u_{i-1}^n, u_i^n\right) & = u_i^n-a \frac{\Delta t}{\Delta x}\left(u_i^n-u_{i-1}^n\right) \\
& = \left(1-a \frac{\Delta t}{\Delta x}\right) u_i^n+\frac{a \Delta t}{\Delta x} u_{i-1}^n .
\end{aligned} \tag{7.28}
$$

In view of (7.24) scheme (7.12) is monotone under the following time step size restriction when $a>0$:

$$
\begin{cases}
\dfrac{\partial H}{\partial u_{i-1}^n} = \dfrac{a \Delta t}{\Delta x} \geq 0 & \\
\dfrac{\partial H}{\partial u_i^n} = 1-\dfrac{a \Delta t}{\Delta x} \geq 0 & \Leftrightarrow \quad \Delta t \leq \dfrac{\Delta x}{a} .
\end{cases} \tag{7.29}
$$

Remark 7.1.3. The time step size restriction in (7.29) is known as *CFL condition* after Courant, Friedrichs and Lewy [89] (English version [90]), which is a necessary condition for the convergence of finite difference methods. This constraint states that there is a limit for the rate in propagation of information [15, 58, 59]. In addition, $\nu:=\frac{a \Delta t}{\Delta x}$ is called *Courant number*.

Now, we give the fundamental theorem of numerical analysis.

7.1.4 The Fundamental Theorem of Numerical Analysis

The fundamental theorem of numerical analysis states that consistency and stability conditions are the necessary and sufficient conditions for convergence of a scheme given a well-posed initial value problem and a finite difference approximation to it.

This can be summarised as

$$
\text{consistency} + \text{stability} \Leftrightarrow \text{convergence} . \tag{7.30}
$$

Sometimes, it is also referred as *Lax-Richtmyer theorem* or *Lax's equivalence theorem* [80]. The rigourous proof can be found, for example, in [92] or [49].

Remark 7.1.4. The point to be stressed out is that the Lax's equivalence theorem can only be applied to linear cases. We shall see the nonlinear cases in the next section.

7.2 Stepping Stones to Convergence

According to [37], the convergence result basically states that solutions of a scheme which is monotone, consistent and stable converge towards a unique continuous viscosity solution provided that a problem admits a comparison principle.

In this section, we investigate the above statement which is a main building block for the convergence of Rouy and Tourin scheme. Since for eikonal-type Hamiltonians the analysis is given in [68], we focus here specially on general-type. As noted previously, the argumentations basically rely on the work by Barles and Souganidis [37] and Souganidis [101]. More details about the theory, we refer to [37, 78, 101] and the references therein.

7.2.1 Construction of a Scheme Function

The ideas explained below mostly came from work by Ishii [48] and by Barles and Perthame [35, 36]. Although they have employed discontinuous concepts, we restrict ourselves only to continuous ones.

What we focus on is the Dirichlet problem for Hamilton-Jacobi equations of the form

$$\begin{cases} H(x,u,Du) & = & 0 & \text{in} \quad \Omega \\ u(x) & = & \varphi(x) & \text{on} \quad \partial\Omega, \end{cases} \tag{7.31}$$

where $H : \Omega \times \mathbb{R} \times \mathbb{R}^n \to \mathbb{R}$ is continuous.

Now, we are interested in constructing a function which has a capability to combine the Hamiltonian and the boundary condition in (7.31) into one expression for efficient treatment of schemes.

As noted before, by assuming that no discontinuity occurs on boundary in (7.31), we can define a function $F : \overline{\Omega} \times \mathbb{R} \times \mathbb{R}^n \to \mathbb{R}$ as

$$F(x,u,Du) = \begin{cases} H(x,u,Du) & x \in \Omega \\ u(x) - \varphi(x) & x \in \partial\Omega. \end{cases} \tag{7.32}$$

Then, (7.31) can be reformulated as

$$F(x,u,Du) = 0 \quad \text{in} \quad \overline{\Omega}, \tag{7.33}$$

where Ω denotes an open subset of $\mathbb{R}^n$, $\overline{\Omega}$ is its closure, the functions $F : \overline{\Omega} \times \mathbb{R} \times \mathbb{R}^n \to \mathbb{R}$ and $u : \overline{\Omega} \to \mathbb{R}$ are locally bounded and continuous both in Ω and on the boundary $\partial\Omega$.

7.2.2 Continuous Viscosity Solutions for General-Type HJE

As we have seen in Definition 2.3.1, continuous viscosity solutions for general-type Hamilton-Jacobi equations (7.31) can be defined as follows.

Definition 7.2.1 (Continuous Viscosity Solution). A continuous function $u \in C^0$ is a viscosity solution of HJE (7.31) if the following conditions are satisfied:

(i) **(Viscosity subsolution)** For any test function $\varphi \in C^1(\Omega)$, if $x_0 \in \Omega$ is a local maximum point for $(u - \varphi)$, then

$$H\left(x_0, u\left(x_0\right), D\varphi\left(x_0\right)\right) \leq 0 \tag{7.34}$$

(ii) **(Viscosity supersolution)** For any test function $\varphi \in C^1(\Omega)$, if $x_1 \in \Omega$ is a local minimum point for $(u - \varphi)$, then

$$H\left(\left(x_1, u\left(x_1\right), D\varphi\left(x_1\right)\right)\right) \geq 0. \tag{7.35}$$

This means that for a locally bounded function $u : \overline{\Omega} \to \mathbb{R}$ to be a viscosity solution of (7.31) u need to satisfy (7.33) in the viscosity sense in view of Definition 7.2.1.

7.3 Theoretical Investigation of Convergence

To approximate (7.33), we consider schemes of the form

$$S\left(\rho, x, u^{\rho}\left(x\right), u^{\rho}\right) = 0 \quad \text{in} \quad \overline{\Omega}, \tag{7.36}$$

where $S : \mathbb{R}^+ \times \overline{\Omega} \times \mathbb{R} \times B\left(\overline{\Omega}\right) \to \mathbb{R}$ and $B\left(\overline{\Omega}\right)$ denotes the space of bounded functions defined on $\overline{\Omega}$ and $\rho > 0$ is a grid parameter.

As mentioned before, the main statement for convergence result is that solutions of (7.36) converge to the continuous viscosity solution of (7.31) as long as schemes are monotone, stable and consistent and provided that the original problem (7.31) admits a comparison principle.

In what follows, we formulate the assumptions for schemes (7.36).

7.3.1 Assumptions on Schemes

The assumptions on schemes comprise:

(S1) monotonicity

(S2) stability

(S3) consistency

(S4) strong uniqueness.

Here, we appreciate one by one.

The first assumption is *monotonicity* of schemes and can be defined as follows.

Definition 7.3.1 (Monotonicity). The scheme S in (7.36) is called *monotone* if $\rho \geq 0$, $x \in \overline{\Omega}$, $t \in \mathbb{R}$, and $u, v \in B\left(\overline{\Omega}\right)$

$$u \leq v \quad \Rightarrow \quad S\left(\rho, x, t, u\right) \geq S\left(\rho, x, t, v\right). \tag{7.37}$$

Remark 7.3.1. According to this definition, the monotone scheme is nonincreasing with respect to u. For this matter, one may raise a question if this notion is different from the one in (7.23) and (7.24). The answer to this question is "no" and can be understood as follows.

The monotonicity in (7.23) is designed for a one-dimensional Cauchy problem

$$\begin{cases} \dfrac{\partial u}{\partial t} + H\left(x, u, Du\right) & = & 0 & \text{in} & \mathbb{R} \times (0, T] \\ u\left(x, 0\right) & = & u_0\left(x\right) & \text{in} & \mathbb{R}, \end{cases} \tag{7.38}$$

where $H : \mathbb{R} \times \mathbb{R} \times \mathbb{R} \to \mathbb{R}$ is continuous.

For discretisation of (7.38), by making use of Euler forward method in time and upwind scheme in spatial domain we obtain

$$\begin{aligned} & \frac{u_i^{n+1} - u_i^n}{\Delta t} + H\left(x_i, u_i^n, \frac{x_i - x_{i-1}}{\Delta x}\right) = 0 \\ \Leftrightarrow \quad & u_i^{n+1} = \underbrace{u_i^n - \Delta t H\left(x_i, u_i^n, \frac{x_i - x_{i-1}}{\Delta x}\right)}_{=:\mathcal{H}}. \end{aligned} \tag{7.39}$$

According to (7.23) and (7.24), $\mathcal{H}$ in (7.39) should be a nondecreasing function for monotonicity. This means that H in (7.39) must be a monotonic nonincreasing function and so is S in (7.36) which approximates H.

The second one is the *stability* of schemes and can be defined as follows.

Definition 7.3.2 (Stability). The scheme S in (7.36) is called *stable* if for all $\rho > 0$, there exists a solution $u^\rho \in B\left(\overline{\Omega}\right)$ of (7.36) with a bound which is independent of ρ.

Remark 7.3.2. As we have studied the notion of stability in previous section, the bound on the accumulated local truncation error leads to the existence of numerical solutions with a corresponding bound.

The third one is *consistency* of schemes and can be defined as follows.

Definition 7.3.3 (Consistency).

$$\limsup_{\substack{\rho \to 0 \\ y \to x \\ \xi \to 0}} \frac{S(\rho, y, \phi(y) + \xi, \phi + \xi)}{\rho} \le F(x, \phi(x), D\phi(x)), \tag{7.40}$$

and

$$\liminf_{\substack{\rho \to 0 \\ y \to x \\ \xi \to 0}} \frac{S(\rho, y, \phi(y) + \xi, \phi + \xi)}{\rho} \ge F(x, \phi(x), D\phi(x)). \tag{7.41}$$

Remark 7.3.3. This new definition seems a little bit different from the one that we encountered in the previous section, but it is also related to the local truncation error in the viscosity sense. Both (7.40) and (7.41) are designed to check how schemes accurately mimic viscosity super- and subsolution notions in Definition 7.2.1, respectively. Specially, the right hand sides of both (7.40) and (7.41) are the limiting process of the method which will be detailed in the proof of Theorem 7.3.1.

Another important assumption is *strong uniqueness* property of (7.31), which also suggests that the same property holds for (7.33). Since we treat only continuous solutions, we can have this property without any difficulty, which basically rely on the *comparison principle*. The result is given in Definition 7.3.4 borrowed from [84], for the proof and theorems involved with this matter, we refer to [12, 23, 60] and the references therein.

Definition 7.3.4 (Strong Uniqueness). It can be said that the *strong uniqueness* holds for the problem (7.31) and (7.33), when

$$u(x) \le v(x) \quad \forall x \in \overline{\Omega}, \tag{7.42}$$

where u and v denote viscosity sub- and supersolution, respectively.

7.3.2 The Convergence Result

The main theorem for convergence of schemes is given below. We elaborate on the proof in [37] thereby clarifying the ideas therein.

Theorem 7.3.1. *Assume that scheme S in (7.36) satisfies (S1), (S2), (S3), and (S4). Then, the solution of u^ρ of (7.36) converges locally uniformly to the unique continuous viscosity solution of (7.31) and (7.33) as $\rho \to 0$.*

Proof. The main idea of this proof utilises strong uniqueness property and the auxiliary functions defined by weak limits which have useful properties in the continuous viscosity framework.

The flow of argumentation is as follows.

First, we define functions $\underline{u}$ and $\overline{u}$ by

$$\underline{u}(x) = \liminf_{\substack{\rho \to 0 \\ y \to x}} u^{\rho}(y) \tag{7.43}$$

and

$$\overline{u}(x) = \limsup_{\substack{\rho \to 0 \\ y \to x}} u^{\rho}(y) . \tag{7.44}$$

Hence, it is clear that $\underline{u} \leq \overline{u}$ holds.

Next, assume for the time being that $\overline{u}$ and $\underline{u}$ are viscosity sub- and supersolution of (7.33) respectively, which we shall validate later. Then, we have $\overline{u} \leq \underline{u}$ by Definition 7.3.4. This means that with the previous result we are able to receive

$$\overline{u} = \underline{u} . \tag{7.45}$$

In other words, we can obtain the unique viscosity solution u such that

$$u \equiv \liminf_{\substack{\rho \to 0 \\ y \to x}} u^{\rho}(y) = \limsup_{\substack{\rho \to 0 \\ y \to x}} u^{\rho}(y) , \tag{7.46}$$

where u^{ρ} is used in scheme function (7.36).

Since viscosity solution u is both viscosity sub- and supersolution at the same time by Definition 7.2.1, this also implies the local uniform convergence of u^{ρ} to u in view of (7.46). Hence, the assertion follows.

As a result, our rest job is to confirm the above claim that $\overline{u}$ and $\underline{u}$ are viscosity sub- and supersolution of (7.33), respectively.

Subsolution $\overline{u}$. The idea of this proof is composed of two parts. First, we build up sequences in such a way, that they satisfy the viscosity subsolution criteria. Afterwards, by taking limits and applying the assumptions on the scheme S, i.e. monotonicity and consistency, we obtain the desired result.

Let x_0 be a local maximum of $\overline{u} - \phi$ on $\overline{\Omega}$ for some $\phi \in C^{\infty}\left(\overline{\Omega}\right)$. Without loss of generality, we may assume that x_0 is a strict local maximum, that $\overline{u}(x_0) = \phi(x_0)$, and finally that $\phi \geq 2 \sup_{\rho} \|u^{\rho}\|_{\infty}$ outside the ball $B(x_0, r)$, where $r > 0$ is such that

$$\overline{u}(x) - \phi(x) \leq 0 = \overline{u}(x_0) - \phi(x_0) \quad \text{in} \quad B(x_0, r) . \tag{7.47}$$

This guarantees that the local maximum occurs only within the ball $B(x_0, r)$.

Then, as $n \to \infty$ by Lemma II 2.4 in [12] there exist sequences $\rho_n \in \mathbb{R}^+$ and $y_n \in \overline{\Omega}$ such that

(i) $\rho_n \to 0$

(ii) $y_n \longrightarrow x_0$

(iii) $u^{\rho_n}(y_n) \longrightarrow \overline{u}(x_0)$

(iv) y_n is a global maximum point of $u^{\rho_n}(\cdot) - \phi(\cdot)$.

By denoting

$$\xi_n =: u^{\rho_n}(y_n) - \phi(y_n) \tag{7.48}$$

and making use of (7.47), as $\xi_n \rightarrow 0$ we have

$$u^{\rho_n}(y_n) \leq \phi(x) + \xi_n \quad \forall x \in \overline{\Omega}. \tag{7.49}$$

Applying monotonicity of S to (7.49) yields

$$S(\rho_n, y_n, u^{\rho_n}(y_n), u^{\rho_n}) \geq S(\rho_n, y_n, \phi(y_n) + \xi_n, \phi + \xi_n) \tag{7.50}$$

Taking limits on the left hand side of (7.56) gives

$$S(\rho_n, y_n, \phi(y_n) + \xi_n, \phi + \xi_n) \leq 0. \tag{7.51}$$

For estimation of (7.51), by using consistency of S in (7.41) we can receive

$$\begin{aligned} & & \liminf_{n} \frac{S(\rho_n, y_n, \phi(y_n) + \xi_n, \phi + \xi_n)}{\rho_n} &\leq 0 \\ \Leftrightarrow \quad F(x_0, \phi(x_0), D\phi(x_0)) &\overset{(7.41)}{\leq} \liminf_{\substack{\rho \to 0 \\ y \to x_0 \\ \xi \to 0}} \frac{S(\rho, y, \phi(y) + \xi, \phi + \xi)}{\rho} &\leq 0, \end{aligned} \tag{7.52}$$

which is desired inequality, since $\overline{u}(x_0) = \phi(x_0)$ by (7.47).

Supersolution $\underline{u}$. The idea here is identical to the subsolution case and only the maximum point is replaced by a minimum point.

Let x_1 be a local minimum of $\underline{u} - \phi$ on $\overline{\Omega}$ for some $\phi \in C^\infty(\underline{\Omega})$. Without loss of generality, we may assume that x_1 is a strict local minimum, that $\underline{u}(x_1) = \phi(x_1)$, and finally that $\phi \leq -2\sup_\rho \|u^\rho\|_\infty$ outside the ball $B(x_1, r)$, where $r > 0$ is such that

$$\underline{u}(x) - \phi(x) \geq 0 = \underline{u}(x_1) - \phi(x_1) \quad \text{in} \quad B(x_1, r). \tag{7.53}$$

This guarantees that the local minimum occurs only within the ball $B(x_1, r)$.

Then, as $n \rightarrow \infty$ by Lemma II 2.4 in [12] there exist sequences $\rho_n \in \mathbb{R}^+$ and $y_n \in \underline{\Omega}$ such that

(i) $\rho_n \longrightarrow 0$

(ii) $y_n \longrightarrow x_1$

(iii) $u^{\rho_n}(y_n) \longrightarrow \underline{u}(x_1)$

(iv) y_n is a global maximum point of $u^{\rho_n}(\cdot) - \phi(\cdot)$.

By denoting

$$\xi_n =: u^{\rho_n}(y_n) - \phi(y_n) \tag{7.54}$$

and making use of (7.47), as $\xi_n \longrightarrow 0$ we have

$$u^{\rho_n}(y_n) \geq \phi(x) + \xi_n \quad \forall x \in \overline{\Omega}. \tag{7.55}$$

Applying monotonicity of S to (7.49) yields

$$S\left(\rho_n, y_n, u^{\rho_n}(y_n), u^{\rho_n}\right) \leq S\left(\rho_n, y_n, \phi(y_n) + \xi_n, \phi + \xi_n\right) \tag{7.56}$$

Taking limits on the left hand side of (7.56) gives

$$S\left(\rho_n, y_n, \phi(y_n) + \xi_n, \phi + \xi_n\right) \geq 0. \tag{7.57}$$

For the estimation of (7.57), by using consistency of S in (7.40) we can receive

$$\begin{array}{rrrcl} & & \limsup\limits_{n} \dfrac{S\left(\rho_n, y_n, \phi(y_n) + \xi_n, \phi + \xi_n\right)}{\rho_n} & \geq & 0 \\ \Leftrightarrow & F\left(x_1, \phi(x_1), D\phi(x_1)\right) \overset{(7.40)}{\geq} & \limsup\limits_{\substack{\rho \to 0 \\ y \to x_1 \\ \xi \to 0}} \dfrac{S\left(\rho, y, \phi(y) + \xi, \phi + \xi\right)}{\rho} & \geq & 0, \end{array} \tag{7.58}$$

which is desired inequality, since $\overline{u}(x_1) = \phi(x_1)$ by (7.53). □

Remark 7.3.4. Since the assumptions of the Rouy and Tourin scheme [26] are the same as here, i.e. monotonicity, stability, consistency and strong uniqueness, this convergence result can be transferred directly.

7.4 The Scheme of Rouy and Tourin

In this section, we study the scheme of Rouy and Tourin by making use of the one-dimensional eikonal equation. This scheme was quite successful to deal with Hamilton-Jacobi equation in the viscosity framework [26].

7.4.1 Construction of a Scheme

Let us consider the following one-dimensional eikonal equation

$$\begin{cases} |\nabla u(x)| & = & 1 & x \in (0,1) \\ u(x) & = & 0 & x \in \{0,1\}. \end{cases} \tag{7.59}$$

Numerical Approximation

Then, a numerical approximation U must satisfy

$$\begin{cases} g_i\left(D_x^+U_i, D_x^-U_i\right) & = & 0 \quad \forall i \in Q \\ U_i & = & 0 \quad \forall i \in \partial Q, \end{cases} \tag{7.60}$$

where

$$g_i\left(a,b\right) = \sqrt{\left(\min\left(0,a,b\right)\right)^2} - 1, \tag{7.61}$$

$$D_x^+ = \frac{U_{i+1} - U_i}{\Delta x}, \tag{7.62}$$

$$D_x^- = \frac{U_{i-1} - U_i}{\Delta x}, \tag{7.63}$$

$$Q = \left\{i \in \mathbb{N} \,|\, x_i \in \left(0,1\right)\right\}, \tag{7.64}$$

and

$$\partial Q = \left\{i \in \mathbb{N} \,|\, x_i \in \{0,1\}\right\}. \tag{7.65}$$

To make sure everything go off without a hitch, we assume the original problem (7.59) fulfils all the requirements for Theorem 4.3.1 in order to guarantee the uniqueness of a solution and so does the scheme g_i with index sets Q and ∂Q in view of Remark 4.3.1. In what follows, we give an exposition of this method.

To solve boundary value problem (7.59), we make use of *method of artificial time* as done in [75]. This means that we obtain $u\left(x,t\right)$ by introducing a pseudo-time variable t and solve this problem with respect to t iteratively until a steady state defined by $u_t = 0$ is attained [26, 75]. For an overview of different numerical methods to solve HJEs, we refer to [21].

According to this method, (7.59) can be turned into a Cauchy problem

$$\begin{cases} u_t + |u_x| - 1 & = & 0 \quad x \in \left(0,1\right) \times t \in \left]0,T\right] \\ u\left(x,t\right) & = & 0 \quad x \in \{0,1\} \times t \in \left]0,T\right] \\ u\left(x,0\right) & = & 0 \quad x \in \left[0,1\right]. \end{cases} \tag{7.66}$$

For the approximation of (7.66), we employ Euler forward method like in (7.7) for the time derivative u_t and a upwind-type scheme of Rouy and Tourin for the spatial derivative u_x [26]. The latter means

$$u_x\left(i\Delta x, \cdot\right) \approx \min\left(0, D_x^+, D_x^-\right) =: \hat{u}_x, \tag{7.67}$$

where

$$D_x^+ = \frac{u_{i+1} - u_i}{\Delta x} \tag{7.68}$$

and

$$D_x^- = \frac{u_{i-1} - u_i}{\Delta x}\,. \tag{7.69}$$

Plugging (7.7) and (7.67) into (7.66) yields

$$\begin{aligned}
& \frac{u_i^{n+1} - u_i^n}{\Delta t} + |\hat{u}_x| - 1 = 0 \\
\Leftrightarrow \qquad & \frac{u_i^{n+1} - u_i^n}{\Delta t} = -\left(|\hat{u}_x| - 1\right) \\
\Leftrightarrow \qquad & u_i^{n+1} = u_i^n - \Delta t\left(|\hat{u}_x| - 1\right) \\
\overset{|\cdot| = \sqrt{(\cdot)^2}}{\Leftrightarrow} \qquad & u_i^{n+1} = \underbrace{u_i^n - \Delta t\left(\sqrt{\hat{u}_x^2} - 1\right)}_{=:\mathcal{G}(u_{i-1}, u_i, u_{i+1})}\,.
\end{aligned} \tag{7.70}$$

Remark 7.4.1. For the choice of the third argument in (7.67), we need to set

$$\hat{u}_x := \frac{u_i - u_{i-1}}{\Delta x} > 0 \tag{7.71}$$

in order to ensure the consistency of the discretisation.

This type of scheme chooses one appropriate direction of information propagation which is meaningful for the problem itself. In other words, the discretisation has the same effect by making use of max operation with $+$ sign of u_i, which means

$$u_x\left(i\Delta x, \cdot\right) \approx \max\left(0, D_x^+, D_x^-\right) =: \hat{u}_x\,, \tag{7.72}$$

where

$$D_x^+ = \frac{u_i - u_{i+1}}{\Delta x} \tag{7.73}$$

and

$$D_x^- = \frac{u_i - u_{i-1}}{\Delta x}\,. \tag{7.74}$$

Analogous to Remark 7.4.1, we need to set

$$\hat{u}_x := \frac{u_{i+1} - u_i}{\Delta x}\,, \tag{7.75}$$

when in (7.72) the second argument is chosen.

7.4.2 Convergence of a Scheme

In the previous section, we have already seen how the convergence of a scheme works in the viscosity framework. Therefore, it suffices here that the assumptions of a scheme are fulfilled. These assumptions are composed of monotonicity, stability, consistency and uniqueness property of a problem.

Monotonicity and Stability

Since the scheme is stable as long as it is monotone, a monotonicity condition on the scheme can also serve as a stability restriction.

For the monotonicity investigation, we follow the notions from (7.23). As we have seen in (7.24), this means that we must show

$$(i)\ \frac{\partial \mathcal{G}}{\partial u_{i-1}^n} \geq 0\,, \quad (ii)\ \frac{\partial \mathcal{G}}{\partial u_i^n} \geq 0\,, \quad (iii)\ \frac{\partial \mathcal{G}}{\partial u_{i+1}^n} \geq 0\,. \tag{7.76}$$

For simplicity, we assume here that the iteration level used for discrete representations of u_x is always the "actual" level n.

Case (i)**.** When the first or second argument in (7.67) is chosen, there is no contribution for the case (i). This means that it holds

$$\frac{\partial \mathcal{G}}{\partial u_{i-1}^n} = 0\,. \tag{7.77}$$

Thus, we only need to consider the case when the third argument in (7.67) is selected.

By taking partial derivative of $\mathcal{G}$ from (7.70) with respect to u_{i-1} we have

$$\begin{aligned} \frac{\partial \mathcal{G}}{\partial u_{i-1}^n} &= -\Delta t\,\frac{\hat{u}_x}{\sqrt{\hat{u}_x^2}}\,\frac{\partial \hat{u}_x}{\partial u_{i-1}} \\ &\overset{(7.71)}{=} -\Delta t\,\frac{\hat{u}_x}{\sqrt{\hat{u}_x^2}}\left(-\frac{1}{\Delta x}\right) \\ &= \frac{\hat{u}_x}{\sqrt{\hat{u}_x^2}}\,\frac{\Delta t}{\Delta x} \\ &\overset{(7.71)}{=} \frac{\hat{u}_x}{\hat{u}_x}\,\frac{\Delta t}{\Delta x} \\ &= \frac{\Delta t}{\Delta x} > 0\,, \end{aligned} \tag{7.78}$$

which is the desired result.

Case (ii)**.** For the case (ii), we need to make case distinctions between the choice of the second and the third argument in (7.67).

To this end, we first take partial derivative of $\mathcal{G}$ from (7.70) with respect to u_i. Then, we have

$$\frac{\partial \mathcal{G}}{\partial u_i^n} = 1 - \Delta t\,\frac{\hat{u}_x}{\sqrt{\hat{u}_x^2}}\,\frac{\partial \hat{u}_x}{\partial u_i} \tag{7.79}$$

with

$$\hat{u}_x = \frac{u_{i+1} - u_i}{\Delta x} < 0 \tag{7.80}$$

or

$$\hat{u}_x = \frac{u_i - u_{i-1}}{\Delta x} \overset{(7.71)}{>} 0. \tag{7.81}$$

Now, let us take the case into account when the second argument in (7.67) is involved. Then, (7.79) is turned into

$$\begin{aligned}
\frac{\partial \mathcal{G}}{\partial u_i^n} &= 1 - \Delta t \frac{\hat{u}_x}{\sqrt{\hat{u}_x^2}} \frac{\partial \hat{u}_x}{\partial u_i} \\
&\overset{(7.80)}{=} 1 - \Delta t \frac{\hat{u}_x}{\sqrt{\hat{u}_x^2}} \left(-\frac{1}{\Delta x} \right) \\
&= 1 + \frac{\hat{u}_x}{\sqrt{\hat{u}_x^2}} \frac{\Delta t}{\Delta x} \\
&\overset{(7.80)}{=} 1 + \frac{\hat{u}_x}{(-\hat{u}_x)} \frac{\Delta t}{\Delta x} \\
&= 1 - \frac{\Delta t}{\Delta x} \overset{(!)}{\geq} 0.
\end{aligned} \tag{7.82}$$

Hence, in order to satisfy (!) in (7.82) the following condition must be satisfied:

$$\begin{aligned}
& 1 - \frac{\Delta t}{\Delta x} \geq 0 \\
\Leftrightarrow \quad & 1 \geq \frac{\Delta t}{\Delta x} \\
\Leftrightarrow \quad & \Delta t \leq \Delta x .
\end{aligned} \tag{7.83}$$

Next, let us consider the case when the third argument in (7.67) comes into play.

Then, (7.79) can be reformulated as

$$\begin{aligned}
\frac{\partial \mathcal{G}}{\partial u_i^n} &= 1 - \Delta t \frac{\hat{u}_x}{\sqrt{\hat{u}_x^2}} \frac{\partial \hat{u}_x}{\partial u_i} \\
&\overset{(7.71)}{=} 1 - \Delta t \frac{\hat{u}_x}{\sqrt{\hat{u}_x^2}} \left(\frac{1}{\Delta x} \right) \\
&\overset{(7.71)}{=} 1 - \frac{\hat{u}_x}{\hat{u}_x} \left(\frac{\Delta t}{\Delta x} \right) \\
&= 1 - \frac{\Delta t}{\Delta x} \overset{(!)}{\geq} 0.
\end{aligned} \tag{7.84}$$

Therefore, we can obtain the same condition as (7.83) to fulfil the inequality (!) in (7.84).

Case (iii)**.** This case is analogous to the case (i). So, when the first or third argument in (7.67) is chosen, there is no contribution for the case (iii). This means it holds

$$\frac{\partial \mathcal{G}}{\partial u_{i+1}^n} = 0. \tag{7.85}$$

Therefore, we only need to consider the case when the second argument in (7.67) is selected.

By taking partial derivative of $\mathcal{G}$ from (7.70) with respect to u_{i-1} we have

$$\begin{aligned}
\frac{\partial \mathcal{G}}{\partial u_{i+1}^n} &= -\Delta t \frac{\hat{u}_x}{\sqrt{\hat{u}_x^2}} \frac{\partial \hat{u}_x}{\partial u_{i+1}} \\
&\overset{(7.68)}{=} -\Delta t \frac{\hat{u}_x}{\sqrt{\hat{u}_x^2}} \left(\frac{1}{\Delta x} \right) \\
&= \frac{-\hat{u}_x}{\sqrt{\hat{u}_x^2}} \frac{\Delta t}{\Delta x} \\
&\overset{(7.68)}{=} \frac{-\hat{u}_x}{-\hat{u}_x} \frac{\Delta t}{\Delta x} \\
&= \frac{\Delta t}{\Delta x} > 0,
\end{aligned} \tag{7.86}$$

which is the desired result.

As a consequence, in view of all three cases in (7.76) we have the following monotonicity condition:

$$\Delta t \leq \Delta x. \tag{7.87}$$

Consistency

In the light of a consistency notion in (7.14), the scheme (7.60) is consistent with (7.59) owing to (7.61).

Comparison Principle

As we have already investigated in Theorem 4.3.1, the original problem (7.59) admits a comparison principle under certain hypotheses.

As a result, the numerical solution of (7.60) converges to a continuous viscosity solution of (7.59) by Theorem 7.3.1.

7.5 Numerical Scheme for VBW Model in 1-D

In this section, we look into the numerical scheme for (6.16) in one-dimensional case.

Let us consider following Phong SfS model in one-dimension

$$JW - \kappa_d I_d e^{-2v} - \kappa_s I_s e^{-2v} \frac{W}{Q} \left(\frac{2Q^2}{W^2} - 1 \right)^{\alpha} = 0, \tag{7.88}$$

where

$$J(x) = (I(x) - \kappa_a I_a) \frac{\mathtt{f}^2}{Q}, \tag{7.89}$$

$$W(x,p) = \sqrt{\mathtt{f}^2 p^2 + (px)^2 + Q(x)^2}, \tag{7.90}$$

with $p = v_x$ and

$$Q(x) = \sqrt{\frac{\mathtt{f}^2}{x^2 + \mathtt{f}^2}}. \tag{7.91}$$

7.5.1 Construction of a Scheme

The procedure here is exactly the same as we did for the scheme of Rouy and Tourin. By employing the method of artificial time for (7.88) we need to solve

$$v_t + \underbrace{JW - \kappa_d I_d e^{-2v} - \kappa_s I_s e^{-2v} \frac{W}{Q} \left(\frac{2Q^2}{W^2} - 1 \right)^{\alpha}}_{=:H} = 0. \tag{7.92}$$

For spatial derivative the following upwind-type scheme

$$v_x \approx \min\left(0, \frac{v_{i+1} - v_i}{\Delta x}, \frac{v_{i-1} - v_i}{\Delta x}\right) =: \hat{v}_x \tag{7.93}$$

is used. When the third argument of (7.93) is taken, as in Remark 7.4.1 $\hat{v}_x$ needs to be set

$$\hat{v}_x = \frac{v_i - v_{i-1}}{\Delta x} > 0 \tag{7.94}$$

for the purpose of ensuring the consistency of dicretisation. Besides, by means of the Euler forward method and with the notation (7.93) the approximation scheme of (7.88) reads as

$$\frac{v_i^{n+1} - v_i^n}{\Delta t} + \underbrace{\left(JW(x_i, \hat{v}_x) - \kappa_s I_s(x_i) e^{-2v_i^n} \frac{W(x_i, v_x)}{Q(x_i)} \left(\frac{2Q(x_i)^2}{W(x_i, \hat{v}_x)^2} - 1 \right)^{\alpha} - \kappa_d I_d(x_i) e^{-2v_i^n} \right)}_{=:\mathcal{H}(x_i, v_i, \hat{v}_x)} = 0. \tag{7.95}$$

Thus, we can obtain the following update rule

$$v_i^{n+1} = \underbrace{v_i^n - \Delta t\, \mathcal{H}\left(x_i, v_i, \hat{v}_x\right)}_{=:\mathcal{G}(x_i, v_i, \hat{v}_x)}. \tag{7.96}$$

For simplicity, here we also assume that the iteration level used for discrete representations of v_x is always the actual level n. This also holds for source term, i.e. $e^{-2v} \approx e^{-2v_i^n}$. All the other terms in (7.95) are assumed to be evaluated at each grid point i.

7.5.2 Convergence of a Scheme

Monotonicity and Stability

For the monotonicity, by virtue of Definition 7.3.1 and Remark 7.3.1 we need to confirm that $\mathcal{H}$ in (7.96) is a nonincreasing function. This is equivalent to show $\mathcal{G}$ in (7.96) to be nondecreasing. As we did for the scheme of Rouy and Tourin, we validate this by the criterion (7.76).

To this end, we make use of the following notations for brevity:

$$W := \sqrt{(\mathtt{f}^2 + x^2)\, \hat{v}_x^2 + Q^2}, \tag{7.97}$$

where $\hat{v}_x$ refers to (7.93) or (7.94) correspondingly depending on the choices.

In addition, we proceed in the sequence of case $(i) \rightarrow (iii) \rightarrow (ii)$, since the procedure between case (i) and case (iii) is analogous with each other.

Case (i)**.** In view of (7.93) there is contribution to the case (i) only when the third argument in (7.93) is taken. In this case, by (7.94) we have

$$\frac{\partial \hat{v}_x}{\partial v_{i-1}} = -\frac{1}{\Delta x}. \tag{7.98}$$

As a next step, taking partial derivative of (7.96) with respect to v_{i-1} yields

$$\begin{aligned}
\frac{\partial \mathcal{G}}{\partial v_{i-1}} &= -\Delta t \frac{\partial \mathcal{H}}{\partial v_{i-1}} \\
&\overset{(7.95)}{=} -\Delta t \frac{\partial}{\partial v_{i-1}} \left(JW - \kappa_s\, I_s e^{-2v_i^n} \frac{W}{Q} \left(\frac{2Q^2}{W^2} - 1 \right)^{\alpha} - \kappa_d\, I_d\, e^{-2v_i^n} \right) \\
&= -\Delta t \frac{\partial}{\partial v_{i-1}} \left(JW - \kappa_s\, I_s e^{-2v_i^n} \frac{W}{Q} \left(\frac{2Q^2}{W^2} - 1 \right)^{\alpha} \right) \\
&= \Delta t \left[-J \underbrace{\frac{\partial W}{\partial v_{i-1}}}_{=:(a)} + \kappa_s\, I_s e^{-2v_i^n} \underbrace{\frac{\partial}{\partial v_{i-1}} \left[\frac{W}{Q} \left(\frac{2Q^2}{W^2} - 1 \right)^{\alpha} \right]}_{=:(b)} \right].
\end{aligned} \tag{7.99}$$

For computational reasons, we perform further calculations of (a) and (b) separately. For (a) we can proceed as

$$\begin{aligned}\frac{\partial W}{\partial v_{i-1}} &\overset{(7.97)}{=} \left(\mathfrak{f}^2+x^2\right)\frac{2\hat{v}_x}{2W}\frac{\partial \hat{v}_x}{\partial v_{i-1}} \\ &\overset{(7.98)}{=} \left(\mathfrak{f}^2+x^2\right)\frac{\hat{v}_x}{W}\left(-\frac{1}{\Delta x}\right) \\ &= -\frac{\left(\mathfrak{f}^2+x^2\right)\hat{v}_x}{W\,\Delta x}.\end{aligned} \tag{7.100}$$

In the case of (b), by applying the chain rule we can obtain

$$\begin{aligned}&\frac{\partial}{\partial v_{i-1}}\left[\frac{W}{Q}\left(\frac{2Q^2}{W^2}-1\right)^{\alpha}\right] \\ &= \frac{1}{Q}\frac{\partial W}{\partial v_{i-1}}\cdot\left(\frac{2Q^2}{W^2}-1\right)^{\alpha}+\frac{W}{Q}\frac{\partial}{\partial v_{i-1}}\left[\left(\frac{2Q^2}{W^2}-1\right)^{\alpha}\right] \\ &\overset{(7.100)}{=} \frac{1}{Q}\left(-\frac{\left(\mathfrak{f}^2+x^2\right)\hat{v}_x}{W\Delta x}\right)\cdot\left(\frac{2Q^2}{W^2}-1\right)^{\alpha}+\frac{W}{Q}\frac{\partial}{\partial v_{i-1}}\left[\left(\frac{2Q^2}{W^2}-1\right)^{\alpha}\right] \\ &\overset{(*)}{=} -\frac{1}{Q}\frac{\left(\mathfrak{f}^2+x^2\right)\hat{v}_x}{W\Delta x}\cdot\left(\frac{2Q^2}{W^2}-1\right)^{\alpha}+\frac{W}{Q}\left[\alpha\left(\frac{2Q^2}{W^2}-1\right)^{\alpha-1}\frac{4Q^2}{W^3}\cdot\frac{\left(\mathfrak{f}^2+x^2\right)\hat{v}_x}{W\Delta x}\right] \\ &= \frac{1}{Q}\cdot\frac{\left(\mathfrak{f}^2+x^2\right)\hat{v}_x}{W\Delta x}\left(\frac{2Q^2}{W^2}-1\right)^{\alpha-1}\left[-\left(\frac{2Q^2}{W^2}-1\right)+\frac{4\alpha Q^2}{W^2}\right] \\ &= \frac{1}{Q}\cdot\frac{\left(\mathfrak{f}^2+x^2\right)\hat{v}_x}{W\Delta x}\left(\frac{2Q^2}{W^2}-1\right)^{\alpha-1}\left[\frac{2\left(2\alpha-1\right)Q^2}{W^2}+1\right].\end{aligned} \tag{7.101}$$

The step $(*)$ in (7.101) can be explained by

$$\begin{aligned}\frac{\partial}{\partial v_{i-1}}\left[\left(\frac{2Q^2}{W^2}-1\right)^{\alpha}\right] &= \alpha\left(\frac{2Q^2}{W^2}-1\right)^{\alpha-1}\frac{\partial}{\partial v_{i-1}}\left(\frac{2Q^2}{W^2}-1\right) \\ &= \alpha\left(\frac{2Q^2}{W^2}-1\right)^{\alpha-1}2Q^2\left(\frac{-2}{W^3}\right)\frac{\partial W}{\partial v_{i-1}} \\ &\overset{(7.100)}{=} \alpha\left(\frac{2Q^2}{W^2}-1\right)^{\alpha-1}\left(\frac{-4Q^2}{W^3}\right)\left(-\frac{\left(\mathfrak{f}^2+x^2\right)\hat{v}_x}{W\Delta x}\right) \\ &= \alpha\left(\frac{2Q^2}{W^2}-1\right)^{\alpha-1}\cdot\frac{4Q^2}{W^3}\cdot\frac{\left(\mathfrak{f}^2+x^2\right)\hat{v}_x}{W\Delta x}.\end{aligned} \tag{7.102}$$

As a final step, plugging (7.100) and (7.101) into (7.99) gives

$$\begin{aligned}
&\frac{\partial \mathcal{G}}{\partial v_{i-1}^{n}} \\
&\quad = \Delta t\left[-J\left(-\frac{\left(\mathrm{f}^{2}+x^{2}\right)\hat{v}_{x}}{W\Delta x}\right)\right] \\
&\qquad + \Delta t\left[\kappa_{s}\,I_{s}e^{-2v_{i}^{n}}\,\frac{1}{Q}\cdot\frac{\left(\mathrm{f}^{2}+x^{2}\right)\hat{v}_{x}}{W\Delta x}\left(\frac{2Q^{2}}{W^{2}}-1\right)^{\alpha-1}\left[\frac{2\left(2\alpha-1\right)Q^{2}}{W^{2}}+1\right]\right] \\
&\quad = \Delta t\left[J\frac{\left(\mathrm{f}^{2}+x^{2}\right)\hat{v}_{x}}{W\Delta x}+\kappa_{s}\,I_{s}e^{-2v_{i}^{n}}\,\frac{1}{Q}\cdot\frac{\left(\mathrm{f}^{2}+x^{2}\right)\hat{v}_{x}}{W\Delta x}\left(\frac{2Q^{2}}{W^{2}}-1\right)^{\alpha-1}\left[\frac{2\left(2\alpha-1\right)Q^{2}}{W^{2}}+1\right]\right] \\
&\quad = \underbrace{\Delta t}_{>0}\,\frac{\overbrace{\left(\mathrm{f}^{2}+x^{2}\right)}^{>0}\overbrace{\hat{v}_{x}}^{\overset{(7.94)}{>}0}}{\underbrace{W}_{\overset{(7.90)}{>}0}\,\underbrace{\Delta x}_{>0}}\left[\underbrace{J}_{\overset{[75]}{>}0}+\underbrace{\kappa_{s}\,I_{s}e^{-2v_{i}^{n}}}_{>0}\,\underbrace{\frac{1}{Q}}_{\overset{(7.91)}{>}0}\left(\underbrace{\frac{2Q^{2}}{W^{2}}-1}_{\overset{[75]}{\geq}0}\right)^{\alpha-1}\underbrace{\left[\frac{2\left(2\alpha-1\right)Q^{2}}{W^{2}}+1\right]}_{>0\text{ for }\alpha\geq\frac{1}{2}}\right] \\
&\Rightarrow \frac{\partial \mathcal{G}}{\partial v_{i-1}^{n}} > 0.
\end{aligned} \tag{7.103}$$

Therefore, case (i) holds for normal specular case when $\alpha \geq \frac{1}{2}$.

We now move on to the case (iii).

Case (iii). For the case (iii), the contribution is only made when the second argument in (7.93) is chosen. In this case, we have

$$\hat{v}_{x} = \frac{v_{i+1}-v_{i}}{\Delta x} < 0 \quad \Leftrightarrow \quad -\hat{v}_{x} > 0 \tag{7.104}$$

and

$$\frac{\partial \hat{v}_{x}}{\partial v_{i+1}} = \frac{1}{\Delta x}. \tag{7.105}$$

The rest steps are the same as in the case (i).

First, we take the partial derivative of (7.96) with respect to v_{i+1}. Then, we have

$$\begin{aligned}
\frac{\partial \mathcal{G}}{\partial v_{i+1}} &= -\Delta t \frac{\partial \mathcal{H}}{\partial v_{i+1}} \\
&\overset{(7.95)}{=} -\Delta t \frac{\partial}{\partial v_{i+1}} \left(JW - \kappa_s I_s e^{-2v_i^n} \frac{W}{Q} \left(\frac{2Q^2}{W^2} - 1 \right)^{\alpha} - \kappa_d I_d e^{-2v_i^n} \right) \\
&= -\Delta t \frac{\partial}{\partial v_{i+1}} \left(JW - \kappa_s I_s e^{-2v_i^n} \frac{W}{Q} \left(\frac{2Q^2}{W^2} - 1 \right)^{\alpha} \right) \\
&= \Delta t \left[-J \underbrace{\frac{\partial W}{\partial v_{i+1}}}_{=:(c)} + \kappa_s I_s e^{-2v_i^n} \underbrace{\frac{\partial}{\partial v_{i+1}} \left[\frac{W}{Q} \left(\frac{2Q^2}{W^2} - 1 \right)^{\alpha} \right]}_{=:(d)} \right].
\end{aligned} \tag{7.106}$$

The further computation of (c) in (7.106) can be expanded by

$$\begin{aligned}
\frac{\partial W}{\partial v_{i+1}} &\overset{(7.97)}{=} \frac{\left(\mathtt{f}^2 + x^2\right) 2\hat{v}_x}{2W} \frac{\partial \hat{v}_x}{\partial v_{i+1}} \\
&\overset{(7.105)}{=} \frac{\left(\mathtt{f}^2 + x^2\right) \hat{v}_x}{W \Delta x}.
\end{aligned} \tag{7.107}$$

By use of the chain rule, (d) in (7.106) can be calculated by

$$
\begin{aligned}
&\frac{\partial}{\partial v_{i+1}}\left[\frac{W}{Q}\left(\frac{2Q^2}{W^2}-1\right)^{\alpha}\right] \\
&= \frac{1}{Q}\frac{\partial W}{\partial v_{i+1}}\cdot\left(\frac{2Q^2}{W^2}-1\right)^{\alpha}+\frac{W}{Q}\frac{\partial}{\partial v_{i+1}}\left[\left(\frac{2Q^2}{W^2}-1\right)^{\alpha}\right] \\
&\overset{(7.107)}{=} \frac{1}{Q}\frac{\left(\mathtt{f}^2+x^2\right)\hat{v}_x}{W\Delta x}\cdot\left(\frac{2Q^2}{W^2}-1\right)^{\alpha}+\frac{W}{Q}\frac{\partial}{\partial v_{i+1}}\left[\left(\frac{2Q^2}{W^2}-1\right)^{\alpha}\right] \\
&\overset{(*)}{=} \frac{1}{Q}\frac{\left(\mathtt{f}^2+x^2\right)\hat{v}_x}{W\Delta x}\cdot\left(\frac{2Q^2}{W^2}-1\right)^{\alpha}-\frac{W}{Q}\left[\alpha\left(\frac{2Q^2}{W^2}-1\right)^{\alpha-1}\frac{4Q^2}{W^3}\cdot\frac{\left(\mathtt{f}^2+x^2\right)\hat{v}_x}{W\Delta x}\right] \\
&= \frac{1}{Q}\cdot\frac{\left(\mathtt{f}^2+x^2\right)\hat{v}_x}{W\Delta x}\left(\frac{2Q^2}{W^2}-1\right)^{\alpha-1}\left[\left(\frac{2Q^2}{W^2}-1\right)-\frac{4\alpha Q^2}{W^2}\right] \\
&= \frac{1}{Q}\cdot\frac{\left(\mathtt{f}^2+x^2\right)\hat{v}_x}{W\Delta x}\left(\frac{2Q^2}{W^2}-1\right)^{\alpha-1}\left[\frac{2\left(1-2\alpha\right)Q^2}{W^2}-1\right] \\
&= -\frac{1}{Q}\cdot\frac{\left(\mathtt{f}^2+x^2\right)\hat{v}_x}{W\Delta x}\left(\frac{2Q^2}{W^2}-1\right)^{\alpha-1}\left[\frac{2\left(2\alpha-1\right)Q^2}{W^2}+1\right].
\end{aligned}
\tag{7.108}
$$

The steps $(*)$ in (7.108) can be computed as

$$
\begin{aligned}
\frac{\partial}{\partial v_{i+1}}\left[\left(\frac{2Q^2}{W^2}-1\right)^{\alpha}\right] &= \alpha\left(\frac{2Q^2}{W^2}-1\right)^{\alpha-1}\frac{\partial}{\partial v_{i+1}}\left(\frac{2Q^2}{W^2}-1\right) \\
&= \alpha\left(\frac{2Q^2}{W^2}-1\right)^{\alpha-1}2Q^2\left(\frac{-2}{W^3}\right)\frac{\partial W}{\partial v_{i+1}} \\
&\overset{(7.107)}{=} \alpha\left(\frac{2Q^2}{W^2}-1\right)^{\alpha-1}\left(\frac{-4Q^2}{W^3}\right)\cdot\frac{\left(\mathtt{f}^2+x^2\right)\hat{v}_x}{W\Delta x} \\
&= -\alpha\left(\frac{2Q^2}{W^2}-1\right)^{\alpha-1}\frac{4Q^2}{W^3}\cdot\frac{\left(\mathtt{f}^2+x^2\right)\hat{v}_x}{W\Delta x}.
\end{aligned}
\tag{7.109}
$$

As a final step for this case, the results of (7.107) and (7.109) can be substituted for

(7.106). This leads to

$$
\begin{aligned}
&\frac{\partial \mathcal{G}}{\partial v_{i+1}^n} \\
&\quad = \Delta t \left[-J \frac{\left(\mathtt{f}^2 + x^2\right) \hat{v}_x}{W \Delta x} \right] \\
&\qquad + \Delta t \left[-\kappa_s \, I_s e^{-2v_i^n} \frac{1}{Q} \cdot \frac{\left(\mathtt{f}^2 + x^2\right) \hat{v}_x}{W \Delta x} \left(\frac{2Q^2}{W^2} - 1 \right)^{\alpha - 1} \left[\frac{2\,(2\alpha - 1)\, Q^2}{W^2} + 1 \right] \right] \\
&\quad = \Delta t \left[J \frac{\left(-\hat{v}_x\right) \left(\mathtt{f}^2 + x^2\right)}{W \Delta x} \right] \\
&\qquad + \Delta t \left[\kappa_s \, I_s e^{-2v_i^n} \frac{1}{Q} \cdot \frac{\left(-\hat{v}_x\right) \left(\mathtt{f}^2 + x^2\right)}{W \Delta x} \cdot \left(\frac{2Q^2}{W^2} - 1 \right)^{\alpha - 1} \left[\frac{2\,(2\alpha - 1)\, Q^2}{W^2} + 1 \right] \right] \\
&\quad = \underbrace{\Delta t}_{>0} \frac{\overbrace{\left(-\hat{v}_x\right)}^{\overset{(7.104)}{>}0} \overbrace{\left(\mathtt{f}^2 + x^2\right)}^{>0}}{\underbrace{W}_{\overset{(7.90)}{>}0} \underbrace{\Delta x}_{>0}} \left[\underbrace{J}_{\overset{[75]}{>}0} + \underbrace{\kappa_s \, I_s e^{-2v_i^n}}_{>0} \underbrace{\frac{1}{Q}}_{\overset{(7.91)}{>}0} \left(\underbrace{\frac{2Q^2}{W^2} - 1}_{\overset{[75]}{\geq}0} \right)^{\alpha - 1} \underbrace{\left[\frac{2\,(2\alpha - 1)\, Q^2}{W^2} + 1 \right]}_{>0 \text{ for } \alpha \geq \frac{1}{2}} \right] \\
&\Rightarrow \frac{\partial \mathcal{G}}{\partial v_{i+1}^n} > 0 \, .
\end{aligned}
\tag{7.110}
$$

Hence, case (iii) also holds for the specular exponent α when $\alpha \geq \frac{1}{2}$.

Now, we come to the case (ii).

Case (ii)**.** For this case, we go into the condition which should imply a stability restriction on the time step size.

Taking partial derivatives of (7.96) with respect to v_i gives

$$
\begin{aligned}
\frac{\partial \mathcal{G}}{\partial v_i^n} &= 1 - \Delta t \frac{\partial \mathcal{H}}{\partial v_i} \\
&\overset{(7.95)}{=} 1 - \Delta t \frac{\partial}{\partial v_i}\left(JW - \kappa_s I_s e^{-2v_i^n} \frac{W}{Q}\left(\frac{2Q^2}{W^2} - 1\right)^{\alpha} - \kappa_d I_d e^{-2v_i^n} \right) \\
&= 1 - \Delta t \left[J \frac{\partial W}{\partial v_i} - \kappa_s I_s \frac{\partial}{\partial v_i}\left[e^{-2v_i^n} \frac{W}{Q}\left(\frac{2Q^2}{W^2} - 1\right)^{\alpha}\right] - \kappa_d I_d e^{-2v_i^n}(-2) \right] \\
&= 1 - 2\Delta t \kappa_d I_d e^{-2v_i^n} - \Delta t \left[J \underbrace{\frac{\partial W}{\partial v_i}}_{=:(e)} - \kappa_s I_s \underbrace{\frac{\partial}{\partial v_i}\left[e^{-2v_i^n} \frac{W}{Q}\left(\frac{2Q^2}{W^2} - 1\right)^{\alpha}\right]}_{=:(f)} \right].
\end{aligned}
\tag{7.111}
$$

The further computation of the term (e) in (7.111) can be received as

$$
\begin{aligned}
\frac{\partial W}{\partial v_i} &\overset{(7.90)}{=} \frac{\left(\mathfrak{f}^2 + x^2\right) 2\hat{v}_x}{2W} \frac{\partial \hat{v}_x}{\partial v_i} \\
&= \frac{\left(\mathfrak{f}^2 + x^2\right) \hat{v}_x}{W} \frac{\partial \hat{v}_x}{\partial v_i}.
\end{aligned}
\tag{7.112}
$$

Since we do not specify yet whether the second or the third argument in (7.93) is chosen, the notation $\frac{\partial \hat{v}_x}{\partial v_i}$ in (7.112) is still alive and this quantity shall be estimated later.

As is done before, we are able to calculate the term (f) in (7.111) by use of the chain rule as follows

$$
\begin{aligned}
&\frac{\partial}{\partial v_i}\left[e^{-2v_i^n}\frac{W}{Q}\left(\frac{2Q^2}{W^2}-1\right)^{\alpha}\right]\\
&= -2e^{-2v_i^n}\frac{W}{Q}\left(\frac{2Q^2}{W^2}-1\right)^{\alpha} + e^{-2v_i^n}\left(\frac{2Q^2}{W^2}-1\right)^{\alpha}\frac{\partial}{\partial v_i}\left(\frac{W}{Q}\right)\\
&\qquad + e^{-2v_i^n}\frac{W}{Q}\frac{\partial}{\partial v_i}\left[\left(\frac{2Q^2}{W^2}-1\right)^{\alpha}\right]\\
&\overset{(7.112)}{=} -2e^{-2v_i^n}\frac{W}{Q}\left(\frac{2Q^2}{W^2}-1\right)^{\alpha} + e^{-2v_i^n}\left(\frac{2Q^2}{W^2}-1\right)^{\alpha}\frac{1}{Q}\frac{\left(\mathtt{f}^2+x^2\right)\hat{v}_x}{W}\frac{\partial\hat{v}_x}{\partial v_i}\\
&\qquad + e^{-2v_i^n}\frac{W}{Q}\frac{\partial}{\partial v_i}\left[\left(\frac{2Q^2}{W^2}-1\right)^{\alpha}\right]\\
&= -2e^{-2v_i^n}\frac{W}{Q}\left(\frac{2Q^2}{W^2}-1\right)^{\alpha} + e^{-2v_i^n}\left(\frac{2Q^2}{W^2}-1\right)^{\alpha}\frac{1}{Q}\frac{\left(\mathtt{f}^2+x^2\right)\hat{v}_x}{W}\frac{\partial\hat{v}_x}{\partial v_i}\\
&\qquad + e^{-2v_i^n}\frac{W}{Q}\cdot\alpha\left(\frac{2Q^2}{W^2}-1\right)^{\alpha-1}2Q^2\left(\frac{-2}{W^3}\right)\frac{\partial W}{\partial v_i}\\
&\overset{(7.112)}{=} -2e^{-2v_i^n}\frac{W}{Q}\left(\frac{2Q^2}{W^2}-1\right)^{\alpha} + e^{-2v_i^n}\left(\frac{2Q^2}{W^2}-1\right)^{\alpha}\frac{1}{Q}\frac{\left(\mathtt{f}^2+x^2\right)\hat{v}_x}{W}\frac{\partial\hat{v}_x}{\partial v_i}\\
&\qquad + e^{-2v_i^n}\frac{1}{Q}\cdot\alpha\left(\frac{2Q^2}{W^2}-1\right)^{\alpha-1}\left(\frac{-4Q^2}{W^2}\right)\frac{\left(\mathtt{f}^2+x^2\right)\hat{v}_x}{W}\frac{\partial\hat{v}_x}{\partial v_i}\\
&= -2e^{-2v_i^n}\frac{W}{Q}\left(\frac{2Q^2}{W^2}-1\right)^{\alpha}\\
&\qquad + e^{-2v_i^n}\left(\frac{2Q^2}{W^2}-1\right)^{\alpha-1}\frac{1}{Q}\frac{\left(\mathtt{f}^2+x^2\right)\hat{v}_x}{W}\frac{\partial\hat{v}_x}{\partial v_i}\cdot\left[\left(\frac{2Q^2}{W^2}-1\right)-\frac{4\alpha Q^2}{W^2}\right]\\
&= -2e^{-2v_i^n}\frac{W}{Q}\left(\frac{2Q^2}{W^2}-1\right)^{\alpha}\\
&\qquad + e^{-2v_i^n}\left(\frac{2Q^2}{W^2}-1\right)^{\alpha-1}\frac{1}{Q}\frac{\left(\mathtt{f}^2+x^2\right)\hat{v}_x}{W}\frac{\partial\hat{v}_x}{\partial v_i}\cdot\left[\frac{2\left(1-2\alpha\right)Q^2}{W^2}-1\right]\\
&= -2e^{-2v_i^n}\frac{W}{Q}\left(\frac{2Q^2}{W^2}-1\right)^{\alpha}\\
&\qquad - e^{-2v_i^n}\left(\frac{2Q^2}{W^2}-1\right)^{\alpha-1}\frac{1}{Q}\frac{\left(\mathtt{f}^2+x^2\right)\hat{v}_x}{W}\frac{\partial\hat{v}_x}{\partial v_i}\cdot\left[\frac{2\left(2\alpha-1\right)Q^2}{W^2}+1\right].
\end{aligned}
\tag{7.113}
$$

At this point, we have done all the necessary computations in order to get hands on the monotonicity conditions for (7.96). By replacing (e) and (f) in (7.111) with the results of (7.112) and (7.113) we receive

$$
\begin{aligned}
\frac{\partial \mathcal{G}}{\partial v_i^n} &= 1 - 2e^{-2v_i^n}\,\kappa_d\,I_d\,\Delta t \\
&\quad - \Delta t\left[J\frac{\left(\mathtt{f}^2+x^2\right)\hat{v}_x}{W}\frac{\partial \hat{v}_x}{\partial v_i}\right] \\
&\quad + \kappa_s I_s \Delta t\left[-2e^{-2v_i^n}\frac{W}{Q}\left(\frac{2Q^2}{W^2}-1\right)^{\alpha}\right] \\
&\quad + \kappa_s I_s \Delta t\left[-\,e^{-2v_i^n}\left(\frac{2Q^2}{W^2}-1\right)^{\alpha-1}\frac{1}{Q}\frac{\left(\mathtt{f}^2+x^2\right)\hat{v}_x}{W}\frac{\partial \hat{v}_x}{\partial v_i}\left(\frac{2\,(2\alpha-1)\,Q^2}{W^2}+1\right)\right] \\
&= 1 - 2e^{-2v_i^n}\,\kappa_d\,I_d\,\Delta t - \;2\,e^{-2v_i^n}\,\kappa_s I_s\left[\frac{W}{Q}\left(\frac{2Q^2}{W^2}-1\right)^{\alpha}\right]\Delta t \\
&\quad - \Delta t\left[J\frac{\left(\mathtt{f}^2+x^2\right)\hat{v}_x}{W}\frac{\partial \hat{v}_x}{\partial v_i}\right] \\
&\quad - \kappa_s I_s \Delta t\left[e^{-2v_i^n}\left(\frac{2Q^2}{W^2}-1\right)^{\alpha-1}\frac{1}{Q}\frac{\left(\mathtt{f}^2+x^2\right)\hat{v}_x}{W}\frac{\partial \hat{v}_x}{\partial v_i}\left(\frac{2\,(2\alpha-1)\,Q^2}{W^2}+1\right)\right] \\
&= 1 - 2e^{-2v_i^n}\left[\kappa_d I_d + \kappa_s I_s\frac{W}{Q}\left(\frac{2Q^2}{W^2}-1\right)^{\alpha}\right]\Delta t \\
&\quad - \Delta t\left[J\frac{\left(\mathtt{f}^2+x^2\right)\hat{v}_x}{W}\frac{\partial \hat{v}_x}{\partial v_i}\right] \\
&\quad - \kappa_s I_s \Delta t\left[e^{-2v_i^n}\left(\frac{2Q^2}{W^2}-1\right)^{\alpha-1}\frac{1}{Q}\frac{\left(\mathtt{f}^2+x^2\right)\hat{v}_x}{W}\left(\frac{2\,(2\alpha-1)\,Q^2}{W^2}+1\right)\frac{\partial \hat{v}_x}{\partial v_i}\right].
\end{aligned}
\tag{7.114}
$$

Since a violation of case (ii) primarily occurs due to the quantity of $\left(\mathtt{f}^2+x^2\right)$ in the last two rows of (7.114), we incorporate a worst case estimate

$$
\hat{v}_x \leq \max\left(|\hat{v}_x|\right) =: |\hat{v}|_{max}\,, \tag{7.115}
$$

where the maximum is taken over all possible cases in (7.93). It follows

$$
\begin{aligned}
\frac{\partial \mathcal{G}}{\partial v_i^n} \;\geq\;& 1 - 2e^{-2v_i^n} \left| \underbrace{\kappa_d I_d + \kappa_s I_s \frac{W}{Q} \left(\frac{2Q^2}{W^2} - 1 \right)^{\alpha}}_{=:A \overset{[75]}{\geq} 0} \right| \Delta t \\
& - |\hat{v}|_{max} \left| \underbrace{J \frac{\left(\mathfrak{f}^2 + x^2\right)}{W}}_{=:B} \frac{\partial \hat{v}_x}{\partial v_i} \right| \Delta t \\
& - |\hat{v}|_{max} \left| e^{-2v_i^n} \underbrace{\kappa_s I_s \left(\frac{2Q^2}{W^2} - 1 \right)^{\alpha - 1} \frac{1}{Q} \frac{\left(\mathfrak{f}^2 + x^2\right)}{W} \left(\frac{2\,(2\alpha - 1)\, Q^2}{W^2} + 1 \right)}_{=:C \overset{[75]}{\geq} 0 \quad \text{if } \alpha > \frac{1}{2}} \frac{\partial \hat{v}_x}{\partial v_i} \right| \Delta t \\
=\;& 1 - 2e^{-2v_i^n} A \, \Delta t - |\hat{v}|_{max} \left(B + e^{-2v_i^n} C \right) \left| \frac{\partial \hat{v}_x}{\partial v_i} \right| \Delta t \, .
\end{aligned} \tag{7.116}
$$

Additionally, in view of (7.93) and (7.94) we have

$$
\begin{aligned}
\frac{\partial \hat{v}_x}{\partial v_i} &= \pm \frac{1}{\Delta x} \\
\Rightarrow \left| \frac{\partial \hat{v}_x}{\partial v_i} \right| &= \frac{1}{\Delta x} =: h_x \, .
\end{aligned} \tag{7.117}
$$

This implies that by (7.116) and (7.117) we can formulate a sufficient condition for monotonicity on the time step size as follows:

$$
\begin{aligned}
& 1 - 2e^{-2v_i^n} A \, \Delta t - |\hat{v}|_{max} \left(B + e^{-2v_i^n} C \right) h_x \, \Delta t \geq 0 \\
\Leftrightarrow \quad & \left[2e^{-2v_i^n} + |\hat{v}|_{max} \left(B + e^{-2v_i^n} C \right) h_x \right] \Delta t \leq 1 \\
\Leftrightarrow \quad & \Delta t \leq \frac{1}{2e^{-2v_i^n} + |\hat{v}|_{max} \left(B + e^{-2v_i^n} C \right) h_x} \, .
\end{aligned} \tag{7.118}
$$

As a consequence, the scheme satisfies monotonicity and thereby stability as long as (7.118) is valid.

Consistency

The scheme (7.96) is consistent with (7.88) due to (7.95).

Comparison Principle

As can be recognised in (7.88), one-dimensional VBW model is described by general-type HJE, which means Hamiltonian depends not only on ∇u but also on u. The good news is that there also exists a comparison theorem for this type of HJE which guarantees uniqueness of a solution.

For the purpose of convergence, we borrow the following theorem from [12] where the proof is provided.

Theorem 7.5.1. *Let Ω be a bounded open subset of $\mathbb{R}^n$. Assume that $\underline{u}, \overline{u} \in C\left(\overline{\Omega}\right)$ are, respectively, viscosity sub- and supersolution of*

$$u(x) + H(x, Du(x)) = 0, \quad x \in \Omega \tag{7.119}$$

and

$$\underline{u} \leq \overline{u} \quad x \in \partial\Omega. \tag{7.120}$$

In addition, assume also that H satisfies

$$|H(x,p) - H(y,p)| \leq \omega\left(|x-y|\left(1+|p|\right)\right), \tag{7.121}$$

for $x, y \in \Omega, p \in \mathbb{R}^n$, where $\omega : [0, +\infty[\to [0, +\infty[$ is continuous nondecreasing with $\omega(0) = 0$. Then $\underline{u} \leq \overline{u}$ in $\overline{\Omega}$.

Therefore, a numerical solution of one-dimensional VBW explicit scheme (7.95) converges to a continuous viscosity solution of (7.88) by Theorem 7.3.1 as grid size vanishes.

Remark 7.5.1. This result can also serve as a proof of the existence of viscosity solutions. In other words, as the mesh size disappear solutions of our scheme converge towards a viscosity solution of (7.88), which means the existence of viscosity solutions.

7.6 Summary

In this chapter, we have studied the Hamilton-Jacobi equation in a numerical point of view.

First, we have studied the basic notions of numerical analysis including local truncation error and consistency, stability, monotonicity, and Lax-equivalence theorem by taking a linear upwind scheme as an example.

After that, we went through the convergence theory for the Rouy and Tourin scheme by following the work by Barles and Souganidis [37].

Then, we have seen how the theory works in the scheme of Rouy and Tourin taking an example of one-dimensional eikonal equation.

Finally, we have shown the convergence of explicit scheme for the Vogel-Breuß-Weickert model in one-dimensional case.

In next chapter, we shall perform numerical experiments in view of what we have seen so far.

Chapter 8

Numerical Experiments

In this chapter, we shall perform numerical experiments in order to validate the convergence results established in previous chapter.

First, we test our method on the one-dimensional eikonal equation for confirming the correctness.

Then, we apply the method to the VBW model. To be more specific, the test involves with the Lambertian and Phong SfS problems in 1-D and 2-D, respectively.

To this end, the main part of the algorithm is coded in both C and Matlab and the results are illustrated by Matlab and Gnuplot.

8.1 Eikonal Equation in 1-D

In this section, we shall see the overview of implementation and experimental results for a one-dimensional eikonal equation. Since we have already investigated the analytic solution of the one-dimensional eikonal equation in Chapter 2, it is a good starting point to validate a numerical scheme.

8.1.1 Numerical Implementation

Our implementation relies on the theory that we have studied in Section 7.4 and the pseudocode is provided in Algorithm 8.1. Here we briefly have a look at parameters in Algorithm 8.1.

Parameters and Variables

Number of Grid Points N. A total number of grid points $N \in \mathbb{N}^+$ for discretisation of the interval $[0,1]$ is needed and it is desirable to be an odd number, otherwise we do not receive a peak at the point $x = \frac{1}{2}$ due to numerical reasons. Then, a computational

Algorithm 8.1 Upwind-type numerical algorithm for an eikonal equation in 1-D

Require: $N > 1$
1: $X \leftarrow \frac{1}{N-1}[0,1,\ldots,N-1]$
2: $U \leftarrow [0,0,\ldots,0]$
3: $dx \leftarrow \frac{1}{N}$
4: $dt \leftarrow dx$
5: $iter \leftarrow 0$
6: **while** $\left\|U^{n+1} - U^n\right\|_\infty > \varepsilon$ **do**
7:     **for** $j = 2$ to $N-1$ **do**
8:         $mx(j) \leftarrow \frac{u(j-1)-u(j)}{dx}$
9:         $px(j) \leftarrow \frac{u(j+1)-u(j)}{dx}$
10:         $dir(j) \leftarrow \min(0, mx(j), px(j))$
11:         $h(j) \leftarrow \sqrt{dir(j)^2} - 1$
12:         $u(j) \leftarrow u(j) - dt * h(j)$
13:     **end for**
14:     $iter \leftarrow iter + 1$
15: **end while**

domain X has the form

$$X := \underbrace{[x(1),\ldots,x(N)]}_{\#\text{ of vector elements } = N} = \frac{1}{N-1}\underbrace{[0,1,\ldots,N-1]}_{\#\text{ of grid points } = N}, \tag{8.1}$$

see "Require" and line 1 in Algorithm 8.1.

Grid Size dx. Since the interval $[0,1]$ is subdivided with N grid points by (8.1), the grid size is given by

$$dx = \frac{1}{N} = x(2) - x(1) = \cdots = x(N) - x(N-1), \tag{8.2}$$

see line 3 in Algorithm 8.1.

Time Step Size dt. As is discussed in Section 7.4, it should be always careful when we choose a time step size to guarantee the stability of a scheme. Based on (7.83) we can recognise that a time step size dt and a mesh size dx are in the same order as long as the scheme is stable. Thus, in order to make the scheme convergent as fast as possible we have selected a largest possible time step size dt as

$$dt = \frac{1}{N}, \tag{8.3}$$

see line 4 in Algorithm 8.1.

Stopping Criterion by ε. The stopping criterion is realised in such a way, that a numerical computation stops if the difference of the two successive iterations is less than a predefind small number ε in the sense of a maximum-norm, see line 6 in Algorithm 8.1. As can be observed in Table 8.1, measuring error in max norm is reasonable, since it is the point of bottleneck for the convergence.

Number of Iterations *iter*. The variable *iter* counts the number of iterations until the above mentioned stopping criterion is satisfied, see line 14 in Algorithm 8.1.

Boundary and Initial Conditions

Another important issue for numerical implementation is about boundary and initial conditions. However, this information for the case of a one-dimensional eikonal equation is already available in (7.66), so we can use them without any pain. Therefore, the initialisation of a solution U has the form

$$U := [u(1), \ldots, u(N)] = [0, 0, \ldots, 0] , \tag{8.4}$$

see line 2 in Algorithm 8.1.

8.1.2 Experimental Result

The first test is performed with $\varepsilon = 10^{-3}$. In this case, the computation stops after nine iterations and Figure 8.1 shows us how a numerical solution evolves and converges to a viscosity solution. To this end, we make use of L_1-, L_2-, and L_∞-error and corresponding error estimations at each iteration step are given in Table 8.1. They are estimated by

$$L_1\text{- error} = \sum_{i=1}^{N} |u_c(i) - u_e(i)| , \tag{8.5}$$

$$L_2\text{- error} = \sqrt{\sum_{i=1}^{N} (u_c(i) - u_e(i))^2}, \tag{8.6}$$

and

$$L_\infty\text{- error} = \max_{i=1,\ldots,N} |u_c(i) - u_e(i)| , \tag{8.7}$$

where u_c and u_e denote computed and exact solution respectively.

Then, we further test by changing a parameter N. Since both dx and dt are described by a same function of N, adjusting N affects both parameters dx and dt as well. Table 8.2 tells us how the iteration numbers change with a fixed constant ε as the number of mesh points N increases. It can be recognised that more iteration numbers are needed as the

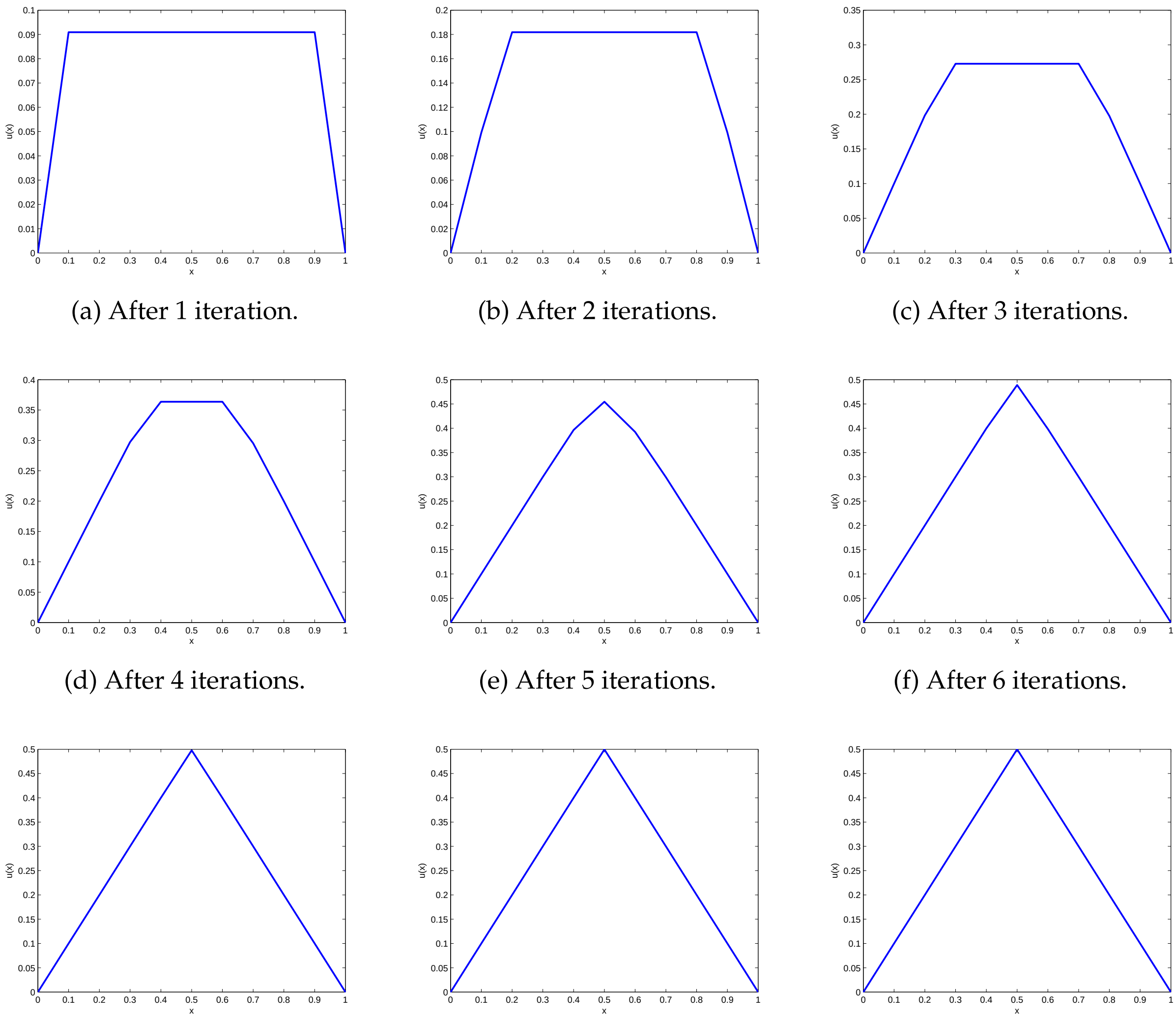

(a) After 1 iteration. (b) After 2 iterations. (c) After 3 iterations.

(d) After 4 iterations. (e) After 5 iterations. (f) After 6 iterations.

(g) After 7 iterations. (h) After 8 iterations. (i) After 9 iterations.

Figure 8.1: Numerical experiments for one-dimensional eikonal equation. The parameters used for this test are: $N = 11$, $dx = dt = \frac{1}{N}$, $\varepsilon = 10^{-3}$. The corresponding error estimations are given in Table 8.1.

number of grid points increases. The results are not surprising but what one might expect based on the theory that we have studied before.

8.2 VBW Model

In this section, we shall see experimental results of one-dimensional VBW explicit scheme on synthetic images. SfS is, however, usually performed in two-dimension, here we

# of iterations	L_1-error	L_2-error	L_∞-error
1	1.6818	0.6854	0.0909
2	1.0289	0.4744	0.0909
3	0.5406	0.2925	0.0909
4	0.2168	0.1458	0.0909
5	0.0575	0.0462	0.0909
6	0.0128	0.0111	0.0345
7	0.0024	0.0022	0.0088
8	$4.1662E-4$	$3.8398E-4$	0.0018
9	$6.5415E-5$	$6.1159E-5$	$3.2184E-4$

Table 8.1: L_1-, L_2-, and L_∞-error estimation after each iteration from $iter = 1$ to 9 for the case of $\varepsilon = 10^{-3}$, cf. Figure 8.1.

# of grid points N	# of iterations	L_1-error	L_2-error	L_∞-error
21	16	$2.4254E-7$	$2.2971E-7$	$1.9124E-6$
41	25	$7.1621E-7$	$6.7076E-7$	$6.0704E-6$
61	35	$4.0103E-7$	$3.7509E-7$	$3.6326E-6$
81	45	$2.7448E-7$	$2.5665E-7$	$2.5751E-6$
101	55	$2.0755E-7$	$1.9392E-7$	$1.9899E-6$

Table 8.2: Necessary iteration numbers and corresponding errors for a predefined constant $\varepsilon = 10^{-5}$ depending on the numbers of grid points N.

briefly explain how we proceed our tests in one-dimension.

8.2.1 Shape from Shading in 1-D

The test idea in one-dimension is exactly the same as in two-dimensional case. Let us have a look at Figure 8.2 to clarify this.

First, we take one row from an input grey value matrix, see Figure 8.2a.

Then, we apply the algorithm to reconstruct the shape of the cross section of the original surface, see Figure 8.2b.

Since applying SfS to the whole two-dimensional image matrix yields three-dimensional surface, its cross section is automatically in two-dimension, which we expect.

8.2.2 Numerical Implementation

The numerical implementation of VBW explicit scheme is based on the theory from Section 7.5. The pseudocode of main part for VBW Lambertian model is given in Al-

$$\begin{array}{c} \\ \\ \\ \rightarrow \\ \\ \\ \\ \end{array}\begin{bmatrix} 255 & 200 & 255 & 200 & 255 \\ 255 & 190 & 255 & 190 & 255 \\ 255 & 180 & 255 & 180 & 255 \\ 170 & 170 & 255 & 170 & 170 \\ 255 & 180 & 255 & 180 & 255 \\ 255 & 190 & 255 & 190 & 255 \\ 255 & 200 & 255 & 200 & 255 \end{bmatrix}$$

(a) Input grey value matrix: "→" indicates the taken row.

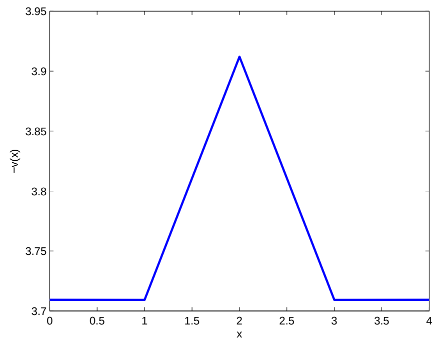

(b) Output of one-dimensional SfS.

Figure 8.2: Illustration of Shape from Shading in one-dimension.

gorithm 8.2, where $E(x,y)$ denotes an input grey value image with $M \times N$ pixels and σ depends on the albedo of the surface and the intensity of the light source [74]. In addition, we briefly touch the issues which are not detailed in Algorithm 8.2.

Points to Consider

Time Step Size dt**.** As we investigated in previous chapter, choosing time step size dt plays a significant role on the stability of an explicit scheme and convergence speed is influenced by this number as well. In order to guarantee monotonicity of a scheme and thereby to fulfil the stability condition, (7.118) must be obeyed pixelwise and it turns out that the right hand side of (7.118) is usually very small. In our experiment, this number is between 10^{-8} and 10^{-7}.

Boundary Conditions. It is also crucial to treat boundary conditions correctly not only for solution theory but also for numerical realisations. When it comes to perspective Shape from Shading problems, there are several options that we can choose [65].

First one is a state constraint boundary condition which was used by Prados in [84] based on the formulation by Hamilton-Jacobi-Bellman equations. In our case, it can be implemented in the form of Dirichlet boundary conditions

$$u(x_1,x_2) = \overline{u}, \tag{8.8}$$

where

$$\overline{u} = \max_{(x_1,x_2)\in\Omega} u(x_1,x_2)\,. \tag{8.9}$$

This condition makes automatically sense owing to the minimisation process in (7.93). One advantage of this method is that we do not need any boundary data which is in general unavailable.

Algorithm 8.2 Upwind-type numerical algorithm for VBW model in 1-D

Require: $E(x,y) > 0$

$I \leftarrow \frac{E(x,y)}{\sigma}$
$V \leftarrow -\frac{1}{2} \ln I\mathtt{f}^2$
$iter \leftarrow 0$
while $\left\|V^{n+1} - V^n\right\|_\infty > \varepsilon$ **do**
  for $i = 1$ to M **do**
    for $j = 1$ to N **do**
      $mx(i) \leftarrow \frac{v(i-1,j)-v(i,j)}{dx}$
      $px(i) \leftarrow \frac{v(i+1,j)-v(i,j)}{dx}$
      $xdir(i) \leftarrow \min(0, mx(i), px(i))$
      $my(j) \leftarrow \frac{v(i,j-1)-v(i,j)}{dy}$
      $py(j) \leftarrow \frac{v(i,j+1)-v(i,j)}{dy}$
      $ydir(j) \leftarrow \min(0, my(j), py(j))$
      $Q(i,j) \leftarrow \frac{\mathtt{f}}{\sqrt{i^2+j^2+\mathtt{f}^2}}$
      $A(i,j) \leftarrow \frac{I\mathtt{f}^2}{Q(i,j)^2} \sqrt{\mathtt{f}^2 \left(xdir(i)^2 + ydir(j)^2\right) + (i * xdir(i) + j * ydir(j))^2 + Q(i,j)^2}$
      $v(i,j) \leftarrow v(i,j) - dt * A(i,j) + dt * e^{-2*v(i,j)}$
    end for
  end for
  $iter \leftarrow iter + 1$
end while

Of course, alternatives are possible. If the solution is known at the boundary under special circumstances, then exact Dirichlet boundary conditions are best choice. When no information is available, homogeneous Neumann boundary conditions can be another choice. In all our tests, we used Neumann boundary conditions.

Initial Condition. Another important factor to influence on convergence speed is the initialisation. Since we use an iterative method and rather small time step size for stability reasons, the initial values should be larger than and as close as possible to the solution. As suggested and shown in [84],

$$v := -0.5 \log I\,\mathtt{f}^2 \tag{8.10}$$

meets the requirements. However, one disadvantage of (8.10) is that due to the properties of a log function the normalised image I is not allowed to have complete black pixels, which means grey values must be strictly positive.

8.2.3 Convergence Tests

We now present test results for both Lambertian- and Phong-type surfaces.

Lambertian Surfaces

For the Lambertian case, we use the classical vase as a test image.

1-D Experiment. Figure 8.3 shows the reconstruction shape for selected rows. The outcome in fact seems reasonable enough to confirm the convergence according to the test method and only one iteration is necessary in order to satisfy the stopping criterion $\varepsilon = 10^{-4}$.

2-D Experiment. Figure 8.4 displays that the shape itself of the vase complies with the behaviour of 1-D case as expected. However, as can be noticed the treatment of the background close to the edge is not that efficient by smoothing effect. Therefore, it can be mentioned that this method does not treat steep gradient well, although the computed result shows the reasonable reconstruction of the shape itself.

Phong Surfaces

The big difference between Lambertian and Phong surface is a specular effect. In order to test correctly, we make use of an ellipsoid scene (8.5a) as an input image which is rendered by a ray tracer.

1-D Experiment. For this test, our experiment is carried out columnwise. Figure 8.5 shows the 1-D outcome is quite reasonable to convince the convergence of the solution within the ellipsoid region. Specially, when it comes to specular point where the highlight effect occurs, they are treated pretty well and the cross section of the original surface is not distorted although it looks a little bit flat. The computational results are described in Table 8.3.

2-D Experiment. As in the case of 1-D, Figure 8.6 also shows the reasonable convergence output. It can be also noticed that the computed solution looks quite well especially around specular points. However, the treatment of edges is not quite efficient, as we have seen in the Lambertian case.

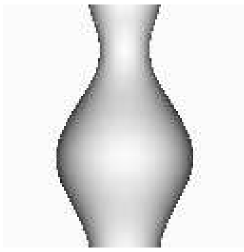

(a) Input image: the classic vase with 128 × 128 pixels. Adapted from [4]

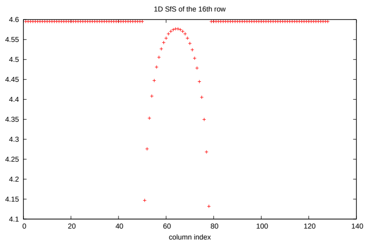

(b) 1D SfS of the 16th row.

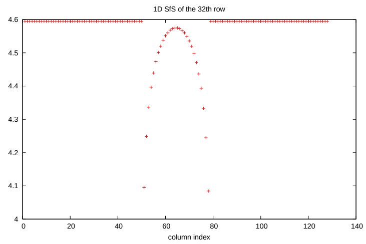

(c) 1D SfS of the 32th row.

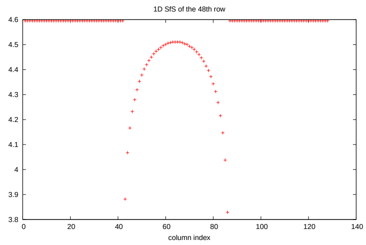

(d) 1D SfS of the 48th row.

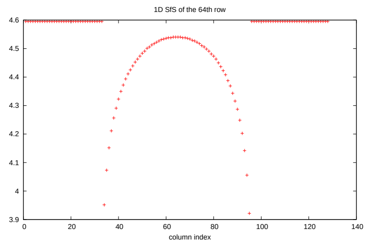

(e) 1-D SfS of the 64th row.

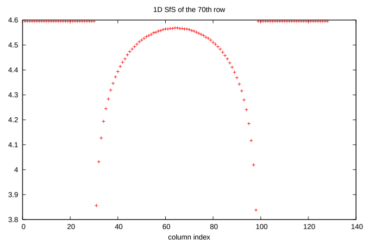

(f) 1-D SfS of the 70th row.

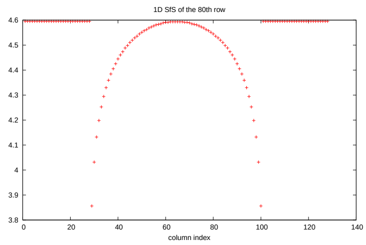

(g) 1-D SfS of the 80th row.

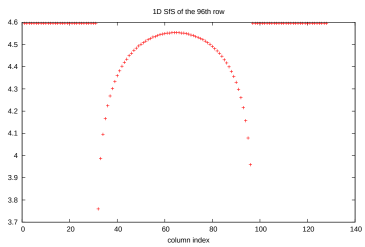

(h) 1-D SfS of the 96th row.

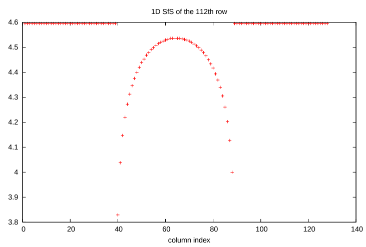

(i) 1-D SfS of the 112th row.

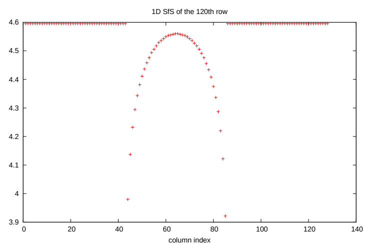

(j) 1-D SfS of the 120th row.

Figure 8.3: The results of 1-D Lambertian SfS. The following parameters are incorporated for this test: $dt = 10^{-8}$, $\sigma = 255$, $dx = 1$, $\mathtt{f} = 100$, $\varepsilon = 10^{-4}$.

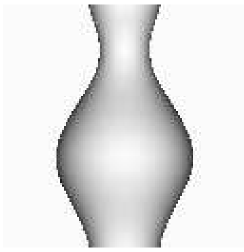

(a) Input image: the classic vase with 128×128 pixels.

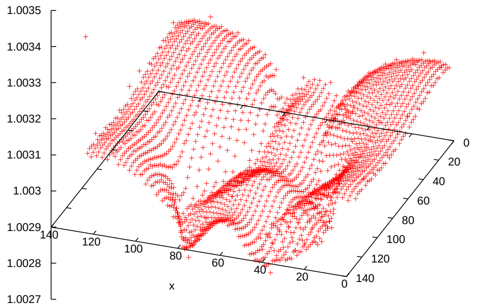

(b) Pixelwise computed solution.

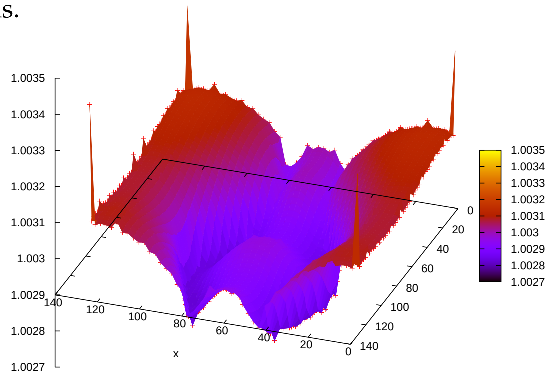

(c) Colour-coded map of (8.4b).

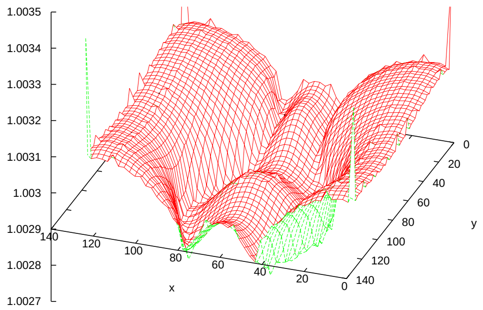

(d) Grid representation of (8.4b).

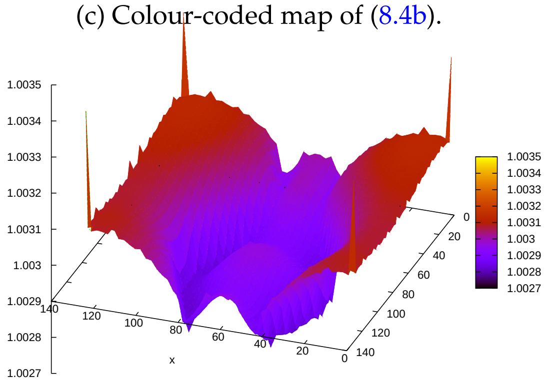

(e) Corresponding surface representation with colour-coded map.

Figure 8.4: The classic Lambertian vase experiment in 2-D. The parameters employed are: $dt = 10^{-8}$, $\sigma = 255$, $dx = dy = 1$, $\mathfrak{f} = 100$, $\varepsilon = 10^{-4}$. The test results are $\|V^n - V^{n-1}\| = 9.999913E - 5$ with $n = 34$ iterations.

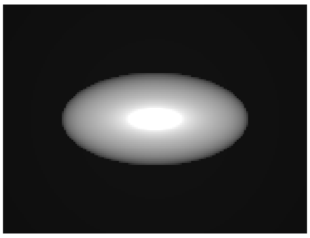

(a) Input image: a Phong-type ellipsoid with 120 × 160 pixels.

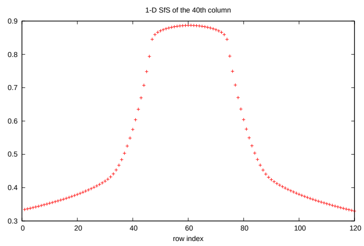

(b) 1-D SfS of the 40th column.

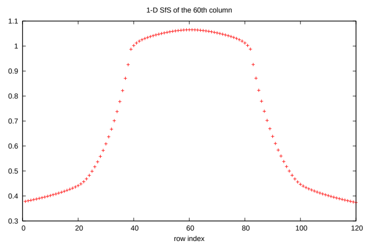

(c) 1-D SfS of the 60th column.

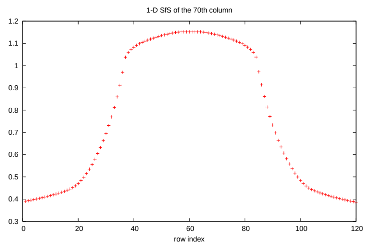

(d) 1-D SfS of the 70th column.

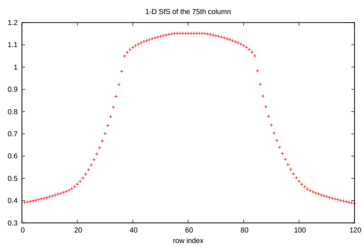

(e) 1-D SfS of the 75th column.

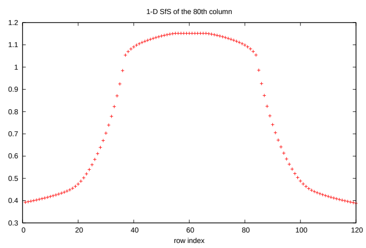

(f) 1-D SfS of the 80th column.

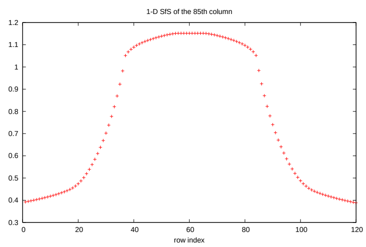

(g) 1-D SfS of the 85th column.

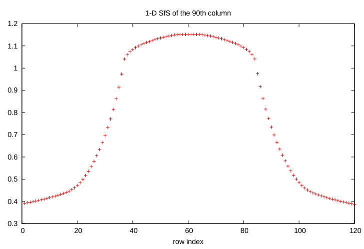

(h) 1-D SfS of the 90th column.

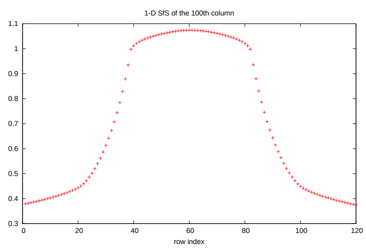

(i) 1-D SfS of the 100th column.

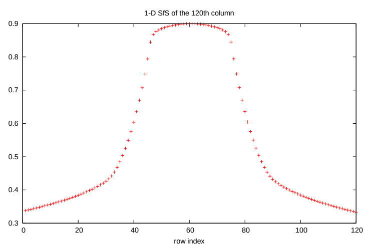

(j) 1-D SfS of the 120th column.

Figure 8.5: The Phong-type ellipsoid experiment in 1-D. The parameters employed are: $dt = 10^{-7}$, $\sigma = 255$, $dx = 1$, $\mathtt{f} = 100$, $\varepsilon = 10^{-4}$, $\kappa_a = 0$, $\kappa_d = 0.7$, $\kappa_s = 0.3$, $I_d = I_s = 1000$, $\alpha = 5$.

selected column index	# of iterations (n)	$\|V^n - V^{n-1}\|_\infty$
40	3560	$9.995699E-5$
60	3459	$9.998679E-5$
70	3431	$9.995699E-5$
75	3427	$9.995699E-5$
80	3423	$9.998679E-5$
85	3423	$9.998679E-5$
90	3427	$9.998679E-5$
100	3456	$9.998679E-5$
120	3554	$9.995699E-5$

Table 8.3: Summary of computational results for 1-D Phong SfS with a stopping criterion $\varepsilon = 10^{-4}$.

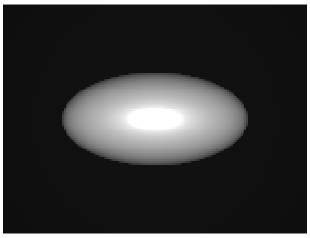

(a) Input image: a Phong-type ellipsoid with 120 × 160 pixels.

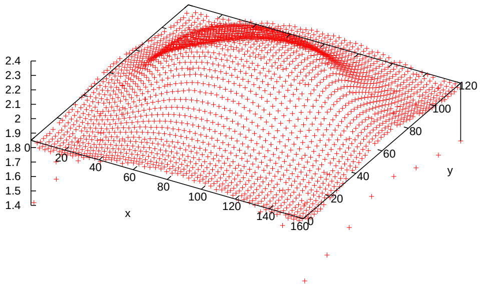

(b) Pixelwise computed solution.

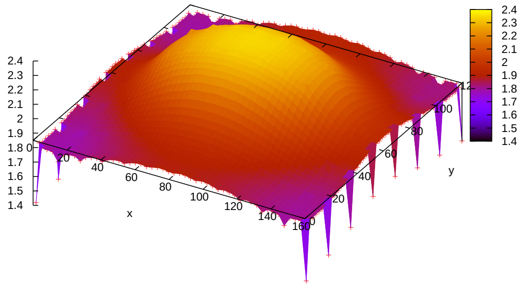

(c) Colour-coded map of (8.6b).

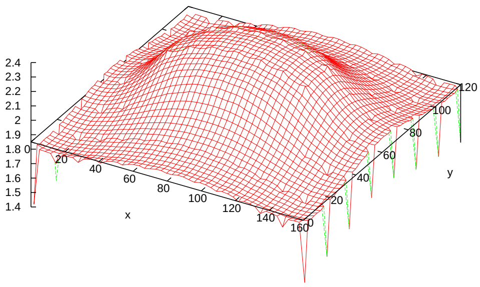

(d) Grid representation of (8.6b).

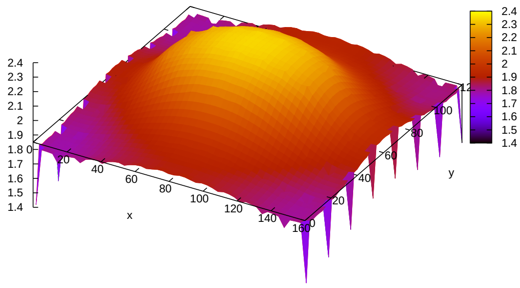

(e) Corresponding surface representation with colour-coded map.

Figure 8.6: The Phong-type ellipsoid experiment in 2-D. The parameters employed are: $dt = 10^{-7}$, $\sigma = 255$, $dx = dy = 1$, $\mathtt{f} = 100$, $\varepsilon = 10^{-4}$, $\kappa_a = 0$, $\kappa_d = 0.7$, $\kappa_s = 0.3$, $I_d = I_s = 1000$, $\alpha = 5$. The test results are $\|V^n - V^{n-1}\| = 9.998679E - 5$ with $n = 3513$ iterations.

Chapter 9

Conclusion

In this thesis, we have explorered the world of Hamilton-Jacobi equations which turned out to be quite effective for Shape from Shading problems.

After Chapter 1 has given a general overview of Shape from Shading problems and modelling issues, the goal of Chapter 2-4 has been to provide the foundation of a continuous viscosity solution framework on which the rest of this work relies.

We have seen that under this notion the long-desired well-posedness properties can be acquired with the help of compatibility condition and comparison principle, which was not possible in the classical one. This notion is not only useful from a theoretical point of view but also from a numerical one, since the convergence of a numerical scheme can be guaranteed in this setup. Therefore, this setting gives us the power to analyse and realise new Shape from Shading models efficiently in both theoretical and practical perspectives, as long as the model involves Hamilton-Jacobi equations.

The next two subsequent chapters have handled modern Shape from Shading models.

Chapter 5 has discussed the perspective Shape from Shading with Lambertian surfaces by Prados and Faugeras including modelling process, eikonal-type generic Hamiltonian - an efficient formulation of the model itself - and well-posedness of the model.

It was shown that singular points played an important role on the uniqueness of solutions. In order to avoid the effect of singular points, a light attenuation term based on the inverse square law was taken into account leading to a general-type Hamiltonian which can satisfy well-posedness properties without being affected by singular points. In consideration of these results, the modelling process should reflect physical phenomena correctly, otherwise an outcome would be unreasonable or have poor qualities.

Chapter 6 has treated one of the simplest non-convex Shape from Shading models handling Phong-type surfaces which look much more realistic than Lambertian ones. As recognised in this case, more realistic modelling often has led to non-convex problems which are, in general, more complicated and difficult to deal with. However, the analysis of critical points enables us to get hands on the valuable information on the behaviour around critical points and the convexities of Hamiltonians. It can even provide conditions to alleviate the non-convex properties theoretically, which can offer us in-depth understanding of the model.

The last part of this work has been involved with numerical sides of the problem.

Chapter 7 has put so much effort to establish the convergence of a numerical scheme for solving general-type Hamilton-Jacobi equations in the viscosity sense and Chapter 8 has presented the experimental results.

Despite the difficulties of monotonicity analysis due to our special interest in the non-convex Hamiltonian we have shown that under certain stability constraints a simple monotone and consistent upwind-type explicit scheme equipped with a strong uniqueness property for the Vogel-Breuß-Weickert model converges toward a continuous viscosity solution in one-dimensional case.

In these contexts, this work can be extended in several ways.

For the modelling aspect, one could employ more physically accurate reflectance model for surfaces in Shape from Shading problems. As long as the mathematical model involves Hamilton-Jacobi equation, properties of viscosity framework can also be transferred into the new model. One example can be found in [5].

For the analysis of these models, a critical point analysis method that we have used in Chapter 6 remains still useful, since in general more realistic models possess non-convex Hamiltonians.

Another work could be expected in higher dimensions. While the theory and the examples in the present thesis mainly focus on 1-D or 2-D grey value data, it is evident that most of its results could be generalised to higher dimension problems, e.g. colour Shape from Shading. Such generalisations could be applied to the situation where more precise operation technique under endoscopy scene is in need for medical purposes.

From the numerical perspective, more efficient schemes like implicit ones can be expected.

Therefore, there is still room for improvements. It would be very nice if this work has inspired its readers to contribute to the related fields.

References

[1] Inverse square law. http://en.wikipedia.org/wiki/Inverse-square_law. 107

[2] Lambert's cosine law. http://en.wikipedia.org/wiki/Lambert's_cosine_law. 68

[3] Shape from Shading. http://jposhea.org/projects/shapefromshading/. 2

[4] The classical vase image. http://server.cs.ucf.edu/~vision/. 159

[5] Abdelrehim H. Ahmed and Aly A. Farag. A New Formulation for Shape from Shading for Non-Lambertian Surfaces. *Computer Vision and Pattern Recognition, IEEE Computer Society Conference on*, 2:1817–1824, 2006. 5, 166

[6] Alec Johnson. The Fundamental Theorem of Numerical Analysis. http://www.math.wisc.edu/~ejohnson/summaries/ftna/ftna.pdf, 2006. 118

[7] Anthony L. Peressini, Francis E. Sullivan, and J. J. Uhl, Jr. *The Mathematics of Nonlinear Programming*. Undergraduate Texts in Mathematics. Springer-Verlag, 1988. 7, 38

[8] Tom M. Apostol. *Calculus*, volume I. John Wiley & Sons, 2nd edition, 1967. 12, 45

[9] Ariel Tankus, Nir Sochen, and Yehezkel Yeshurun. Reconstruction of Medical Images by Perspective Shape-from-Shading. *Pattern Recognition, International Conference on*, 3:778–781, 2004. 1

[10] Ariel Tankus, Nir Sochen, and Yehezkel Yeshurun. Shape-from-Shading Under Perspective Projection. *International Journal of Computer Vision*, 63(1):21–43, 2005. 3

[11] Gilles Aubert and Pirre Kornprobst. *Mathematical Problems in Image Processing: Partial Differential Equations and the Calculus of Variations*, volume 147 of *Applied Mathematical Sciences*. Springer, 2nd edition, 2006. 7, 14, 15

[12] Martino Bardi and Italo Capuzzo-Dolcetta. *Optimal control and viscosity solutions of Hamilton-Jacobi-Bellman equations*. Modern Birkhäuser Classics. Birkhäuser, Boston, reprint of the 1997 edition, 2008. 7, 16, 17, 18, 53, 54, 56, 110, 128, 129, 130, 148

[13] Stanley H. Benton. *The Hamilton-Jacobi Equation: A Global Approach*, volume 131. Academic Press, 1977. 43

[14] Berthold Klaus Paul Horn and Michael J. Brooks. *Shape from Shading*. Artificial intelligence series. The MIT Press, 1989. 1, 2

[15] Michael Breuß. Lecture Note "Numerical Algorithms for Visual Computing II". http://www.mia.uni-saarland.de/Teaching/NAVC-WS0809/NAVC02-08.pdf, 2008/2009. 118, 122, 124

[16] Michael J. Brooks. Two Results Concerning Ambiguity in Shape From Shading. In *AAAI-83*, pages 36–39, 1983. 2, 64, 66

[17] Anna R. Bruss. The eikonal equation: some results applicable to computer vision. *Journal of Mathematical Physics*, 23(5):890–896, May 1982. 2

[18] Bui Tuong Phong. Illumination for Computer Generated Pictures. *Communications of the ACM*, 18(6):311–317, June 1975. 106

[19] C. J. Seelye. Conditions for a Positive-Definite Quadratic Form Established by Induction. *The American Mathematical Monthly*, 65(5):355–356, May 1958. 80

[20] Chenyu Wu, Srinivasa G. Narasimhan, and Branislav Jaramaz. Shape reconstruction from endoscopic images. In *8th Annual Meeting of the International Society for Computer Assisted Orthopaedic Surgery (CAOS' 08)*, June 2008. 1

[21] Chiu Yen Kao, Stanley Osher, and Jianliang Qian. Lax-Friedrichs sweeping scheme for static Hamilton-Jacobi equations. *Journal of Computational Physics*, 196(1):367 – 391, 2004. 132

[22] Michael G. Crandall and Pierre-Louis Lions. Condition d'unicité pour les solutions generalisées équations Hamilton-Jacobi de premier ordre. *Comptes Rendus de l'Académie des Sciences. Série I.*, 292(3):183–186, 1981. 15, 16

[23] Michael G. Crandall and Pierre-Louis Lions. Viscosity Solutions of Hamilton-Jacobi equations. *Transactions of the American Mathematical Society*, 277(1):1–42, May 1983. 15, 16, 53, 54, 110, 128

[24] Angel de la Fuente. *Mathematical Methods and Models for Economists*. Cambridge University Press, 2000. 84

[25] Jean-Denis Durou and Didier Piau. Ambiguous Shape from Shading with Critical Points. *Journal of Mathematical Imaging and Vision*, 12(2):99–108, 2000. 64

[26] Elisabeth Rouy and Agnès Tourin. A viscosity solutions approach to Shape-from-Shading. *SIAM Journal on Numerical Analysis*, 29(3):867–884, June 1992. 53, 64, 73, 103, 117, 118, 131, 132

[27] Emiliano Cristiani, Maurizio Falcone, and Alessandra Seghini. Some Remarks on Perspective Shape-from-Shading Models. In Fiorella Sgallari, Almerico Murli, and Nikos Paragios, editors, *Scale Space and Variational Methods in Computer Vision – First International Conference, SSVM 2007, Ischia, Italy, May 30 - June 2, 2007. Proceedings*, volume 4485 of *Lecture Notes in Computer Science*, pages 276–287, Berlin Heidelberg, 2007. Springer. 1, 3

[28] Emmanuel Prados, Oliver Faugeras, and Elisabeth Rouy. Shape from shading and viscosity solutions. Technical Report 4638, INRIA, November 2002. 64

[29] Emmanuel Prados, Oliver Faugeras, and Fabio Camilli. Shape from Shading: a well-posed problem? Technical Report 5297, INRIA, August 2004. 3, 64, 66, 67, 105, 110

[30] Emmanuel Prados, Olivier D. Faugeras, and Elisabeth Rouy. Shape from Shading and Viscosity Solutions. In *Computer Vision – ECCV 2002: 7th European Conference on Computer Vision Copenhagen, Denmark, May 28-31, 2002 Proceedings, Part II*, volume 2351/2002 of *Lecture Notes in Computer Science*, pages 790–804, Berlin Heidelberg, 2002. Springer. 64

[31] Emmanuel Prados and Olivier D. Faugeras. ”Perspective Shape from Shading” and Viscosity Solutions. In *9th IEEE International Conference on Computer Vision (ICCV 2003), 14-17 October 2003, Nice, France*, pages 826–831. IEEE Computer Society, 2003. 64, 67, 75

[32] Lawrence C. Evans. *Partial Differential Equations*, volume 19 of *Graduate Studies in Mathematics*. American Mathematical Society, 1998. 7, 8

[33] Bernd Freytag. Lecture Note “Introduction to Numerical Hydrodynamics”. http://www.astro.uu.se/~bf/course/numhd_course_20100124.pdf, 2010. 118

[34] G. Barles. *Solutions de Viscosité des Equations de Hamilton-Jacobi*. Springer, 1994. 16

[35] G. Barles and B. Perthame. Discontinuous solutions of deterministic optimal stopping time problems. *Modélisation mathématique et analyse numérique*, 21(4):557–579, 1987. 125

[36] G. Barles and B. Perthame. Exit Time Problems in Optimal Control and Vanishing Viscosity Method. *SIAM Journal on Control and Optimization*, 26(5):1133–1148, 1988. 125

[37] G. Barles and P. E. Souganidis. Convergence of approximation schemes for fully nonlinear second order equations. *Asymptotic Analysis*, 4:271–283, 1991. 117, 118, 125, 128, 148

[38] Felix R. Gantmacher. *The Theory of Matrices*, volume I. Chelsea Publishing Company, New York, 1960. 80

[39] George T. Gilbert. Positive Definite Matrices and Sylvester's Criterion. *The American Mathematical Monthly*, 98(1):44–46, January 1991. 80

[40] Guo-hui Wang, Jiu-qiang Han, and Xin-man Zhang. Three-dimensional reconstruction of endoscope images by a fast shape from shading method. *Measurement Science and Technology*, 20(12), 2009. 1

[41] Jacques Hadamard. *Lectures on Cauchy Problem in Linear Partial Differential Equations*. Yale University Press, 1923. 10

[42] Jean-Baptiste Hiriart-Urruty and Claude Lemaréchal. *Convex Analysis and Minimization Algorithms I*, volume 305 of *Grundlehren der Mathematischen Wissenschaften*. Springer, 1996. 7, 16, 18, 38

[43] Jean-Baptiste Hiriart-Urruty and Claude Lemaréchal. *Convex Analysis and Minimization Algorithms II*, volume 306 of *Grundlehren der Mathematischen Wissenschaften*. Springer, 1996. 38, 40

[44] Jean-Baptiste Hiriart-Urruty and Claude Lemaréchal. *Fundamentals of Convex Analysis*, volume 19 of *Grundlehren Text Editions*. Springer, 2004. 7, 16, 18

[45] Berthold Klaus Paul Horn. *Shape From Shading: A Method for Obtaining the Shape of a Smooth Opaque Object From One View*. PhD thesis, Massachusetts Institute of Technology, 2004. 2

[46] Hugo Touchette. Legendre-Fenchel transforms in a nutshell. http://www.maths.qmul.ac.uk/~ht/archive/lfth2.pdf, 2007. 7, 36

[47] Hitoshi Ishii. A Simple Direct Proof of Uniqueness for Solutions of the Hamilton-Jacobi Equations of Eikonal Type. *American Mathematical Society*, 100(2):247–251, 1987. 53, 54, 55, 56

[48] Hitoshi Ishii. A boundary value problem of the Dirichlet type for Hamilton-Jacobi equations. *Annali della Scuola Normale Superiore di Pisa - Classe di Scienze*, 16(1):105–135, 1989. 125

[49] John Strikwerda. *Finite Difference Schemes and Partial Differential Equations*. SIAM, 2nd edition, 2004. 124

[50] C. R. Johnson. Positive Definite Matrices. *The American Mathematical Monthly*, 77(3):259–264, March 1970. 80

[51] Keith W. Morton and David Francis Mayers. *Numerical Solution of Partial Differential Equations: An Introduction*. Cambridge University Press, 2nd edition, 2005. 118

[52] Kenneth Hoffman and Ray Kunze. *Linear Algebra*. Prentice-Hall, Englewood Cliffs, New Jersey, 2nd edition, 1971. 80

[53] Andreas Kirsch. *An Introduction to the Mathematical Theory of Inverse Problems*, volume 120 of *Applied Mathematical Sciences*. Springer, 1996. 7

[54] Konrad Königsberger. *Analysis 1*. Springer-Lehrbuch. Springer, Berlin - Heidelberg - New York, 6th edition, 2004. 45

[55] Ryszard Kozera. Uniqueness in Shape from Shading Revisited. *Journal of Mathematical Imaging and Vision*, 7(2):123–138, 1997. 66

[56] Kyoung Mu Lee and C.-C. Jay Kuo. Shape from shading with a generalized reflectance map model. *Computer Vision and Image Understanding*, 67(2):143–160, 1997. 4

[57] Johann Heinrich Lambert. *Photometria sive de mensure de gratibus luminis, colorum umbrae*. Eberhard Klett, 1760. 68

[58] Randall J. LeVeque. *Numerical Methods for Conservation Laws*. Lecture in Mathematics: ETH Zürich. Birkhäuser, 1992. 118, 120, 123, 124

[59] Randall J. LeVeque. *Finite Volume Methods for Hyperbolic Problems*, volume 31 of *Cambridge Texts in Applied Mathematics*. Cambridge University Press, Cambridge - New York - Melbourne - Madrid - Cape Town, 2002. 118, 123, 124

[60] Pierre-Louis Lions. *Generalized Solutions of Hamilton-Jacobi Equations*, volume 69 of *Research Notes in Mathematics*. Pitman Publishing, 1982. 16, 43, 46, 47, 53, 54, 110, 128

[61] M. Breuß, O. Vogel, and J. Weickert. Efficient Numerical Techniques for Perspective Shape From Shading. In A. Handlovičová, P. Frolkovič, K. Mikula, and D. Ševčovič, editors, *Algorithmy 2009 – 18th Conference on Scientific Computing Vysoké Tatry Podbanské, Slovakia, March 15 20, 2009* , pages 11–20, 2009. 118

[62] Melvyn A. Fuss and Daniel L. McFadden. *Production Economics: A Dual Approach to Theory and Applications*, volume I, chapter "Definite Quadratic Forms Subject to Constraint", pages 365–373. Elsevier North-Holland, Amsterdam, 1978. 80

[63] Carl D. Meyer. *Matrix Analysis and Applied Linear Algebra*. SIAM, Philadelpia, PA, 2000. 80

[64] Michael Artin. *Algebra*. Prentice-Hall, Upper Saddle River, New Jersey, 1991. 80

[65] Michael Breuß, Emiliano Cristiani, Jean-Denis Durou, Maurizio Falcone, and Oliver Vogel. Numerical Algorithms for Perspective Shape from Shading. Technical Report 240, Universität des Saarlandes, Saarbrücken, 2009. 156

[66] Michael G. Crandall, Hitoshi Ishii, and Pierre-Louis Lions. User's Guide to Viscosity Solutions of Second Order Partial Differential Equations. *Bulletin of the American Mathematical Society*, 27(1):1–67, July 1992. 16

[67] Michael G. Crandall, Lawrence C. Evans, and Pierre-Louis Lions. Some Properties of Viscosity Solutions of Hamilton-Jacobi Equations. *Transactions of the American Mathematical Society*, 282(2), April 1984. 7, 16, 53, 110

[68] Michael G. Crandall and Pierre-Louis Lions. Two Approximations of Solutions of Hamilton-Jacobi Equations. *Mathematics of Computation*, 43(167):1–19, July 1984. 125

[69] Michael G. Crandall and Pierre-Louis Lions. On existence and uniqueness of solutions of Hamilton-Jacobi equations. *Nonlinear Analysis: Theory, Methods & Applications*, 10(4):353–370, April 1986. 16, 53, 110

[70] Milton Abramowitz and Irene A. Stegun. *Handbook of Mathematical Functions: with Formulas, Graphs, and Mathematical Tables*. Dover Publications, 1965. 108

[71] Wolfgang Nolting. *Grundkurs Theoritische Physik 2: Analytische Mechanik*. Springer-Lehrbuch. Springer, Berlin Heidelberg, 7th edition, 2007. 7, 34

[72] John A. Oliensis. Shape from shading as a partially well-constrained problem. *Computer Vision, Graphics, and Image Processing: Image Understanding: Image Understanding*, 54(2):163–183, 1991. 64

[73] John A. Oliensis. Uniqueness in shape from shading. *International Journal of Computer Vision*, 6(2):75–104, 1991. 66

[74] Oliver Vogel, Michael Breuß, and Joachim Weickert. A Direct Numerical Approach to Perspective Shape-from-Shading. In H. Lensch, B. Rosenhahn, H.-P. Seidel, P. Slusallek, and J. Weickert, editors, *Vision, Modeling, and Visualization 2007*, pages 91–100, Saarbrücken, Germany, November 2007. 118, 156

[75] Oliver Vogel, Michael Breuß, and Joachim Weickert. Perspective Shape from Shading with Non-Lambertian Reflectance. In *Proceedings of the 30th DAGM symposium on Pattern Recognition*, pages 517–526, Berlin, Heidelberg, 2008. Springer-Verlag. 5, 105, 118, 132, 140, 143, 147

[76] Optical Society of America. *Handbook of Optics: Design, Fabrication, and Testing; Sources and Detectors; Radiometry and Photometry*, volume II. McGraw-Hill, 3rd edition, 2009. 68, 69

[77] Optical Society of America. *Handbook of Optics: Geometrical and Physical Optics,Polarized Light,Components and Instruments*, volume I. McGraw-Hill, 3rd edition, 2009. 11, 68, 69

[78] Daniel Ostrov. Viscosity Solutions and Convergence of Monotone Schemes for Synthetic Aperture Radar Shape-From-Shading Equations with Discontinuous Intensities. *SIAM Journal on Applied Mathematics*, 59(6):2060–2085, 1999. 125

[79] Alex P. Pentland. Local Shading Analysis. *Pattern Analysis and Machine Intelligence, IEEE Transactions on*, PAMI-6(2):170–187, March 1984. 3, 64

[80] Peter David Lax and Robert Davis Richtmyer. Survey of the stability of linear finite difference equations. *Communications on Pure and Applied Mathematics*, 9(2):267–293, 1956. 11, 124

[81] Peter N. Belhumeur and David J. Kriegman and Alan L. Yuille. The Bas-Relief Ambiguity. *International Journal of Computer Vision*, 35(1):33–44, 1999. 64

[82] Pierre-Louis Lions, Elisabeth Rouy, and A. Tourin. Shape-from-shading, viscosity solution and edges. *Numerische Mathematik*, 64:323–353, 1993. 64

[83] Yehuda Pinchover and Jacob Rubinstein. *An Introduction to Partial Differential Equations*. Cambridge University Press, 2005. 7, 8

[84] Emmanuel Prados. *Application of the theory of the viscosity solutions to the Shape From Shading problem*. PhD thesis, University of Nice - Sophia Antipolis, 2004. 1, 2, 3, 67, 73, 74, 75, 94, 96, 110, 128, 156, 157

[85] Emmanuel Prados and Oliver Faugeras. A mathematical and algorithmic study of the Lambertian SFS problem for orthographic and pinhole cameras. Technical Report 5005, INRIA, November 2003. 1, 4, 64, 67, 71, 73, 74, 75, 94, 96, 110

[86] Emmanuel Prados and Oliver Faugeras. A Generic and Provably Convergent Shape-from-Shading Method for Orthographic and Pinhole Cameras. *International Journal of Computer Vision*, 65(1/2):97–125, 2005. 100

[87] Emmanuel Prados and Oliver Faugeras. Shape from Shading: A Well-Posed Problem? *Computer Vision and Pattern Recognition, 2005. CVPR 2005. IEEE Computer Society Conference on*, 2:870–877, 2005. 66, 105, 110

[88] Emmanuel Prados and Olivier D. Faugeras. Unifying Approaches and Removing Unrealistic Assumptions in Shape from Shading: Mathematics Can Help. In *ECCV04*, 2004. 64, 67, 73, 74, 75, 94, 110

[89] R. Courant, K. Friedrichs, and H. Lewy. Über die partiellen Differenzengleichungen der mathematischen Physik. *Mathematische Annalen*, 100(1):32–74, 1928. 124

[90] R. Courant, K. Friedrichs, and H. Lewy. On the Partial Difference Equations of Mathematical Physics. *IBM Journal*, pages 215–234, March 1967. 124

[91] R. K. P. Zia, Edward F. Redish, and Susan R. McKay. Making Sense of the Legendre Transform. http://www.citebase.org/abstract?id=oai:arXiv.org:0806.1147, 2009. 7, 36

[92] Robert David Richtmyer and K. W. Morton. *Difference Methods for Initial-Value Problems*. Wiley-Interscience, 1967. 124

[93] R. Tyrrell Rockafellar and Peter R. Wolenski. Convexity and Duality in Hamilton-Jacobi Theory, 1998. 43

[94] Ralph Tyrell Rockafellar. *Convex Analysis*. Princeton Landmarks in Mathematics and Physics. Princeton University Press, 1970. 16, 18

[95] Walter Rudin. *Principles of Mathematical Analysis*. McGraw-Hill, 3rd edition, 1976. 98

[96] Ruo Zhang, Ping-Sing Tsai, James Edwin Cryer, and Mubarak Shah. Shape from Shading: A Survey. *IEEE Transactions on Pattern Analysis and Machine Intelligence*, 21(8):690–706, 1999. 1

[97] S. Bakshi and Y. H. Yang. Shape From Shading for Non-Lambertian Surfaces. In *IEEE International Conference on Image Processing, Austin, Texas Nov 13-16, 1994*, volume 2, pages 130–134, 1994. 4

[98] S. M. Samuels. A Simplified Proof of a Sufficient Condition for a Positive Definite Quadratic Form. *The American Mathematical Monthly*, 73(3):297–298, March 1966. 80, 82, 84

[99] S. N. Kružkov. Generalized Solutions of the Hamilton-Jacobi Eeuqtions of Eikonal Type. I. Formulation of the Problems; Existence, Uniqueness and Stability Theorems; Some Properties of the Solutions. *Math. USSR Sbornik*, 27(3):406–446, 1975. 15, 54

[100] Dirk Schieborn. *Viscosity Solutions of Hamilton-Jacobi Equations of Eikonal Type on Ramified Spaces*. PhD thesis, Eberhard-Karls-Universität Tübingen, 2006. 15

[101] Panagiotis E. Souganidis. Approximation Schemes for Viscosity Solutions of Hamilton-Jacobi Equations. *Journal of Differential Equations*, 59:1–43, 1985. 117, 118, 125

[102] Michael Spivak. *Calculus On Manifolds: A Modern Approach to Classical Theorems of Advanced Calculus*. Westview Press, 5th edition, 1971. 45

[103] Stephen P. Boyd and Lieven Vandenberghe. *Convex Optimization*. Cambridge University Press, Cambridge, seventh printing with corrections edition, 2007. 111

[104] Gilbert Strang. *Linear Algebra and Its Applications*. Harcourt Brace Jovanovich College Publishers, 3rd edition, 1988. 80, 84

[105] Takayuki Okatani and Koichiro Deguchi. Shape Reconstruction from an Endoscope Image by Shape from Shading Technique for a Point Light Source at the Projection Center. *Computer Vision and Image Understanding*, 66(2):119–131, 1997. 1

[106] William Rowan Hamilton. On a General Method of Expressing the Paths of Light, and of the Planets, by the Coefficients of a Characteristic Function, 1833. 10

[107] William Rowan Hamilton. On the Application to Dynamics of a General Mathematical Method previously Applied to Optics, 1834. 10

[108] Chenyu Wu, Srinivasa G. Narasimhan, and Branislav Jaramaz. Shape-from-shading under near point lighting and partial views for orthopedic endoscopy. In *Workshop on Photometric Analysis For Computer Vision (PACV 2007)*, October 2007. 1

List of Figures

List of Tables

List of Algorithms

Index